Preliminary Report

of

The Hakuhō Maru Cruise KH-68-4

(Southern Cross Cruise)

November 14, 1968 ~ March 3, 1969

Central and South Pacific

Ocean Research Institute
University of Tokyo

1970

Contents

Introduction 3
I. Object 4
II. Scientists Aboard 5
III. Outline of the Cruise 6
IV. Hydrocast 8
IV.1. Salinity 8
IV.2. Dissolved Oxygen 8
IV.3. Reactive Phosphate 10
IV.4. Reactive Silicate 10
IV.5. Nitrite 10
IV.6. Nitrate 11
IV.7. pH and Total Alkalinity 12
V. Large Volume Water Sampling 24
VI. Observation with *in situ* S.T.D. System 25
VII. Piston Coring 36
VIII. Individual Research Works 63
VIII.1. Chemistry 63
VIII.1.1. Ammonia and Ammonium Ion 63
VIII.1.2. Nitrogen and Argon 63
VIII.1.3. ^{18}O of Dissolved Oxygen 66
VIII.1.4. Carbon Dioxide in the Atmosphere and in the Surface Sea Water 67
VIII.1.5. Borate and Fluoride Ion 68
VIII.1.6. Bromine 68
VIII.1.7. Iodide and Iodate 69
VIII.1.8. Tatal Phosphorus and Total Silicate 69
VIII.1.9. Arsenic 70
VIII.1.10. Calcium and Other Elements 70
VIII.1.11. Calcium Carbonate Chemistry 70
VIII.1.12. Strontium and Barium in Sea Water and Sediment 71
VIII.1.13. Iron, Aluminum, and Silicon in Suspended Matter 72
VIII.1.14. Trace Elements (Chromic and Chromate Ion) in Sea Water and Sediment 72
VIII.1.15. Chemical Composition of Marine Plankton 74
VIII.1.16. Organic Matter 75
VIII.1.17. ^{14}C in Sea Water and in Air 76
VIII.1.18. Distribution of ^{90}Sr and ^{137}Cs in the Pacific Waters 77
VIII.1.19. ^{210}Pb and ^{210}Po 78
VIII.1.20. Samples for the Studies on Distribution of Natural Radioactive Nuclides in Deep-Sea Deposit 78
VIII.1.21. Uranium, Thorium, and Plutonium Isotopes 78
VIII.1.22. Monitoring of Artificial Radioactive Nuclides in Sea Water 79

VIII.2. Geophysics 80
VIII.2.1. Measurement of Gravity and Magnetic Force at Sea during KH-68-4 Cruise 80
VIII.2.2. Gravity Measurement on Land 103
VIII.2.3. On Line Real Time Processing Program of the Gravity Data 106
VIII.2.4. Batch Processing Program for Computing the Corrected Depth, Bouguer Correction and the Eotvos Correction 119
VIII.2.5. Terrestrial Heat Flow..... 133
VIII.2.6. Possibility of Magnetization Measurement of the Pelagic Sediments on Board 134
VIII.2.7. Observation of Atmospheric Electricity 138
VIII.3. Biological Works 141
VIII.3.1. Sighting Records of Whales and Sea-birds 141
VIII.3.2. Plankton Sampling and Observation of the DSL..... 142
VIII.3.3. Jet Net..... 170

Introduction

It is my great pleasure to compile the cruise report of our Southern Cross Cruise with the memories that all the scientists aboard had done their chemical, geophysical and biological research works with intimate collaboration and no one had slight inquries during the whole one hundred and ten days cruise in mid Pacific.

We were deeply impressed by many research works on oceanography in the Oceanographic Institutes in Wellington and in Sydney, and were happy to have chances to talk with many scientists. I hope our visit will become the first step of collaboration of oceanographic works between scientists of New Zealand, Australia and Japan.

We, scientists aboard, were much indebted to the officers and crew of R. V. Hakuhō Maru for assisting us in doing our research works day and night: also to the Japan Embassy in Wellington and the Japan Consul in Sydney for their kind arrangements during our stay in Wellington and Sydney, respectively: to the business personnels of the Institute and Ship Agent (Burns, Philp & Co. Ltd.). Without efforts of these people the cruise would not be successful.

Yoshio Horibe
Chief Scientist in charge
Ocean Research Institute
University of Tokyo

I. Object

The principal object of the Southern Cross Cruise is to study the chemical characteristics of waters of the Central and South Pacific. Recently, the techniques of chemical and radioactive measurements have been developed into high conditions so that the results of these measurements are expected to be very important for the understanding of large scale circulation and mixing processes of the ocean water. The Southern Cross Cruise was the first Japanese attempt to challenge to the ocean exploration from the view point of chemistry, and the results will help extend and refine the present various circulation models of the Pacific waters.

Air-sea interactions, sea water-sediments interactions, and chemistry of sea water were also studied by measuring the chemical species and radioactivities in air, sea water, and sediments. Along all the course of the cruise, gravity, earth's magnetic total force, and atmospheric electricity were measured, and sighting observation was performed. Also, the heat flow measurements and measurement of magnetic polarity of sediments were carried out at various stations.

II. Scientists Aboard

HORIBE, Yoshio	Ocean Res. Inst., Univ. of Tokyo	Isotope oceanography
TOMODA, Yoshibumi	Ocean Res. Inst., Univ. of Tokyo	Submarine geophysics
TSUBOTA, Hiroyuki	Ocean Res. Inst., Univ. of Tokyo	Chemical oceanography
KANAMORI, Satoru	Water Res. Lab., Nagoya Univ.	Geochemistry
SUGIMURA, Yukio	Meteor. Res. Inst.	Nuclear oceanography
WATANUKI, Kunihiko	Dept. of Chem., Univ. of Tokyo	Geochemistry
YOSHIMURA, Hirozo	Japan Meteor. Agency	Chemical oceanography
KUWAMOTO, Toru	Dept. of Chem., Univ. of Kyoto	Geochemistry
KOBAYASHI, Kazuo	Ocean Res. Inst., Univ. of Tokyo	Submarine geophysics
TOYOTA, Yoshimasa	Tokai Univ., College of Marine Science and Technology	Geochemistry
TSUNOGAI, Sizuo	Dept. of Chem., Hokkaido Univ.	Geochemistry
NAKAI, Toshisuke	Ocean Res. Inst., Univ. of Tokyo	Physical oceanography
SHIGEHARA, Koji	Ocean Res. Inst., Univ. of Tokyo	Isotope oceanography
KITAZAWA, Kazuhiro	Ocean Res. Inst., Univ. of Tokyo	Submarine geophysics
KAWAMURA, Akito	Whales Res. Inst.	Marine biology
FUJITA, Tetsuo	Kyoto Univ. of Education	Analytical chemistry
NAGASAKA, Koichi	Maizuru Marine Observatory	Submarine geophysics
KOIZUMI, Kinichiro	Ocean Res. Inst., Univ. of Tokyo	Geophysics
KUREHA, Kazuo	Ocean Res. Inst., Univ. of Tokyo	Biology
TANO, Minoru	Ocean Res. Inst., Univ. of Tokyo	Chemistry
HASUMOTO, Koji	Ocean Res. Inst., Univ. of Tokyo	Biology
OTOBE, Hirotaka	Ocean Res. Inst., Univ. of Tokyo	Oceanography
KANADA, Masahiro	Res. Inst. Atmospherics, Nagoya Univ.	Physics
YANAGI, Katsumi	Water Res. Lab., Nagoya Univ.	Chemistry
TOKUYAMA, Akira	Water Res. Lab., Nagoya Univ.	Chemistry
MAYEDA, Masaru	Tokyo Univ. of Education	Chemistry
YASUJIMA, Tadahide	Tokyo Univ. of Education	Chemistry
HIRAO, Yoshimitu	Tokyo Univ. of Education	Chemistry
MURAI, Shigeo	Dept. of Chem., Univ. of Kyoto	Chemistry

III. Outline of the Cruise

The cruise was divided into four legs, as is shown in Figure 1. Leg I was from Tokyo to Apia, Western Samoa, leg II was from Apia to Wellington, New Zealand, leg III was from Wellington to Sydney, Australia via Ross Sea (170° W, 69.5°S), Scott Island, and Balleny Islands, and leg IV was from Sydney to Tokyo via Noumea, New Caledonia. Leg I, II, and III passed through mainly the deep part of the Central and South Pacific.

Table 1 shows sampling, measurements and observation done in each leg, and all the stations of water sampling, S.T.D. observation (including water sampling), piston coring, and heat flow measurement are shown in Tables 2, 6, 8, and 21, respectively.

Table 1. Observation items

	Leg			
	I	II	III	IV
1. Hydrocasts with 2 liter Nansen and 6 liter van Dorn samplers	○	○	○	
2. Large volume sampling	○	○	○	
3. Core sampling	○	○	○	
4. Heat flow measurement	○	○	○	
5. Measurement with *in situ* S.T.D. System	○ (30°–20°N, 2°N–3°S)			
6. CO_2 measurement in atmosphere	○	○	○	
7. Gravity measurement	○	○	○	○
8. Magnetic intensity measurement	○	○	○	○
9. Atmospheric electricity measurement	○	○	○	○
10. Sighting observation	○	○	○	○

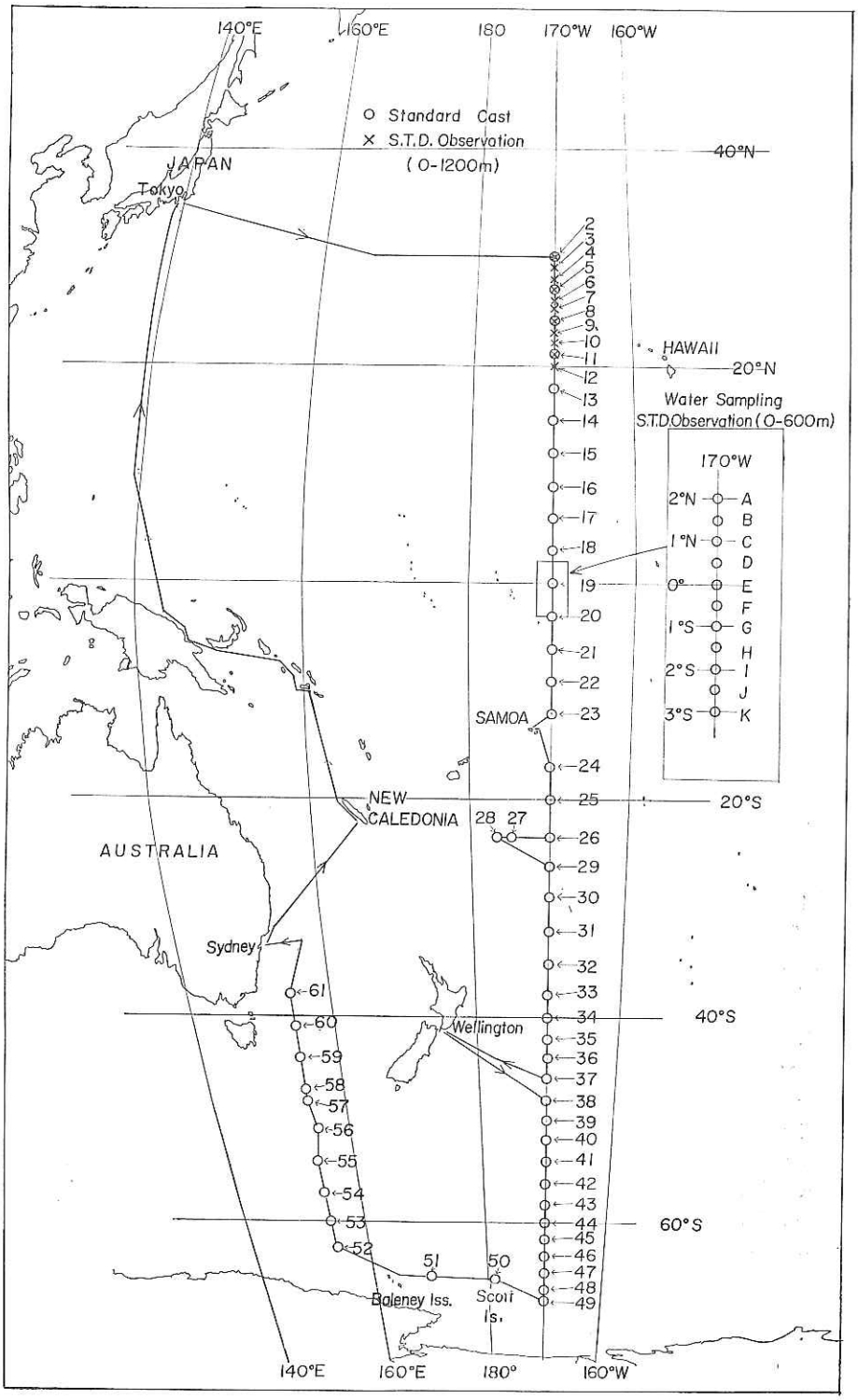

Fig. 1. Map of cruise track and stations.

IV. Hydrocast

by
Y. Horibe, Y. Sugimura, K. Watanuki, S. Kanamori,
H. Tsubota, H. Yoshimura, and T. Nakai

Standard hydrocasts were done along 170°W longitude and along 155°E longitude at 53 stations which are shown in Table 2.

The hydrocast was carried out with a winch equipped with 14,000 m stainless steel tapered wire. At one station, two casts were done, one was for the upper 1,200 meter, and the other was for from 1,200 m to bottom. Standard depth for Nansen sampler were 10, 30, 50, 75, 100, 150, 200, 300, 400, 500, 600, 700, 800, 1,000, and 1,200 m for the upper 1,200 meters, and 1,200, 1,500, 2,000, . . . (every 500 m) . . . bottom, for deeper cast.

A sonar pinger (EG and G Model 220) was attached at the end of the wire, and ship echo sounder (1 second scanning) served as detector, so that we could recognize the distance between sonar pinger and sea floor and could obtain bottom water as near as possible. Although we could recognize the distance between sonar pinger and bottom as near as 5 m in most cases, we experienced that we had no direct and echo signals at some stations near equator. As the diesel-electric, two screw two rudder propulsion system and bow thruster of the Hakuhō Maru allowed us to move the ship in all directions, we could minimize the wire angle during the hydrocast. Van Dorn sampler (a pair of 6 liter) or 1.7 liter plastic sampler (General Oceanics Nonmetallic Water Sampling Bottles Model RMS–1.7) were attached 10 m below the Nansen sampler when they were needed. Two protected reversing thermometers and one unprotected reversing thermometer were attached to the each Nansen sampler.

1 liter of water sample in Nansen sampler was used for routine analyses. The chemical data for routine analyses are salinity, dissolved oxygen, inorganic phosphate, soluble silicate, nitrite, nitrate, pH, and total alkalinity. The remaining 1 liter water of Nansen bottle and water of plastic sampler were used for special purposes of chemistry.

IV. 1. Salinity

120 ml sea water was put in a brown glass bottle and its surface was washed with fresh water and was kept in an air-bath which had electronically cooling and heating device and its temperature was adjusted to room temperature. Temperature of all sample waters, (number of bottles were about 40 at each station) in the air bath became equal to room temperature at least in two hours so that the temperature fluctuation had not been obsereved during salinity measurement. A salinometer of Auto Lab Model 601 MK III was used. One ampoule of Standard Sea Water (IAPO) was used for samples of one station and substandard (filtered sea water) was measured for every 10 samples. All the measurement could be finished within four hours (two hours for temperature equilibrium and two hours for measurement) after hydrocast.

IV. 2. Dissolved Oxygen

The amount of dissolved oxygen was determined by the modified Winkler method,

Table 2. Stations of standard hydrocast

Station Number	Position		Time		Depth (m)
	Longitude	Latitude	Date	Hour	
2	170°03.1W	30°02.1N	Nov. 22, 1968	1540–2240	5400
5	169°58.6W	26°54.8N	Nov. 24, 1968	1030–1535	4520
8	169°56.8W	23°58.5N	Nov. 25, 1968	1340–1843	4640
11	170°02.1W	21°00.8N	Nov. 26–27, 1968	1945–0210	4270
13	170°02.8W	17°59.0N	Nov. 27–28, 1968	2157–0328	5220
14	170°02.9W	14°58.4N	Nov. 28–29, 1968	1804–0325	5665
15	169°49.5W	11°59.7N	Nov. 29, 1968	1753–2350	5050
16	170°01.0W	9°01.7N	Dec. 1– 2, 1968	2050–0125	5200
17	169°53.1W	6°05.1N	Dec. 3, 1968	0100–0542	5580
18	169°56.4W	3°02.0N	Dec. 3– 4, 1968	1919–0310	5470
19	170°12.1W	00°03.2N	Dec. 5, 1968	0743–1427	5500
20	170°01.6W	3°01.9S	Dec. 6, 1968	1820–2330	5130
21	170°04.6W	6°09.3S	Dec. 7, 1968	1240–1740	4970
22	169°52.9W	9°04.6S	Dec. 8, 1968	1930–2332	4400
23	170°03.4W	11°59.7S	Dec. 9, 1968	1750–2205	5050
24	170°02.6W	17°00.7S	Dec. 15, 1968	0730–1510	5000
25	170°03.2W	19°59.7S	Dec. 16, 1968	0440–0900	5300
26	169°58.3W	23°10.6S	Dec. 17, 1968	0335–0805	5800
27	174°40.1W	23°11.0S	Dec. 18, 1968	0915–2010	10200
28	176°30.4W	23°16.1S	Dec. 19, 1968	0457–0708	2080
29	169°59.0W	26°01.7S	Dec. 20–21, 1968	2130–0235	5600
30	170°01.1W	29°00.2S	Dec. 22, 1968	0155–0755	5550
31	169°59.7W	31°58.8S	Dec. 22–23, 1968	2131–0222	5650
32	169°59.1W	35°00.0S	Dec. 23–24, 1968	2345–0330	5200
33	169°59.9W	38°00.9S	Dec. 25, 1968	0216–0819	5100
34	170°03.2W	39°59.5S	Dec. 26, 1968	1240–1640	5200
35	170°01.8W	42°01.2S	Dec. 27, 1968	0153–0640	4100
36	170°00.1W	44°00.0S	Dec. 27, 1968	1632–2030	5000
37	169°58.6W	46°01.3S	Dec. 28, 1968	0621–1155	5200
38	170°05.1W	48°00.6S	Jan. 10, 1969	0640–1620	5280
39	170°00.9W	49°52.4S	Jan. 11, 1969	0310–0702	5190
40	169°53.7W	52°00.4S	Jan. 12, 1969	0635–1137	5060
41	169°55.6W	53°58.2S	Jan. 12–13, 1969	2335–0625	5210
42	169°58.0W	55°55.0S	Jan. 14, 1969	0715–1225	4700
43	169°58.4W	57°55.1S	Jan. 14–15, 1969	2353–0347	4550
44	169°54.6W	59°59.8S	Jan. 15, 1969	1745–2340	4650
45	169°57.6W	61°58.9S	Jan. 16, 1969	1055–1440	3350
46	170°01.7W	63°58.9S	Jan. 17, 1969	0525–0800	2700
47	170°00.0W	66°00.0S	Jan. 17, 1969	1938–2310	3250
48	170°06.9W	68°00.1S	Jan. 18, 1969	1348–1720	3695
49	169°57.3W	69°29.4S	Jan. 19, 1969	1047–1540	4230
50	179°56.6E	66°44.0S	Jan. 20–21, 1969	2045–0025	3800
51	170°08.0E	66°30.0S	Jan. 21, 1969	1805–2055	3180
52	154°53.6E	63°03.8S	Jan. 23–24, 1969	1845–0027	3005
53	155°02.5E	60°00.3S	Jan. 24, 1969	1607–1855	3000
54	155°01.9E	57°05.3S	Jan. 25, 1969	1240–1550	3620
55	155°08.0E	53°56.9S	Jan. 26–27, 1969	2200–0150	4200
56	155°23.9E	51°10.4S	Jan. 27–28, 1969	2158–0418	4465
57	155°04.2E	47°59.6S	Jan. 29, 1969	0256–0820	4775
58	155°02.9E	46°54.9S	Jan. 29, 1969	1735–2107	4700
59	155°02.4E	44°03.1S	Jan. 30, 1969	1337–1740	4650
60	155°02.3E	41°01.8S	Jan. 31, 1969	1410–1850	4595
61	154°56.2E	38°02.2S	Feb. 1, 1969	1750–2240	4500

using Metrohm piston buret of 10 ml capacity. Titration was done between 5 and 24 hours after the addition of manganese chloride and potassium iodide solution.

Reagents

(1)	$MnCl_2\ 4H_2O$	400 g in 1 liter 0.02 N HCl solution
(2)	NaOH	360 g } in 1 liter distilled water
	KI	100 g }
(3)	Starch	0.2% solution which was prepared every five days.
(4)	$Na_2S_2O_3\ H_2O$	2.5 g } in 1 liter cold distilled water which was
	Na_2CO_3	1.0 g } boiled before cooling
(5)	HCl	6 N
(6)	KIO_3 solution	0.01 N solution made by Sagami Chemical Research Center as the standard solution for oceanographic work.

The mean deviation of titration was 0.01 ml O_2/l, and no correction was applied for dissolved oxygen in reagents added, because the amount of dissolved oxygen in reagents were less than 0.005 ml O_2/l. Seven bottles of standard potassium iodate solution were used during the whole course of the cruise, and the differences of concentration between bottles corresponded less than 0.01 ml O_2/l.

IV. 3. Reactive Phosphate

The reactive phosphate was measured by the acidified molybdate method described in "Guide Book for Oceanographic Observation" (Oceanographical Society of Japan, in press, in Japanese).

1 ml of acidified ammonium molybdate solution was added to 50 ml unfiltered sea water samples from Nansen bottle, and the solution was reduced with one drop of 2.15% stannous chloride solution. The final ammonium molybdate concentration was 0.05% and the acidity was 0.27 N. The absorbancy was measured after 15 minutes at wave length of 700 mμ with a photo-electric photometer-recorder system which is widely used on board the Japanese oceanographic vessels. The discrepancy of the values between two aliquots of the same water sample did not exceed more than 3% of the reported value in any case.

CSK standard solution which contains known amount of potassium dihydro-phosphate was diluted with artificial sea water to make four solutions of different concentration, and the calibration curve was made for every series of the analysis. Ampoules of CSK standard solution were prepared by Sagami Chemical Research Center under the supervision of Dr. K. Sugawara.

IV. 4. Reactive Silicate

1.0 ml of 10% ammonium molybdate and 1.0 ml of 6 N sulfuric acid were added to 50 ml unfiltered sea water from Nansen bottle and its absorbancy was measured at wave length of 420 mμ, with the same photoelectric photometer as that used for phosphorus determination. A calibration curve was prepared in each series of analysis, using a set of standard solutions of sodium silicate which was diluted with artificial sea water. Discrepancy of measured values between two aliquots of the same sample was usually less than 3% of the reported value.

IV. 5. Nitrite

The procedure was based on the method described in "A Manual of Sea Water

Analysis" by J. D. H. Strickland and T. R. Parsons (1965). The nitrite in sea water was treated with sulphanilamide in acid solution. The resulting diazo compound reacted with N-(1-naphthyl)-ethylendiamine to form wine red coloured azo dye, and its absorbancy was measured by spectrophotometry.

Reagents. Sulphanilamide solution: 5 g of sulphanilamide was dissolved in a solution of 50 ml of 12 N HCl and 300 ml of distilled water, and then was diluted to 500 ml with distilled water. N-(1-naphthyl)-ethylendiaminhydrochloride: 1.0 g of the reagent was dissolved in distilled water and diluted to one liter. The solution was stored in a brown coloured glass bottle.

Procedure. 20 ml of sea water from Nansen sampler was taken in the graduated test tube with stopper. 0.8 ml of sulphanilamide solution was added with a dispencer pipette to each sample, and was mixed by shaking. After 2 to 5 minutes 0.8 ml of naphthyl ethylendiamine solution was added and mixed with sea water immediately. After 10 minutes absorbancy of the solution was measured in a 5 cm cell at the wave length of 543 mμ with a spectrophotometer (Hitachi model 101). The analysis was done not later than 10 hours after the collection of samples. All the samples collected were clear and the turbidity correction was not applied. The content of nitrite was read from the calibration curve which was made by the use of CSK standard solutions. The reproducibility of the standard solution is shown in Table 3. The experimental error did not exceed 2%.

Table 3. Reproducibility of CSK standard solution

NO_2–N μg at/l	Absorbance		
0.00	0.003	0.005	0.004
0.25	0.061	0.064	0.064
0.50	0.121	0.123	0.124
1.00	0.242	0.242	0.244
1.99	0.488	0.488	0.491

IV. 6. Nitrate

Nitrate in sea water was determined for all the samples collected in the hydrographic casts. The procedure was based on the method improved by E. D. Wood, F. A. J. Armstrong, and F. A. Richards (J. Mar. Biol. Ass. U. K., *47*, 23–31 (1967).) The nitrate in sea water was reduced to nitrite by passing sea water through a column containing copperized cadmium filings, and the nitrite thus produced was determined by the method described earlier.

Five columns for the reduction of nitrate to nitrite were used for routine analysis of nitrate in sea water on board. The reduction column which contained copperized cadmium filing is shown in Figure 2. The column was treated with 50 ml wash-solution (EDTA–HCl solution) prior to the reduction of nitrate in sea water. Sample sea water was passed through the column at a rate of 5–6 ml/min, and 5 ml of reduced sea water sample was pipetted and diluted to 20 ml with distilled water.

Standard solution, which contain known amount of nitrate (20 μg atom NO_3–N per liter) in 30% artificial sea water, were used as a reference sample. Average deviation of the analysis of reference sample was 1.2% and reducing efficiency was estimated to be more than 99%. Estimated overall average deviation of the nitrate content in sea water was 4% of the reported value.

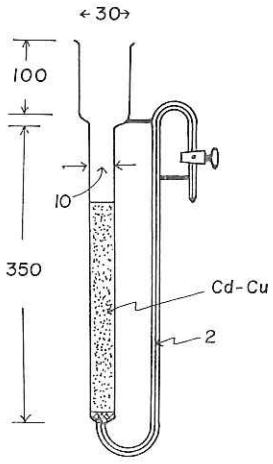

Fig. 2. Cd-Cu reduction column for nitrate determination. (Unit; mm)

IV. 7. pH and Total Alkalinity

pH measurement was done by the method described in "A manual of Sea Water Analysis" by J. D. H. Strickland and T. R. Parsons (Bulletin No. 125, 29–36 (1965), Fish. Res. Bd. Canada).

Total alkalinity (A) was calculated by the equation

$$A = V_e \frac{C}{V_0} \times 1000 \quad \text{(meq/l)}$$

where C is the concentration (normality) of HCl solution added to sea water sample, V_0 is the volume of sea water sample, and V_e is the volume of HCl solution which is equivalent to the total alkalinity of the sample, and can be obtained experimentally, using Gran's plot.

Reagents and pH meter. Three buffer solutions were prepared by the use of Merck's buffer reagents.

phosphate buffer:	0.025 m Na_2HPO_4 and 0.025 m KH_2PO_4
phthalate buffer:	0.01 m KH-phthalate
borate buffer:	0.01 m borax

500 ml of phosphate buffer and 1 liter of phthalate buffer were prepared every 5 and 10 days, respectively. The solutions were kept in glass bottles with rubber stopper. 200 ml of borate buffer was prepared every time when it was needed. Hitachi Model F–5 pH meter of precision type was used throughout the cruise. The instrument is guaranteed to have precision of 0.005 pH unit. Beckmann glass electrode with a bulb of GP glass and silver-silver chloride internals and Hitachi-Horiba reference electrode with a frit junction and calomel internals were used.

Procedure. The sample was taken into a 100 ml polyethylene bottle directly from a Nansen bottle. The contact of sample water with air during sampling was avoided by applying the same technique as that for dissolved oxygen.

The polyethylene bottle was immersed into a constant temperature bath to adjust the temperature of sample to the room temperature. A portion of the sample was transferred to another polyethylene bottle with a 50 ml pipet for the total alkalinity determination. The electrodes were immersed directely into the remaining sample water to read pH value.

For the total alkalinity determination, 1.30 ml of titrant (0.1 N HCl and 0.6 N NaCl mixed solution) was added to 50 ml of sea water sample while stirring with a magnet stirrer.

The pH measurements were carried out every time after successive additions of 0.05 ml HCl solution. Three pH values lower than 4 were obtained to be plotted in Gran's plot. The relation between 10^{-pH} and V is linear, and the value of V at $10^{-pH}=0$ gives the value of V_e.

Accuracy. 10 aliquots of surface sea water samples in 100 ml polyethylene bottles were analyzed during the cruise aboard, and the results are shown in Table 4. The results show very good reproducibility. However, due to the uncertainties of the pH values of standard buffer solution, insufficient temperature control of water sample, and nonlinear drift of pH meter setting, values of pH and total alkalinity during the whole cruise were estimated to be certain within $\pm$ 0.01 and $\pm$ 0.01 meq/l, respectively.

Table 4. pH and alkalinity of a surface sea water for the reproducibility determination

Sample No.	pH obs*	pH	V_e(ml)	A(meq/l)
1	8.23_1	8.23_3	1.15_3	2.33_1
2	8.23_7	8.24_1	1.15_5	2.33_5
3	8.23_8	8.24_0	1.15_5	2.33_5
4	8.23_6	8.24_0	1.15_4	2.33_3
5	8.23_6	8.24_1	1.15_3	2.33_1
6	8.23_6	8.23_8	1.15_4	2.33_3
7	8.23_5	8.23_9	1.15_4	2.33_3
8	8.23_5	8.23_7	1.15_3	2.33_1
9	8.24_4	8.23_8	1.15_4	2.33_3
10	8.24_6	8.24_1	1.15_3	2.33_1
Average		8.24_1		2.33_3
standard deviation		± 0.003		± 0.002

* These values were corrected for the drift, assuming that it is a linear function of the time.

Results

Cross sections of temperature, salinity, dissolved oxygen, pH, PO_4–P, SiO_2–Si, NO_3–N along 170°W (30°N–69.5°S) and 155°E (38°S–63°S) are shown in Figures 3–16. All these values and interpolated temperature, and salinity are tabulated in a separate table (Oceanographic Data of KH–68–4 (Southern Cross Cruise) of the Hakuhō Maru, Ocean Research Institute, University of Tokyo, 1970), and can be obtained on request to the Institute.

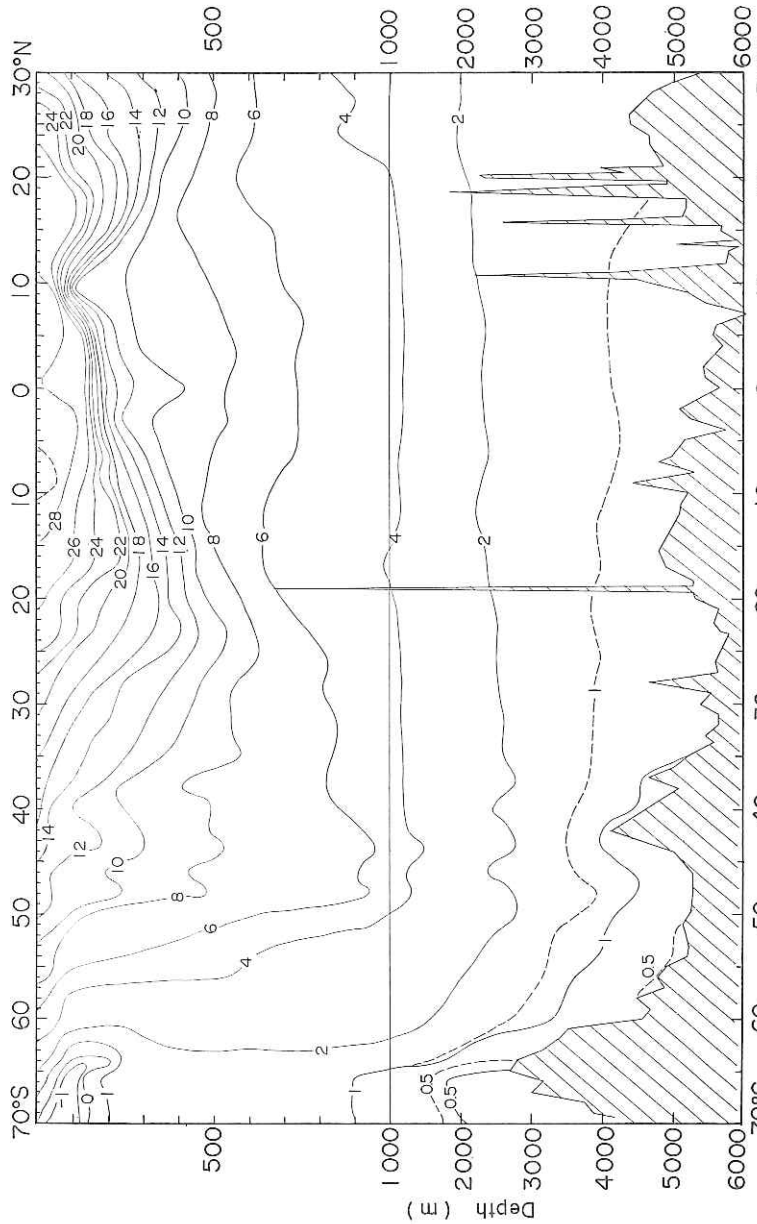

Fig. 3. Temperature profile, 170°W, 30°N–69.5°S. (Unit; °C).
----- potential temperature

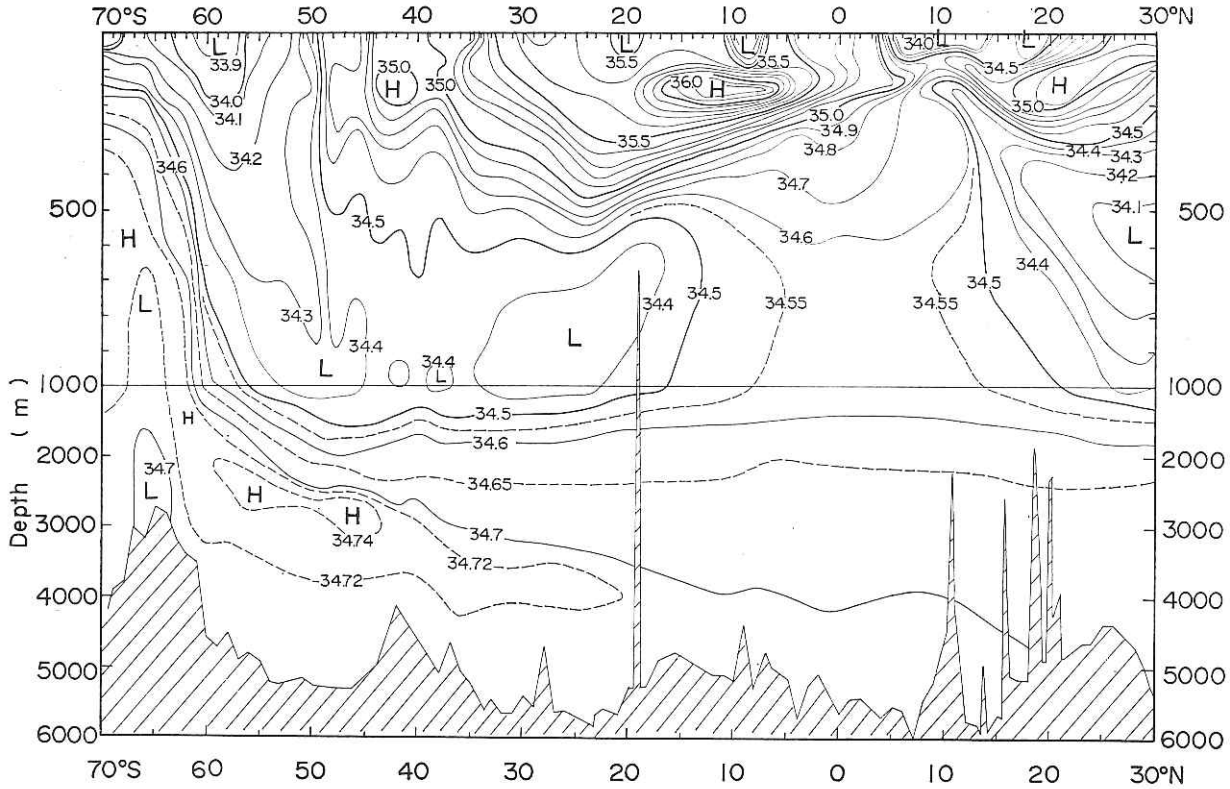

Fig. 4. Salinity profile, 170°W, 30°N–69.5°S. (Unit; ‰).

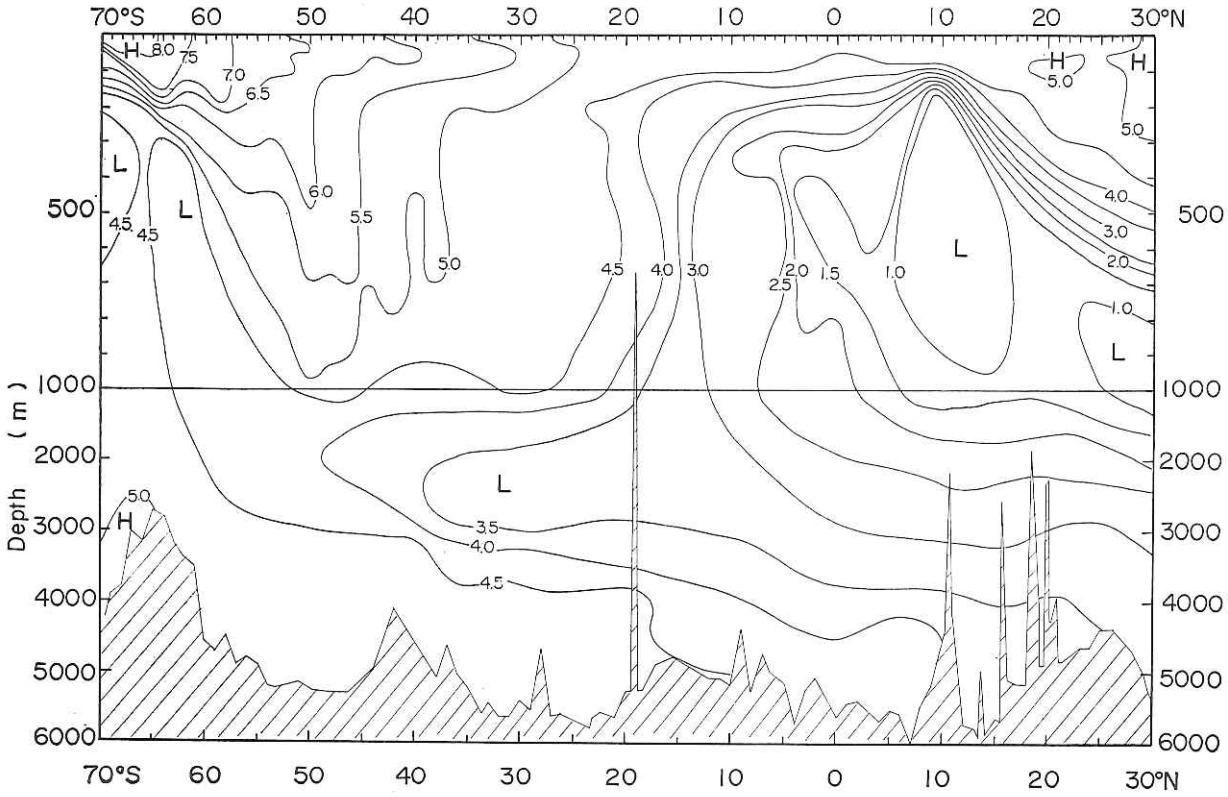

Fig. 5. Dissolved oxygen profile, 170°W, 30°N–69.5°S. (Unit; ml/l).

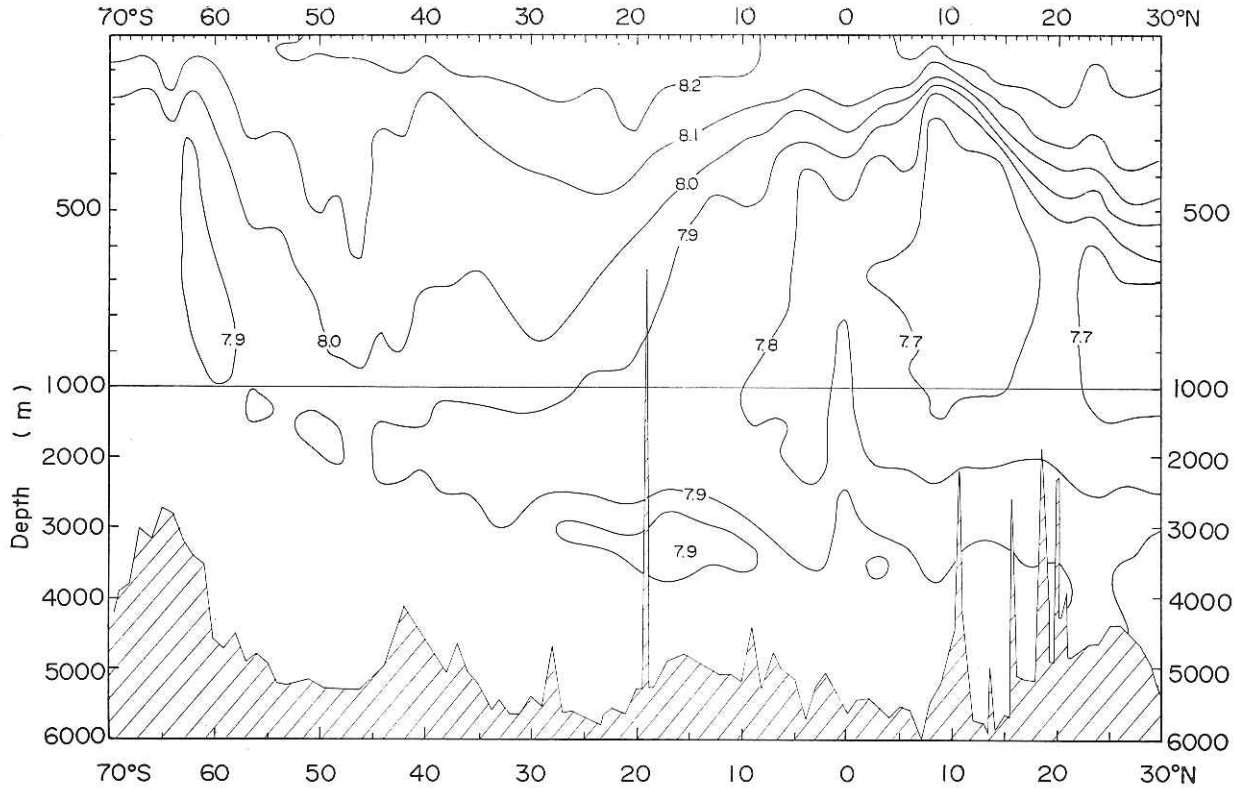

Fig. 6. pH profile, 170°W, 30°N–69.5°S.

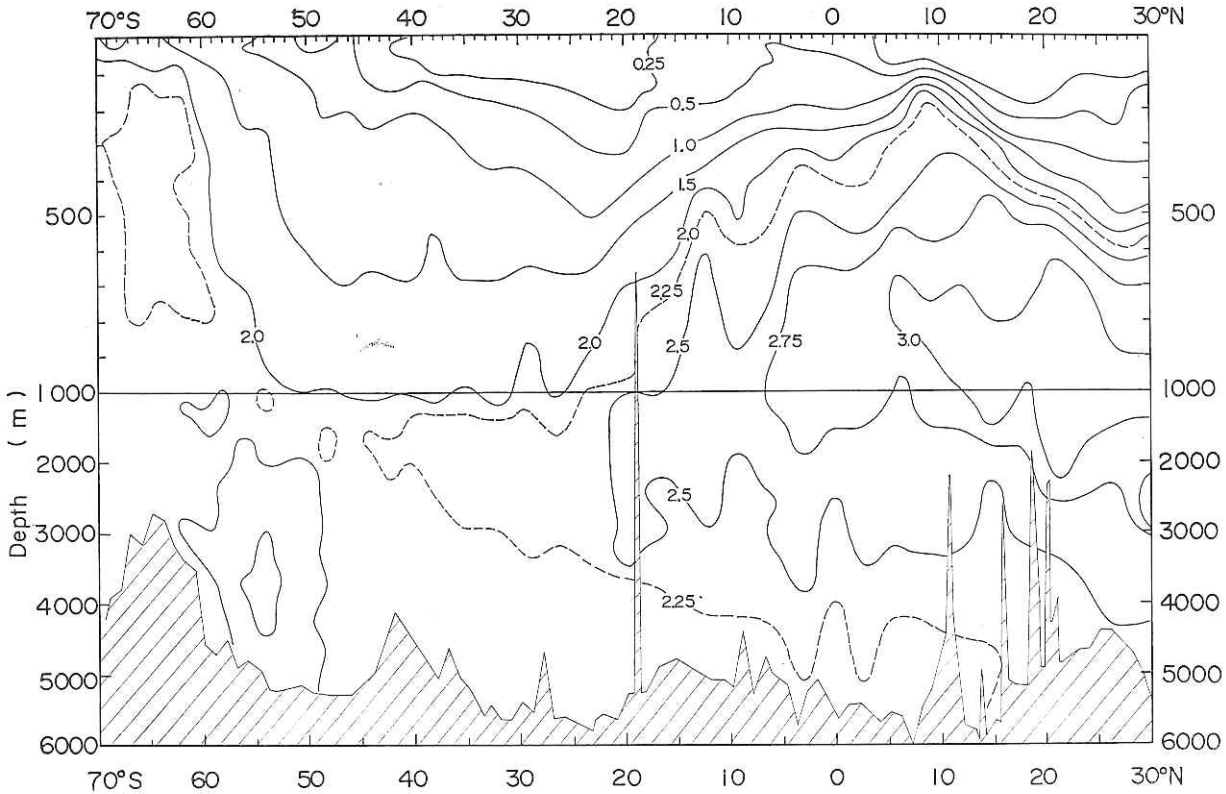

Fig. 7. Reactive phosphate profile, 170°W, 30°N–69.5°S. (Unit; μg at/l).

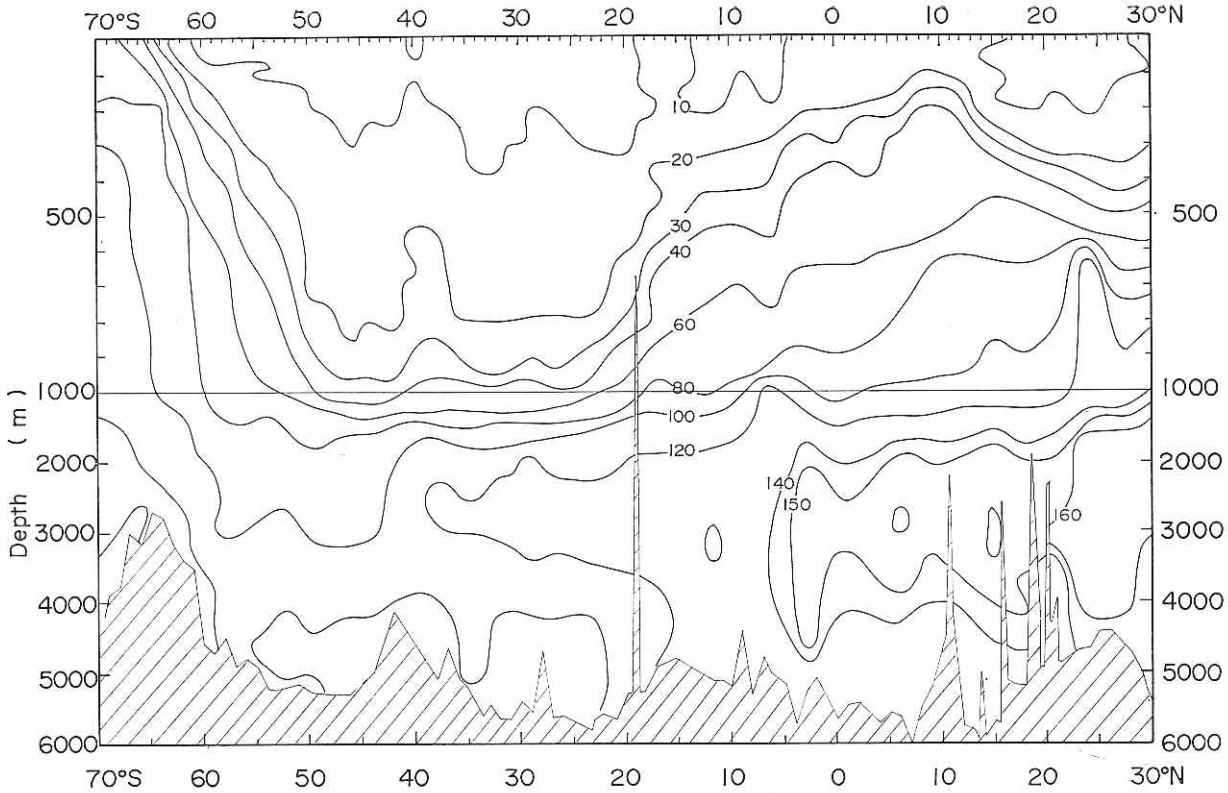

Fig. 8. Reactive silicate profile, 170°W, 30°N–69.5°S. (Unit; μg at/l).

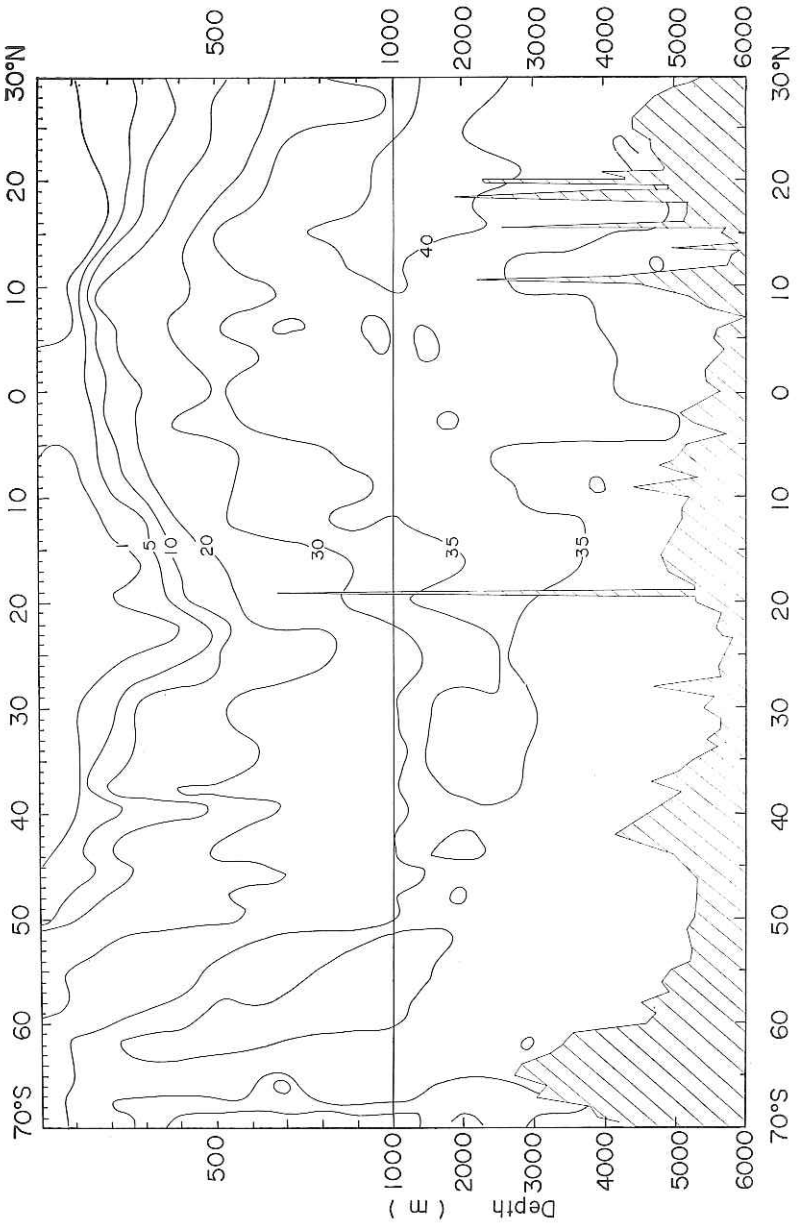

Fig. 9. Nitrate-nitrogen profile, 170°W, 30°N–69.5°S. (Unit; μg at/l).

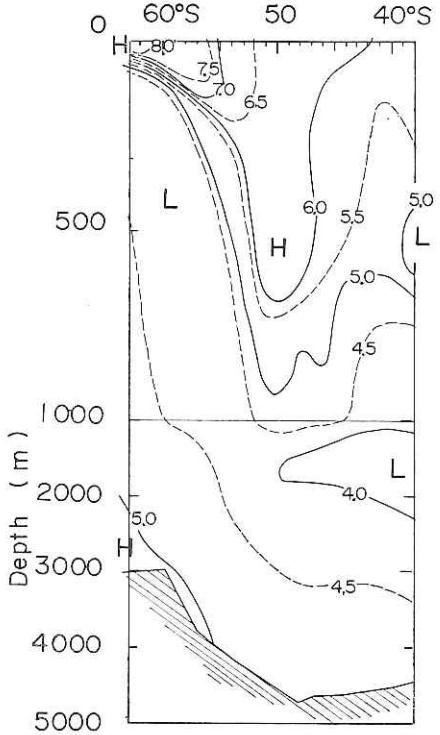

Fig. 12. Dissolved oxygen profile, 155°E, 63°S–38°S. (Unit; ml/l).

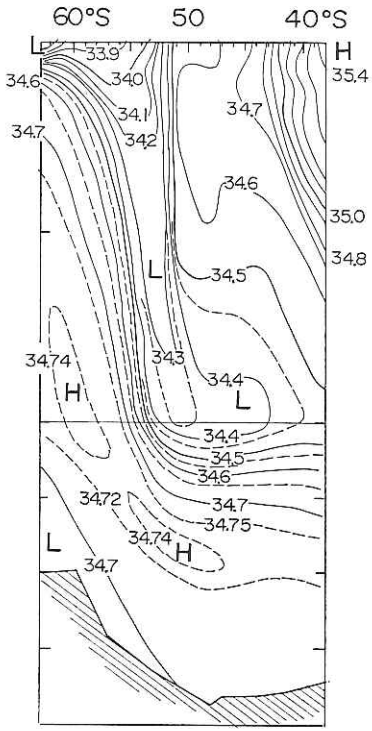

Fig. 11. Salinity profile, 155°E, 63°S–38°S. (Uuit; ‰)

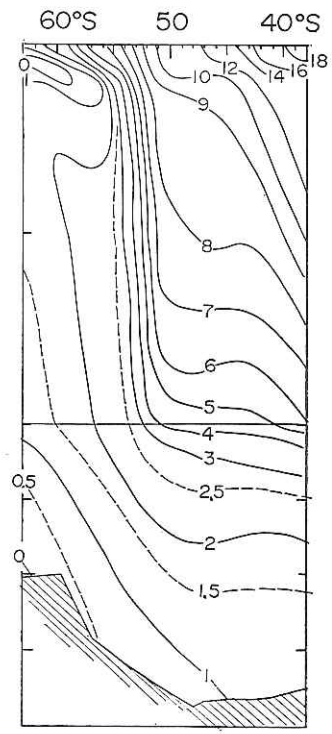

Fig. 10. Temperature profile, 155°E, 63°S–38°S. (Unit; °C)

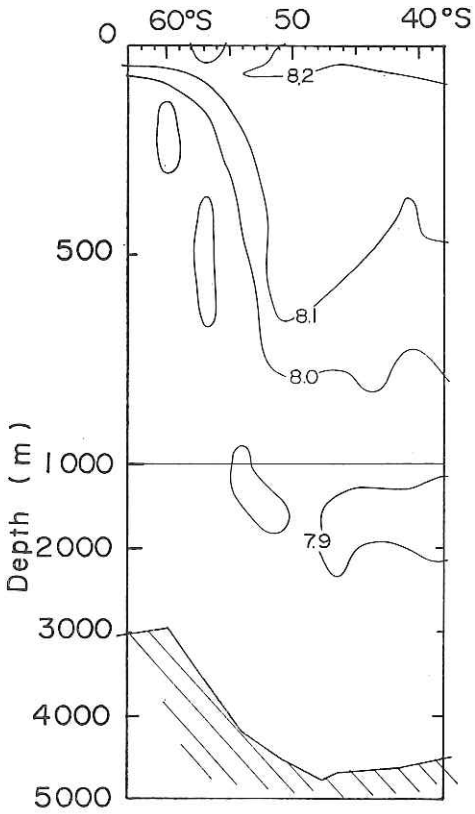

Fig. 13. pH profile, 155°E, 63°S–38°S.

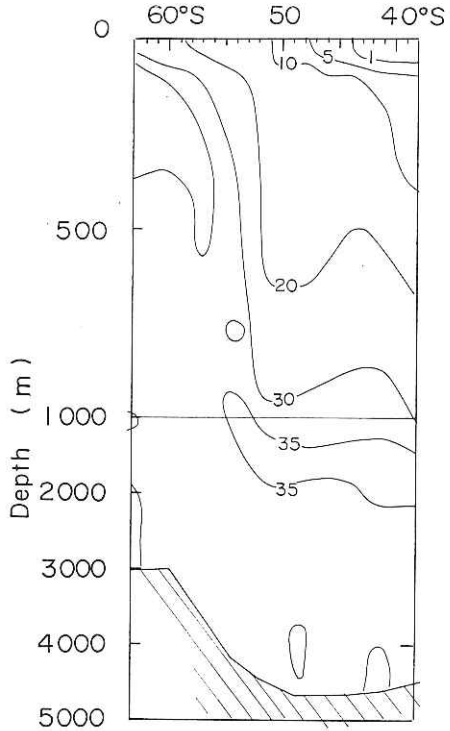

Fig. 16. Nitrate-nitrogen profile, 155°E, 63°S–38°S. (Unit; μg at/l).

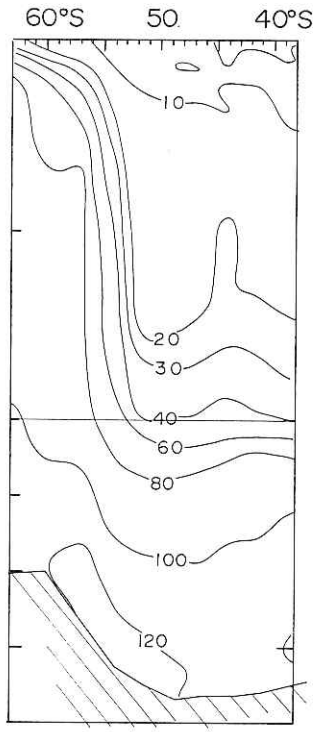

Fig. 15. Reactive silicate profile, 155°E, 63°S–38°S. (Unit; μg at/l).

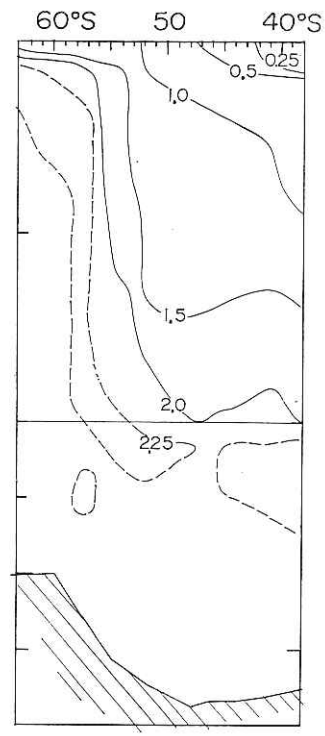

Fig. 14. Reactive phosphate profile, 155°E, 63°S–38°S. (Unit; μg at/l).

V. Large Volume Water Sampling

by
Y. Sugimura

For the studies of thorium isotopes, plutonium, cesium 137, strontium 90, polonium 210, lead 210, chromium, suspended matters, and plant pigments, water samples of large volume were collected at several stations along 170°W longitude. A barrel water sampler of 200 liter and two 400 liter large volume samplers (General Oceanics Model DT-2) were used.

Locations and depth of water sampling are shown in Table 5.

Table 5. Stations for large volume water sampling

Station No.	Location		Depth (m)
2–2	30°07.3′ N	170°04.8′ W	0, 30, 50, 75, 100, 150, 200, 500, 1000
16–2	9°01.5′ N	169°59.7′ W	0, 30, 50, 75, 100, 150, 200, 500, 1000
16–3	9°01.7′ N	170°01.4′ W	0, 500, 1000, 2000
21–3	6°11.7′ S	170°13.5′ W	0, 30, 50, 75, 100, 150, 200, 500, 1000 4000
26–2	23°11.1′ S	169°56.2′ W	0, 30, 50, 75, 100, 150, 200, 500, 1000
29–4	26°02.2′ S	169°55.1′ W	0, 500, 1000, 3000, 5000
33–4	37°59.7′ S	169°54.5′ W	0, 30, 50, 75, 100, 150, 200, 500, 1000, 5000
40–2	51°59.3′ S	169°53.0′ W	0, 30, 50, 75, 100, 150, 200, 500, 1000, 3000
48–2	68°01.5′ S	170°06.5′ W	

VI. Observation with *in situ* S.T.D. System

by
Y. Horibe, and T. Nakai

An *in situ* S.T.D. system (Bissett-Berman Model 9006) was used for the detail description of subtropical eastward current (K. Yoshida, and Y. Kidokoro, J. Oceanogr. Soc. Japan, **23**, 88–91 (1968)), and for the chemical studies of Cromwell Current with combination with Rosette Multi Sampler (Model RMS–12). The latter instrument worked very satisfactorily to get 1.7 liter water samples at the depth where temperature and salinity showed characteristic water type. Water samples obtained were used for the determination of salinity (for checking the S.T.D. system), dissolved oxygen, pH, total alkalinity, and inorganic phosphate on board, and the remaining samples were brought back for the measurement of deuterium, boron, calcium, fluorine, bromine, and iodine. Outline of stations are shown in Table 6.

Table 6. Outline of stations of *in situ* S.T.D. observation

	Subtropical Eastward Current study	Cromwell Current study
Station	11 stations Stn. No. 2, 3, 4, 5, 6, 7, 8, 9, 10, 11, 12	11 stations Stn. No. A, B, C, D, E, F, G, H, I, J, K
Date	November 22–27, 1968	December 4–6, 1968
Position	170°W, 30°N–20°N	170°W, 2°N–3°S
Distance between stations	60 nautical miles	30 nautical miles
Observed depth	0–1,200 meter	0–600 meter
Remarks		Ten water samples were taken at every station with Rosette samplers.

Operation

Specially designed winch which equipped with friction- and stock-drum was used for the operation of the underwater unit. S.T.D. deck unit, digital frequency counter, cable length- and speed-meter, and Rosette deck unit were mounted in one rack on board.

Downward speeds of the underwater unit were 0.75 and 0.5 m/s in subtropical and Cromwell Current studies, respectively, and at much slower rate (usually 0.25 m/s) in thermocline area. Water sampling depth was determined from the data of downward cast and the samples were taken during the upward cast. The results of both down- and up-ward cast were consistent fairly well as is shown in Figure 18 and we could get the samples of desired temperature and salinity in most cases.

Calibration

As this was for the first time for us that we used *in situ* S.T.D. system, it was necessary to know how exactly the recorder could show the data of depth, temperature and

salinity. For this purpose, we attached the array of Rosette sampler (10 of RMS–12 sampler) on the sea cable 1 meter above the underwater unit of S.T.D. system. Recorder readings of depth, temperature, and salinity were compared with the calculated values from signal frequency data, and these values were quite consistent within the experimental error, when the recorder pens were adjusted properly. Recorder readings of depth and temperature could be checked with the data of reversing thermometers which were attached to the deepest sampler, and that of salinity could be checked with the data of salinity measurement of water in samplers. The salinity measurement of water in samplers was done aboard with Auto Lab salinometer Model 601 MK III. The readings of protected reversing thermometers were quite consistent with those of S.T.D. recorder, and the depth calculated from reversing thermometers showed the same depth as that of S.T.D. recorder. Salinity obtained from S.T.D. recorder showed higher values than those of salinometer by +0.05‰ at station No. 2 to No. 11, and +0.03‰ at stations *A* to *K*, as are shown in Table 7.

Table 7. Comparison of salinities obtained from S.T.D. recorder with those of salinometer at deepest sampling layer

Station Number	Salinity (‰)		
	S.T.D. recorder	Salinometer	Difference
2	34.54	34.49*	0.05
5	34.53	34.48*	0.05
6	34.55	34.498	0.052
8	34.57	34.52*	0.05
10	34.59	34.537	0.053
11	34.59	34.54*	0.05
		Mean difference	0.051
A	34.61	34.580	0.030
B	34.61	34.581	0.029
C	34.61	34.582	0.029
D	34.62	34.588	0.032
E	34.64	—	—
F	34.60	34.570	0.030
G	34.60	34.576	0.024
H	34.61	34.590	0.020
I	34.61	34.573	0.037
J	34.62	34.589	0.031
K	34.63	34.598	0.032
		Mean difference	0.029

* Interpolated values from Nansen cast.

Results

Two of the S.T.D. system data sheets are shown in Figure 17 and 18 as examples. Figure 17 is a downward cast from surface to 1200 m depth at station 9 (22°59.8 N, 170°00.4 W), and figure 18 is a down- and up-ward casts from surface to 600 m at station E(0°02.3 N, 170°10.2 W), arrows show the depth at which water samples were taken with Rosette samplers.

Profiles of temperature, and salinity obtained from S.T.D. data, and of calculated thermosteric anomaly from 30°N to 20°N along 170°W longitude are shown in Figure

19, 20 and 21, respectively. Profiles of temperature, salinity, dissolved oxygen, pH, and PO_4–P from 2°N to 3°S are shown in Figure 22, 23, 24, 25 and 26, respectively. The values of these parameters are tabulated in "Oceanographic Data of KH–68–4 (Southern Cross Cruise) of the Hakuhō Maru, Ocean Research Institute, University of Tokyo, 1970", and can be obtained on request to the Institute.

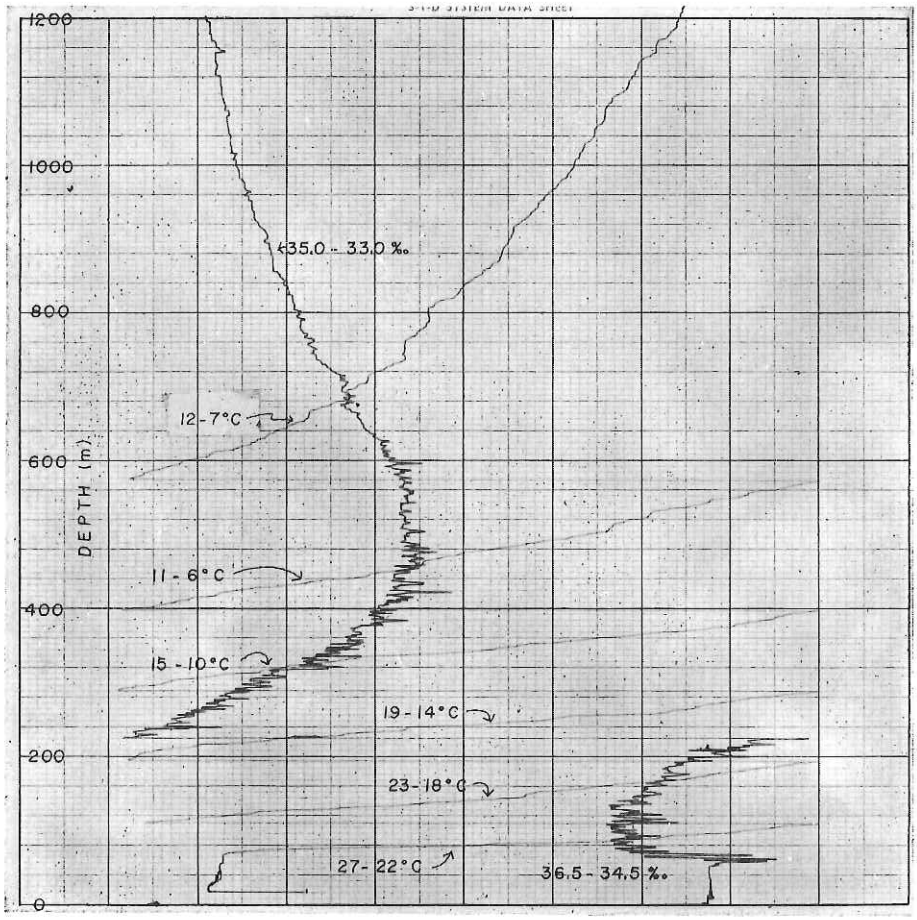

Fig. 17. S.T.D. date sheet at station 9 (22°59.8N, 170°00.4W). Downward cast from surface to 1200 m.

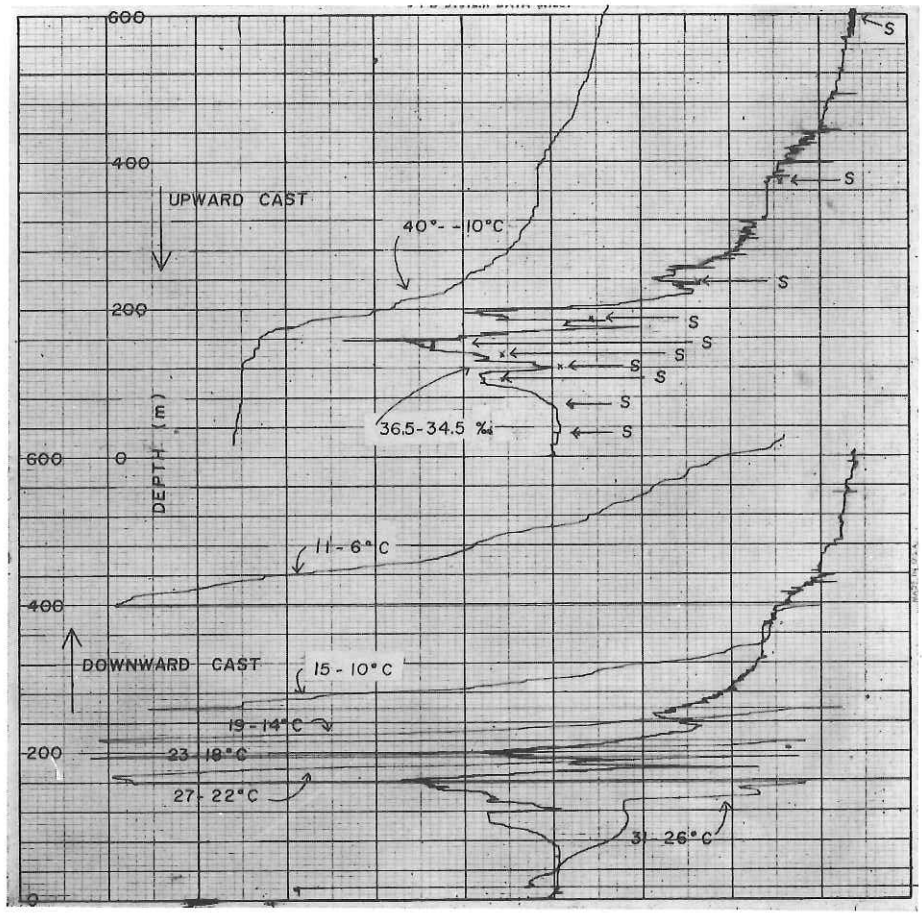

Fig. 18. S.T.D. data sheet at station E (0°02.3N, 170°10.2W). Downward and upward casts from surface to 600 m depth. Arrows show the depth where the water samples were taken with Rosette samplers.

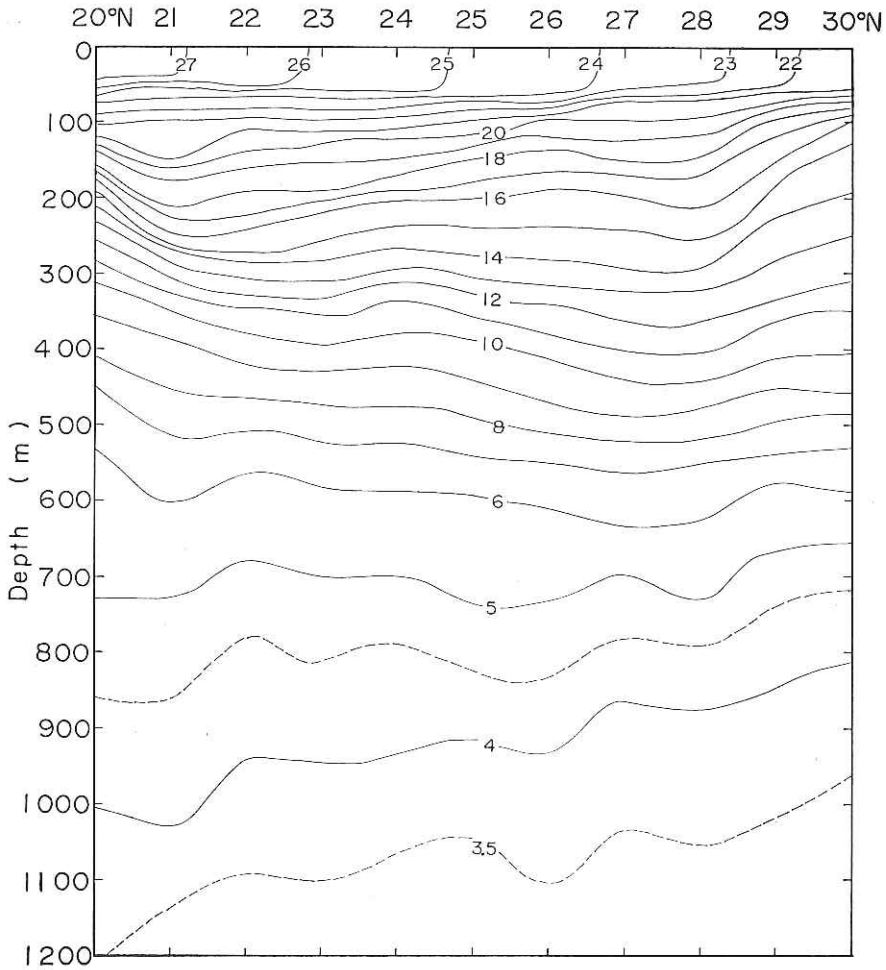

Fig. 19. Temperature profile between 30°N and 20°N along 170°W longitude. (Unit; °C).

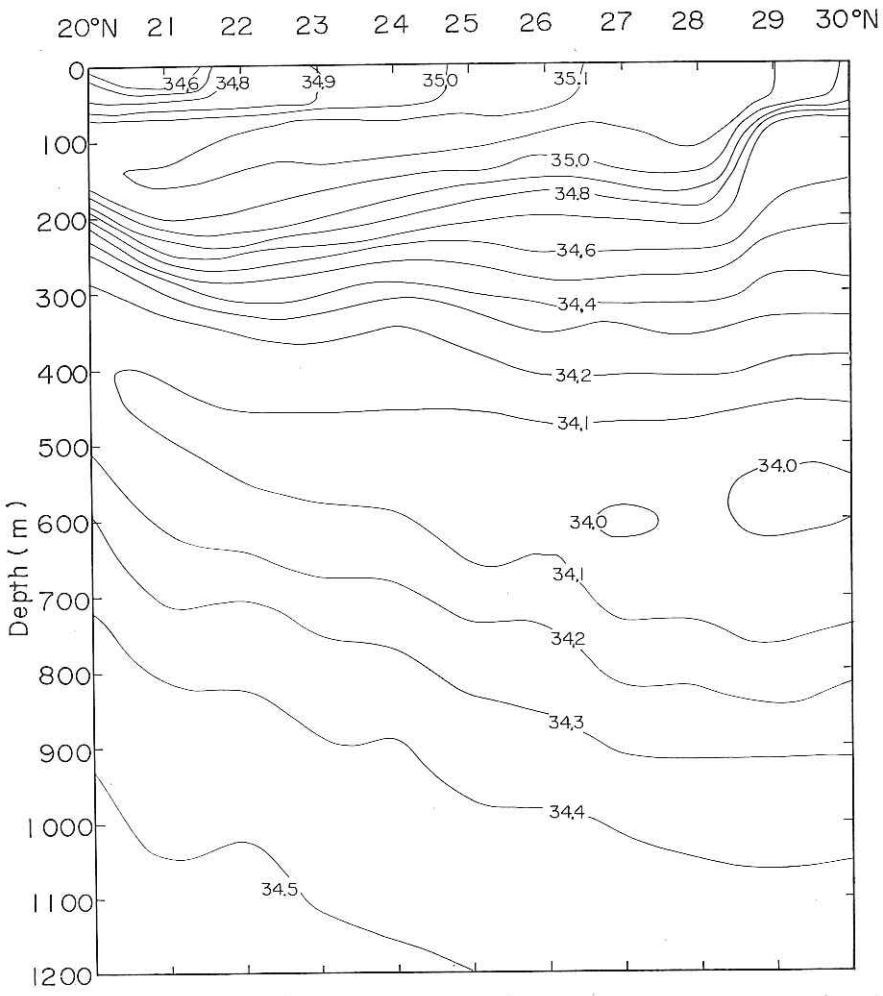

Fig. 20. Salinity profile between 30°N and 20°N along 170°W longitude. (Unit; ‰).

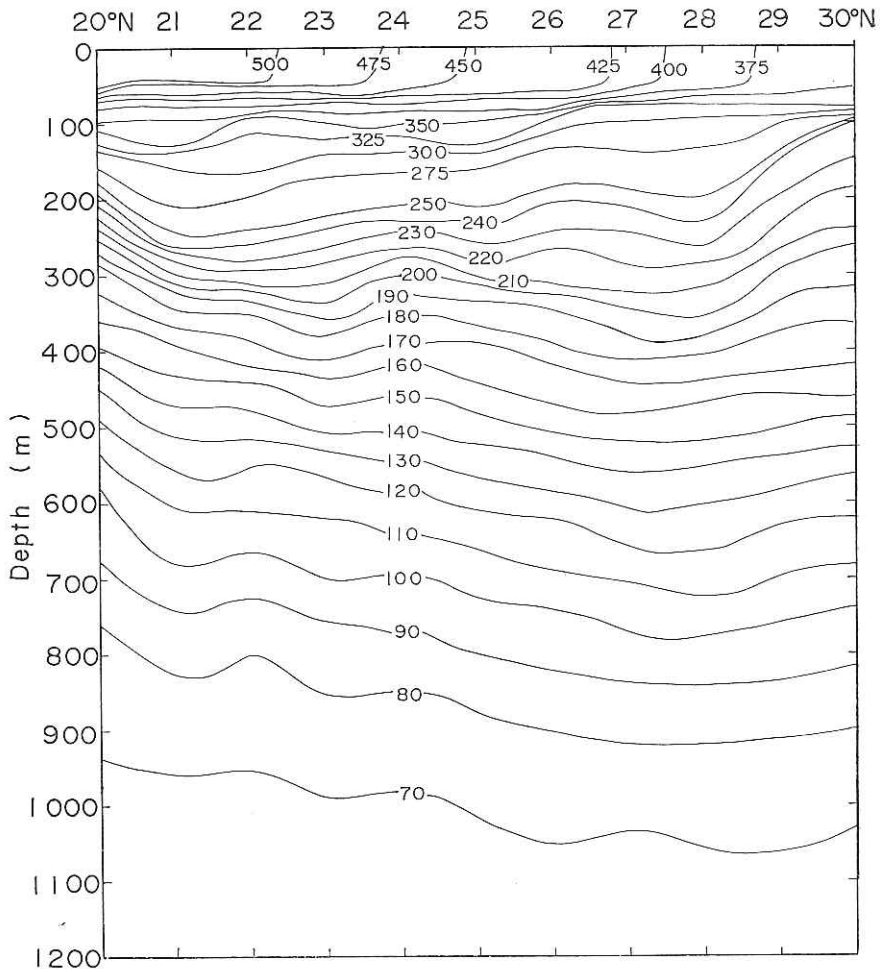

Fig. 21. Thermosteric anomaly profile between 30°N and 20°N along 170°W longitude. (Unit; cl/ton)

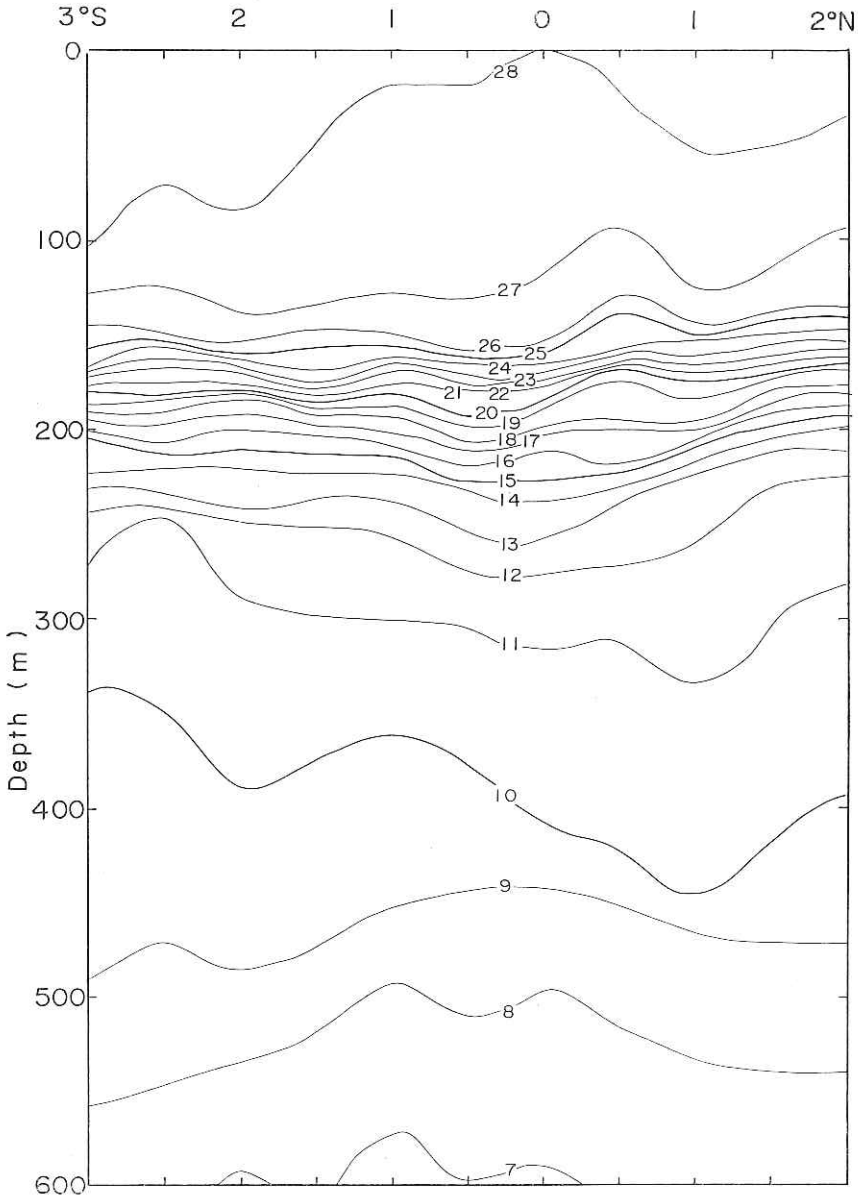

Fig. 22. Temperature profile between 2°N and 3°S along 170°W longitude. (Unit; °C).

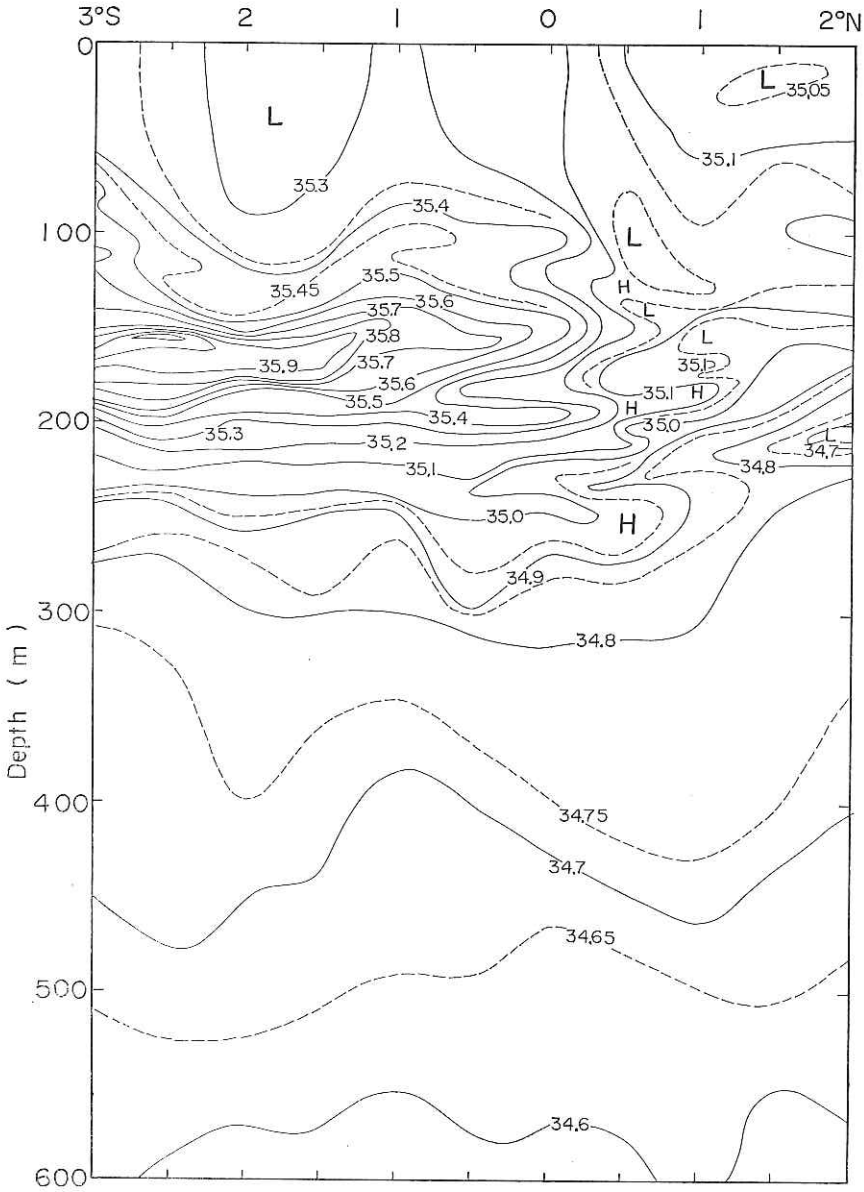

Fig. 23. Salinity profile between 2°N and 3°S along 170°W longitude. (Unit; ‰)

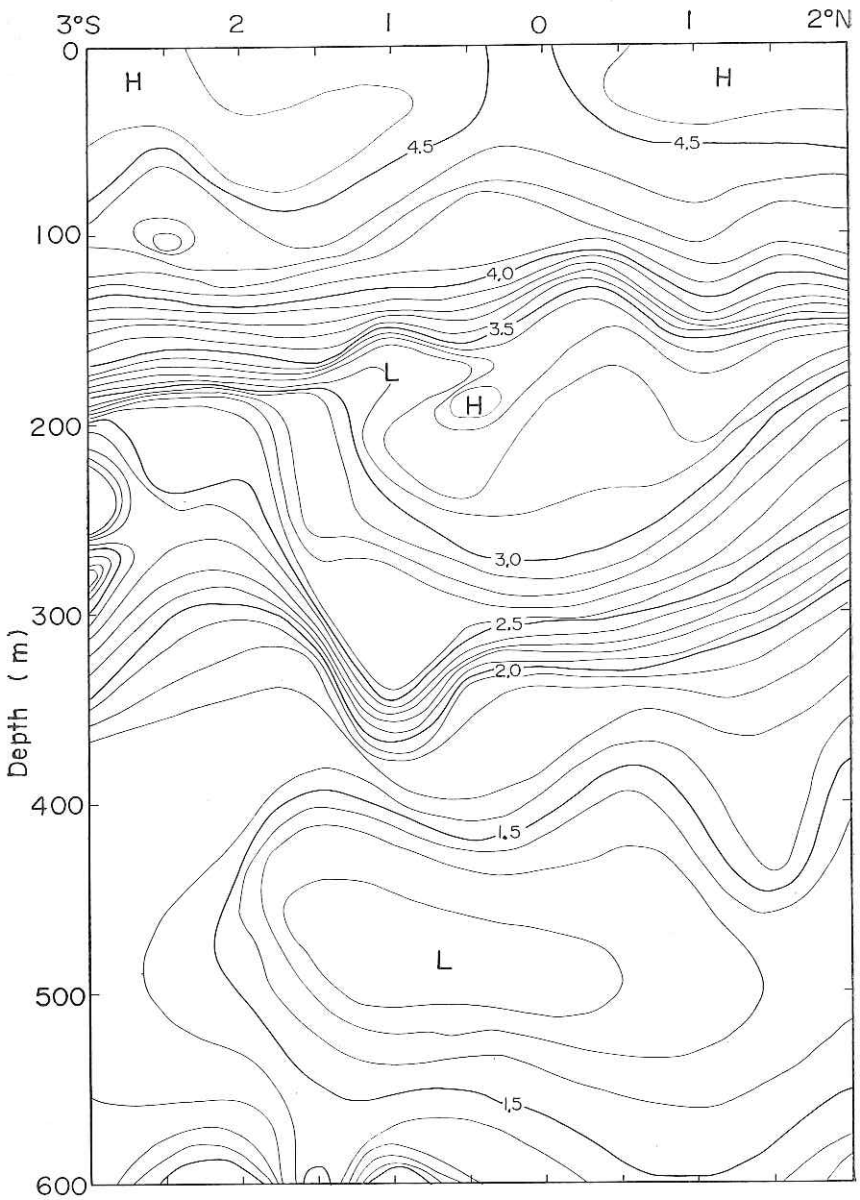

Fig. 24. Dissolved oxygen profile between 2°N and 3°S along 170°W longitude. (Unit; ml/l)

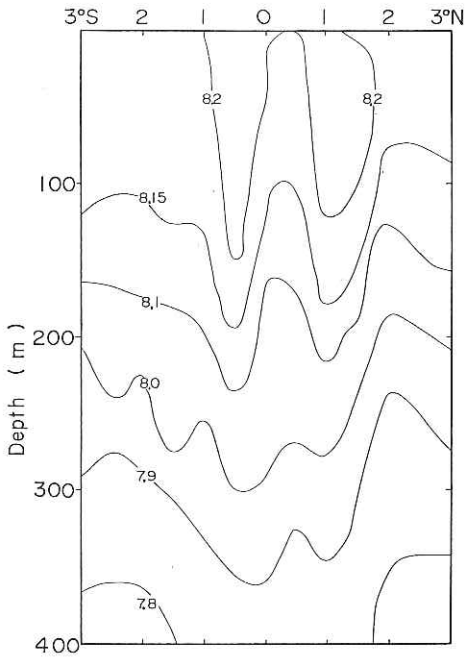

Fig. 25. pH profile between 3°N and 3°S along 170°W longitude.

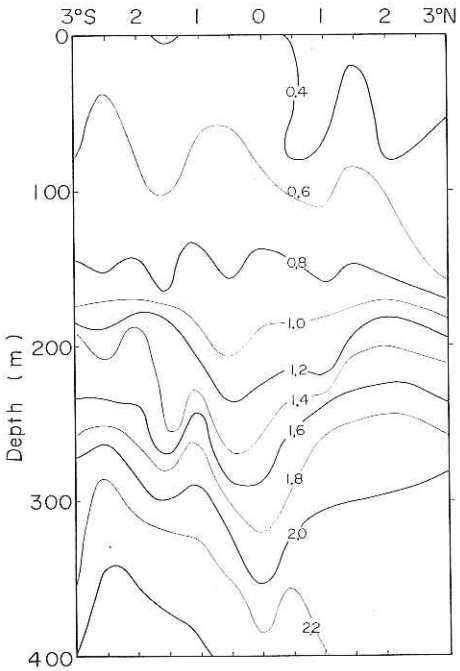

Fig. 26. Reactive phosphate profile between 3°N and 3°S along 170°W longitude.
(Unit; μg at/l)

VII. Piston Coring

by
K. Kobayashi, and K. Kitazawa

Ocean floor sediments were collected at twenty stations using piston corers made of aluminum alloy (with a small amount of Mg; JIS H4143, I.D. = 68 mm, wall thickness = 6 mm, length = 12 m) as are shown in Figure 27. The details of the corer were described in "Preliminary Report of the Hakuhō Maru, Cruise KH-68-3". A corer with larger diameter (I.D. = 136 mm, wall thickness = 6 mm, length = 6 m) was also used to obtain a large amount of pelagic clays for the analysis of radioactive isotopes of cosmic origin.

In both sizes of corers a piston was tightly sealed in pipe using two O-rings so that appreciable negative pressure is generated when the piston is pulled up. Judging from the comparison of the penetration length with length of the main cores taken, this negative pressure seems to balance with the friction between sediment and the inner wall of the pipe. In most cases the penetration length measured by the sediment attached on the outer surface of pipe was nearly equal to the length of main core. Therefore neither compression nor flow-in of sediment in the core barrel was probable. Inner tube (core liner) was not used. Core catcher was not attached to the cutting edge but no trouble occurred unless the sediment were too soft (muddy) or sandy as seen in station 49–3 and 60–2. In station 49–3, 12 m corer was successful, while 6 m corer was failed because the 12 m pipe penetrated to a depth with sufficiently fine-grained and nonporous sediment. Among the other three unsuccessful corings, two were mainly due to a trouble with the winch or winch wire. The trouble with a coring at station 2–4 was supposed to be originated from an inclined hit on the bottom and thereafter the head weight was readjusted to lower the center of mass of the corer.

Sediment was extruded from the Al pipe using a loose piston, after the corer was recovered to the working deck. A pin-mark was put on one side of a core during the extrusion so that twisting of the core was avoided or, if any, clearly recorded. Record of the magnetic north at hit was tested by clamping a small magnet by the top of the piston but proved unsuccessful. Only relative horizontal orientation was obtained by the pin-mark. Each core was cut into a length of less than 2 meters and contained in vinylchloride containers of 2 m length, numbered as #1 to #54 and L1–L3, #6A. Top side (upward or toward the surface of sediment) was taped white and bottom side (downward) was taped red. Each core was then cut longitudinally into half. One half of the core was distributed to chemists for their geochemical studies, as is shown in Table 9, and 20 mm cubic samples for paleomagnetic measurement were taken from the remaining half which was to be brought back to the Ocean Research Institute for microscopic examination in laboratory.

Descriptions of colors and some distinct characteristics completed on board are represented in figures 28–54. Five photographs of interesting parts of cores and included nodules and rocks are also reproduced (plates 1–5). Several cores show white or black streaks which are almost exactly perpendicular to the axis of the core. Some color boundaries are also perpendicular to the axis and least disturbed as seen in plate 2 (core 37–2). These observations seem to indicate that the corer hit the sediment vertically.

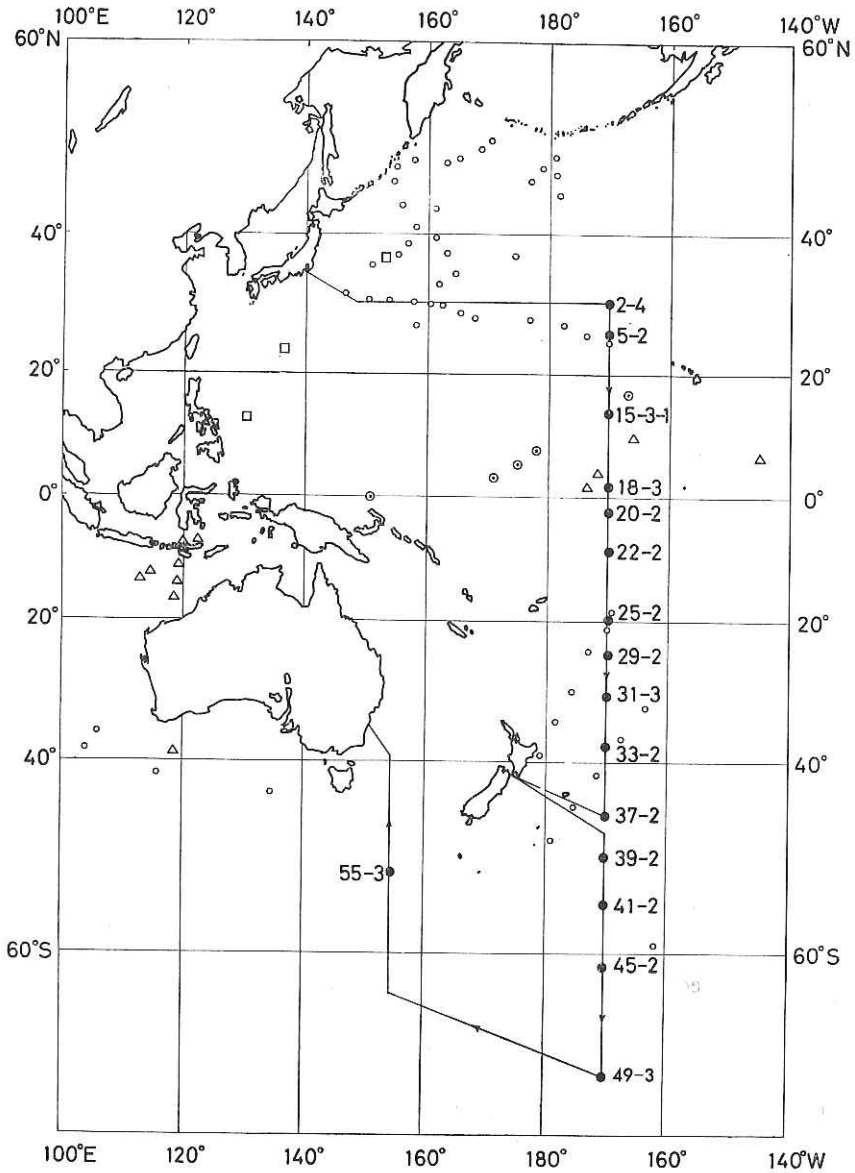

Fig. 27. Sediment cores with paleomagnetic measurement.

⊙: ORI previous data

●: Core station of the present cruise

□: ORI data with Lamont sample

○: Lamont data

△: Scripps data

Table 8. List of core samples

Station No.	Latitude	Longitude	Water depth (m)	Core length (cm)	Remarks
5–2	26°51′N	170°01′W	4565	238	uniform reddish brown clay
15–3–1	12°00′N	169°59′W	5770	989	reddish brown clay, Mn nodule at top, micronodule? near the bottom
18–3	01°59′N	170°01′W	5360	983	reddish brown clay with white & black patches.
20–2	02°28′S	170°00′W	5500	992	reddish brown clay with white & black patches & layers.
22–2	10°57′S	169°59′W	5110	316	large dia. core, reddish brown clay with solid (rock?) layers at 30 cm & 96 cm from top.
25–2	19°59′S	170°02′W	5280	716	uniform reddish brown clay with nodules at 155 cm & 700 cm from the top.
29–2	25°54′S	170°20′W	5485	918	reddish brown clay with brown ash layers at 157–194 cm & 330–352, 376–389 cm, white ash at 599–606 cm from top. small white & black patches also abundant.
31–3	32°09′S	169°56′W	5550	706	brown clay with white ash layers at 102–108 and 690–704 cm from the top.
33–2	38°00′S	169°58′W	5070	5	solid Mn slab.
37–2	46°01′S	169°53′W	5210	395	greenish grey clay with brownish layer at 0–18 cm from top, dark patches & streaks.
39–2	50°07′S	169°59′W	5150	495	dull yellow to gold clay, a hard rock fragment at 480 cm from top.
41–2	54°14′S	169°38′W	5100	322	brownish yellow clay, Mn nodules at the top & 195 cm.
45–2	61°57′S	169°54′W	3345	173	globigerina & diatom ooze, at 130 cm globigerina appears broken or solved but diatoms observed. reddish brown clay at 145–156 cm.
49–4	69°28′S	169°53′W	4200	973	yellowish brown clay with solid rock fragments at 30, 35, 168, & 792 cm from the top.
55–3	53°14′S	155°12′E	4050	390	light brown clay with micronodules abundant at 45–90 cm.

The same core (37–2) has streaks, mottles and color boundaries obliquely oriented to the core axis, but they may possibly be inclined in situ, since co-existence of both horizontal and inclined streaks and boundaries was found in a short vertical succession of this core.

Some streaks and color boundaries (e.g. 32 cm & 38–42 cm in station 37–2) show convex curvature towards the top on their rims. However, the curvature is seen only within 10 mm from both rims (side surfaces). Inner part is still horizontal. This shape is thought to be formed by a superficial deformation of core owing to the friction between the inner surface of the pipe and the sediment when the sediment was extruded. Such deformation

does not seem to have occurred when the corer hit the bottom, because no streaks with concave curvature were found. Frictional condition may be different when the pipe hits very rapidly. Although the paleomagnetic samples were taken from inside of the core to avoid such disturbance, further improvement of the method of extrusion of sediment may be needed.

Circular mottles were found in most of the cores. They are usually circular or elliptical in section. No evidence of vertical elongation was seen. There are many circular rings. Most of them are colored (brownish) white and some are black (see plates 2 and 3). Origin of such circular rings are not clear and will be further examined in laboratory on land.

Two layers of white or brownish white ash were found in core Stn. 31–3 at depths of 102–108 cm and 690–704 cm. This volcanic ash may possibly correspond to that reported by D. Ninkovich (Earth Planet. Sci. Letters, 4, 89–102, 1968). The locality of our core (32°09.2′S, 169°56.3′W) is nearest to his RC9 115 sample in which two colorless layers occur at depth of 139–141 cm and 378–383 cm and magnetic reversals between 310 and 390 cm, 400 and 650 cm, 690 and 910 cm, respectively. Magnetic polarity of the present core will soon be measured and compared with his result.

Several manganese nodules and rock fragments were found in various part of cores. Manganese nodules are spherical or agglomerates of spherical masses (see plate 5). A nodule has granular surface. It is very interesting that the nodules were found buried in deep part of cores. For instance, they were found at 475 cm, 820 cm, 895 cm and 915 cm from the top of Station 15–3–1 core together with their surface occurrence. Further study of such a core will provide a great deal of information on the origin of the nodule. It seems most unlikely that these nodules were hit by the cutting edge of the corer and pushed down to such depths. There are two evidences against this suspicion; 1. there is no damage in nodules but it should have been recorded if they were hit by the edge. 2. many circular mottles are seen undisturbed above and below the levels at which the nodules were found.

Small brownish black spheres (d = 0.1–1 mm) were microscopically observed at various depths of some cores. They resemble the cosmic spherules but are nonmagnetic. They are supposed to be micronodules.

Rock fragments particularly found in core of stations 49–4, 55–3 and some others are likely to be ice-rafted from the Antarctica. Origin of rocks in station 25–2 (155 cm) etc. are not yet fully understood.

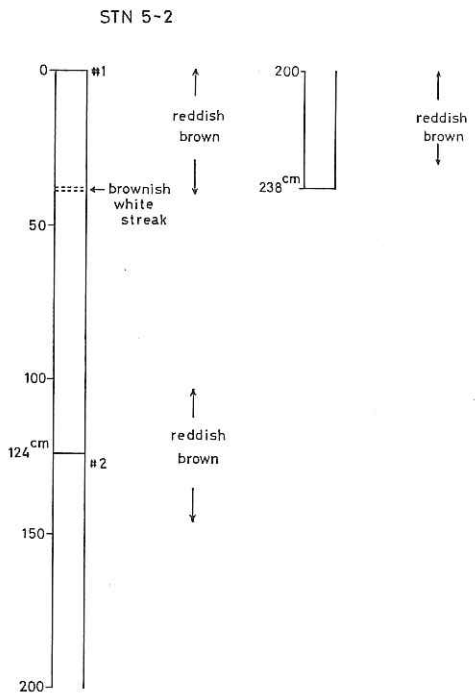

Fig. 28. Core description. Description of colors and distinct characteristics.

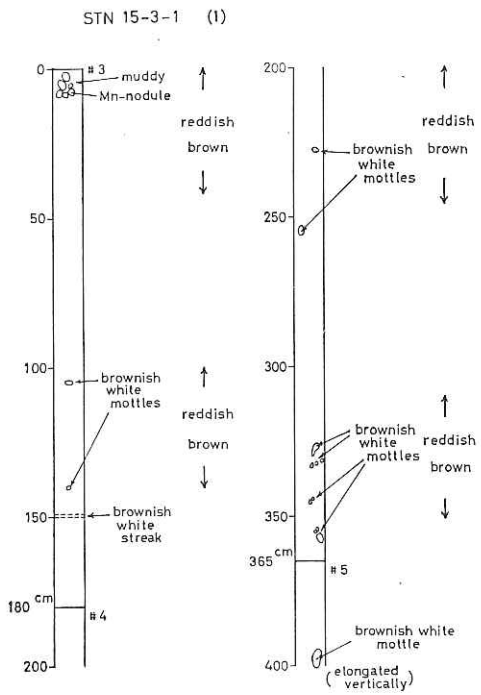

Fig. 29. Core description. Description of colors and distinct characteristics.

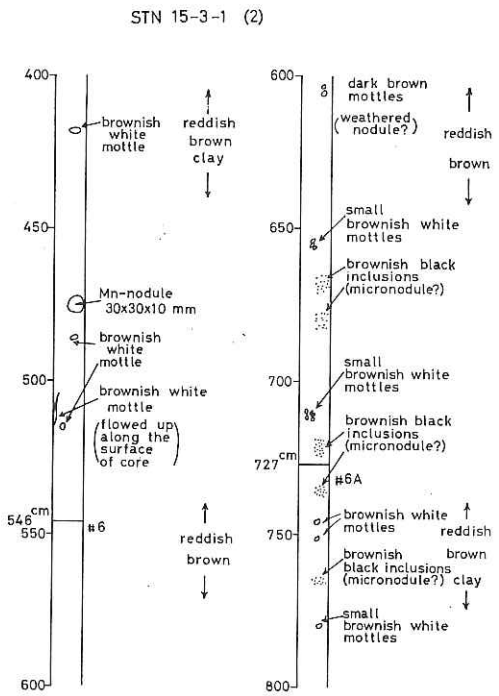

Fig. 30. Core description. Description of colors and distinct characteristics.

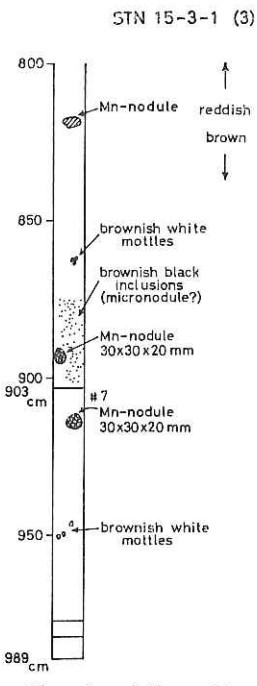

Fig. 31. Core description. Description of colors and distinct characteristics.

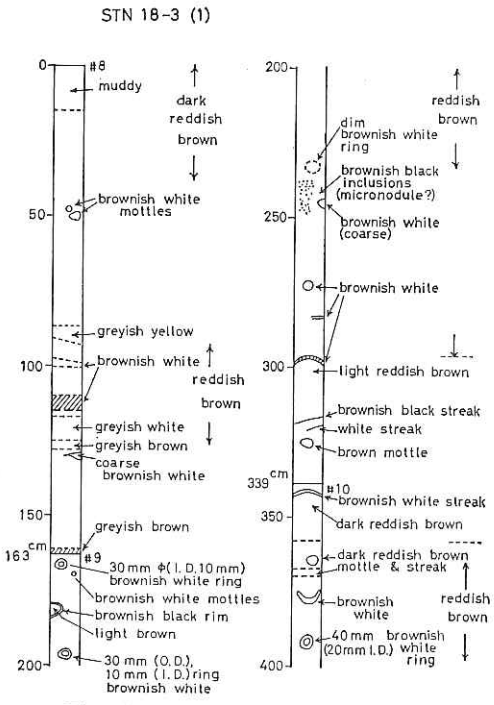

Fig. 32. Core description. Description of colors and distinct characteristics.

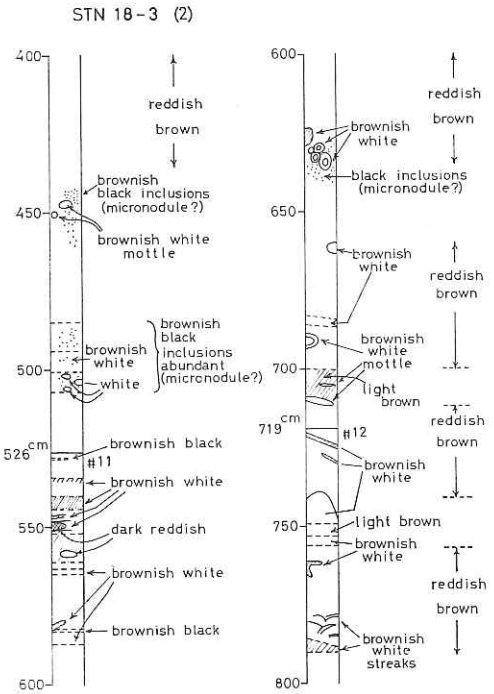

Fig. 33. Core description. Description of colors and distinct characteristics.

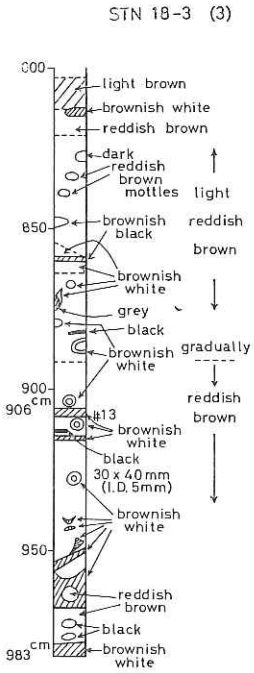

Fig. 34. Core description. Description of colors and distinct characteristics.

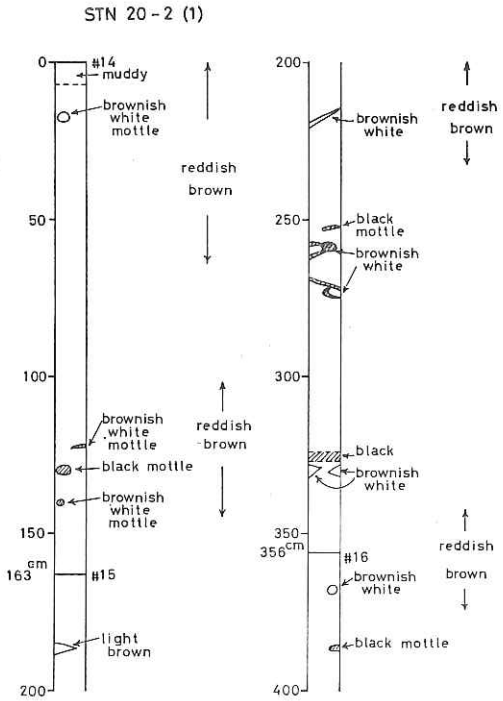

Fig. 35. Core description. Description of colors and distinct characteristics.

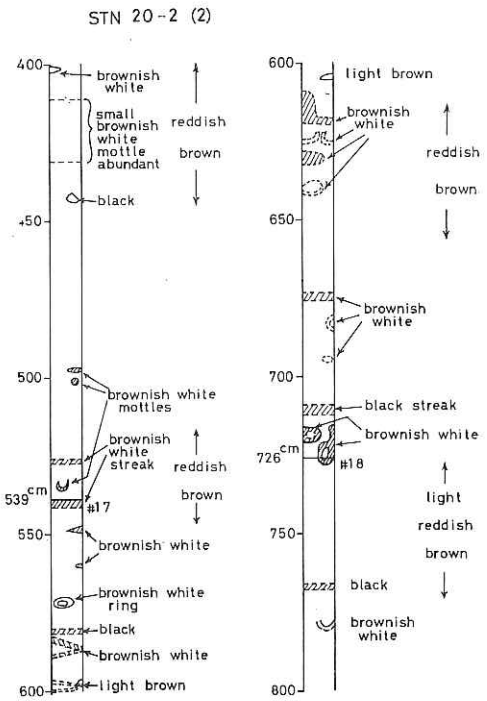

Fig. 36. Core description. Description of colors and distinct characteristics.

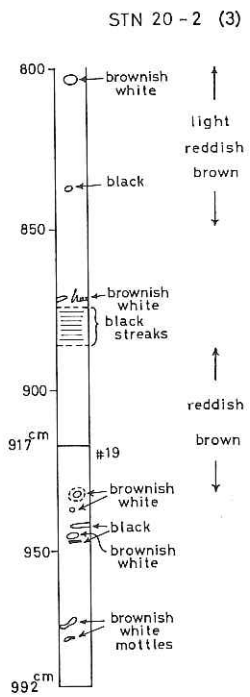

Fig. 37. Core description. Description of colors and distinct characteristics.

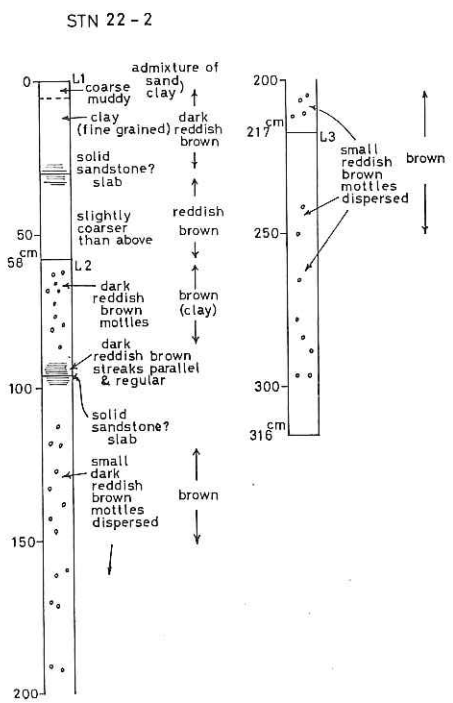

Fig. 38. Core description. Description of colors and distinct characteristics.

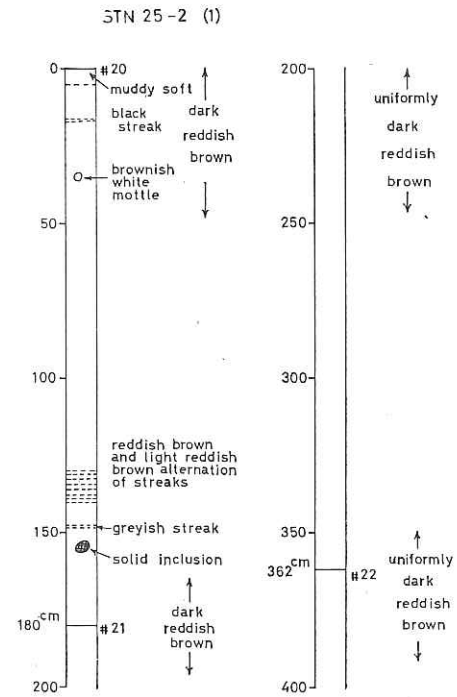

Fig. 39. Core description. Description of colors and distinct characteristics.

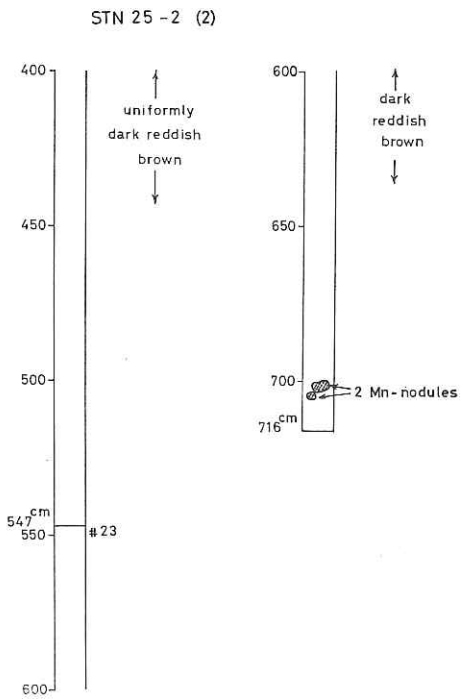

Fig. 40. Core description. Description of colors and distinct characteristics.

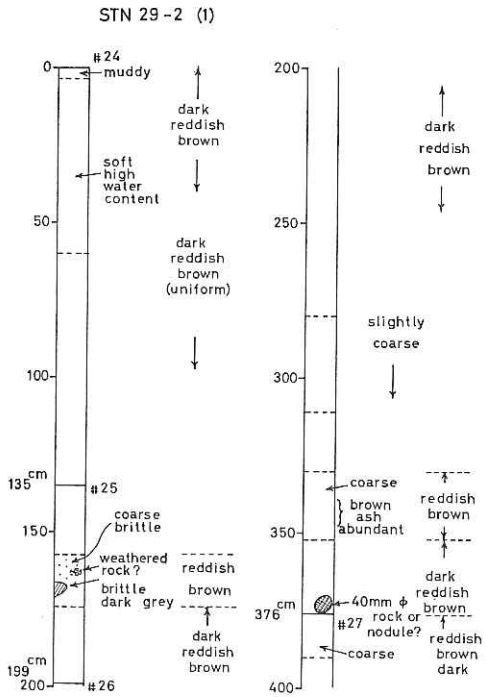

Fig. 41. Core description. Description of colors and distinct characteristics.

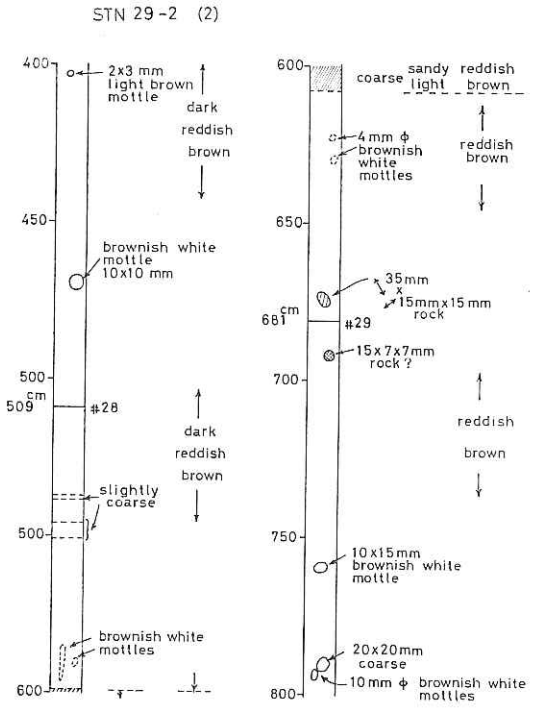

Fig. 42. Core description. Description of colors and distinct characteristics.

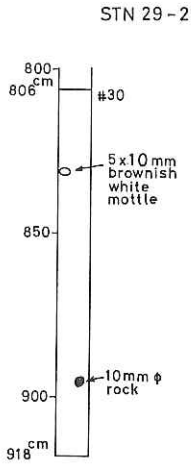

Fig. 43. Core description. Description of colors and distinct characteristics.

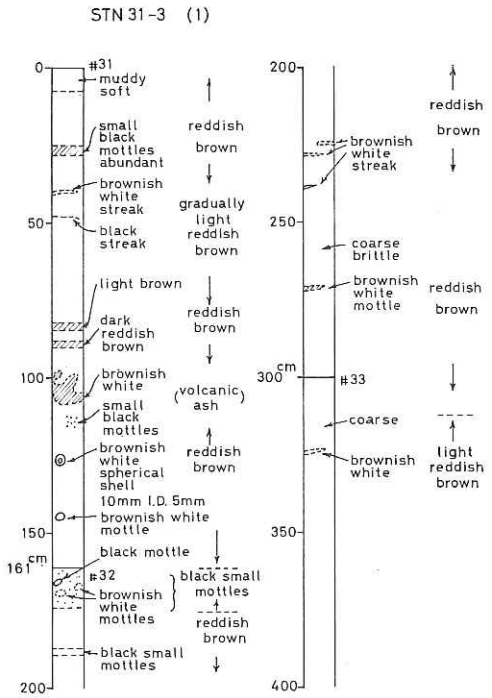

Fig. 44. Core description. Description of colors and distinct characteristics.

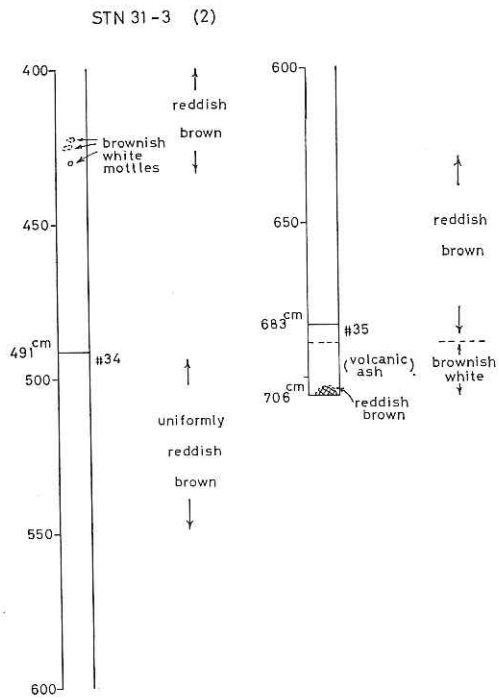

Fig. 45. Core description. Description of colors and distinct characteristics.

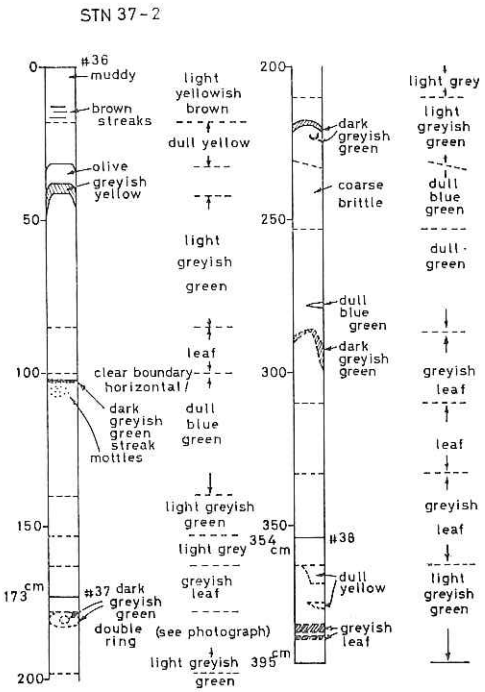

Fig. 46. Core description. Description of colors and distinct characteristics.

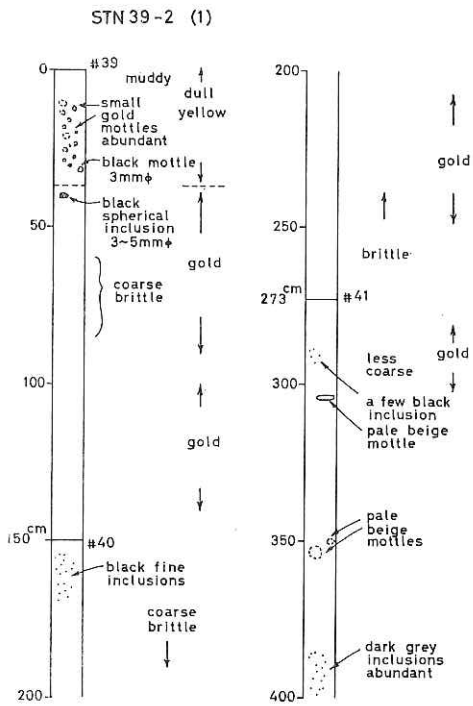

Fig. 47. Core description. Description of colors and distinct characteristics.

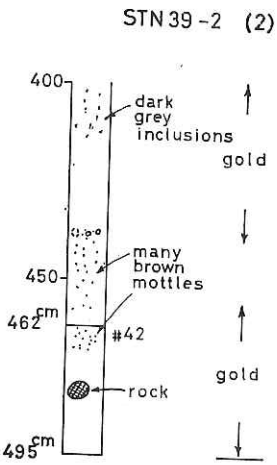

Fig. 48. Core description. Description of colors and distinct characteristics.

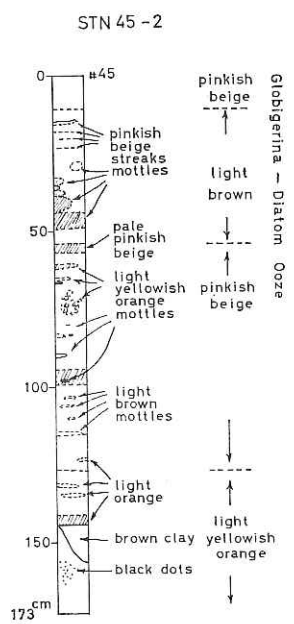

Fig. 49. Core description. Description of colors and distinct characteristics.

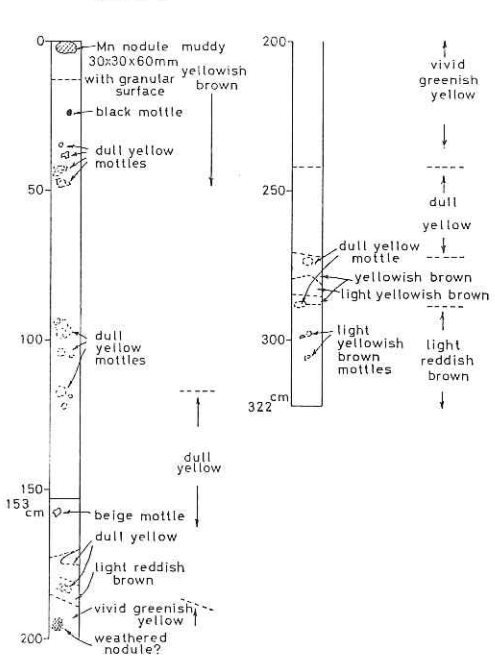

Fig. 50. Core description. Description of colors and distinct characteristics.

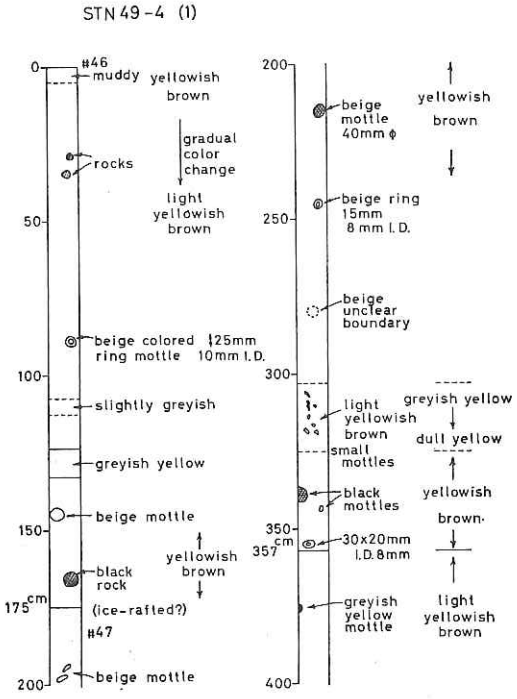

Fig. 51. Core description. Description of colors and distinct characteristics.

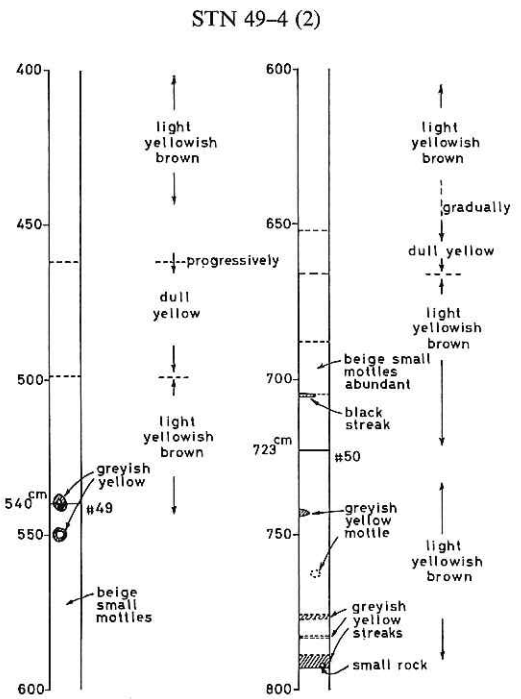

Fig. 52. Core description. Description of colors and distinct characteristics.

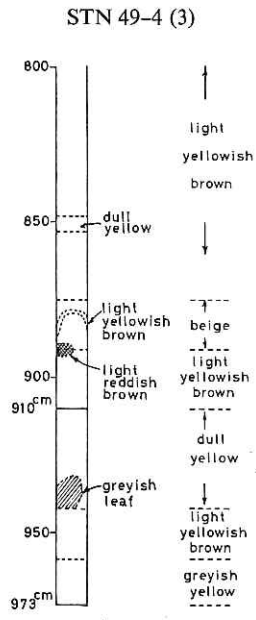

Fig. 53. Core description. Description of colors and distinct characteristics.

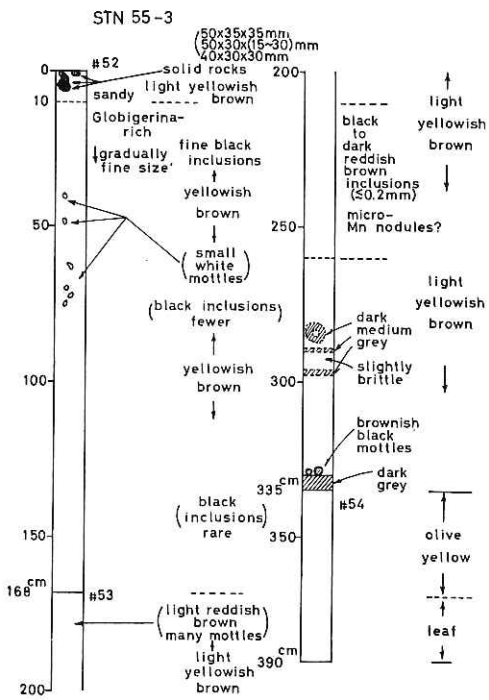

Fig. 54. Core description. Description of colors and distinct characteristics.

Plate 1. Stn. 37–2. Color boundaries in core. Left; toward top (surface of sediment),
1st core from the top of sheet: 72–120 cm, a color boundary between 'leaf' (left) and dull blue green (right) is perpendicular to the axis and not disturbed.
2nd core (middle of photo): 183–231 cm, a straight color boundary from light gray to light grayish green is seen in the middle, convex dark grayish green streak is on the right-hand side, and coarse, brittle part on the right end.
3rd core (bottom): sample in the cutting edge, slightly irregular streaks.

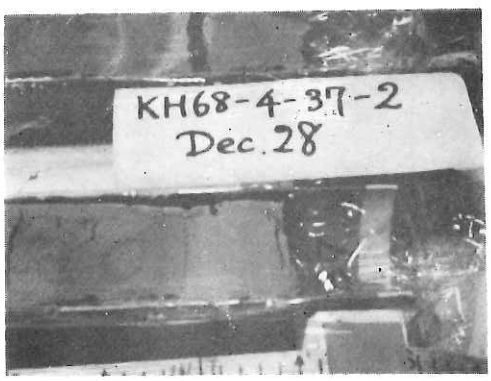

Plate 2. Dark grayish green double ring. Stn. 37–2. Core in the bottom half of photo; 173–188 cm. Left; toward bottom (downward).
Grayish leaf color in the right end and light grayish green with dark grayish green ring on the left are seen.

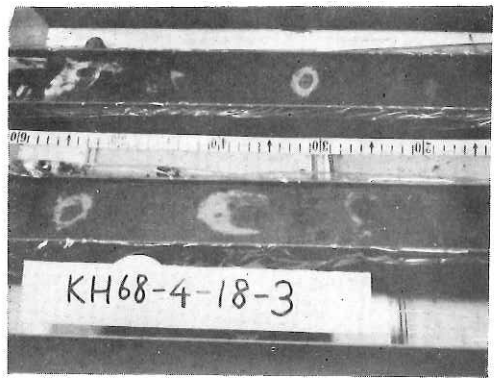

Plate 3. White rings and mottles. Stn. 18–3. Left; toward bottom (downward), right; toward top.
1st core (in the top of photo): 910–958 cm.
2nd core: 350–398 cm, reddish brown sediment with brownish white ring, mottle and dark reddish brown mottle (on the right-hand side).

Plate 4. Brownish white or colorless ash layers, Stn. 31–3. Left; toward bottom, right; toward top (surface of sediment). Middle core: from cutting edge (683–706 cm). Core in the bottom of photo: 75–124 cm, reddish brown sediment with brownish white mottle.

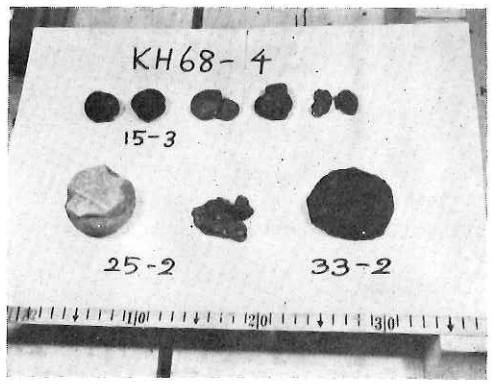

Plate 5. Manganese nodules and rock fragments included in cores 15–3, 25–2 and 33–2.

Core Log

Date Nov. 23, '68 Ship Hakuhō maru Cruise KH-68-4 Station 2-4
Latitude 30°14.2'N Longitude 170°04.7'W
Location north-central Pacific
Weather rain & stormy wind due to a front
Bottom rough, hilly. flank of a hill

Length Main Pipe	12 m	No. of Pipe 1 Material	Al(Mg)Alloy
I.D. of Pipe	68 mm	Wall Thickness	6 mm
Core Head Wt.	780 kg	Trigger Wt.	44 kg+20 kg
Length Main Line	25 m	Length Trigger Line	25 m
Time lowered	10:08	Uncorr. Water Depth	5473 m
Time hit	11:46	Uncorr. Water Depth	5480 m
Wire Angle at Hit	10°	Wire-out at Hit	5750 m
Time surfaced	13:07	Winch #1	
Response at Hit	not clear	Response at Pull-out	not clear
Length Main Core	0 cm	Length Trigger Core	0 cm

State of Cutting Edge & Pipe Pipe bent at 7 m from the top.
Remarks. Core head wt. may be top-heavy so that the inclined hit is probable.

Date Nov. 24, '68 Ship Hakuhō maru Cruise KH-68-4 Station 5-2
Latitude 26°50.5'N Longitude 170°00.7'W
Location northern flank of the north Hawaiian Rise
Weather cloudy Sea small swell
Bottom relatively smooth

Length Main pipe	6 m	No. of Pipe 1 Material	Al(Mg)Alloy
I.D. of Pipe	68 mm	Wall Thickness	6 mm
Core Head Wt.	570 kg	Trigger Wt.	44 kg
Length Main Line	15 m	Length Trigger Line	15 m
Length Free Fall	m		
Time lowered	15:50	Uncorr. Water Depth	4560 m
Time hit	17:03	Uncorr. Water Depth	4564 m
Wire Angle at Hit	2°	Wire-out at Hit	4633 m
Time surfaced	18:03		
Response at Hit	not clear	Response at Pull-out	gentle change 500 kg
Length Main Core	238 cm	Length Trigger Core	25 cm
Length Penetration	600 cm		

State of Cutting Edge & Pipe good, no damage
Method of Core Extrusion extruding by hands using piston & bars
Method of Core Storage lapped by vinyl sheet & contained in 2 m pipes after cutting into halves
No. of Storage Pipes 2
Length of Cores in Pipes #1; 124 cm, #2; 114 cm
No. of Cubic Samples for Paleomagnetism 93 (#1581-1674)

Date Nov. 26, '68 Ship Hakuhō maru Cruise KH-68-4 Station 11-2
Latitude 21°06.3'N Longitude 170°00.8'W
Location north flank of the Necker Ridge
Weather clear Sea calm
Bottom 7 miles from a seamount, flat

Length Main Pipe	12 m	No. of Pipe 1 Material	Al (Mg) Alloy
I.D. of Pipe	68 mm	Wall Thickness	6 mm
Core Head Wt.	780 kg	Trigger Wt.	44 kg
Length Main Line	25 m	Length Trigger Line	25 m
Time lowered	13:18	Uncorr. Water Depth	4835 m
Time hit	14:45	Uncorr. Water Depth	4832 m
Wire Angle at Hit	3°	Wire-out at Hit	4894 m
Time surfaced	16:03	Winch #1	
Response at Hit	not clear	Response at Pull-out	not clear
Length Main Core	0 cm	Length Trigger Core	45 cm

State of Cutting Edge & Pipe Pipe bent at 7 m from the top (head).
Remarks. The trigger may have gone on the way down because of trouble in the winch wire damper. Repaired later soon.

Date Nov. 30, '68 Ship Hakuhō maru Cruise KH-68-4 Station 15-3-1
Latitude 12°00.0'N Longitude 169°58.5'W
Location west-central Pacific
Weather clear, moderate breeze Sea generally good, small swell
Bottom basin between two ridges, hilly, hit on a gentle slope

Length Man Pipe	12 m	No. of Pipe 1 Material	Al (Mg) Alloy
I.D. of Pipe	68 mm	Wall Thickness	6 mm
Core Head Wt.	780 kg	Trigger Wt.	60 kg
Length Main Line	25 m	Length Trigger Line	25 m
Time lowered	09:43	Uncorr. Water Depth	5775 m
Time hit	11:33	Uncorr. Water Depth	5770 m
Wire Angle at Hit	5°	Wire-out at Hit	5800 m
Time surfaced	12:52	Winch #1	
Response at Hit	clear	Response at Pull-out	quick 1 ton
Length Main Core	989 cm	Length Trigger Core	53 cm
Length Penetration	~900 cm		

State of Cutting Edge & Pipe no particular damage
Method of Core Extrusion extruding by hands using piston & bars
Method of Core Storage the same as St 5-2
No. of Storage Pipes 6 Length of Cores in Pipes #3; 180 cm
#4; 185 cm, #5; 181 cm, #6; 181 cm, #6A; 176 cm, #7; 74 cm
No. of Cubic Samples for Paleomagnetism 473 (#1743-2216)

Date Dec. 4, '68 Ship Hakuhō maru Cruise KH-68-4 Station 18-3
Latitude 01°59.5′N Longitude 170°00.5′W
Location equatorial Pacific
Weather clear Sea very smooth, no swell
Bottom almost flat, slightly hilly

Length Main Pipe	12 m	No. of Pipe 1 Material	Al (Mg) Alloy
I.D. of Pipe	68 mm	Wall Thickness	6 mm
Core Head Wt.	780 kg	Trigger Wt.	60 kg
Length Main Line	25 m	Length Trigger Line	25 m
Time lowered	10:22	Uncorr. Water Depth	5360 m
Time hit	11:45	Uncorr. Water Depth	5360 m
Wire Angle at Hit	3°	Wire-out at Hit	5413 m
Time surfaced	13:05	Winch #1	
Response at Hit	clear, 1 ton	Response at Pull-out	soft 0.7 ton
Length Main Core	983 cm	Length Trigger Core	44 cm
Length Penetration	?		

State of Cutting Edge & Pipe good
No. of Storage Pipes 6 Length of Cores in Pipes #8; 163 cm, #9; 176 cm, #10; 187 cm, #11; 193 cm, #12; 187 cm, #13; 77 cm.
No. of Cubic Samples for Paleomagnetism 376 (#2229–2605)

Data Nov. 30, '68 Ship Hakuhō maru Cruise KH-68-4 Station 15-3-2
Latitude 11°59.1′N Longitude 169°57.7′W
Location the same as 15-3-1
Weather clear Sea calm
Bottom about 1 mile away from a hill

Length Main Pipe	6 m	No. of Pipe 1 Material	Al (Mg) Alloy
I.D. of Pipe	136 mm	Wall Thickness	6 mm
Core Head Wt.	570 kg	Trigger Wt.	44 kg
Length Main Line	15 m	Length Trigger Line	15 m
Time lowered	13:50	Uncorr. Water Depth	5770 m

Remarks. The winch wire went off when the winch restarted at its wire-out of 5545 m. 1 day work for repair.

Date Dec. 6, '68 Ship Hakuhō maru Cruise KH-68-4 Station 20-2
Latitude 02°28.4′S Longitude 169°59.7′W
Location south of the equator near the Phoenix Islands
Weather clear, 7 m/s wind Sea smooth, no swell
Bottom very rugged, hit on the bottom of a low.

Length Main Pipe	12 m	No. of Pipe 1 Material Al (Mg) Alloy	
I.D. of Pipe	68 mm	Wall Thickness	6 mm
Core Head Wt.	780 kg	Trigger Wt.	60 kg
Length Main Line	25 m	Length Trigger Line	25 m
Time lowered	09:33	Uncorr. Water Depth	5380 m
Time hit	11:06	Uncorr. Water Depth	5500 m
Wire Angle at Hit	2°	Wire-out at Hit	5542 m
Time surfaced	12:20	Winch #1	
Response at Hit	clear	Response at Pull-out	not clear
Length Main Core	992 cm	Length Trigger Core	74 cm
Length Penetration	~1300 cm		

State of Cutting Edge & Pipe good, plenty of mud attached with wt.
No. of Storage Pipes 6 Length of Cores in Pipes #14; 163 cm
#15; 193 cm, #16; 183 cm, #17; 187 cm, #18; 191 cm, #19; 75 cm
No. of Cubic Samples for Paleomagnetism 395 (#2634–3029)

Date Dec. 9, '68 Ship Hakuhō maru Cruise KH-68-4 Station 22-2
Latitude 10°56.8′S Longitude 169°59.3′W
Location south-central Pacific
Weather clear, 3 m/s wind Sea slight swell
Bottom near flank of a seamount, almost flat

Length Main Pipe	6 m	No. of Pipe 1 Material Al (Mg) Alloy	
I.D. of Pipe	136 mm	Wall thickness	6 mm
Core Head Wt.	570 kg	Trigger Wt.	44 kg
Length Main Line	15 m	Length Trigger Line	15 m
Time lowered	09:20	Uncorr. Water Depth	5110 m
Time hit	11:19	Uncorr. Water Depth	5110 m
Wire Angle at Hit	1.5°	Wire-out at Hit	5174 m
Time surfaced	12:30	Winch #1	
Response at Hit	clear	Response at Pull-out	very strong at 5138 m wire-out
Length Main Core	316 cm	Length Trigger Core	45 cm

State of Cutting Edge & Pipe Cutting edge lost
No. of Storage Pipes 3 Length of Cores in Pipes L1; 58 cm, L2; 159 cm, L3; 99 cm
No. of Cubic Samples for Paleomagnetism 101 (#4393–4415, #520–599)
Remarks. 3/4 sent to Inst. for Nuclear Physics for analysis of cosmic-ray bombarded isotopes, 1/4 preserved in ORI

Date Dec. 16, '68 Ship Hakuhō maru Cruise KH-68–4 Station 25–2
Latitude 19°59.1′S Longitude 170°01.6′W
Location south of the Niue Island
Weather clear, no appreciable breeze Sea smooth, no swell
Bottom rugged, hit on the top of a 100 m hill

Length Main Pipe	12 m	No. of Pipe 1	Material Al (Mg) Alloy
I.D. of Pipe	68 mm	Wall Thickness	6 mm
Core Head Wt.	780 kg	Trigger Wt.	60 kg
Length Main Line	25 m	Length Trigger Line	25 m
Time lowered	09:41	Uncorr. Water Depth	5315 m
Time hit	11:24	Uncorr. Water Depth	5280 m
Wire Angle at Hit	0°	Wire-out at Hit	5338 m
Time surfaced	12:42	Winch #1	
Response at Hit	clear	Response at Pull-out	large (1 ton)
Length Main Core	716 cm	Length Trigger Core	42 cm

State of Cutting Edge & Pipe Cutting edge crushed in, no damage with pipe
No. of Storage Pipes 4
Length of Cores in Pipes #20; 180 cm, #21; 182 cm, #22; 185 cm, #23; 169 cm
No. of Cubic Samples for Paleomagnetism 275 (#3039–3313)

Date Dec. 20, '68 Ship Hakuhō maru Cruise KH-68–4 Station 29–2
Latitude 25°54.4′S Longitude 170°19.5′W
Location flank of 2 seamounts
Weather slightly cloudy, 2 m/s breeze Sea smooth, very slight swell
Bottom very flat

Length Main Pipe	12 m	No. of Pipe 1	Material Al (Mg) Alloy
I.D. of Pipe	68 mm	Wall Thickness	6 mm
Core Head Wt.	780 kg	Trigger Wt.	60 kg
Length Main Line	25 m	Length Trigger Line	25 m
Time lowered	13:42	Uncorr. Water Depth	5485 m
Time hit	15:14	Uncorr. Water Depth	5485 m
Wire Angle at Hit	3°	Wire-out at Hit	5545 m
Time surfaced	16:28	Winch #1	
Response at Hit	rather clear	Response at Pull-out	very clear, 1 ton
Length Main Core	918 cm	Length Trigger Core	60 cm

State of Cutting Edge & Pipe Pipe bent at 5 m from the bottom
No. of Storage Pipes 7 Length of Cores in Pipes #24; 135 cm, #25; 64 cm, #26; 177 cm, #27; 133 cm, #28; 172 cm, #29; 125 cm, #30; 112 cm
No. of Cubic Samples for Paleomagnetism 328 (#3314–3641)

Date Dec. 23, '68 Ship Hakuhō maru Cruise KH-68-4 Station 31-3
Latitude 32°09.2′S Longitude 169°56.3′W
Location east of the Kermadec trough
Weather cloudy, 5 m/s breeze Sea smooth, no swell
Bottom hilly but moderately smooth area chosen

Length Main Pipe	12 m	No. of Pipe 1	Material Al (Mg) Alloy
I.D. of Pipe	68 mm	Wall Thickness	6 mm
Core Head Wt.	780 kg	Trigger Wt.	60 kg
Length Main Line	25 m	Length Trigger Line	25 m
Time lowered	07:50	Uncorr. Water Depth	5575 m
Time hit	09:22	Uncorr. Water Depth	5550 m
Wire Angle at Hit	1°	Wire-out at Hit	5608 m
Time surfaced	10:40	Winch #1	
Response at Hit	rather clear	Response at Pull-out	very strong, 5582 m
Length Main Core	706 cm	Length Trigger Core	50 cm

State of Cutting Edge & Pipe Cutting edge crushed out, pipe bent at 5 m from the bottom
No. of Storage Pipes 5
Length of Cores in Pipes #31; 161 cm #32; 139 cm, #33; 191 cm, #34; 192 cm, #35; 23 cm
No. of Cubic Samples for Paleomagnetism 308 (#3603–3910)
Remarks. White volcanic ash (at least two layers) found at 102–108 cm & 690–704 cm from the top.

Date Dec. 25, '68 Ship Hakuhō maru Cruise KH-68-4 Station 33-2
Latitude 38°00.3′S Longitude 169°57.8′W
Location east off North Island, N. Z.
Weather cloudy, 3 m/s breeze Sea very calm, no swell
Bottom flat, flank of a seamount

Length Main Pipe	11 m	No. of Pipe 1	Material Al (Mg) Alloy
I.D. of Pipe	68 mm	Wall Thickness	6 mm
Core Head Wt.	780 kg	Trigger Wt.	60 kg
Length Main Line	25 m	Length Trigger Line	24 m
Time lowered	08:42	Uncorr. Water Depth	5070 m
Time hit	09:55	Uncorr. Water Depth	5070 m
Wire Angle at Hit	3°	Wire-out at Hit	5112 m
Time surfaced	11:25	Winch #1	
Response at Hit	clear	Response at Pull-out	very strong (1 ton)
Length Main Core	5 cm	Length Trigger Core	38 cm

State of Cutting Edge & Pipe Pipe bent at 1 m from the bottom
Remarks. A solid manganese slab obtained.

Date Dec. 28. '68 Ship Hakuhō maru Cruise KH-68–4 Station 37–2
Latitude 46°00.6′S Longitude 169°53.0′W
Location southeast off Chatham Island, southern flank of the Chatham Rise
Weather clear, 5 m/s wind Sea moderate swell
Bottom slightly rugged, flat in minor scale

Length Main Pipe	6 m	No. of Pipe 1	Material Al (Mg) Alloy
I.D. of Pipe	68 mm	Wall Thickness	6 mm
Core Head Wt.	570 kg	Trigger Wt.	60 kg
Length Main Line	15 m	Length Trigger Line	15 m
Time lowered	12:40	Uncorr. Water Depth	5200 m
Time hit	14:09	Uncorr. Water Depth	5210 m
Wire Angle at Hit	0°	Wire-out at Hit	5259 m
Time surfaced	15:30	Winch #1	
Response at Hit	clear	Response at Pull-out	undetectable
Length Main Core	395 cm	Length Trigger Core	41 cm

State of Cutting Edge & Pipe good
No. of Storage Pipes 3 Length of Storaged Cores #36; 173 cm, #37; 181 cm, #38; 41 cm
No. of Cubic Samples for Paleomagnetism 151 (#3911–4061)

Date Jan. 11, '69 Ship Hakuhō maru Cruise KH-68–4 Station 39–2
Latitude 50°07.2′S Longitude 169°58.9′W
Location southeast off the Chatham Rise
Weather cloudy, 5 m/s wind Sea small to large swell
Bottom rugged, hit near the top of a 100 m hill

Length Main Pipe	6 m	No. of Pipe 1	Material Al (Mg) Alloy
I.D. of Pipe	68 mm	Wall Thickness	6 mm
Core Head Wt.	570 kg	Trigger Wt.	60 kg
Length Main Line	15 m	Length Trigger Line	15 m
Time lowered	09:44	Uncorr. Water Depth	5200 m
Time hit	11:11	Uncorr. Water Depth	5150 m
Wire Angle at Hit	6.5°	Wire-out at Hit	5186 m
Time surfaced	12:35	Winch #1	
Response at Hit	clear	Response at Pull-out	not detected
Length Main Core	495 cm	Length Trigger Core	53 cm

State of Cutting Edge & Pipe pipe OK, cutting edge slightly bent
No. of Storage Pipes 4
Length of Storaged Cores #39; 150 cm, #40; 123 cm, #41; 189 cm, #42; 33 cm
No. of Cubic Samples for Paleomagnetism 188 (#4063–4250)

Date Jan. 13, '69 Ship Hakuhō maru Cruise KH-68-4 Station 41-2
Latitude 54°13.9′S Longitude 169°38.0′W
Location south Pacific near Antarctic Ocean
Weather 10–15 m/s wind Sea rough swell
Bottom rugged, northern flank of a 500 m hill

Length Main Pipe	6 m	No. of Pipe 1	Material Al (Mg) Alloy
I.D. of Pipe	68 mm	Wall Thickness	6 mm
Core Head Wt.	570 kg	Trigger Wt.	60 kg
Length Main Line	15 m	Length Trigger Line	15 m
Time lowered	09:24	Uncorr. Water Depth	5000 m
Time hit	11:02	Uncorr. Water Depth	5100 m
Wire Angle at Hit	5°	Wire-out at Hit	5258 m
Time surfaced	12:17	Winch #1	
Response at Hit	clear	Response at Pull-out	clear
Length Main Core	322 cm	Length Trigger Core	67 cm

State of Cutting Edge & Pipe good, no damage
No. of Storage Pipes 2
Length of Storaged Cores #43; 153 cm, #44; 169 cm
No. of Cubic Samples for Paleomagnetism 128 (#4254–4381)

Date Jan. 16, '69 Ship Hakuhō maru Cruise KH-68-4 Station 45-2
Latitude 61°57.0′S Longitude 169°54.2′W
Location northern slope of Antarctic-Pacific Rise
Weather cloudy to clear 12 m/s wind Sea moderate swell
Bottom very rugged

Length Main Pipe	6 m	No. of Pipe 1	Material Al (Mg) Alloy
I.D. of Pipe	68 mm	Wall Thickness	6 mm
Core Head Wt.	570 kg	Trigger Wt.	60 kg
Length Main Line	15 m	Length Trigger Line	15 m
Time lowered	15:02	Uncorr. Water Depth	3300 m
Time hit	16:13	Uncorr. Water Depth	3345 m
Wire Angle at Hit	2°	Wire-out at Hit	3349 m
Time surfaced	17:03	Winch #1	
Response at Hit	clear	Response at Pull-out	clear
Length Main Core	173 cm	Length Trigger Core	23 cm

State of Cutting Edge & Pipe good, no damage
No. of Storage Pipes 1 Length of Storaged Cores #45; 173 cm
No. of Cubic Samples for Paleomagnetism 74 (#4416–4489)
Remarks. Globigerina diatom ooze with some layers & admixture of reddish brown clay.

Date Jan. 19, '69 Ship Hakuhō maru Cruise KH-68–4 Station 49–3
Latitude 69°29.7′S Longitude 169°58.0′W
Location near the ice pack off Antarctic continent
Weather clear Sea very smooth
Bottom flat, south flank of the Antarctic Pacific Rise

Length Main Pipe	6 m	No. of Pipe 1	Material Al (Mg) Alloy
I.D. of Pipe	68 mm	Wall Thickness	6 mm
Core Head Wt.	570 kg	Trigger Wt.	60 kg
Length Main Line	15 m	Length Trigger Line	15 m
Time lowered	08:26	Uncorr. Water Depth	4230 m
Time hit	09:34	Uncorr. Water Depth	4205 m
Wire Angle at Hit	1°	Wire-out at Hit	4204 m
Time surfaced	10:36	Winch #1	
Response at Hit	clear	Response at Pull-out	not clear
Length Main Core	0 cm	Length Trigger Core	70 cm
Length Penetration	~600 cm		

State of Cutting Edge & Pipe good
Remarks. The main core may have been washed away because it is too soft and loose.

Date Jan. 19, '69 Ship Hakuhō maru Cruise KH-68–4 Station 49–4
Latitude 69°28.4′S Longitude 169°53.0′W
Location near ice pack off Antarctic continent
Weather clear Sea very smooth
Bottom flat, south flank of the Antarctic Pacific Rise

Length Main Pipe	12 m	No. of Pipe 1	Material Al (Mg) Alloy
I.D. of Pipe	68 mm	Wall Thickness	6 mm
Core Head Wt.	780 kg	Trigger Wt.	60 kg
Length Main Line	25 m	Length Trigger Line	25 m
Time lowered	16:00	Uncorr. Water Depth	4210 m
Time hit	17:11	Uncorr. Water Depth	4200 m
Wire Angle at Hit	0°	Wire-out at Hit	4170 m
Time surfaced	18:22	Winch #1	
Response at Hit	clear	Response at Pull-out	not clear
Length Main Core	973 cm	Length Trigger Core	47 cm

State of Cutting Edge & Pipe good
No. of Storage Pipes 6
Length of Storaged Cores #46; 175 cm, #47; 182 cm, #48; 183 cm, #49; 183 cm, #50; 187 cm, #51; 63 cm.
No. of Cubic Samples for Paleomagnetism 376 (#4500–4875)

Date Jan. 27, '69 Ship Hakuhō maru Cruise KH-68–4 Station 55–3
Latitude 54°13.5′S Longitude 155°12.1′E
Location south of the Tasman Sea
Weather 15 m/s N wind, clear Sea rough wave, low swell
Bottom nearly flat

Length Main Pipe	6 m	No. of Pipe 1	Material Al (Mg) Alloy
I.D. of Pipe	68 mm	Wall Thickness	6 mm
Core Head Wt.	570 kg	Trigger Wt.	60 kg
Length Main Line	15 m	Length Trigger Line	15 m
Time lowered	09:25	Uncorr. Water Depth	4060 m
Time hit	10:42	Uncorr. Water Depth	4050 m
Wire Angle at Hit	6°	Wire-out at Hit	4190 m
Time surfaced	11:50	Winch #1	
Response at Hit	not clear	Response at Pull-out	clear
Length Main Core	390 cm	Length Trigger Core	0 cm

State of Cutting Edge & Pipe good
No. of Storaged Pipes 3
Length of Storaged Cores #52; 168 cm, #53; 168 cm, #54; 53 cm.
No. of Cubic Samples for Paleomagnetism 133 (#4876–5008)

Date Feb. 1, '69 Ship Hakuhō maru Cruise KH-68–4 Station 60–2
Latitude 38°26.6′S Longitude 155°05.0′E
Location Tasman Sea
Weather cloudy, warm no breeze Sea very calm
Bottom rugged over 300 m, north flank of a seamount

Length Main Pipe	6 m	No. of Pipe 1	Material Al (Mg) Alloy
I.D. of Pipe	68 mm	Wall Thickness	6 mm
Core Head Wt.	780 kg	Trigger Wt.	60 kg
Length Main Line	15 m	Length Trigger Line	15 m
Time lowered	09:45	Uncorr. Water Depth	4500 m
Time hit	11:04	Uncorr. Water Depth	4330 m
Wire Angle at Hit	4°	Wire-out at Hit	4394 m
Time surfaced	12:36	Winch #1	
Response at Hit	clear	Response at Pull-out	vague
Length Main Core	0 cm	Length Trigger Core	46 cm
Length Penetration	400 cm		

State of Cutting Edge & Pipe no damage with pipe, slight bend with edge.
Remarks. Mn nodule fragments attached in the edge, may have prevented from penetrating further.

Table 9. List of distributed cores for geochemical studies

Organization (personel)	Item of study	No. of core sample														
		5	11	15	18	20	25	29	31	37	39	41	45	49	55	60	Ex.
Meteorological Res. Inst. (Y. Sugimura)	Geochronology & natural radio-nuclides	M/8	M/8	M/8	M/8	M/8	M/8	M/8	M/8	M/8	M/8	M/8	M/8	M/8	M/8	P	
Nagoya Univ. (S. Kanamori)	Carbonate geochemistry	M/8	M/8	M/8	M/8	M/8	M/8	M/8	M/8	M/8	M/8	M/8	M/8	M/8	M/8	*	
Nagoya Univ. (T. Koyama)	Fossil pigments & carbohydrate	M/8	M/8	M/8	M/8	M/8	M/8	M/8	M/8	M/8	M/8	M/8	M/8	M/8	M/8	*	
Univ. of Tokyo (K. Watanuki)	Alkaline earth & Mineral composition	M	M	M	M	M	M	M	M	M	M	M	M	M	M	*	
Tokai Univ. (Y. Toyota)	V, Fe, Al content	M	M	M	M	M	M	M	M	M	M	M	M	M	M	*	
Hokkaido Univ. (S. Tsunogai)	Equilibrium behavior of Ca	HP	*	HP	HP	*	*	HP	HP	*	P	*	P	*	P	*	
Univ. of Kyoto (T. Kuwamoto)	Cr content	HP	*	HP	HP	*	*	HP	HP	*	P	*	P	*	P	*	
Kyoto Univ. of Education (T. Fujita)	Mn and Ti content	HP	*	HP	HP	*	*	HP	HP	*	P	*	P	*	P	*	
Jap. Meteor. Agency (H. Yoshimura)	Ni and P content	HP	*	HP	HP	*	*	HP	HP	*	P	*	P	*	P	*	
Ocean Res. Inst. (H. Tsubota)	Interstitial water	P	P	P													
Phys. chem. Inst. (M. Shima)	Cosmic dust	M/8	M/8	*	*	*	*	*	*	*	*	*	*	*	*	*	
Tokyo Metropol. Univ. (R. Ishiwatari)	Marine humus	*	*	*	*	*	*	M	*	*	*	*	*	*	M	*	
Nuclear Res. Inst. (S. Tanaka)	^{26}Al and ^{10}Be	*	*	*	*	*	*	*	*	*	*	*	*	*	*	*	M

M: MAIN CORE P: PILOT CORE HP: HEAT FLOW CORE.
* Not distributed.

VIII. Individual Research Works

VIII. 1. Chemistry

VIII.1.1. Ammonia and Ammonium Ion

by

S. Tsunogai

It is an interesting problem to study the origin of ammonia in marine atmosphere, and some works had been done in the area of the Northwest Pacific.

Air was sucked into water bottle and dilute sulfuric acid bottles which were placed in series, and ammonium in aerosol and gaseous ammonia were absorbed in water and surfuric acid, respectively, at the roof of the bridge. 35 samples of gaseous ammonia, 31 aerosol samples, and 13 rain water samples were collected during the whole cruise. (Part of the results was read at the Autumn Meeting of the Geochemical Society of Japan, Kyoto, 1969.)

VIII.1.2. Nitrogen and Argon

by

Y. Horibe and M. Tano

Theoretical and experimental results of the dissolved gases in sea water showed that the knowledge of dissolved gas content can give us precise understanding of the surface phenomena in the ocean and also of behavior of oxygen in sea water. Mass spectrometry may be the best method for the analysis of gases, and recent development of mass spectrometric technique coupled with the stable large research vessel is expected to make possible the use of mass spectrometer on board.

Apparatus. The mass spectrometer used is a modified version of Hitachi Model RMS-4, which is usually used for the determination of structure of organic compounds and of composition of organic material together with gas chromatograph. Schematic outline is shown in Figure 55. The mass spectrometer is composed of two units, one is analyzer tube, sample-inlet- and pumping-assembly, and the other is control- and recording-unit. The analyzer tube is Nier-type with the radius of 125 mm, and the magnetic field can be changed electronically to scan the mass range from M/e = 2 to M/e = 150 at

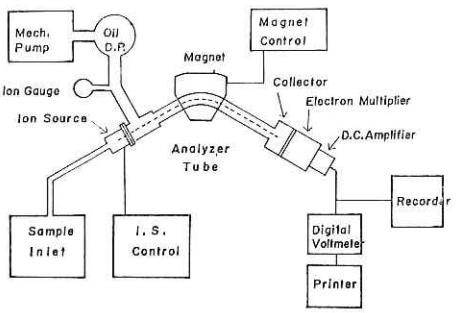

Fig. 55. Schematic diagram of shipborne mass spectrometer.

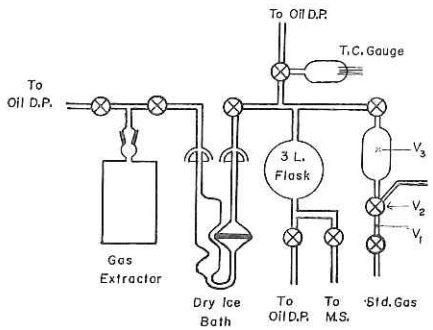

Fig. 56. Sample (sea water) inlet system.

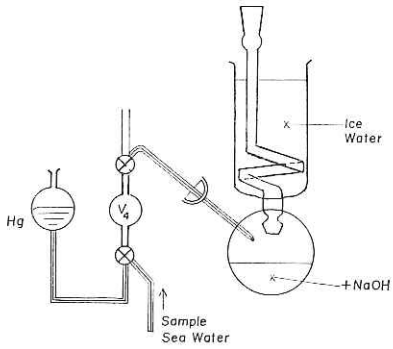

Fig. 57. Gas extractor of the sample inlet system.

various speeds. A copper-beryllium electron multiplier and a direct coupled DC amplifier are used for the determination of ion current. All the power supply and electronic circuits are transisterized except a vacuum tube 5886 of the DC pre-amplifier. Output of DC amplifier is furnished to a 3 pen recorder which monitors the output voltage (peak height), and to a digital voltmeter (Takeda Riken TR 6191) couple with a printer (Takeda Riken TR 6154 BS) which prints out the output voltage. Analyzer tube is pumped with a 150 liter three stage oil diffusion pump which is cooled with circulating cold water. The oil diffusion pump worked very satisfactorily even when the ship roled more than 20 degree, and we had no difficulty for pumping aboard during the whole 110 days of the cruise.

Sample Inlet System. Sample inlet system is shown schematically in Figure 56 and Figure 57. As the dissolved gas should be completely extracted from a known amount of water sample and be dry, the extraction system is composed of gas extractor, U-tube with fritted disk for removal of water vapor, 3 liter gas reservoir, and a thermocouple gauge. Gas pipet which serves to introduce a known amount of air or pure gas is attached to measure the sensitivities of the specific gas.

The sample inlet system is evacuated with a 100 liter oil diffusion pump of the same design as that of the analyzer tube, and the pressure of inlet system can be measured with thermocouple gauge (RCA 1946). Sea water sampler consists of two three-way stopcocks and sample bulb of known volume (2.5–3.0 ml) in between. A small bulb which contains mercury is connected with one arm of lower three-way stopcock. One arm of the upper three-way stopcock is connected with gas extractor with a ball joint. The sample sea water is taken from Nansen sampler into a 100 ml bottle which is usually used for sample bottle of the Winkler method. The sample sea water is pipetted into bulb V_4. By turning two three-way stopcocks, mercury pushes the sea water sample into the gas extractor by the atmospheric pressure. Thus, the sample sea water and small amount of mercury are introduced into the bottom bulb of gas extractor. As carbon dioxide is the most abundant component of the dissolved gases and it is convenient not to extract carbon dioxide for the measurement of nitrogen, oxygen and argon, a few pellets of sodium hydroxide are put in the extractor bottom bulb, so as to fix carbon dioxide as carbonate.

The upper part of gas extractor is cooled with ice-water, and U-tube with fritted disk in dry ice slush bath to remove water vapor from the extracted gas. The bulb of gas extractor is heated with small flame of an alcohol lamp till the pressure increase in gas reservoir can not be observed with thermocouple gauge. Although some of the sea water is distilled over into U-tube in this extraction process, ten aliquots of sea water sample can

be treated with one gas extractor and U-tube.

Analysis. Sensitivities of nitrogen, oxygen and argon can be measured by putting known amount of pure gas into 3 liter gas reservoir with gas pipets V_1, V_2, and V_3. Sample gas was introduced into analyser tube through stopcock (to M.S.), and scanning of magnetic field is started from M/e = 26 after 30 seconds. It took 3 minutes to scan from M/e = 28 to M/e = 44. Peak height could be read from printer output. Analysis of one sea water sample (including extraction of gas) took less than 10 minutes.

Results. One of the advantages of mass spectrometric method is that the analysis of nitrogen, oxygen and argon can be done with the same aliquot of water sample. Other advantages is that the mass spectrometric method takes less time for one sample as compared to the classical volumetic method or gas chromatographic method, so that we can analyse the gas content of all the sea water sample of different depth of one hydrocast in a short time. Only one drawback is to use dry ice, and the disadvantage can be avoided by carrying a deep freezer which keeps dry ice without any loss by sublimation. Dry ice may be obtained almost in any places in the world, and we did not find any difficulties to get necessary amount of dry ice throughout the whole course of the cruise in 1968–1969.

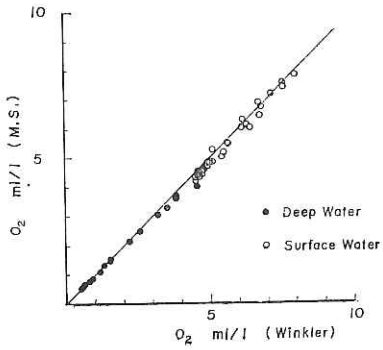

Fig. 58. Comparison of dissolved oxygen content in sea water obtained by the Winkler method and mass spectrometric method.

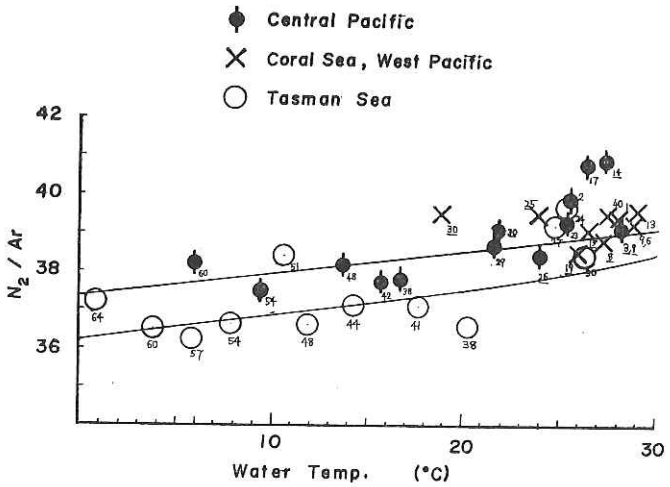

Fig. 59. N_2/Ar-temperature relation of the Pacific and South Tasman Sea. The number in the figure shows latitude in south hemisphere and bar under the number shows north latitude.

Oxygen data obtained by mass spectrometric method are compared with those of the Winkler method, as are shown in Figure 58. The average deviation of the concentration of dissolved gases is about $\pm 1\%$. Sensitivity for gas decreased gradually during analysis, presumably because surface conditions of the electron multiplier might change with time by the impact of ions. The effect may be the reason why the average deviation was relatively high. It is expected that the average deviation be made smaller by improving the stability of electron multiplier.

Nitrogen-argon ratios of surface sea water which were measured at the same time as those of oxygen concentration show very interesting features of Tasman Sea, Coral Sea and the West Pacific, as are shown in Figure 59. The ratios of Tasman Sea are lower than those calculated from equilibrium solubility ratio at any temperature, and those of Coral Sea are the same as those of the equilibrium value. (Part of the results was read at the Spring Meeting of the Oceanographical Society of Japan, Tokyo, 1969, and at the Autumn Meeting of the Geochemical Society of Japan, Kyoto, 1969).

VIII.1.3. Oxygen-18 of Dissolved Oxygen

by

Y. Horibe and K. Shigehara

Dole and Rakestraw found that the oxygen-18 of the dissolved gas in sea water of the Northeast Pacific is enriched as the oxygen content decreases. The same tendency was found in sea water of the Northwest Pacific. This phenomenon is explained to be due to the preferential consumption of light isotope of dissolved oxygen in sea water. In the north region to Kurile Islands, however, we found that oxygen-18 content of the dissolved oxygen above the oxygen minimum layer is lower than those of the deeper water, when they are compared at the same oxygen content. The phenomenon suggests that there might be some processes which decrease the oxygen-18 content above the oxygen minimum layer, and the process might be closely related to the movement of water masses above the oxygen minimum layer.

It may be interesting to find some other places in the Pacific where the same phenomenon as above occures.

Water samples were taken from various depth at 16 stations (Station 2, 11, 14, 16, 18, 19, 21, 24, 27, 30, 33, 35, 38, 41, 44, and 48).

The extraction of dissolved oxygen in sea water was done aboard as soon as the sea water samplers were brought up on deck. Oxygen extraction flasks are shown in Figure

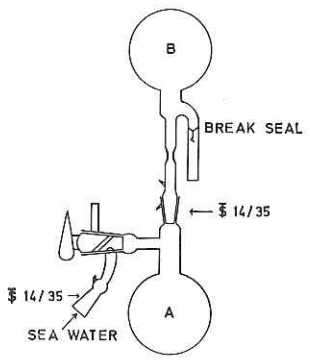

A, B : 500ml or 1l PYREX FLASK

Fig. 60. Oxygen extraction flasks for ^{18}O analysis.

60. 500 ml sea water in Nansen sampler or 1000 ml sea water in van Dorn sampler was introduced into evacuated glass flask A of oxygen-extraction flasks which was flushed with helium gas before pumping with mechanical pump. The flasks were turned upside down several times to extract oxygen gas to other storage flask B. More than 95% of volume of dissolved gases was extracted to the storage flask which was sealed off and brought back to the laboratory for isotope analysis. (Part of the results was read at the Autumn Meeting of the Geochemical Society of Japan, Kyoto, 1969.)

VIII.1.4. Carbon Dioxide in the Atmosphere and in the Surface Sea Water

by

Y. Sugimura, and Y. Hirao

Our survey of the partial pressure of CO_2 in the surface sea water and in the atmosphere in the Pacific and the Antarctic Oceans followed in general the method employed in the cruise of the previous Antarctic Expedition (JARE-8, 1966-67) by one of the authors (Y. S., 1968).

A nondispersive infra-red gas analyzer with a strip chart recorder was installed in one of the laboratory to monitor the concentration of CO_2 of dry air continuously.

Atmospheric CO_2. Atmospheric CO_2 was measured directly by sucking the air at deck height (5 m above sea level) through intake cup protected against sea spray. (The air was passed rapidly through polyethylene tubing on the weather decks and inside the ship). To remove the water vapour, the line was connected with an electric desiccant system made of thermoelectric elements. The air was then rewarmed to ambient temperature, and was passed through the analyzer cell.

The equilibrator. The CO_2 in surface sea water was determined by recording the concentration of CO_2 in a closed volume of air which was circulated countercurrentwise through exchange column so as to be in equilibrium with a renewed supply of sea water. The water was pumped up continuously from an intake in the ship's hull 4 to 5 m below the water surface.

As the concentration of CO_2 in sea water is highly dependent upon temperature, temperature change from outside the ship to the equilibrator was kept so small (less than 1°C) that little error was introduced. The relative accuracy of the data for the water during this cruise is ± 3 ppm. The determination of partial pressure of CO_2 in surface water was carried out every one hour through the course of the expedition. More than two thousands measurements of atmospheric air and ocean surface water have been processed.

Rough description of the results. During the eastward traverse from Tokyo to 170°W, the atmospheric CO_2 concentration was almost constant, and, the CO_2 concentration in the surface water was undersaturated relative to the air throughout the section, showing minimum at about 175°E.

Along the meridional section of 170°W, the CO_2 concentration in the water varied almost systematically, peak value occuring close to the equator and minimum was found in the east side of New Zealand.

As to the Subantarctic and the Antarctic waters, the CO_2 concentration in the waters were generally undersaturated until 66°S, however further south in the Ross Sea, the water was undersaturated as much as 70 ppm than that of the air.

In the Tasman Sea water, striking low values were observed over a broad zone between 20°S and 50°S.

As pointed out in a previous paper by one of the authors (Y.S. 1968), there is a close relationship between oceanographic condition of the surface water and the concentration

of CO_2 in surface water. (Part of the results was read at the Autumn Meeting of the Oceanographical Society of Japan, Nagoya, 1969).

VIII.1.5. Borate and Fluoride Ion

by

S. Kanamori, and A. Tokuyama

One of the authors (S. K.) showed that an observation of the distribution of borate in the sea is usefull

1) for discrimination of water masses or water types
2) for illustration of currents or slow movements of water.

The behavior of fluoride ion is expected to show a similar trend as that of borate. The analytical method by the use of ion specific electrode was also reported by the author (S. K.).

In this cruise, water samples for analysis of borate and fluoride ions were taken to study

1) chemical character of Antarctic Bottom Water and other water masses,
2) the chemical reactions which would occur in Antractic Bottom Water by mixing with another masses or types of water and by interaction with bottom sediments during its flowing up to north along bottom surface, and
3) material balance of borate and fluoride between atmosphere and ocean through the distribution of borate and fluoride ions.

Sea water samples were collected from all layers observed at all stations except stations 1, 3, 4, 7, 9, 12, and reserved in soft glass bottles for laboratory experiments in Nagoya University.
(Part of the results was read at the Autumn Meeting of the Geochemical Society of Japan, Kyoto, 1969.)

VIII.1.6. Bromine

by

Y. Toyota

Bromine is one of the major constituents of sea salt. It is generally accepted that the bromine to chlorine ratio in sea water is 0.00348 from the results of many workers. The careful inspection of the previous data suggests that small variations of relative composition (Br/Cl) do exist and it might be related to the difference in water masses.

The author's object is to study on the applicability of bromine to chlorine ratio as a tracer of Antarctic Bottom Water and other water masses, and on the interaction between Antarctic Bottom Water and bottom sediments through the distribution of bromine in sea water and sediments of the South Pacific Ocean and Southern Ocean.

200 ml sea water samples were taken from Nansen samplers of hydrocast at all sattions (Station No. 2 to 61, and station No. A to K) except station No. 53 to 58 and 60. Bromine and other bromine compounds such as bromate, if any, in sea water were oxidized to bromate with hypochlorite, and total bromate was measured by iodometric titration. The reproducibility increased appreciably under constant conditions of analysis by the use of automatic titrator and a constant temperature water bath ($\pm 0.1°C$), and the standard deviation of the Br/Cl is less than $\pm 0.2\%$ of the reported value. Preliminary experiments were carried out on board and promising results were obtained. Precise analysis of all samples will be done under the best conditions of the laboratory in Tokai University.

VIII.1.7. Iodide and Iodate

by

S. Tsunogai

311 sea water samples were collected at 24 stations to measure iodide and oidate concentrations in the Pacific, especially in the tropical ocean. The distribution of these ions will be useful for the understanding of the mechanism of evaporation of iodine from ocean surface and of formation of iodide in sea water.

(Part of the results was read at the Autumn Meeting of the Geochemical Society of Japan, Kyoto, 1969.)

VIII.1.8. Total Phosphorus and Total Silicate

by

H. Yoshimura

A number of samples were taken to measured total phosphorus and total silicate in sea water of all depth of hydrocast at stations shown in Table 10.

For the total phosphorus analysis, 50 ml of sea water was treated by Menzel's method (Limnol. Oceanogr., **10**, 280–282 (1965)), to liberate phosphorus combining with organic matter, and the determination of phosphate was done by ammonium molybdate ascorbic acid method (J.D.H. Strickland, and T. R. Parsons, A mannual of sea water analysis. Bull. No. 125, 47–50 (1965) Fish. Res. Bd. Canada). All the procedures were done on board, and total phosphorus profile along 170°W are shown in Figure 61.

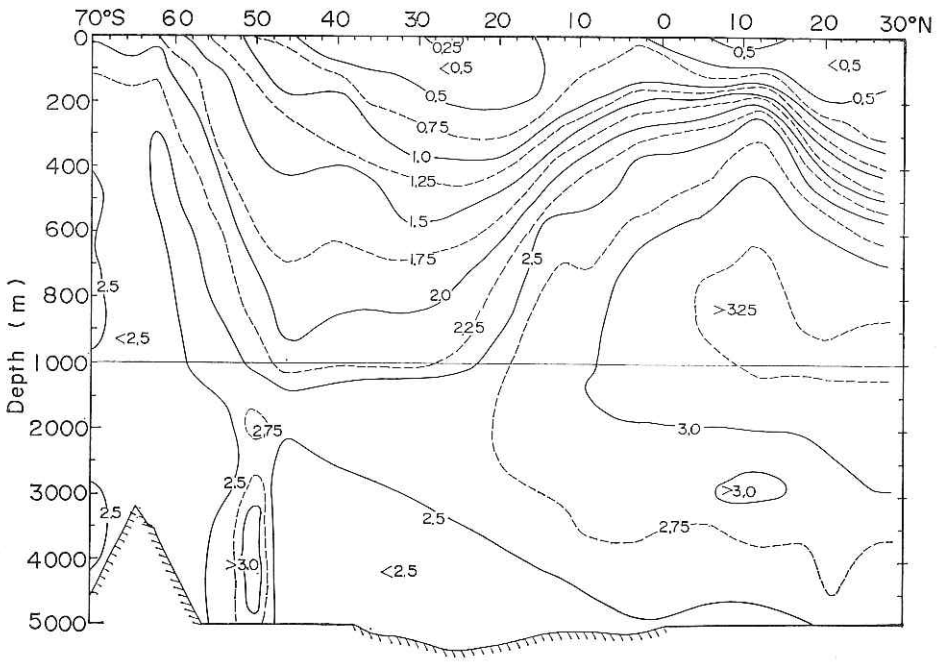

Fig. 61. Total phosphorus profile along 170°W. (Unit; μg at/l).

Table 10. Stations for total phosphorus and silicate

Phosphorus	170°W-longitude	Station No.	5, 11, 13, 15, 17, 20, 22, 23, 25, 29, 31, 34, 37, 39, 41, 43, 45, 47, 49
	155°E-longitude	Station No.	52, 53, 54, 55, 56, 57, 58, 59, 60, 61
Silicate	170°W-longitude	Station No.	5, 13, 17, 22, 25, 29, 31, 31, 34, 37, 43, 47

VIII.1.9. Arsenic

by

S. Kanamori, and A. Tokuyama

As the results of extensive study on the distribution of arsenic in the Northwest Pacific, it was concluded that each water mass has its characteristic concentration of arsenic, and deep and bottom waters are rich in arsenic (10–15 μgAs/l), while surface and intermediate waters are very poor in arsenic (1.5 μg As/l). Such distribution of arsenic is expected to be affected by the flow of Antarctic Bottom Water.

Sea water samples for analysis of arsenic were collected from all layers observed at all stations except stations 1, 3, 4, 7, 9, 12 and stored after addition of a small amount of concentrated hydrochloric acid to prevent mold growth.

The analysis of these water samples is carried out in Nagoya University, and

1) the distribution of arsenic in the South Pacific Ocean and the Southern Ocean will be understood,
2) the characteristic concentration of arsenic prevailing in each water masses will be found out and compared with those in the Northwestern Pacific Ocean, and
3) the contribution from antarctic bottom water to the distribution of arsenic in the Pacific Ocean will be evaluated.

VIII.1.10. Calcium and Other Elements

by

S. Tsunogai

1097 sea water samples were collected at 59 stations to determine calcium content in sea water. Samples were brought back to the laboratory of Hokkaido University to measure its calcium content accurately by complexometric titration. Distribution of calcium in sea water might be able to give some knowledge on the deep sea circulation of the Pacific. Chlorinity will be measured at the same time, and the author expects that calcium content may explain the discrepancy between salinity from electrical conductivity and chlorinity by titration. Also, 293 sea water samples of 5–10 liter at various depth and 20 surface water of 20 liter were filtered to get suspended solid substances. The solid substances were brought back to the laboratory, to analyze calcium, sodium, poassium, and silicone. The results will serve to study the dissolution and precipitation of calcium carbonate and silicate minerals in surface and deep water.

VIII.1.11. Calcium Carbonate Chemistry

by

S. Kanamori and A. Tokuyama

It is important to find whether or not a sea water (in situ if possible) is saturated with mineral calcium carbonate from a view point of calcium carbonate geochemistry,

because it directly concerns with many important geochemical problems such as the geochemical balance of calcium between sea water and bottom sediments. The degree of saturation of calcium carbonate is calculated from salinity, alkalinity and pH values, but there remains an unavoidable uncertainty which arises from the complex nature of sea water as an concentrated salt solution.

Degree of saturation of sea water with respect to calcium carbonate can be measured directly by the "Carbonate Saturometer", in which the change in pH value after addition of calcium carbonate powder to sample water is traced and decrease in pH indicates precipitation of calcium carbonate from sample water and increase in pH indicates solution of added calcium carbonate powder. The calculation of percentage of saturation is possible with suitable assumption. This method is more direct and leaves less uncertainty than the calculation from salinity, and pH.

Samples for experiments of "Carbonate Saturometer" were collected at stations 36, 39, 42, 46, 50, 51, 53, and 55. Preliminary experiments showed that the water shallower than about 300 m was supersaturated, while the water deeper than about 500 m was understaturated with respect to inorganic precipitate of aragonite.

Most of the collected samples will be used for measurements under precisely controlled conditions in the laboratory of Nagoya University.

Any calcarious detritus found in bottom sediments offers us a good chance to find out an evidence of solution, recrystallization or another processes which are important to understand the chemical history of ocean. A mineralogical study and chemical analysis of calcium carbonates in core samples of bottom sediments are undertaken, with special interest upon any evidence of chemical reaction proceeded after deposition.

One eighth of each core sediment was cut off at every one meter. Each piece was put into the special container and stored in cold store room at the temperature of 0–5°C.

VIII.1.12. Strontium and Barium in Sea Water and Sediments

by

K. Watanuki

Outline. The behavior of alkaline earth elements is very interesting as geochemical processes. Distribution and abundance of calcium in rocks, minerals, sea water, and sediment were studied by many researchers. But distribution and abundance of other alkaline earth elements are not so well known in sea water and sediment. Author tried to determine the content of strontium in sea water by the atomic absorption technique aboard. The content of strontium was found to be between 6.25 and 7.50 ppm for the surface water. The content of barium in sea water and deep sea sediment will be determined in the laboratory.

The method of analysis. The determination of strontium was carried out by the use of HITACHI 139 atomic absorption spectrophotometer. The spectral line employed was Sr 4607Å and optimum condition for hollow cathode lamp was 15 mA, 200 V. The gas pressure of acetylene was 0.4 kg/cm^2 and that of air was 1.4 kg/cm^2. The flow rate of acetylene was 1.5 l/min. and that of air was 7 l/min.

When the sea water sample was diluted with distilled water to five times, the analytical curve for strontium showed good linearity. The other samples are prepared by adding 1 ppm or 5 ppm of strontium to the sample. The absorption of 4607 Å was measured with HITACHI 139 atomic absorption spectrometer of 10 cm width flame.

One of the results is shown in Figure 62 and Table 11.

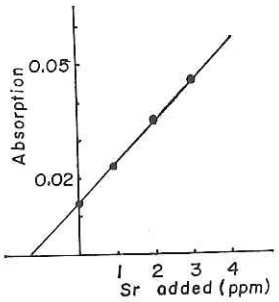

Fig. 62. Linearity of analytical curve for determination of strontium in sea water by atomic absorption spectrometry.

Table 11. Relation between added strontium content and absorption coefficient of sea water

Sample	Absorption coefficient
Sea Water	0.0141
Sea Water + 1 ppm Sr added	0.0232
Sea Water + 2 ppm Sr added	0.0353
Sea Water + 3 ppm Sr added	0.0453

VIII.1.13. Iron, Aluminum, and Silicon in Suspended Matter

by

Y. Toyota

The suspended mattters in sea water were collected in the Western North Pacific, Indian, and Antarctic Ocean near Scott Island and George V Land, and the contents of Fe, Al, and Si were analyzed by the author previously. Plot of the Fe–Al–Si weight percentage for each region on a triangular diagram shows that the points of samples from the Western North Pacific, Indian and Antarctic Oceans do not fall on the sphere of clay minerals and pelagic sediments. Only the Fe–Al–Si weight percent of the sample from Sagami Bay was similar to that of vermiculite, glauconite and pelagic sediments.

The purpose of the study is to account for the composition, origin of suspended matter and distribution of these three elements between suspended matter and sea water. The author could take samples in the ocean area which has not been surveyed on the problem. 10 liter sea water samples at different depth were taken at stations No. 2, 16, 21, 26, 33, 40 and 47. The suspended matter in sea water was seperated from sea water with Millipore Filter Type HA immediately after sampling. The contents of Fe, Al and Si in suspended matter will be determined in Tokai University as it needs delicate laboratory works.

VIII.1.14. Trace Elements (Chromic and Chromate Ions) in Sea Water and Sedements

by

T. Kuwamoto and S. Murai

1. Introduction. In the field of marine geochemistry the study of the distribution and the circulation of trace elements existing in sea water has been one of the important problems. It is well known that some trace elements are not so much concentrated in sea water but are notably concentrated in sediments. Especially, on the study of trace

elements in sea water it has become important, in recent years, to know the behaviors and valency states of chemical species dissolved in sea water. For example, some works on the valency state of chromium in sea water were done. Goldschmidt (1954) and Krauskopf (1956) suggested hexavalent state, and Huynh Ngoc and Fukai (1967), Arrhenius and Bonatti (1965) supported the idea of hexavalent state. On the other hand, Sillen (1961) suggested that uncharged soluble chromic hydroxide might be present in sea water and Riley (1966) reported that chromium is present in the trivalent state in sea water. Recently, Fukai (1967) concluded from the results of his experiments that the total chromium content of sea water is higher than those so far reported, being 0.5 $\mu g/l$, when haxavalent chromium has been measured and the occurrence of trivalent and hexavalent chromium may be related to the oxido-reduction process *in situ*.

From these points of view, the writers investigated the contents of chromic ion and chromate ion in sea water along 170°W longiude of the Pacific Ocean by using the new procedures of preconcentration of chromium with sub bismuth nitrate (basic bismuth nitrate) precipitate.

2. Experimental. Sampling of sea water. Sampling of sea water was made along 170°W and 155°E from November, 1968 to February, 1969.

Analytical procedure. To 5 liter sea water, add 5 ml-5 M ammonia and adjust to the pH of 8 aproximately, and then add 300–500 mg of sub bismuth nitrate precipitate (basic bismuth nitrate) to the sample solution. Stir and stand for about 4 hours. Measure pH of supernatant solution, if necessary. Filter off the precipitate with millipore filter HA (0.45 μ) and wash the precipitate with 0.01 N ammonia thoroughly. The precipitate is used for the analysis of chromic ion and the filtrate is used for the analysis of chromate ion.

Procedure of the determination of chromic ion. The obtained precipitate is washed with 2 N sulphuric acid on the millipore filter, transfer the filtrate to a 50 ml volumetric flask, dilute with distilled water to 50 ml, and then divide the solution exactly to half. To the one sample solution add 0.5 ml of 0.1 N permanganate and heat it in steam bath for 20 minutes. If the pink colour disappears, add more as required to remain a slight excess. Decolorize the permanganate by adding 3 to 5 drops of 5% sodium azide to destroy, but avoid excess. Remove promptly from steam bath and place it in a tray of cold water. Filter it if necessary, and transfer the solution to a 50 ml volumetric flask. Add 2 ml of 0.5 M sodium fluoride and 2 ml of 0.2% diphenyl carbazide. Mix and allow 1 minutes for colour development. After that, add 5 ml of 6 N hydrochloric acid and dilute to 50 ml with distilled water. Measure the extinction of pink colour at wave length of 540 mμ. The obtained value is the total sum of chromic and the part of chromate ion that is due to the contamination to the precipitate. Therefore, this value must be corrected experimentally.

The corrected value is obtained as follows; To the other half sample add 2 ml of 0.5 M sodium fluoride and 2 ml of 0.2% diphenylcarbazide. After colour development measure the extinction of pink colour at 540 mμ and then subtract this value from the total value. Colour too weak to be read may be rised with addition of standard chromate solution.

The procedure of the determination of chromate ion. To the filtrate add 15 ml of concentrated hydrochloric acid and 14 ml of 0.5 M sodium sulfite. Stir and stand for 1 hours. After aging, (chromate ion is reduced to chromic ion) add 55 ml of 5 N ammonia solution and determine chromic ion according to the procedure of analysis of chromic ion.

The correction of the observed value. As the recovery of chromium ions cannot

be obtained in these procedure, the quantity of chromium ion in sample is not correct. Therefore, it is necessary to correct the observed values by using the standard additional method.

In the case of additional method net extinction readings are obtained on two solutions(unknown sample solution and unknown sample solution plus measured amount of a standard solution of the element), the quantity of test element in each of these solution is determined from absorbancy and calibration curve. Subtraction of the quantity of elements in the former solution from that found in the latter solution yields the amount of test element equal to that added when there is no depression and enhancement. But, usually, the quantity of test element found by subtraction is greater or less than that added. In such case, the true metal content is found from the following relationship.

$$\frac{X_{\text{found}} \times C_{\text{added}}}{C_{\text{added}}} = X_{\text{actually present}}$$

X = the concentration of unknown, C = the amount of standard added

3. Results

Results of analysis. The range in concentration of each form of chromium in sea water is as follows,

chromic ion in sea water	0.04–0.72 μg/l (av. 0.25 μg/l)
chromate ion in sea water	0.06–0.40 μg/l (av. 0.2 μg/l)
total chromium in sea water	0.10–0.94 μg/l (av. 0.4 μg/l)

(Analytical procedure was read on the Meeting of Analytical Chemistry at Hiroshima, 1968.)

VIII.1.15. Chemical Composition of Marine Plankton

by

T. Fujita

Studies on the distribution of trace elements in the ocean have just begun, and a little is known on their distribution, chemical forms and the physical, chemical and biological processes which might have much effect on their distribution. Biological activities may influence the concentration of trace elements in the ocean, and it is the major object of this work to study the concentration of trace elements of marine organism and in sea water, and to know the relations between them. Marine plankton which is widely distributed in the ocean was chosen as a representative of marine organisms, and the author expects to get plankton samples and surface sea water samples from different part of the Pacific, so that he can draw pictures on the world wide distribution pattern of trace elements in the ocean.

Sampling. Plankton samples and surface sea water samples (20 liter) were taken at 30 stations which are shown in Table 12. Most of the plankton samples were collected by towing a 2 meter plankton net equipped with GG 53 nylon bolting cloth (50 cm calibre). Towing from surface to 150 meter depth was conducted several times at one station to collect enough quantity of plankton to analyse trace elements. Plankton of individual species was sorted mechanically with a bamboo tweezers from the mixed plankton samples collected at 19 stations (stations No. 5, 20, 21, 25, 31, 34, 35, 37, 40, 43, 45, 47, 48, 50, 52, 54, 55, 56, and 59), and 13 zooplankton and 8 phytoplankton samples of individual species were prepared. Samples of individual species were washed well with distilled water and drained on nylon bolting cloth. The plankton samples of individual species, mixed plankton samples, and surface water samples were brought back to the laboratory to determine manganese, titanium and chromium contents.

Table 12. Collection data for plankton samples

Station number	Date	Time	Collection* volume (ml)	Major composition
		h m h m		
2	Nov. 22 '68	15.00—17.00	100	Copepoda
5	Nov. 24 '68	8.30—11.00	200	Copepoda, Sagita
8	Nov. 25 '68	13.00—14.30	120	Copepoda, Sagita
16–2	Dec. 1 '68	21.00—23.00	110	Copepoda, Salpa
18	Dec. 3 '68	20.00—23.00	140	Copepoda, Sagita
19	Dec. 5 '68	6.30—10.00	250	Copepoda
20	Dec. 6 '68	18.00—23.00	260	Copepoda, Amphipoda
21–3	Dec. 7 '68	20.00—22.00	220	Copepoda, Sagita
24	Dec. 15 '68	8.00—12.00	30	Copepoda
25	Dec. 16 '68	6.30—10.00	230	Copepoda
26–2	Dec. 17 '68	9.00—11.30	60	Copepoda
29	Dec. 20 '68	22.00—2.30	100	Copepoda, Sagita
31–2	Dec. 23 '68	0.00—5.00	150	Copeopda, Euphausia
33–4	Dec. 25 '68	16.00—20.00	50	Copepoda
34	Dec. 26 '68	14.00—16.00	300	Salpa
35	Dec. 27 '68	6.30—8.30	340	Salpa
37	Dec. 28 '68	9.30—11.30	250	Copepoda
38	Jan. 10 '69	3.00—6.00	95	Euphausia
40	Jan. 12 '69	3.00—6.00	310	Copepoda
43	Jan. 15 '69	0.00—3.30	330	Phytoplankton
45–2	Jan. 16 '69	16.00—19.00	1200	Phytoplankton
47	Jan. 17 '69	20.00—22.00	2430	Phytoplankton, Salpa
48	Jan. 18 '69	15.00—19.00	2050	Phytoplankton
49	Jan. 19 '69	12.00—16.00	210	Copepoda
50	Jan. 20 '69	20.30—22.30	640	Phytoplankton, Salpa
52	Jan. 23 '69	19.00—21.30	2420	Phytoplankton
54	Jan. 25 '69	14.30—16.30	1600	Phytoplankton
55–2	Jan. 26 '69	1.00—3.00	950	Copepoda
56	Jan. 28 '69	0.00—3.30	95	Amphipoda, Copepoda
59	Jan. 30 '69	16.30—19.00	40	Euphausia

* A collection volume are shown by quantity of precipitating plankton sample.

VIII.1.16. Organic Matter

by

K. Yanagi

Studies of distribution and decomposition of organic matter is useful for the better understanding of organic fertility in the ocean, and analyses of plant pigment and carbohydrates in sea water and in particulate matter, and of the organic substances including carbohydrate, protein and lipid in bottom sediment are very important for these studies.

Experimental aboard. Samples for total plant pigments and total organic matter (org.-C & -N) were taken by filtering 5 liter sea water sample through glass fiber filter with pore size of about 1 μ. Sea water samples were taken by the use of van Dorn samplers from 9 to 10 layers not deeper than 500 m, usually from the depth of 0, (10), 30, 50, 75, 100, 150, 200, 300, and 500 m at stations No. 2, 8, 13, 16, 20, 21, 23, 25, 26, 29, 31, 33, 35, 37, 40, 43, 45, 47, 48, 52, 56, and 60.

To determine compositions of pigments and carbohydrate, it was necessary to treat

a large amount of sea water. Sea water samples of 100 liter were taken from the depth of 0, 30, 50, 75, 100, 150, and 200 m, and sea water samples of 180 liter were taken from 500 and 1000 m at the stations No. 2, 16, 33, 40 and 48.

Plant pigments in particulate matter were extracted with 90% acetone and analyzed by the technique of thin layer chromatography on cellulose with the use of fluorometer for the determination of chlorophylls and their derivatives. The method aboard enabled us to have very accurate data of pigments, because these pigments are easily decomposable even at very low temperature, and could not be brought back to the laboratory without changing their concentration.

Sea water samples of 100 ml were taken in plastic bottle from all layers of hydrocast at all stations to analyze carbohydrate. They were ketp freezed and brought back to the laboratory of Nagoya University.

60 liter of sea water samples were taken from the depth of 0, 30, 50, 75, 100, 150, 200, 500, 1000 and 3000 m at station No. 48 and were filtered with glass fiber filter and the filtrates were reserved with 150 ml of concentrated sulfuric acid for the determination of dissolved organic compounds.

Preliminary Results. As was expected, the layer of maximum content of total pigment in tropical region was found at about 150 m. It became shallower with the increase of latitude. In antarctic region, it was shallower than 50 m. The amount of total pigment in the maximum layer as 0.2–0.3 μg/l in tropical region, and 1.0–1.5 μg/l in antarctic region, respectively.

It was very interesting that chlorophyll was found even below the depth of 500 m in some region.

(Part of the results was read at the Autumn Meeting of the Oceanographical Society of Japan, Nagoya, 1969.)

VIII.1.17. ^{14}C *in Sea Water and in Air*

by

Y. Horibe and H. Tsubota

Measurement of radio carbon content in sea water and in air is a useful method to trace the origin and movement of water masses and to estimate their mixing rate. Many investigations were done in these ten years, and still there remain many problems in the circulation and mixing of the South Pacific waters.

One of the technical problem is the necessity of large volume of water sample for precise measurement of ^{14}C content, and in this cruise we could not get as much water as those of the preceding works. We reexamined how much water would be needed for ^{14}C analysis for the purpose and reached the conclusion that it might need at least 5 liter of sea water.

Although chemical technique to extract CO_2 from 5 liter sea water sample is simple, an extremely low background detector of ^{14}C counting is needed. 20‰ of accuracy is estimated to be got by 2 days counting of 250 cc CO_2 sample.

Extraction of CO_2 from sea water and from air. CO_2 gas was extracted from 5 liter sea water samples from van Dorn sampler and was absorbed in CO_2 free sodium hydroxide solution. $SrCO_3$ was precipitated from the solution by adding $SrCl_2$ at pH 9.5.

5 liter sea water sample was acidified with 50 ml of concentrated hydrochloric acid and CO_2 free air was bubbled through for 40 min at the flow rate of 500 ml/min. The carbonate in sea water was completely removed as CO_2 in this process, and it was confirmed that there remained no carbonate in sample sea water. The extracted CO_2 was absorbed in 4 N sodium hydroxide solution, and 8 N hydrochloric acid was added to adjust the pH

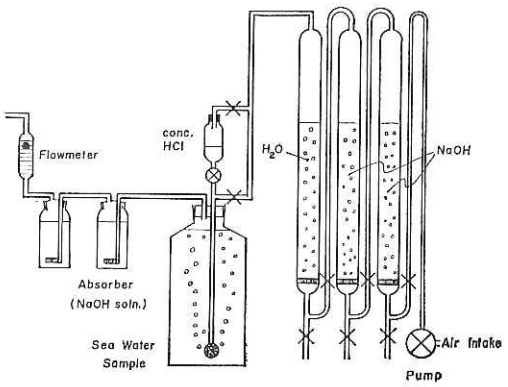

Fig. 63. CO_2 extraction and absorption apparatus for ^{14}C analysis.

of solution to 9.5. 10 ml of saturated strontium chloride solution was added to precipitate strontium carbonate which was washed and sealed in a small plastic tube. The CO_2 extraction and collection line are shown in Figure 63.

CO_2 in air was also collected by bubbling about 800 liter air through absorption bottle in Figure 63.

VIII.1.18. Distribution of ^{90}Sr and ^{137}Cs in the Pacific Waters

by

Y. Sugimura and T. Yasujima

The distribution of artificial radioactivity of both horizontal and vertical directions in the open ocean has been studied for a long time in our laboratory from the point of investigation of water movement in the ocean.

During the cruise, sea water samples of 200 liter each, 10 of deep and 15 of surface samples were subjected to the analysis of ^{90}Sr and ^{137}Cs.

As to the strontium-90 separation, carbonate precipitate was formed aboard in the polyethylene tank at the cold solution by adding each 2 kg of NH_4Cl and Na_2CO_3, followed by stirring with water mixing pump for 5 hours. The mixture was stood for one day and the precipitate which contained ^{90}Sr was placed in a glass bottle. Further purification and determination of the nuclide will be carried out at the laboratory on land.

The inorganic ion exchange method was used for the separation of cesium-137 by using crystalline ammonium molybdophosphate (AMP).

The supernatant solution of above described procedure containing ^{137}Cs was replaced in another polyethylene tank and the acidity of the solution was adjusted to pH = 3 by adding dilute nitric acid. 20 grams of fine crystalline AMP was added into the solution and mixed thoroughly with the aid of water mixing pump for 5 hours.

The crystal which adsorbed ^{137}Cs was separated from the solution by syphoning off the supernatant after standing over night. The crystal of AMP was placed in a small polyethylene bottle and the determination of γ-activity of ^{137}Cs will be carried out at the laboratory on land.

(Part of the results was read at the Autumn Meeting of the Geochemical Society of Japan, Kyoto, 1969)

VIII.1.19. ^{210}Pb *and* ^{210}Po.

by

S. Tsunogai

^{210}Pb and ^{210}Po (91 samples of surface, 48 samples of various depth) were separated from 30–50 liter sea water together with calcium carbonate precipitation after addition of carriers of lead and bismuth. Activities of these nuclides will be measured at the laboratory of Hokkaido University. The results will serve for the estimation of circulation and mixing rate of surface water.

(Part of the results was read at the Autumn Meeting of the Geochemical Society of Japan, Kyoto, 1969).

VIII.1.20. Samples for the Studies on Distribution of Natural Radioactive Nuclides in Deep-sea Deposit

by

Y. Sugimura

The sediments of the Central and South Pacific Ocean are characterized by low rate of sedimentation and high surface ratio of Io and Th. In connection with the deep circulation of the Pacific waters, the studies on the distribution of radionuclides in the Pacific deep-sea sediment have been intended in our laboratory.

Thirteen sediment core samples obtained by means of the piston corer (68 mm in dia. and 4 to 10 m long) will be able to use for the study.

The sample shared in one-eighth along the long axis direction was cut every 1 m long, and it was covered with polyvinylchloride sheet, following the store in a board tube.

The determination of natural radionuclides (uranium isotopes, thorium isotopes, radium etc.,) in the sediment and the study of Io-Th geochronology will be carried out at laboratory on land by means of wet chemistry and α-spectrometry.

VIII.1.21. Uranium, Thorium and Plutonium Isotopes

by

Y. Sugimura, M. Mayeda and T. Yasujima

To clarify the relationship between general oceanic circulation and the distribution of natural radio elements in the Pacific waters, this study was intended.

Uranium isotopes. Samples of sea water, 50 in surface and 180 in deep, were collected during this cruise along the meridional section of 170°W. Uranium was analyzed on board by the absorption spectrophotometric method with Arsenazo-III after separation with a chelating resin Dowex A–1 in the presence of CDTA as a masking agent at pH=3.

As far as the isotopic ratio of $^{234}U/^{238}U$, the measurement of α-activities will be carried out in laboratory on land, using an α-ray spectrometer which consisted of the solid state detector coupled with a multichannel pulse height analyzer.

Thorium and plutonium isotopes. Each 500 liter of sea water, 12 in deep and 38 in surface, was subjected to analysis. Sample of sea water, collected by using the large volume of bag sampler from deep or direct pumping up from the surface was placed into a polyethylene tank on board, following the addition of ferric ion as chloride form. Most of thorium isotopes and plutonium isotopes were coprecipitated with ferric hydroxide. To decompose the organic matters containing in the hydroxide precipitate, it was digested successively with concentrated nitric acid, hydrochloric acid and perchloric acid, dried up and the residue was dissolved in nitric acid.

Separation and purification of thrium isotopes were carried out by using two steps of anion exchange method on board.

The content and the isotopic ratio of thorium and plutonium isotopes will be determined by the α-ray spectrometric method after electroplating them on a platinum or stainless steel disk at the laboratory on land.

The result of determination will be given later in elsewhere with a discussion from radioactive equilibria and oceanographical points of view.
(Part of the results was read at the Autumn Meeting of the Geochemical Society of Japan, Kyoto, 1969.)

VIII.1.22. Monitoring of Artificial Radioactive Nuclides in Sea Water

by

H. Tsubota

Continuous monitoring of the radiation level of surface sea water was necessary to estimate the concentration of artificial radioactive nuclides in sea water which was used to prepare distilled water and to many purposes aboard. When any anomalies of radioactivity were found, a large volume of surface sea water was taken to identify the species of radionuclides. The knowledge of the species of radioactive nuclides helps us discuss general circulation and mixing phenomena on the Pacific as were shown by many previous workers.

Instruments. The scintillation detector ($2'' \times 2''$ NaI (Tl) crystal and photomultiplier) was placed in a double wall cylindrical plastic vessel. Surface sea water passed through between two walls so that the detector was surrounded by the flowing fresh surface sea water. The plastic vessel is placed in lead shield of 5 cm thick. The output of Aloka TRM 1B rate meter was continuously recorded with a strip chart recorder (Toa Dempa EPR 2TB). The schematic diagram of the apparatus is shown in Figure 64. The sensitivity of the instrument was as high as natural radiation level of sea water (0.4×10^{-7} μc- γ/cm^3), and 10^{-7} μc of γ-disintegration per cm^3 in water could be discriminated clearly. γ-spectrum of the sample sea water could be obtained when rate meter recorder system was replaced with a 400 channel pulse height analyzer system.

Results. The monitoring system worked satisfactorily during the whole course of the expedition. The surface sea waters in the North and Equatorial Pacific seemed to have rather higher concentration of radioactive nuclides than those of the Antarctic region, when the latitudinal variation of background caused by cosmic radiations were taken into consideration. Slight increases of radioactivity were sometimes found in coastal waters and waters over banks. Anomalous patterns were also observed near equator. They seemed to be caused by artificial radionuclides, but the level were not high to give warning. The conventional warning level aboard was fixed at 1×10^{-7} μc γ-disintegration per cm^3.

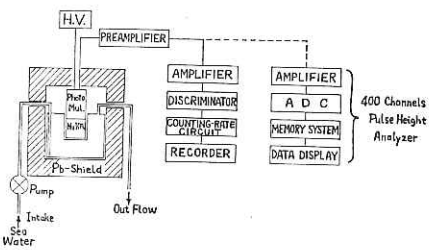

Fig. 64. Block diagram for the monitoring of artificial radioactive nuclides in sea water.

VIII. 2. Geophysics

VIII.2.1. Measurement of Gravity and Magnetic Force at Sea during KH-68-4 Cruise

by

Y. Tomoda, K. Kitazawa and K. Koizumi

1. Gravity and magnetic data acquisition and processing during KH-68-4 Cruise

1·1. Introduction

During this research cruise, the earth's total magnetic field was measured by the use of the proton magnetometer at every 1 min throughout the cruise except when the ship was drifting for oceanographic observation.

At the beginning of the cruise, the proton magnetometer Model 61 was used. As the meter cannot cover the area of magnetic field larger than 6000 γ, another set of magnetometer Model 65 was improved by adding three sets of external tuning condenser boxes for head tuning, $f \times 1$ tuning and $f \times 2$ tuning, and used from Dec 15th till the end of the cruise.

The earth's gravitational field was measured by the use of the T.S.S.G. (UMITAKA) with string gravity meter "Z-68-7-14".

At the beginning of the cruise, the gravity data processing was carried out by the PAPER TAPE SYSTEM which is the same system as used in the previous cruise, KH-68-3 and the gravity analysis was made by a computer FACOM 270-20 on board the ship by the use of the gravity analysis program described in the "Preliminary Report of the Hakuhō Maru Cruise KH-68-3". In addition to the PAPER TAPE SYSTEM, a small electronic computer T.D.K. P-3 was used on line for auxiliary purpose.

In the middle of December, ON LINE REAL TIME GRAVITY DATA PROCESSING PROGRAM for FACOM 270-20 was compiled. The results of the PAPER TAPE SYSTEM and the ON LINE SYSTEM were compared at first for one day and the identity of the results obtained by two methods was confirmed. Since then, the gravity analysis was carried out by the ON LINE SYSTEM.

On December 7th, the No. 8 laboratory in which the computer was installed was flooded with sea water from an eroded cooling tank of the air conditioner. It took about one day to repair the computer, during which we were compelled to use PAPER TAPE SYSTEM for the gravity analysis. During the period between the time of occurrence of the damage and the start of the PAPER TAPE SYSTEM the analysis was continued with the help of the T.D.K. P-3 auxiliary system.

1·2. Flow chart of gravity and magnetic data processing

Flow chart of data processing of gravity and magnetic data is shown in Figure 65.

1·2·1. The output of the T.S.S.G. is the oscillation period of the string gravity meter mounted on the vertical gyroscope sampled at interval of 0.5 sec. The 1st branch of the output is fed to the R.T.C. of the FACOM 270-20 through an interface device between the gravity meter and the R.T.C., and the 2nd branch to the tape puncher which is ready to start PUNCHING whenever the computer is wrong or busy for BATCH PROCESSING or for the debugging of new programs.

The 3rd branch of the output of the gravity meter is the oscillation frequency of the string gravity meter and is fed to the small computer T.D.K. P-3 through an interface device (T.S.S.G.D.P.U.).

The 1st branch of the output is processed by FACOM 270-20 according to the "ON LINE REAL TIME GRAVITY DATA PROCESSING PROGRAM" described in another section of this report.

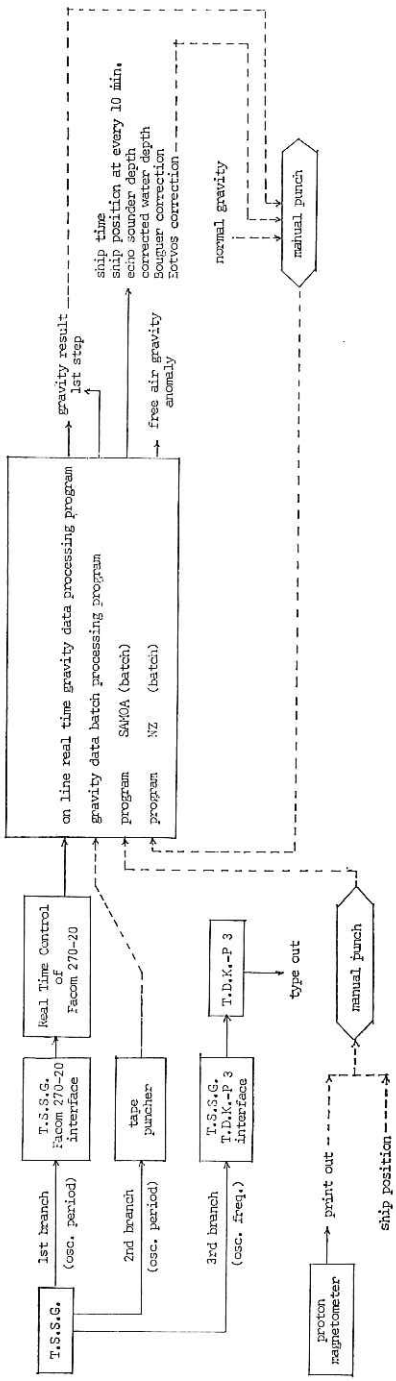

Fig. 65. Flow chart of gravity and magnetic data processing.

```
LEFT APIA
681214P    -20E     -26Q
1420H     978341X   978652Y   0Z
  30H               978626Y   *
  40H               978541Y   *
  50H               978513Y   *
1500H     978341X   978515Y   89Z
  10H               978507Y   89Z
  20H               978507Y   89Z
  30H               978513Y   89Z
  40H               978491Y   89Z
  50H               978464Y   89Z
1600H     978346X   978460Y   84Z
  10H               978491Y   56Z
  20H               978492Y   56Z
  30H               978493Y   56Z
  40H               978468Y   56Z
  50H               978456Y   56Z
1700H     978353X   978446Y   46Z
  10H               978440Y   46Z
  20H               978440Y   46Z
  30H               978425Y   46Z
  40H               978412Y   46Z
  50H               978407Y   46Z
1800H     978363X   978410Y   49Z
  10H               978416Y   49Z
  20H               978426Y   49Z
  30H               978435Y   49Z
  40H     978370X   978422Y   50Z
  50H               978410Y   50Z
1900H     978372X   978416Y   50Z
  10H               978429Y   40Z
  20H               978398Y   40Z
  30H               978397Y   40Z
  40H               978395Y   40Z
  50H               978395Y   40Z
2000H     978381X   978395Y   37Z
  10H               978401Y   37Z
  20H               978397Y   37Z
  30H               978405Y   37Z
  40H               978415Y   37Z
  50H               978412Y   37Z
2100H     978390X   978419Y   35Z
  10H               978425Y   35Z
  20H               978429Y   35Z
  30H               978431Y   35Z
  40H               978434Y   35Z
  50H               978431Y   35Z
2200H     978400X   978429Y   33Z
  10H               978430Y   35Z
  20H               978427Y   33Z
  30H               978430Y   33Z
  40H               978433Y   33Z
  50H               978439Y   33Z
2300H     978410X   978443Y   34Z
  10H               978446Y   34Z
  20H               978450Y   34Z
  30H               978454Y   34Z
  40H               978459Y   34Z
  50H               978459Y   34Z
```

Fig. 66. Format.

The output of the computer is the gravity value with which the effect of the longitudinal velocity of the ship (Eotvos Effect) is not corrected.

1·2·2. Flow of informations on total magnetic force, water depth, and ship position.

The output of the proton magnetometer is given as digital prints but not as paper tape punching. The printed data at every minute are plotted in a figure and the values at every 5 min are manually punched on paper tapes together with the data of ship position and water depth, according to the format described in another section of the report.

The ship position is usually given at an interval of 30 or 60 min, from a table prepared by the officers of the ship. The position is not determined by direct measurement but given after being smoothed for a certain duration so that it is expected to be the most probable position of the ship. The water depth is measured by the use of an echo sounder and the data are read out from the chart record at an interval of 10 min.

Corrected water depth, Bouguer correction and Eotvos correction are calculated by the use of the "Batch processing program (program name SAMOA)", from punched tapes containing the data of total magnetic force, ship position and water depth. The Eotvos correction is used for the next stage of the gravity analysis.

When the computer excutes "SAMOA", simultaneously with the on line processing, the outputs of gravity analysis are punched out on the paper tapes through the FACOM WRITER. In this case, the print out is carried out by the use of the OKI TYPER.

1·2·3. After the value of Eotvos correction is obtained, the gravity value calculated in the process mentioned in 1·2·1 is manually punched on the paper tapes, together with the standard gravity and the Eotvos correction according to the format shown in Figure 66. Erroneous gravity value is checked and excluded in this stage.

Further problems in the data processing method.

In the present method of gravity data processing, its ability depends on the speed of manual punching.

During the present cruise the final results were obtained for the track from Tokyo to Sydney, which corresponds to about 2/3 of the whole results.

The first step to be done is the automatic data acquisition of total magnetic force. At the present stage, erroneous data of the proton magnetometer occupies small per cent of the total data (less than 5%) but it is not so easy to reject such data by soft ware programming.

The second step should be automatic data aquisition of water depth. There are many problems in measuring the water depth. The echo sounder installed on board is insufficient as a terminal device for the computer of real time processing. S/N ratio of the echo sounder is low especially when either the depth is more than 5000 m, or the bottom is irregular, or the sea is rough. To discriminate the bottom echo from the noise by the use of this computer will prove to be unwise when the ability of the computer is considered. It will be the best way to use the paper tape output system: batch processing with a powerful analogue filter to improve the S/N ratio of the echo sounder. Ship position, corrected water depth, Bouguer correction, total magnetic force are tabulated in "Geophysical Data of KH–68–4 (Southern Cross Cruise) of the Hakuhō Maru, Ocean Research Institute, University of Tokyo, 1970", and can be obtained on request.

2. Free air gravity anomaly, bottom topography and total magnetic force profiles.

At present, free air gravity anomaly is calculated for the track from Tokyo to Sydney. In the free air gravity profile, large amount of latitude effect is seen. This is caused by the uncorrect scale constant of the gravity meter due to the elastic contribution of the string "Z–68–7–14" and so local free air gravity anomaly will be discussed here.

Position index maps are shown in Figs. 66a–d to see easily the relation between the anomaly and the ship position.

2·1. Profile 1 (Tokyo–Station 2:29°59′ N, 170°02′ W) (Figure 68)

From the geomagnetic point of view, the profile is that of the longitudinal boundary of the western Pacific. In the northern part, magnetic anomaly is large and existence of the lineation of local magnetic anomaly is expected. In the southern part, on the other hand, local magnetic anomaly is generally small, with the exception of those anomalies which exactly correspond to the sea mountains.

Magnetic anomaly becomes large on the east of the North West Pacific Rise. The peak to peak amplitude of local magnetic anomaly at the Northwest Pacific Basin is about 200 γ–300 γ in the west part of the rise and is 300 γ–400 γ in the east part. Magnetic anomaly corresponding to seamounts existing at position index Nov. 20–20 is very small. This seems to be the general character of the seamounts surrounding the Darwin Rise. Anomaly suddenly disappears on the east of the Hawaiian Island and some isolated magnetic anomalies correspond to seamounts. These characteristics are the same with seamounts belonging to the western part of the Marcus Necker Rise.

The minimum free air gravity anomaly at the Japan Trench in the profile is −310 mgal and the gradient of free air anomaly is 94 mgal/1000 m on the oceanic side of the trench and 53 mgal/1000 m on the continental side. The continental side of the trench at this section is more nonisostatic as compared with that of the northern section of the trench.

Free air gravity anomaly on the seamount (position index Nov. 21A–17) is interpreted as caused by the excess mass above the surrounding basin. This characteristic feature shows remarkable difference from the seamounts in the western area of the Marcus Necker Rise or on the Emperor Seamountains, where the seamount is surrounded by topographic or gravimetric trenches.

Profile 2 (Station 2: 29°59′ N, 170°02′ W—Apia, Western Samoa) (Figure 69, Figure 69A, Figure 69B)

The amplitude of magnetic anomaly is generally small (smaller than 100–200 γ) in the northern part of the Marcus Necker Rise and the seamount in the Hawaiian Ridge seems to be reversely magnetized. The seamount has large gravimetric trenches on both sides, like those seamounts belonging to the Emperor Ridge, etc.

At the central part of the Marcus Necker Rise (position index from Station 6 to Station 16), magnetic anomalies approximately correspond to seamounts and although the anomalies are not so large the direction of magnetization seems to be normal. Free air gravity anomalies on these seamounts truly reflect the topography on the flank or at the crest and are negative around them.

A large seamount at the southern end of the Marcus Necker Rise (position index from Station 15 to Station 16) is worth noticing. Free air gravity anomaly is very small compared with the shape and the scale of the seamount. Height of the seamount is about 4000 m above the surrounding basin and yet free air gravity anomaly is only 100 mgal. Considering that the horizontal extent of the seamount is 100 km, it is reasonably considered to be in isostatic equilibrium.

The basin between the Marcus Necker Rise and the Phoenix Islands is characterized by large magnetic anomalies. The bottom topography is generally flat with small irregularity supperposed on it. The maximum magetic anomaly is 800 γ, and the characteristics are similar to those in the North Australia Basin, the Scotia Basin or the Bismark Sea. The area may be interpreted to be formed by the ocean spreading, but like other basins mentioned above no crest of the ridge is recognized.

In the south of the basin (position index from Station 20—Station 23), magnetic anomaly becomes small and disappears at the small gravity trench north east of Apia in Western Samoa. Free air gravity anomaly is as irregular as the bottom topography, but the correspondence between the two is not so clear. This is because the irregular topography is small in its horizontal scale and gravity field disturbance caused by them is attenuated. Magnetic anomaly is very small there in spite of the irregular topography, suggesting that the crustal strucure is continental.

Three magnetic, bathymetric and gravity profiles were obtained between the island of Western Samoa and the basin north east of the island. The contoured maps of total magnetic force and the bathymetric maps were made and shown in Figure 69A and 69B.

Profile 3 (Figure 70)

Magnetic anomaly from Apia to the west of the Niue Island is very small and the anomaly of 200 γ–300 γ begins to appear at the west of Niue Is. and continues to Station 23.

The profile from Station 33 to Station 37 (position index from Dec. 24–12 to Dec. 28–06) is the eastern end of the Chatham Rise. The water depth gradually becomes shallower and is 200 m at its shallowest point. The rise is characterized by several seamounts at position index Station 32–33, Dec. 26–07, Dec. 26–20 and Dec. 27–36. Some of these seamounts can not be recognized from free air gravity anomaly, perhaps due to attenuation, while the magnetic anomaly is recognized exactly corresponding to each of these seamountains.

As the region lies in the middle magnetic latitude, it is difficult to estimate the direction of magnetization, but the magnetization of seamount seems to be reverse relatively to the other seamounts in the region.

Profile 4–1, 4–2 (Tonga Trench) (Figure 71)

4–1 is the profile from 23°11′S, 169°55′W to 23°S, 176°30′W; passing the deepest point of the trench. 4–2 is the profile from 23°16′S, 176°30′W to the Station 29 (25°57′S, 170°16′W).

The minimum free air gravity anomaly in the profile 4–2 is −302 mgal at the deepest point of the trench where the water depth is 10716 m. On the oceanic side of the trench, the gradient of free air anomaly is 98 mgal/1000 m and on the continental side, 66 mgal/1000 m.

Using the results of seismic prospecting in the region of the Tonga Ridge and Trench and examining the difference between the gravity and seismic data, an adjusted crustal section was computed as shown in Figure 72 (Worzel 1965). In the crustal section, the upper surface of the basaltic layer (7.5–6.5 km layer) lies at the depth of about 7 km from the surface of the earth. The depth of this surface is somewhat moved downward to 13 km, at the deepest point of the trench, and horizontal extent of this subsiding region is about 15 miles. This crustal structure will give a good evidence that the origin of magnetic anomaly lies at the surface of the basaltic layer. Because, the magnetic anomalies in both sections are 200–300 γ and seem constant on both side of the trench, though the granitic layer is about 7 km on the continental side and becomes thinner than 2 km on the oceanic side. Depth of the layers other than the basaltic layer is considerably different on both side of the trench and if the origin of magnetic anomaly is assumed to exist in those layers different amplitude of magnetic anomaly will be expected.

Profile 5–1 (position index Dec. 28–16 to Jan. 01–10)

5–2 (Jan. 07–15 to Jan. 10–00) (Figure 73–1, Figure 73–2)

Profile from the South Pacific Basin, the Chatham Rise to Wellington, New Zealand.

Both of the above profiles are the typical examples in which magnetic anomaly

suddenly disappears at the margin of the continental shelf. Magnetic anomaly on the continental shelf of New Zeland is generally smaller than 100 γ. These chracteristics are true for the other sections surveyed by the Umitaka Maru in 1965 and 1966, in the sections from Wellington to the Bounty Island, Wellington to the Antipode Island and off the west coast of the South Island. One exception is the isolated anomaly off Christchurch, where sharp magnetic anomalies larger than 500 γ were observed during this cruise, although the results are not shown in the profile.

Large isolated magnetic anomaly on the continental slope or at the continental margin is also remarkable in this region. The anomaly at position index Dec. 30–10 is closely correlated with the anomaly at position index Jan. 08–00, and is expected to be linked to the anomaly on the oceanic side of the Bounty or Antipode Is. The anomaly will be interpreted to be caused by the difference in the crustal structure between the continent and the oceanic floor. This kind of magnetic anomaly can be seen at the Sandy Cope of the east coast of Australia, at the continental margin of the Rowley Shelf of the northern territory of West Australia or at the continental margin of the East China Sea.

From the gravimetric point of view, the isostatic equilibrium is expected to be perfectly achieved at the continental margin of New Zealand, resulting in the sudden change from continental to oceanic structure.

East coast of the North Island of New Zealand is separated from the Chatham Rise by a trough where the maximum water depth is 3000 m. Free air gravity anomaly near and around the trough truly reflects the bottom topography in such a manner as to suggest that the region subsided. The subsiding region seems to be linked to the Tonga Trench. However, if the trench is caused by the downward motion of the mantle convection, it seems difficult to explain the origin of this trough by the same reason, because the scale of the mantle convection becomes too small.

Profile 6 (South East Pacific Basin to the South Pacific Antarctic Ridge) (Figure 74)

The profile is mainly divided into 3 regions; oceanic basin adjacent to the Ridge (position index Jan. 10–16 to Jan. 13–00, Jan. 18–23 to Jan. 19–05), the flank province of the Ridge (Jan. 13–00 to Jan. 16–09, Jan. 18–05 to Jan. 18–23) and the crest province of the Ridge (Jan. 16–09 to Jan. 18–23).

In the northern region of the ridge, magnetic anomaly in the basin or in the flank province of the ridge is 200–300 γ and the two regions are divided by a region where the anomaly is smaller than 100 γ (position index Jan. 12–17 to Jan. 12–20). This feature can also be seen in the southern region of the ridge where the basin and the flank province are divided by a smaller anomaly region at the positions indexed from Jan. 18–07 to Jan. 18–21.

At the crest province of the ridge, the Rift Valley causes a pair of magnetic anomaly whose amplitude is 1800 γ–2000 γ. The width of the Rift Valley is about 30 miles. At the valley, water depth is about 800 m deeper than the mean depth of the crest on both sides of the valley. Free air gravity anomaly at the valley is about 30 mgal smaller than the value at the crest.

The bottom topography in the flank province is a group of mountains whose height from the base is 500 to 1000 m and at the crest it is generally flat, whose uneveness is reduced to 1/3–1/4 of that of the flank. However, magnetic anomaly in the crest province is twice or three times larger than that in the flank province. This suggests that magnetic anomaly at the ridge cannot be interpreted to be caused by the induced magnetization of the rock.

Free air gravity anomaly in the flank province varies in accordance with the bottom

topography and the flank province is distinguished from the crest province by giant gravimetric valleys.

Gradual change of topography at the crest province is little reflected on the free air gravity anomaly. Moreover, it is generally flat, which suggests that the region was not flattened by the sedimentation or the fall of volcanic ashes filling the valleys as irregular as in the flank province.

Profile 7 (Scott Island to the Sturge Island.) (Figure 75)

The gravimetric and magnetic surveys near and around the Scott Island and the Scott Bank south of the Island were already carried out in the 3rd southern sea expedition of the Umitaka Maru in 1965. During the present cruise a negative free air gravity anomaly was found east of the Island where the free air anomaly is about 40 mgal lower than the averaged anomaly. At the shallowest point about 500 m apart from the Island, water depth is 50 m and free air gravity anomaly is 160 mgal higher than at the surrounding basin. The depth change of 1000 m corresponds to 40 mgal change in gravity.

In the profile from the Scott to Sturge Islands, magnetic anomaly is about 500 γ. A gravimetric trench can also be seen in the east region of the Sturge Island where the free air gravity anomaly is about 30 mgal lower than the average value and the width of the trench is about 80 miles.

Profile 8 (Sturge Island to the Tasman Sea) (Figure 76–1, 76–2)

The profile is the east part of the South Indian Antarctic Ridge. The trend of the ridge in this section is north east to south west and linked to the South Pacific Antarctic Ridge with a bridge of the Macquarie Ridge.

The crest of the ridge is magnetically identified at the positions indexed by Jan. 23–12 and Jan. 24–08. The Rift Valley lies between the position indices Jan. 23–14 and Jan. 23–17. The valley is about 900 m deeper than the crest and free air gravity anomaly is 38 mgal lower than the value at the crest. The bottom topography in the flank province is not so rough as in the case of the South Pacific Antarctic Ridge described above. No gravimetric valley can be seen at the boundary between the crest and the flank province. On the contrary, two negative free air gravity anomalies whose amplitude and horizontal extent are 30–20 mgal and 20–30 miles respectively lie between the flank and the basin.

In the basin north of the ridge, magnetic anomaly is 300–500 γ. It gradually becomes small and is 100–200 γ at the region from Jan. 20–00 to Jan. 31–19. The anomaly at the central part of the Tasman Basin is 100–200 γ. The ship crossed the top of a seamount in the Tasman Basin. Magnetic anomaly is very small there compared with usual isolated seamounts in the basins.

Profile 9 (Sydney to Noumea) (Figure 77)

The profile is along the east coast of Australia from Sydney to Smoky Cape and from Smoky Cape to Noumea, New Caledonia crossing the northern part of the Tasman Basin, the Lord Howe Rise and the New Caledonia Basin. Free air gravity anomaly in the profile is not calculated yet.

At the continental margin off Smoky Cape, a magnetic trench is recognized between position indices Feb. 10–10 and Feb. 10–13, where the anomaly is smaller than 100 γ. In the Tasman Basin from indices Feb. 10–13 to Feb. 11–04, the anomaly is about 200 γ but it disappears at the foot of the East Tasman Rise. The Bank at position indices Feb. 11–12 and Feb. 11–14 belongs to a series of sea mountains running north to south from the southern end of the Coral Sea to the seamount described in the profile 8. The bank is about 3000 m shallower than the surrounding basin and the ship crossed the summit of the bank. Magnetic anomaly at the bank is only 300 γ and the characteristic feature is similar to the bank at position index Feb. 02–23 in the profile 8.

Magnetic anomaly becomes large at the east part of the Lord Howe Rise and disappears at the west of the New Caledonia Basin. The peak to peak amplitude of the anomaly is 600 γ with wave length of about 150 miles. The anomaly is expected to run parallel to the trend of the Rise which the ship crossed almost perpendicularly. Therefore, from the scale of the anomaly, it seems likely that the anomaly is caused by the same origin as that existing at the margin of the continental and oceanic structures, suggesting that the anomaly indicates the location of tectonic boundary between New Caledonia and the Tasman Sea. It is also noteworthy that no magnetically indicated boundary is recognized between New Caledonia and the New Caledonia Basin.

Profile 10 (Noumea to New Guinea) (Figure 78)

The profile is along the west coast of New Caledonia, across the east part of the Coral Sea, the Slot, the northern part of the Solomon Sea, along the south east coast of New Britain and the north coast of New Guinea.

Along the west coast of New Caledonia, magnetic anomaly is extremly small (smaller than 100 γ) as often seen on the shelf of a stable continental crust. From the results of surface geology of New Caledonia, it has been found that some part of the island is covered with peridotite which is the rock occurring in the upper mantle, and the fact led us to suspect that there was a large magnetic anomaly here. The fact that the actually observed anomaly was small in this region may suggest that the layer of the peridotite is not so thick and that New Caledonia is heaved up by the underthrusting motion of the thick continental mass continuing to the New Caledonia Basin.

Magnetic anomaly along the east coast of the Coral Sea is also very small, though the region is bounded by zones of small magnetic anomaly at the north end of New Caledonia (position index Feb. 17–02) and west of the Indispensable Reefs or east of the Rennell Island which is the eastern end of the Louisiade Archipelago.

Magnetic anomaly at the Solomon Sea, from the Rennell Is to the Guadalcanal Island or from Bougainville to New Britain is about 100–200 γ and is similar to those of the West Indies.

The anomaly of long wave length seems to exist in the Slot or Solomon trench, but it will be discussed later after removing the effect of the regional field because, in this case, the ship often altered its course.

Profile 11 (New Guinea to Tokyo) (Figure 79)

The profile is along the north coast of New Guinea (from Vitiaz Strait to Aitape), the western end of the Bismark Archipelago, across the west Caroline Basin, near the Yap across the Mariana Basin and to the Sagami Bay.

Along the north coast of New Guinea between New Guinea and the islands linked to the New Britain Island such as the Long Island, the Kar Kar Island and the Manan Is., magnetic anomaly is about 300 γ and its amplitude does not decrease even at the continental margin of New Guinea. This characteristic feature resembles that of the continental margin of north America where the old oceanic ridge comes up to the continent.

Large magnetic variations are noted to exist between the Manan Is. and New Guinea on the Hydrographic chart. The ship approached to the island and cruised along its south west coast. Maximum anomaly in total force observed is 500 γ, which is not so large, and yet affects much the compass deviation, because the region lies in magnetically low latitude. Maximum compass deviation expected from the anomaly in total force is 2.5° and about 2° deviation was observed in the magnetic compass.

Though large magnetic anomaly was found in the previous survey (Results of KH–67–3) in the eastern region of the Bismark Archipelago between 148° to 151°E, small anomaly is recognized in the western part. The anomaly becomes extremely small at the

Rise at position index Feb. 22–15.

Magnetic anomaly suddenly appears at the west Caroline Basin and disappears at the west Caroline Rise. The anomaly will be explained as caused by the same origin as in the case of North Australia Basin etc. described in the Profile 2.

Magnetic anomaly from the west Caroline Rise to the Sagami Bay is 0–100 γ, and occurs independently of the characteristics of bottom topography such as the Yap Trench, the Yap Island, the Mariana Basin east of the Philippine Sea. As was shown by several profiles crossing the west part of the Izu Mariana Islands, the area of small anomaly extends westward and covers the Philippine Basin, where its southern part is bounded by the Mariana Island or the Caloline Island. The existence of the region of 200–300 γ is limited to a narrow band along the Palau Kyushu Ridge.

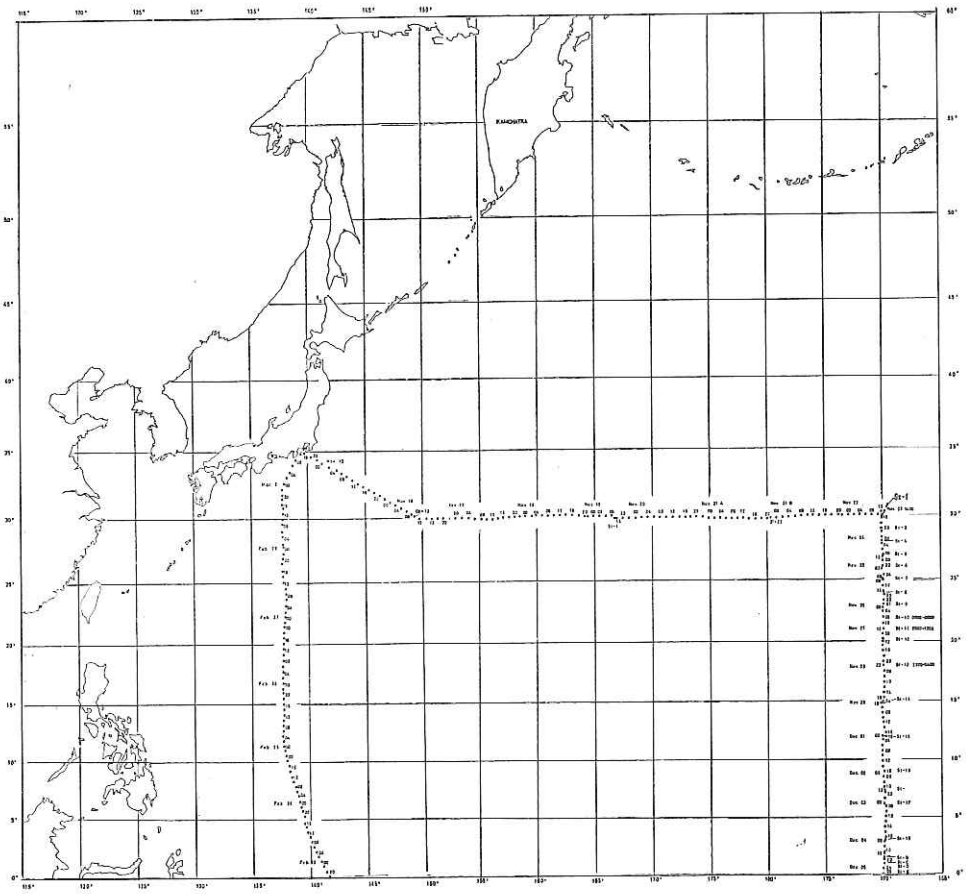

Fig. 67–a. Position index map for free air gravity anomaly and ship position.

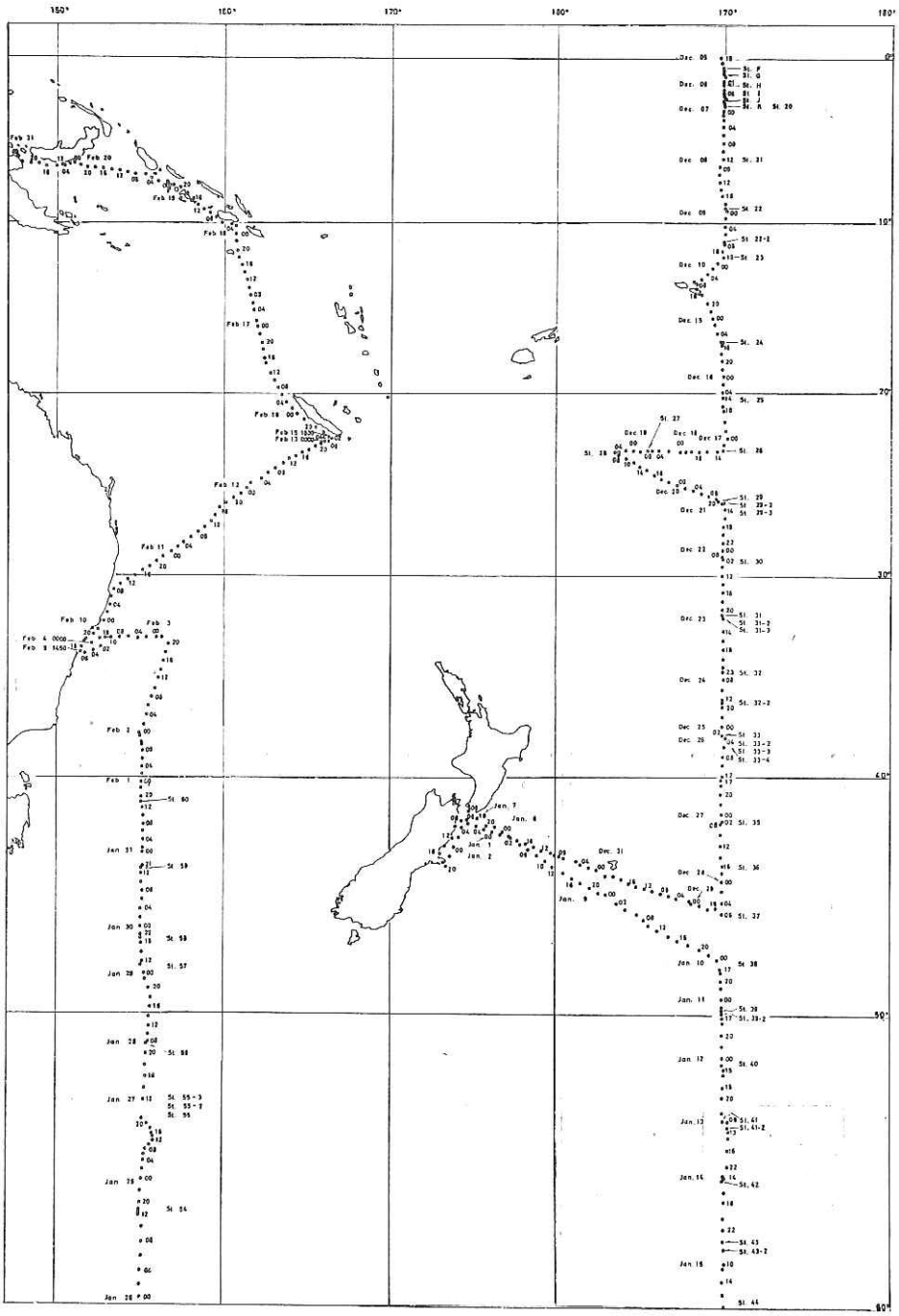

Fig. 67–b. Position index map for free air gravity anomaly and ship position.

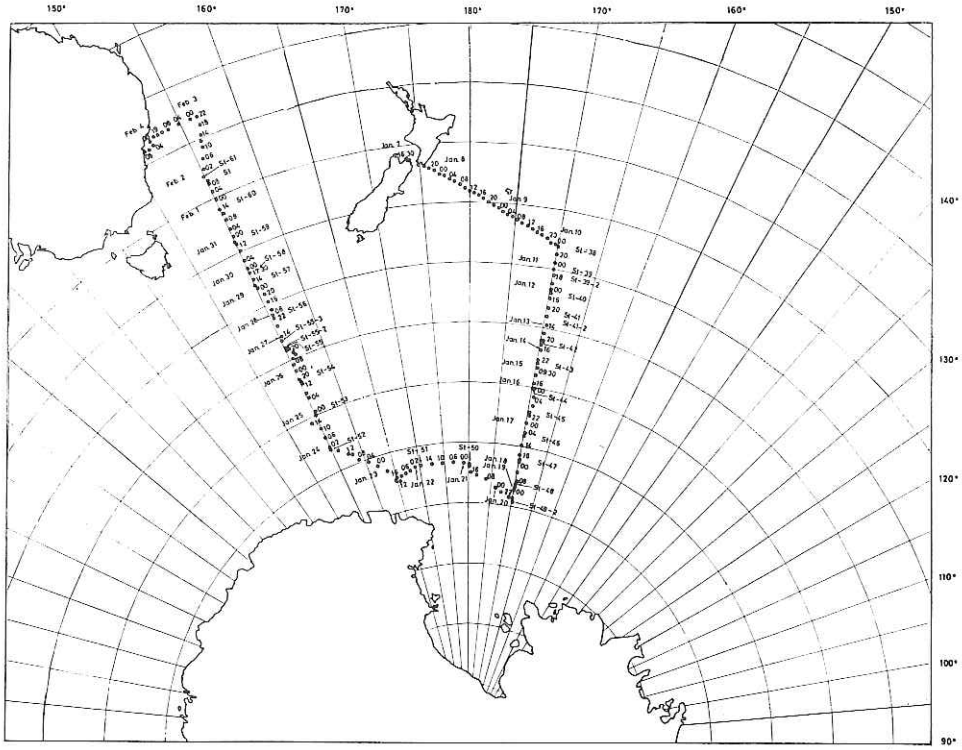

Fig. 67–c. Position index map for free air gravity anomaly and ship position.

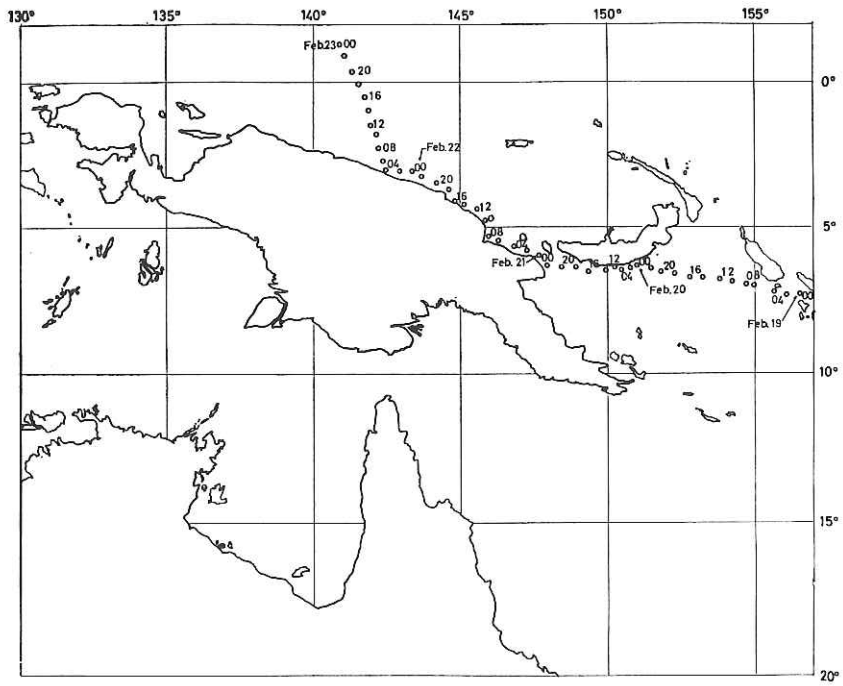

Fig. 67–d. Position index map for free air gravity anomaly and ship position.

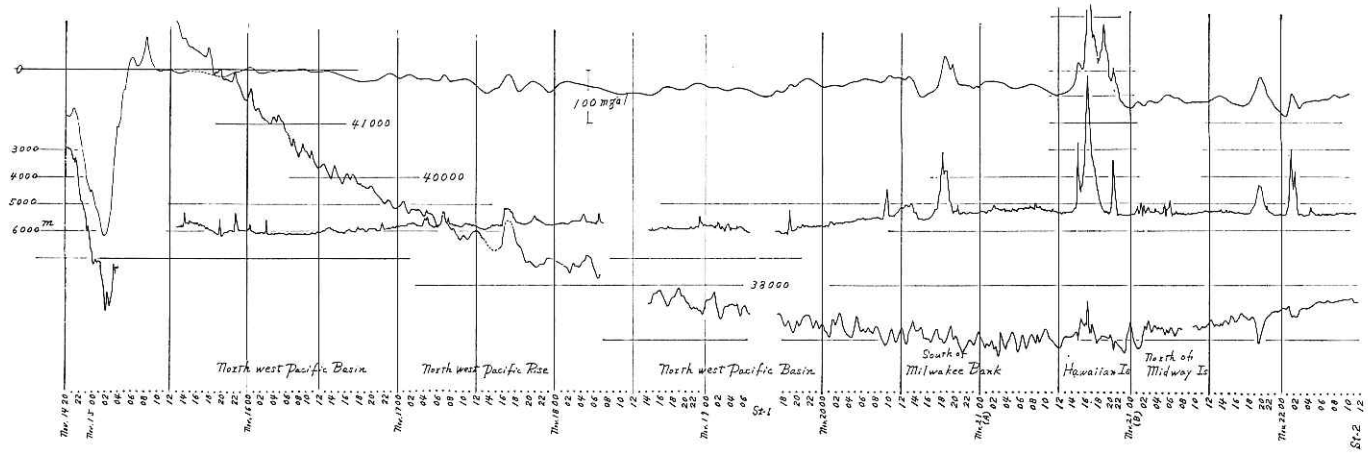

Fig. 68. Free air gravity anomaly, total magnetic force, and bottom topography. Profile 1 (Tokyo—Station 2).

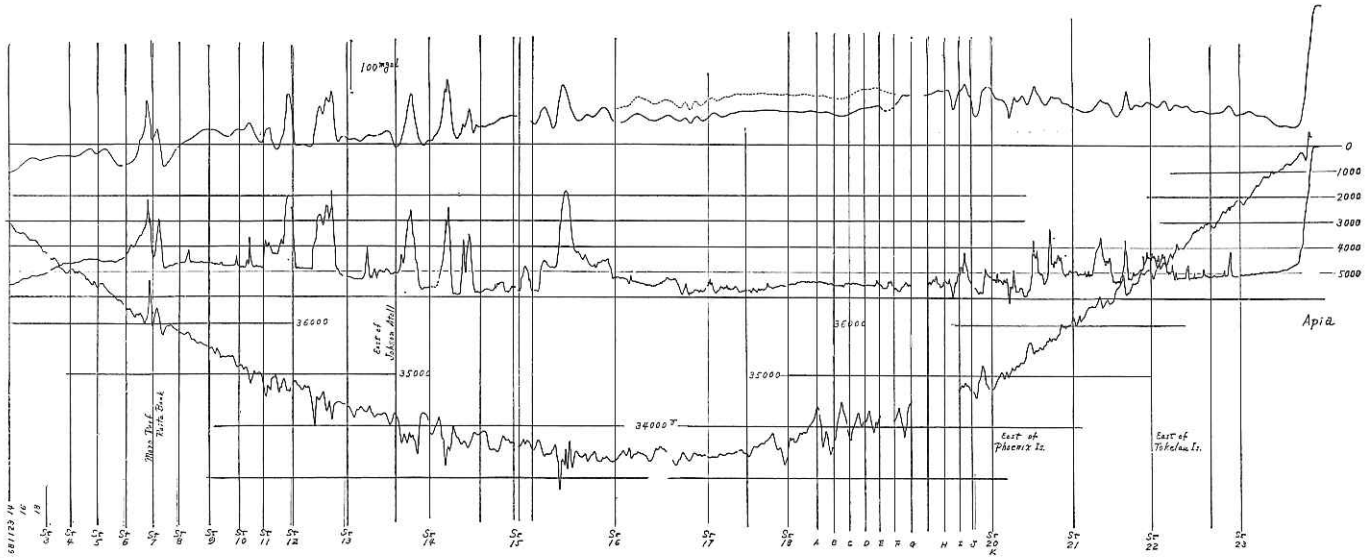

Fig. 69. Free air gravity anomaly, total magnetic force, and bottom topography. Profile 2 (Station 2—Apia, Western Samoa).

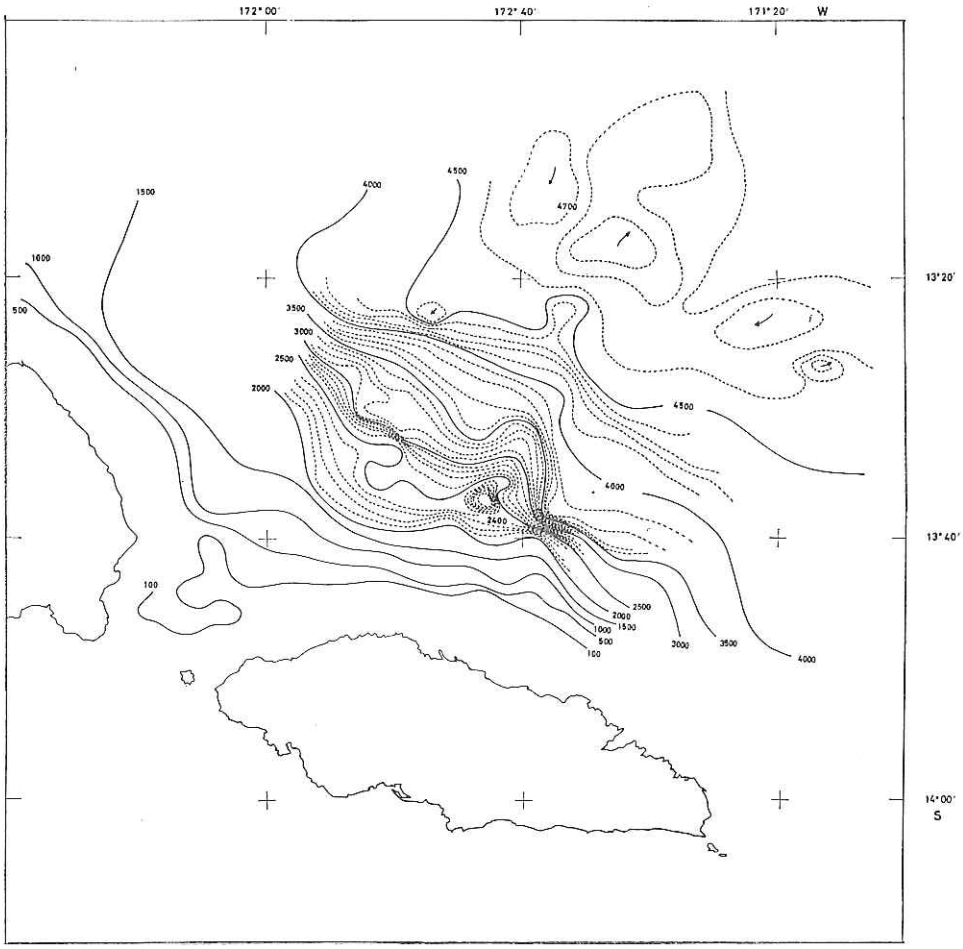

Fig. 69–A. Bathymetric map, north of Western Samoa.

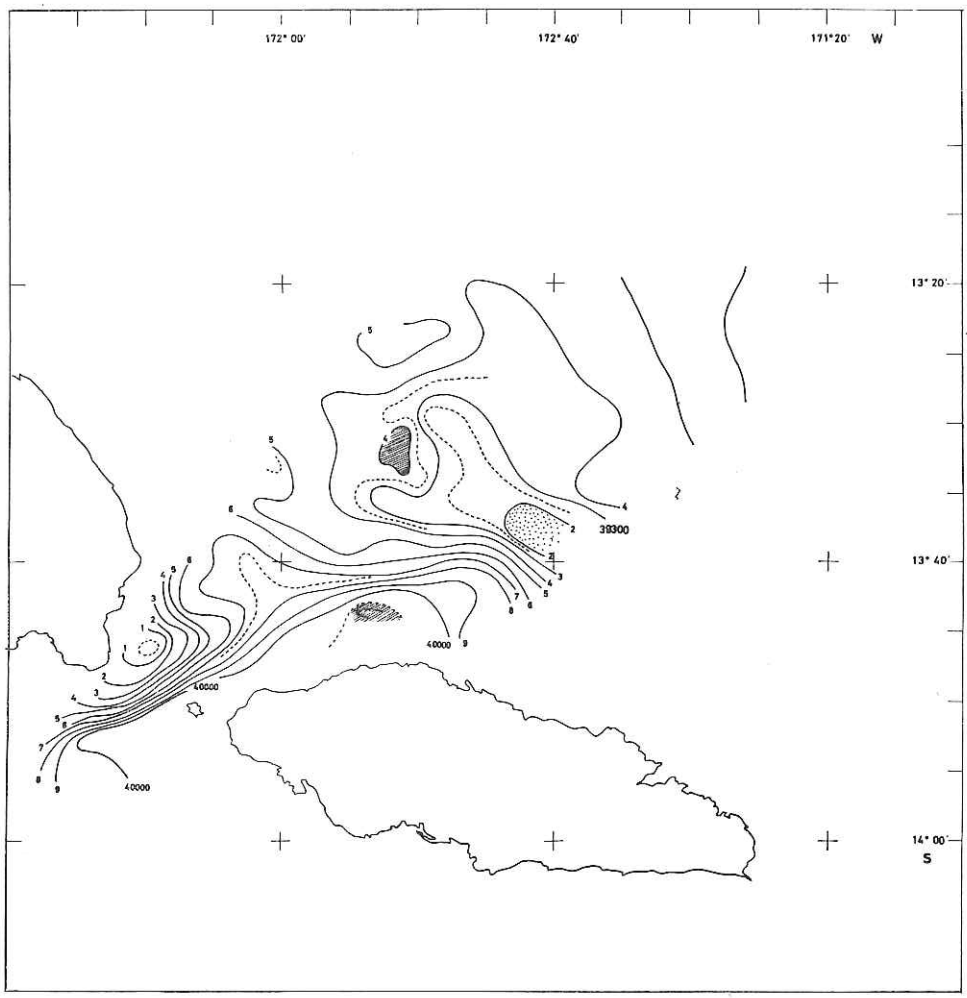

Fig. 69–B. Magnetic map, north of Western Samoa.

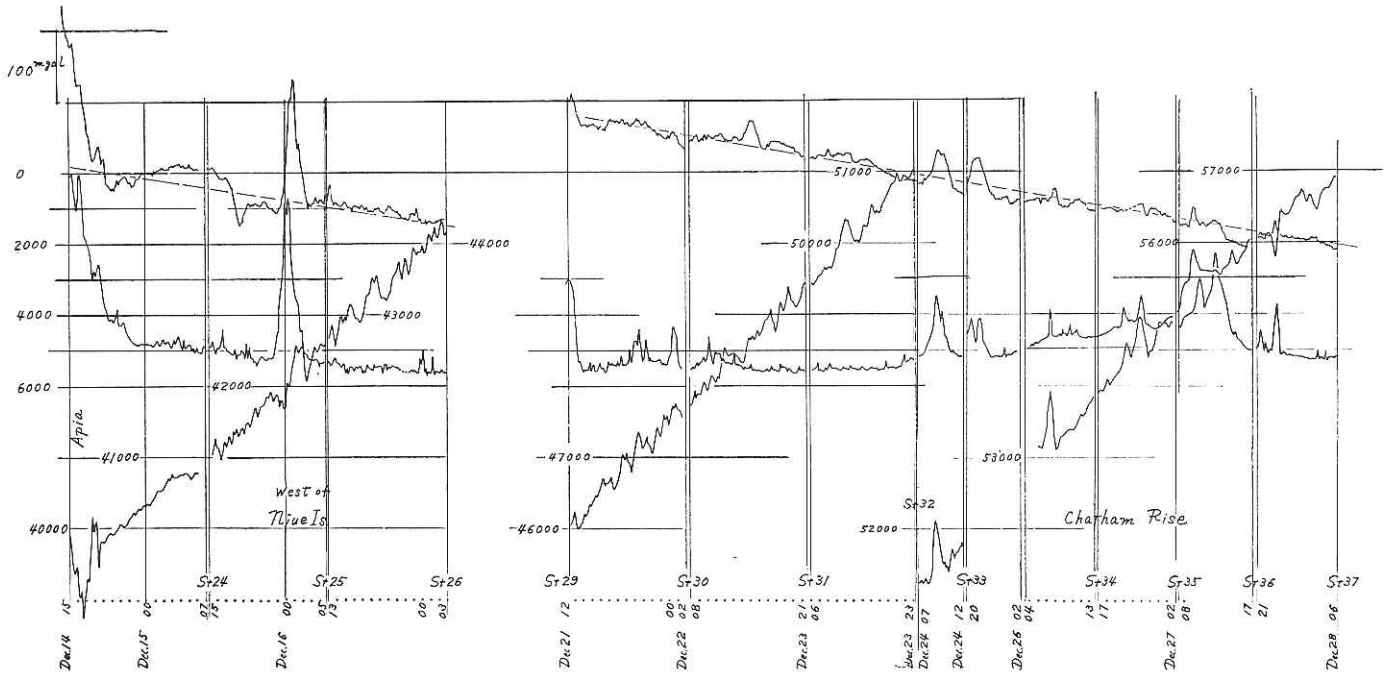

Fig. 70. Free air gravity anomaly, total magnetic force, and bottom topography. Profile 3 (Apia—West of Niue Island).

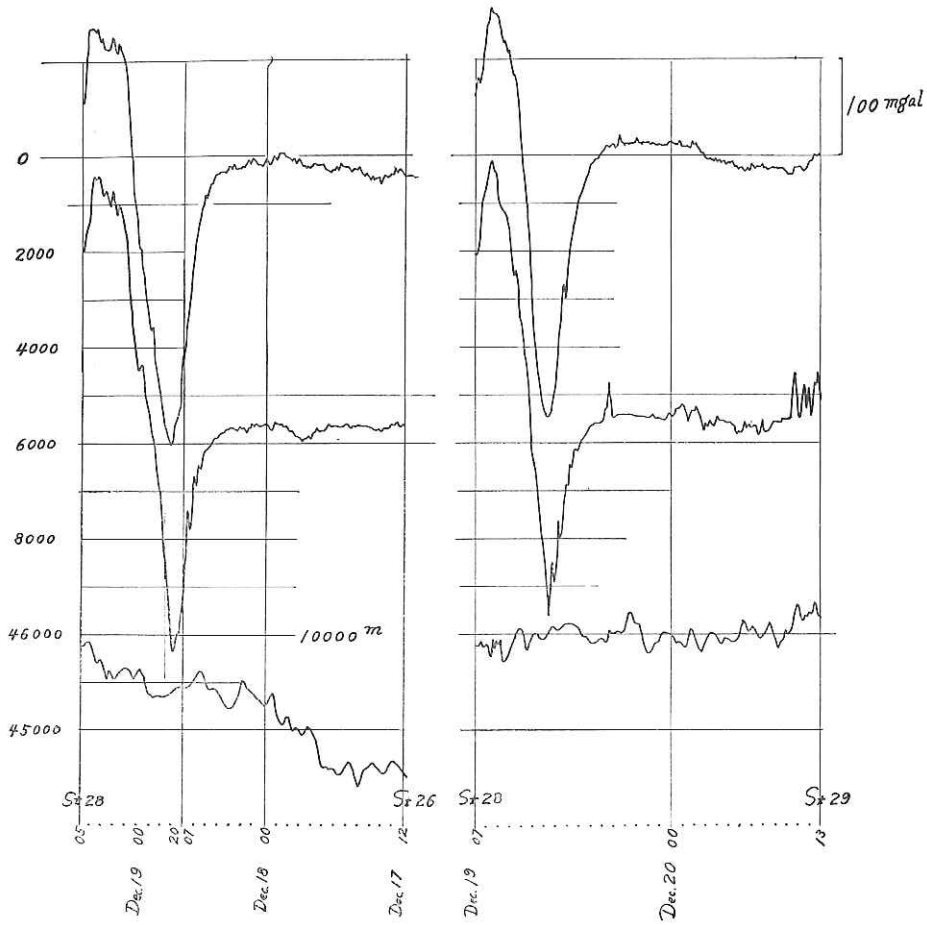

Fig. 71. Free air gravity anomaly, total magnetic force, and bottom topography. Profile 4–1, 4–2 (Tonga Trench).

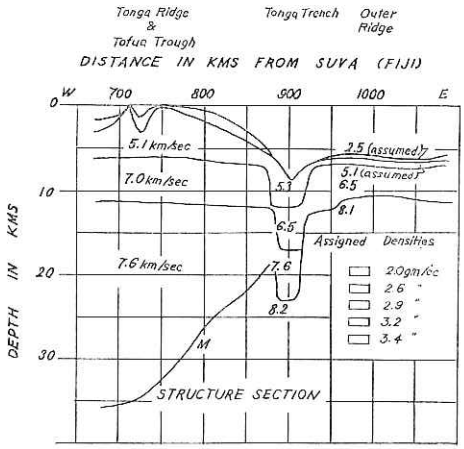

Fig. 72. Crustal section of Tonga Trench.

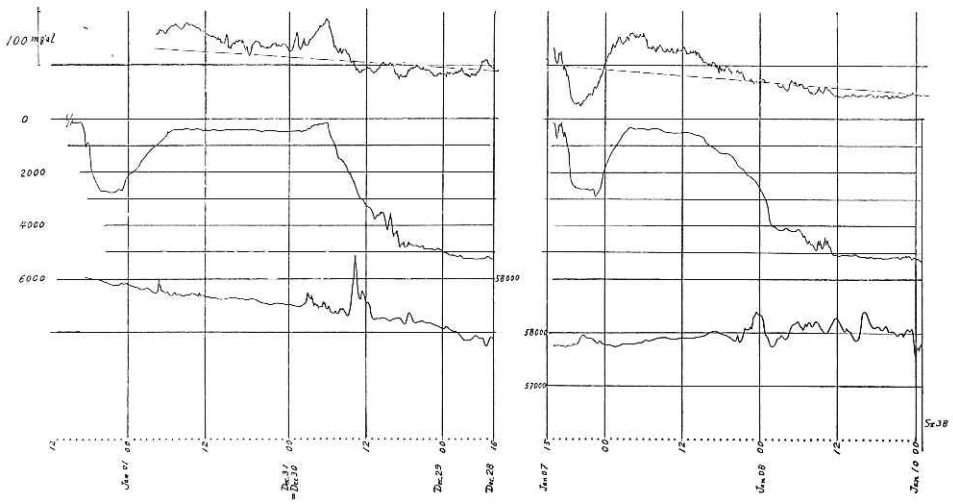

(1) (2)

Fig. 73–1, 73–2. Free air gravity anomaly, total magnetic force, and bottom topography. Profile 5–1, 5–2 (South Pacific Basin, Chatham Rise to Wellington).

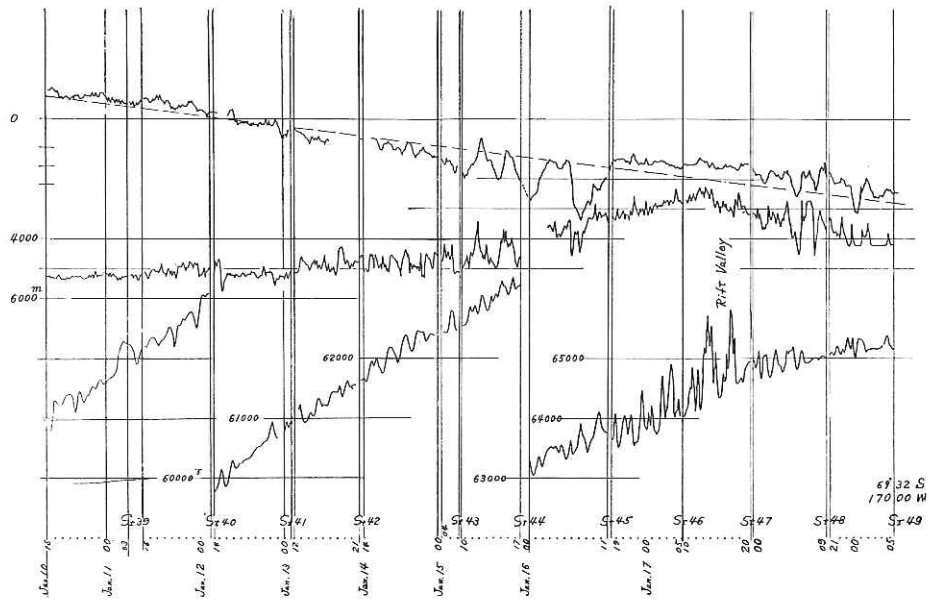

Fig. 74. Free air gravity anomaly, total magnetic force, and bottom topography. Profile 6 (South East Pacific Basin—South Pacific Antarctic Ridge).

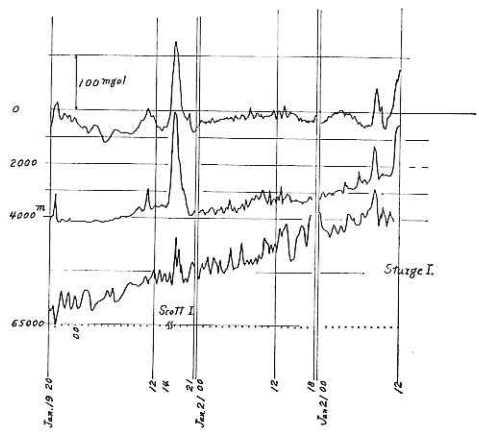

Fig. 75. Free air gravity anomaly, total magnetic force, and bottom topography. Profile 7 (Scott Island—Sturge Islands).

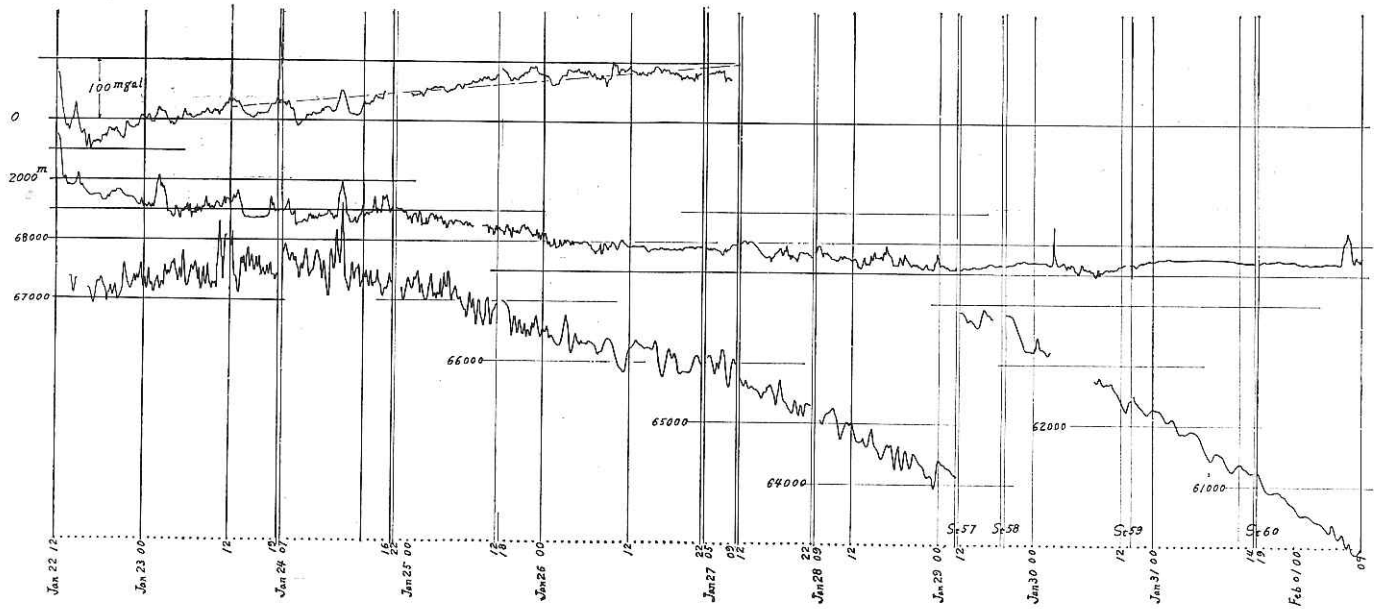

Fig. 76–1. Free air gravity anomaly, total magnetic force, and bottom topography. Profile 8 (Sturge Islands—Tasman Sea).

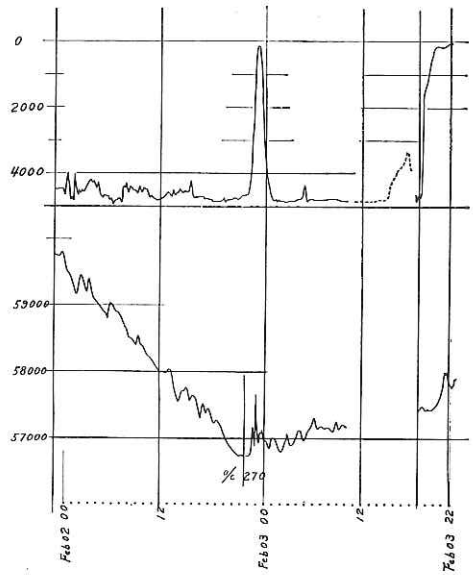

Fig. 76–2. Total magnetic force, and bottom topography. Profile 8 (Sturge Islands—Tasman Sea).

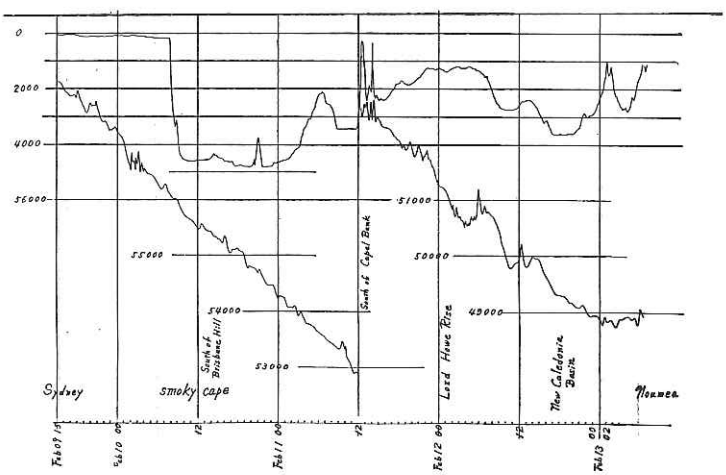

Fig. 77. Total magnetic force, and bottom topography. Profile 9 (Sydney—Noumea).

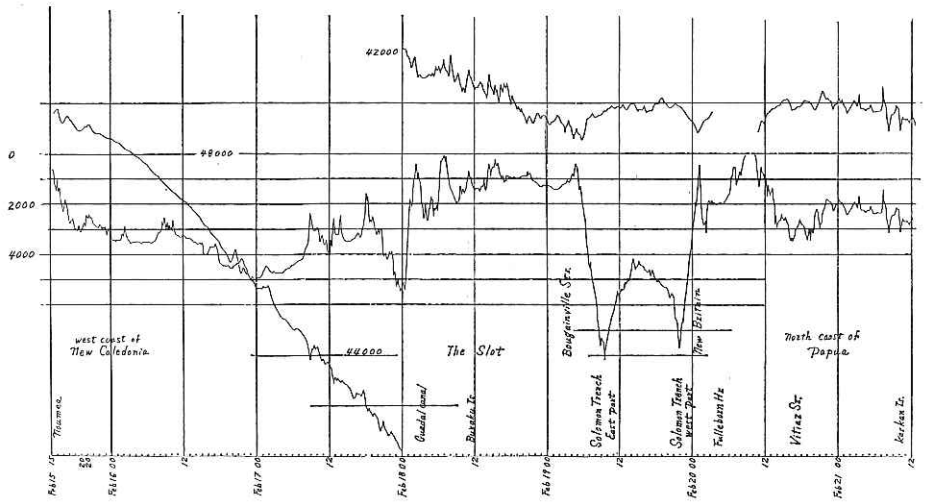

Fig. 78. Total magnetic force, and bottom topography. Profile 10 (Noumea—New Guinea).

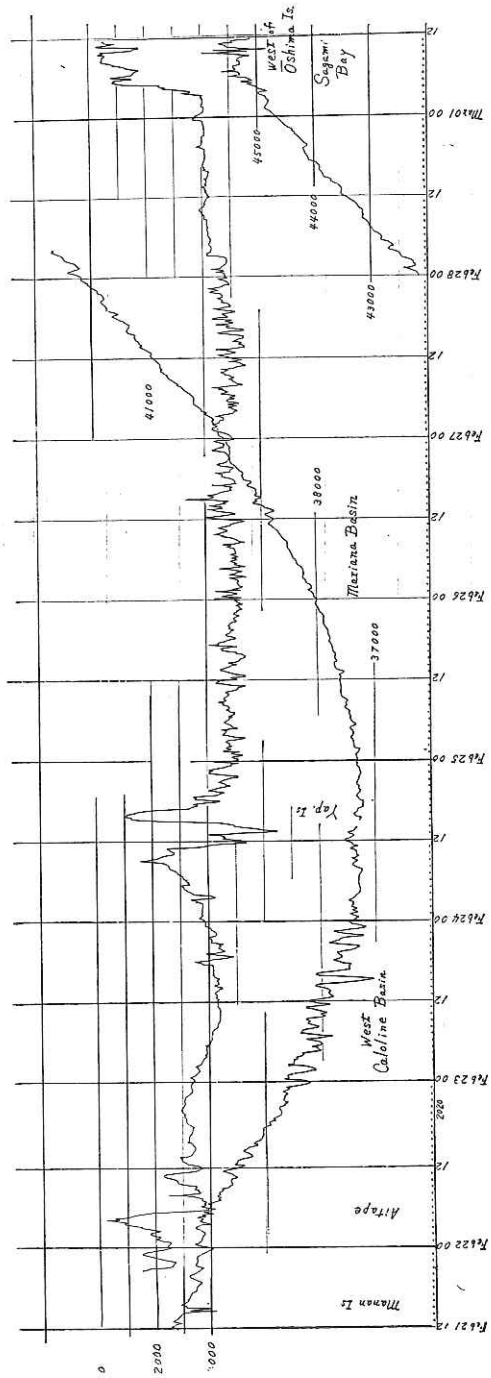

Fig. 79. Total magnetic force, and bottom topography. Profile 11(New Guinea—Tokyo).

VIII. 2.2. Gravity Measurement on Land

by

K. Koizumi

In order to calibrate the ship borne gravity meter (T.S.S.G.), gravity measurement was carried out at the wharfs whenever the ship arrived at the ports. The measurement was carried out by the use of the Lacoste Romberg land gravity meter 'G 124' at Apia (Western Samoa), Wellington (New Zealand), Sydney (Australia) and Noumea (New Caledonia).

The gravity value at these stations was determined relative to the gravity base at Harumi (Wharf of the Ocean Research Institute), Tokyo.

In the case of Noumea, the ship could not reach the wharf and the land gravity value was measured at the pier of the ferryboat about 1 mile apart from the ship.

The location of these land stations, scale reading of the gravity meter, free air gravity anomaly are shown in Table 13, Figures 80, 81, 82, and 83.

The discrepancy between the old and new measurements is about 10 mgal at Berth No. 3 Circular Quay at Sydney. The former measurement was determined relative to the gravity base station at the Dominion Observatory in Wellington and the latter was referred to the temporary gravity base at Harumi, Tokyo. The difference will be interpreted as the result of uncorrectly assumed gravity value at Harumi.

The free air gravity anomaly at Apia in Western Samoa is +302 mgal. Compared with the Islands in the central Pacific, the value is comparable to the value at Hawaii (Pearl Harbor; 207 mgal), Samoa (Pago Pago: 306 mgal) and 278 mgal of Penrhyn Island.

The free air gravity anomaly at Noumea is +113 mgals. The value is not so large when we consider the geological evidence that the ultra basic rock of upper mantle lies near the surface. According to the results of surface geology of New Caledonia, the peridotite or serpentine is found parralel to the Island, and the Nickel ores are found in the metamorphic rock adjacent to the ultra basic rock.

The existence of high density of peridotite or serpentine will result in higher positive anomaly than in the case of the Hawaii or Samoa Islands.

According to Arthur Holmes, this fact will be interpreted as the oceanic floor has riden over the adjoining continental crust, like 'Cyprus'.
(Arthur Holmes, Principle of Physical Geology 1965)

The crustal structure will be discussed later by the use of the gravity value at sea near Noumea and off the west coast of New Caledonia measured in this cruise.

Table 13.

	Date D/M/Y	Time J.S.T.:L.T.	Latitude	Longitude	Scale reading	Gravity value	Free air anomaly
Tokyo	11/11/68	14/30	35°38.58N	139°46.45E	3307.430	979.800	
Apia	11/12/68	07/30	13°49.17S	171°45.36W	2189.930	978.645	+302 mgals
	11/12/68	11/30					
Well.	02/01/69	05/20	41°17.45S	174°47.30E	3791.570	980.301	+ 5 mgals
N.Z.	02/01/69	08/20					
Sydney	04/02/69	10/20	33°51.70S	151°12.79E	3215.200	979.705	+ 55 mgals
	04/02/69	11/20					
Noumea	13/02/69	19/55	22°16.26S	166°26.01E	2438.055	978.902	+113 mgals
	13/02/69	21/55					
Tokyo			35°38.58N	139°46.45E			

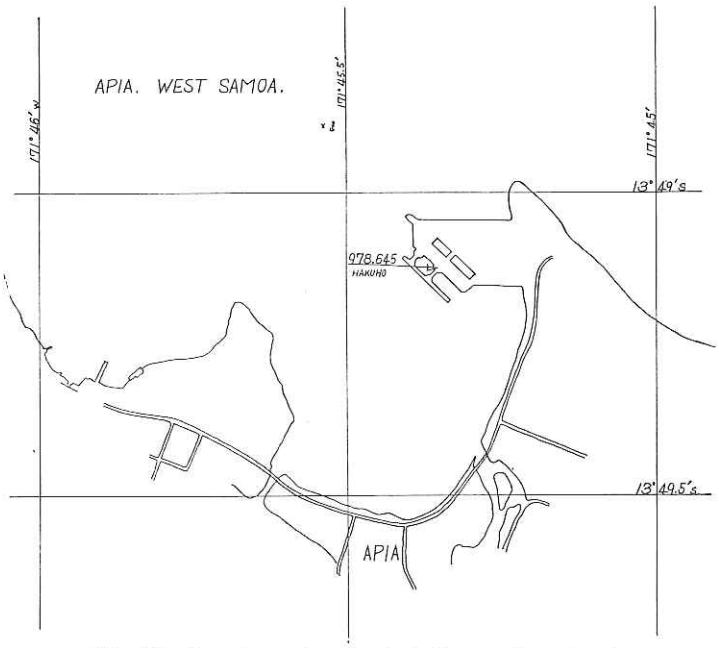

Fig. 80. Location of station Apia for gravity on land.

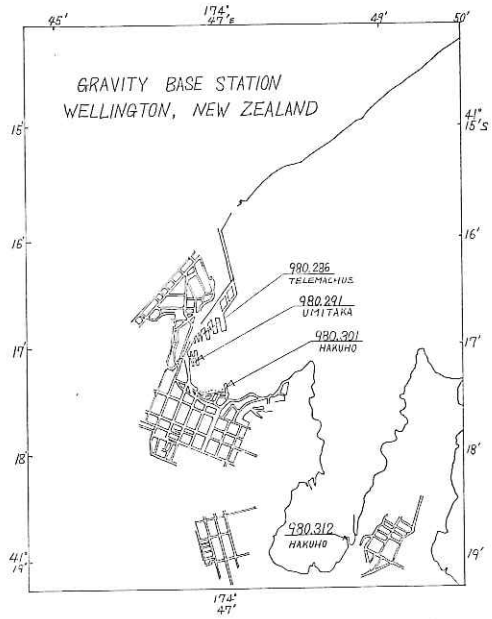

Fig. 81. Location of station Wellington for gravity on land.

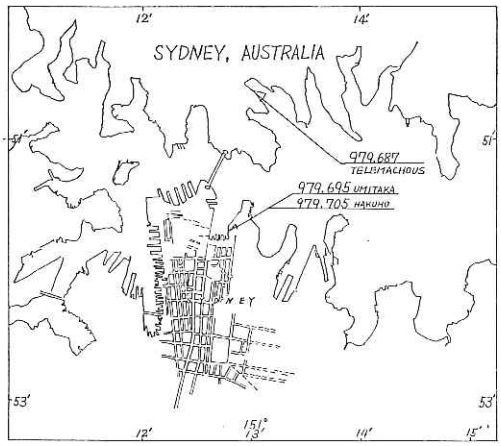

Fig. 82. Location of station Sydney for gravity on land.

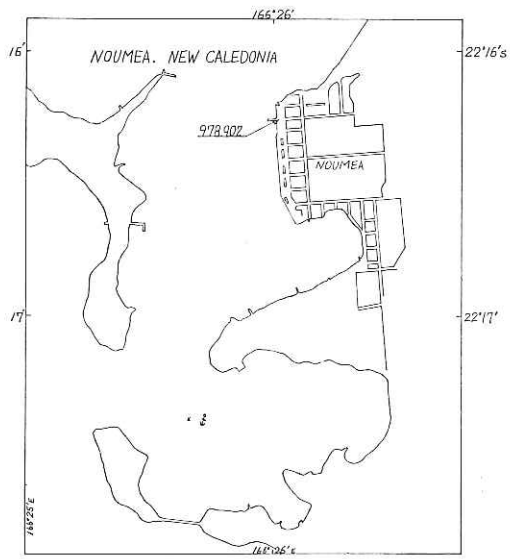

Fig. 83. Location of station Noumea for gravity on land.

VIII.2.3. On Line Real Time Processing Program of the Gravity Data

by

T. Igarashi

1. Introduction

The gravity meter (T.S.S.G.) installed on R. V. Hakuho Maru provides the output information of 6 bits times 3 plus a sign bit, i.e. 19 bits in total every 0.5 sec.

Until this cruise the routine procedure has been in such a way that the 19 bits information is automatically perforated on the paper tapes and the gravity values are calculated on land by the BATCH processing using the electronic computers after each research cruise.

Because of the increase of the gravity data it has become impossible to analyze these data by means of the former manner and there is a serious requirement to know the gravity values on board the ship.

For these reasons the electronic computer FACOM 270–20 which is capable of process control and general scientific calculations has been installed on the ship. The computer was installed in the No. 8 Laboratory of the ship on April 1968. In order to analyze the gravity data by the use of this computer, the BATCH processing program was compiled and tested during the preceding cruise. (Preliminary Report of the Hakuhō Maru Cruise KH 68–3)

On line processing program of the gravity data was completed in the middle of Dec., 1968 during this cruise, and since then gravity data have been continuously analyzed by the program.

The computer has worked perfectly well throughout the whole cruise and the gravity values at more than 10,000 sites have been determined. The configuration of the FACOM 270–20 system used in this cruise is shown in Figure 84.

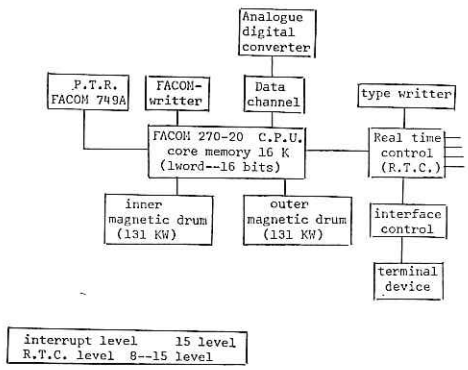

Fig. 84. Block digram of FACOM 270–20 on board.

2. Interface between the gravity meter and the R.T.C.

2·1. The R.T.C. (Real Time Control) of the computer has the following digital input terminal.

Digital input; Contact operate .....8 words (16 bits 8)
Electric signal input .....4 words (16 bits 4)
Interrupt; Contact operate .....16 points

The contact operate digital input and the interrupt circuit has a low pass filter whose time constant is about 25 milli sec and 13 milli sec respectively.

Direct connection of the ground side of the terminal device and the ground side of the R.T.C. input terminal may possibly induce electric noise and it is desirable to use contact operate terminal of the R.T.C., electrically separated by a relay. However this plan was given up because of the following reasons.

1) reliable relays which are capable of working with such a short time interval as 100–150 m sec are not available.

2) Because of the capacitor involved in the input circuit of the R.T.C., some amount of time delay in transmitting the data is caused so as to result in a time difference between the interrupt signal and the input information signal.

In the present cruise, the electric signal input (1 word; 16 bits) of the R.T.C. was adopted.

2·2. Interface between R.T.C. and the gravity meter.

The control signals (1 sign bit, 6 signal bits and 1 feed bit) of the tape puncher which is the terminal device of the T.S.S.G., were transferred to the R.T.C. through 8 lines with the transmission length of 100 m each.

The signals are converted into bipolar voltage fitted to the standard of the R.T.C. input, say $+1 \text{---} -8$V and $0 \text{---} +8$V, by the use of 7 sets of the I. C. Comparater. The feed signal was used as the interrupt signal by the use of the switching transister circuit connected to the contact operate terminal for interrupt. The capacitor in the interrupt circuit of the R.T.C. was removed.

3. The Format of the input Data

As described above, the output signal of the T.S.S.G. was at first used to the tape puncher. One set of data consists of 18 bits + 1 sign bit, and these digits which are put forth successively are divided into 3 segments, each consisting of 6 bits as shown in Figure 85.

One group of data consisting of 1000 data, is sent forth within a time interval of 9 min 30 sec and no data in the following 30 sec is sent force to the computor (Figure 86). Among these 1000 data, 800 are used for the calculation of the gravity.

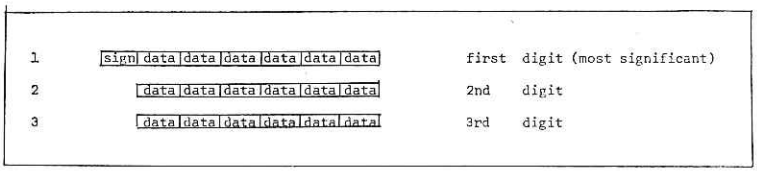

Fig. 85. One set of input data.

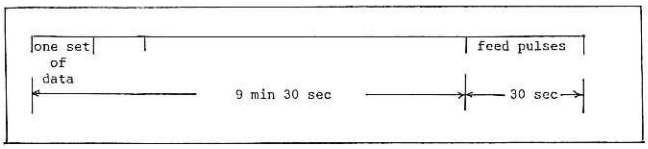

Fig. 86. Time chart of data processing.

4. Gravity calculations

The formula of computing the gravity are expressed by the following equations, where

$$K_1\left(\sum_{i=0}^{n} w_i/T_{i-k}\right)\Big/\left(\sum_{i=0}^{n} w_i T_{i-h}\right) = G(k)$$

$$K_2 \left\{ \sum_{i=0}^{n} w_i (1/T_{i-k})^2 - (\Sigma\, T_i / \Sigma\, T_i) \right\}^2 \Delta G(k)$$

$$g(k) = G(k) + \Delta G(k)$$

T_i; input data

w_i; weight function

K_1; numerical constant proper to the frequency of oscillation of the string gravity meter.

K_1; numerical constant for the second order correction for the finite sampling interval.

5. Flow chart of real time processing program of the gravity data (Figure 87).

5·1. Data processing is chiefly divided into high level and low level processings. The high level porcessing is a part of program concerned with the R.T.C. and plays a role of writing the data on the magnetic drum. The low level processing works as the BATCH processing of the data written on the drum. Some parts of the low level processing are executed within the time interval between the consecutive write in operations on the drum, and the other parts of the processing which requires all data are executed in the time between the end of write in and the arrival of the first data of the next group. The content of the data processing method included in the low level processing is almost the same as GRAVITY DATA BATCH PROCESSING PROGRAM and will not be described here. (See Preliminary Report of the Hakuhō Maru Cruise KH–68–3)

5·2. Flow chart of high level processing program

The following items are processed in the high level.

1) Discrimination of useful data. That is, judgment whether the data should be written in the drum or abandoned.

2) Grouping of one set of data and the compilation of the data.

3) Discrimination of erroneous data.

The item 1) is executed by the FEED CONTROL. As described above, one group of data are placed between the spaces of 30 sec during which the content of the data is zero. As the input data are the oscillation periods of the string in the gravity meter, the values never become zero. One set of the transferred data consists of three segments, each consisting of 6 bits information, i.e. three characters in octal form. Therefore it can not be expected that the most significant digit in the octal form becomes zero. This means that the information can not be expected to come from the gravity meter when more than three zero signals are succeeded.

By the use of this condition, if the contents of 6 bits input information are zero, the R.T.C. reads new digits by the next interrupt. If the zero continues 4 times, the computer judges that the information means space between the group of data and reads the new data until none zero digits are read in, without executing any function except read in function.

The item 2) is executed by SING BITS SENSE and X SENSE. When the read in digits are none zero, the data are first checked by the X. When the drum is already filled enough data for gravity computation, say, 800 words, the X is set to 1 and the following data are discriminated as the excess ones. The compuer does not execute any function without read in.

When the X is not set ($X = 0$), the computer judges whether the data are the most significant digits or not according to the sign bits. If the sign bits are 1, these digits together with the following two digits are compiled as one set of data of 16 bits. When the

number of data becomes 50 which is equal to the capacity of 1 record of the drum, then the 50 sets of data are written on the drum. When the data are wirtten in the 16 RECORDS of the drum, say 800 data are written, the low level interrupt takes place and the computations are executed and thereafter the final results are printed out.

The item 3) is executed by the use of the ERROR CONTROL and COUNT. When the computer reads any one of the data, the number 1 is set in the ERROR COUNT, and this is reset if 16 records are written on the drum. This means that, if a group of data is read in but the number of the data is not enough to EXECUTE the required computation, the group of the data is abandoned. When a group of data is abandoned the content of the error count is 1, and is added to the data number so that the abandoned group can be recognized when the final results of gravity are printed out with the data number.

6. On line real time processing program of the gravity data written in the FASP is shown in Table 14. An example of the results of the computation is shown in Table 15.

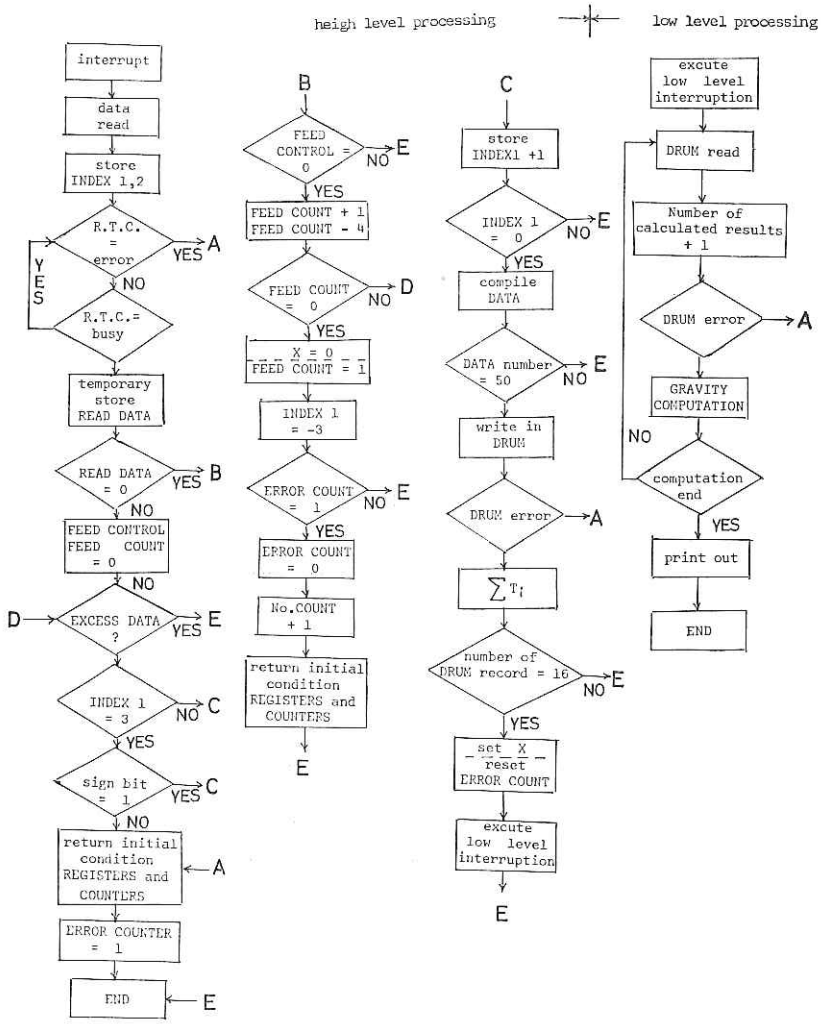

Fig. 87. Flow chart of real time processing program of the gravity data.

Table 14. High level processing program.

```
    XIO.L,READ,#2@          ——————  read R.T.C.
    L.R,IND1@
    ST.L,#1@
    L.R,IND2@
    ST.L,#2@
    B.L,P3@
    IND1;DN,-3@             ——————  specify figures
    IND2;DN,-100@           ——————  specify Number of DATA written
                                    in 1 record of the Drum
    IND3;DN,-16@            ——————  specify Number of Recor          Parameter Area
                                    written in the Drum
    EVEN@
    READ;DN,#2110,DATA@
    SENCE;DN,#B000,0@
    PARK;BSS,100@           ——————  store temporary read DATA
    CONT1;DN,0@
    CONT2;DN,#FFFF@
    CONT5;DN,4@
    CONT6;DN,1@
    CONT7;BSS,1@
    CONT8;BSS,1@
    CONT9;BSS,1@
    ERR;BSS,1@
    ZERO;DN,0,0@
    KAKUM;DN,-100@
    KAKUD;DN,-16@
    M3;DN,-3@
    D8;DN,#80@
    MASK;BSS,1@
    DRADD;DN,#400@          ——————  Drum write,head address (1) when channel 1
    DR1;DN,#400@
    DR2;DN,#410@            ——————  Drum write,head address(2) when channel 2
    CH1;DN,CHNEL1@
    CH2;DN,CHNEL2@
    DRR;DN,#400@
    DATA;BSS,1@
    DATA1;BSS,3@
    EVEN@
    TOTAL1;BSS,2@           ——————  Σ x_i
    TOTAL2;BSS,2@           ——————  Σ x_i²
    WS1;BSS,1@
    AB1;DN,#D7C@
    AB2;DN,#D7D@
    P3;XIO.L,SENCE,#2@      }       read R.T.C. and sense(read END and check ERROR)
    B.L,P2,Z@               }
    B.R,P4@                 }
    P2;EOR.R,CONT6@         }
    B.L,ERROR,Z@            }
    B.R,P3@                 }
    P4;L.R,DATA@
    ST.L,*1,DATA1+3@
    B.L,P5,Z@
    L.R,CONT8@
    B.L,=END,Z@             ——————  discriminate FEED DATA and abandon
    L.R,CONT9@              }
    A.R,CONT6@              }
    ST.R,CONT9@             }
    S.R,CONT5@              }
    B.L,P55,Z@              }       discriminate FEED DATA
    ST.R,CONT7@
    L.R,CONT2@
    ST.R,CONT8@
    LD.L,ZERO@
    STD.L,TOTAL1@
    STD.L,TOTAL2@
```

Table 14. (Continued)

```
    L.R,M3@
    ST.L,IND1@
    L.R,ERR@
    B.L,P7,Z@          ERROR check
    B.L,=END@
    P7;L.R,ZERO@
    ST.R,ERR@          ERROR RESISTER clear
    B.L,P40@
    P5;L.R,ZERO@
    ST.R,CONT8@
    ST.R,CONT9@
    P55;L.R,CONT7@
    B.L,=END,Z@        discriminate EXCESS DATA
    L.L,#1@
    S.L,M3@
    B.L,P8,Z@          discriminate Most Significant Digit
    L.R,DATA1@
    SR.S,7@
    B.L,P8,Z@          discriminate SIGN BIT
    ERROR;L.R,KAKUM@
    ST.L,IND2@
    L.L,KAKUD@
    ST.L,IND3@
    L.L,M3@            ERROR processing
    ST.L,IND1@
    LD.L,ZERO@
    STD.L,TOTAL1@
    STD.L,TOTAL2@
    L.R,CONT2@
    ST.R,ERR@
    L.L,DRR@
    ST.L,DRADD@
    B.L,=END@
    P8;AX.S,*1,1@
    B.R,P6@            verify "Read in 3 Character"
    B.R,P10@
    P6;STX.L,*1,IND1@
    B.L,=END@
    P10;SLD.S,32@
    L.L,DATA1+2@
    SRCR.S,6@
    L.L,DATA1+1@       complie DATA
    SRCR.S,6@
    L.R,D8@
    EOR.L,DATA1@
    SRCR.S,4@
    STD.L,*2,PARK+100@
    AD.L,TOTAL1@       calculate -∑ Xi
    STD.L,TOTAL1@
    LD.L,*2,PARK+100@
    SLD.S,14@
    ST.L,WS1@          ∑ Xi²
    M.L,WS1@
    SRAD.S,8@
    AD.L,TOTAL2@
    STD.L,TOTAL2@
    L.L,M3@
    ST.L,IND1@
    AX.S,*2,2@
    B.R,P11@           verify "Read in 50 sets of DATA"
    B.R,P12@
    P11;STX.L,*2,IND2@
    B.L,=END@
```

Table 14. (Continued)

```
P12;CTL.L,MASK,#4@
L.L,DRADD@
ST.R,DRA@
NOE3;L.L,#64@
B.L,P20;Z@
P30;LX.L,*1,*@
B.L,=STDR@                          write in DRUM
VFD,3/2,13/1@
DN,PARK@
DRA;DN,#400@
DN,-1@
B.R,*@
CTL.L;MASK,#5@
L.L,KAKUM@
ST.L,IND2@
L.L,DRADD@
A.L,CONT6@
ST.L,DRADD@                         verify"Drum write in and Data read end"
L.L,IND3@
ST.L,#3@
AX.S,*3,1@
B.R,P13@
B.R,P14@
P13;STX.L,*3,IND3@
B.L,=END@
P14;L.L,KAKUD@
ST.L,IND3@
LD.L,TOTAL1@
STD.L,#D78@
LD.L,TOTAL2@
STD.L,#D7A@                         excute computation and
                                    set Parameter for the next Data
LD.L,ZERO@
STD.L,TOTAL1@
STD.L,TOTAL2@
EVEN@
NON2;B.L,CHNEL1@
CHNEL1;L.L,CONT2@
ST.L,#D7C@
L.L,AB2@
ST.L,NOE3+1@
L.L,DR2@
ST.L,DRADD@
ST.L,DRR@
L.L,DR1@
ST.L,#D7E@
L.L,AB1@
ST.L,#D7F@                          Switch processing to the channel 2
L.L,CH2@
ST.R,NON2+1@
B.L,P15@
CHNEL2;L.L,CONT2@
ST.L,#D7D@
L.L,AB1@
ST.L,NOE3+1@
L.L,DR1@
ST.L,DRADD@
ST.L,DRR@
L.L,DR2@
ST.L,#D7E@                          Switch processing to the channel 1
L.L,AB2@
ST.L,#D7F@
L.L,CH1@
ST.R,NON2+1@
```

Table 14. (Continued)

```
P15;ST.L,CONT7@
L.L,ZERO@
ST.L,ERR@
LX.L,*1,*@
B.L,=PINT@          excute "Gravity Analysis" according to
DN,#2805@           the low level processing program
B.L,=END@
P20;L.L,CONT2@      } set ERROR RESISTER
ST.L,ERR@           }
B.L,ERROR@
P40;L.L,#D80@       process Data Number if ERROR
A.L,CONT6@
ST.L,#D80@
B.L,=END@
END@
¥XORG-D84PN-080101¥STOP
```

low level processing program

```
LX.L,*1,-800@
L.L,CV2@
ST.L,BP@
LD.L,#D7A@
BB.L,FCVT@
STD.L,TPSG@
L.L,CV1@
ST.L,BP@
LD.L,#D78@
BB.L,FCVT@
STD.L,TISG@
FD,TPSG@
STD.L,ANSW1@
FM,ANSW1@
STD.L,ANSW1@
L.L,#D7F@
ST.L,NOE1+1@
L.L,#D80@
A.L,ONE@
ST.L,#D80@
L.L,#D7E@
SL.S,8@
ST.L,DRA@
P6;STX.L,*1,INDEX1@
BB.L,DREAD@
L.L,DRA@
A.L,RONE@
ST.L,DRA@
LX.I,*1,INDEX1@
LX.L,*2,-100@
P5;LD.L,*2,DATA2+100@
BB.L,FCVT@
STD.L,*1,DATA1+900@
AX.L,*1,2@
B.R,P3@
B.R,P4@
P3;AX.S,*2,2@
B.R,P5@
B.R,P6@
P4;LX.L,*1,-8@
P1;STX.L,*1,INDEX1@
BB.L,DREAD@
L.L,DRA@
A.L,RONE@
```

$$\left(\sum X_i \Big/ \sum X_i^2\right)^2$$

Drum Data read out parametef control program

Table 14. (Continued)

```
        ST.L,DRA@
        LX.L,*1,-800@
        P7;LD.L,*1,DATA1+900@
        STD.L,*1,DATA1+800@
        AX.L,*1,2@
        B.R,P7@
        LX.L,*1,-100@
        P8;LD.L,*1,DATA2+100@
        BB.L,FCVT@
        STD.L,*1,DATA1+900@
        AX.L,*1,2@
        B.R,P8@
        LX.L,*2,0@
        JMP9;LX.L,*3,0@
        L.L,D2@
        ST.L,KKK+1@
        LD.L,DDO@
        STD.L,AAAA@
        SLD.S,32@
        LX.S,*3,-16@
        AN;STD.L,*3,ANSW2+16@
        AX.S,*3,2@
        B.R,AN@
        JMP10;LD.L,*3,OMEGA@
        STD.L,WS1@
        FLW,FZERO@
        LD.L,*2,DATA1@
        STD.L,WS2@
        FMW,WS1@
        FAW;OHK2@
        FSTW,OHK2@
        FLW,DONE@
        FDW,WS2@
        STD.L,WS2@
        FMW,WS1@
        FAW,ONETH@
        FSTW,ONETH@
        LD.L,WS2@
        FM,WS2@
        FS,ANSW1@
        STD.L,ANSW2@
        FM,ANSW2@
        FM,WS1@
        FA,ANSW3@
        STD.L,ANSW3@
        AX.L,*2,2@
        L.L,#3@
        S.L,INDEX3@
        B.L,KKK,Z@
        L.L,MINAS2@
        ST.L,KKK+1@
        LD.L,DOO@
        STD.L,AAAA@
        KKK;AX.L,*3,2@
        B.R,AAAA@
        B.R,JMP10@
        M3;B.L,JMPA@
        EVEN@
        DOO;B.L,M3@
        DDO;B.L,JMP10@
        AAAA;B.L,JMP10@
        DATA8;EFLD,8@
        CQ;DN,KOTAI@
```

Parameters for computation control program

Table 14. (Continued)

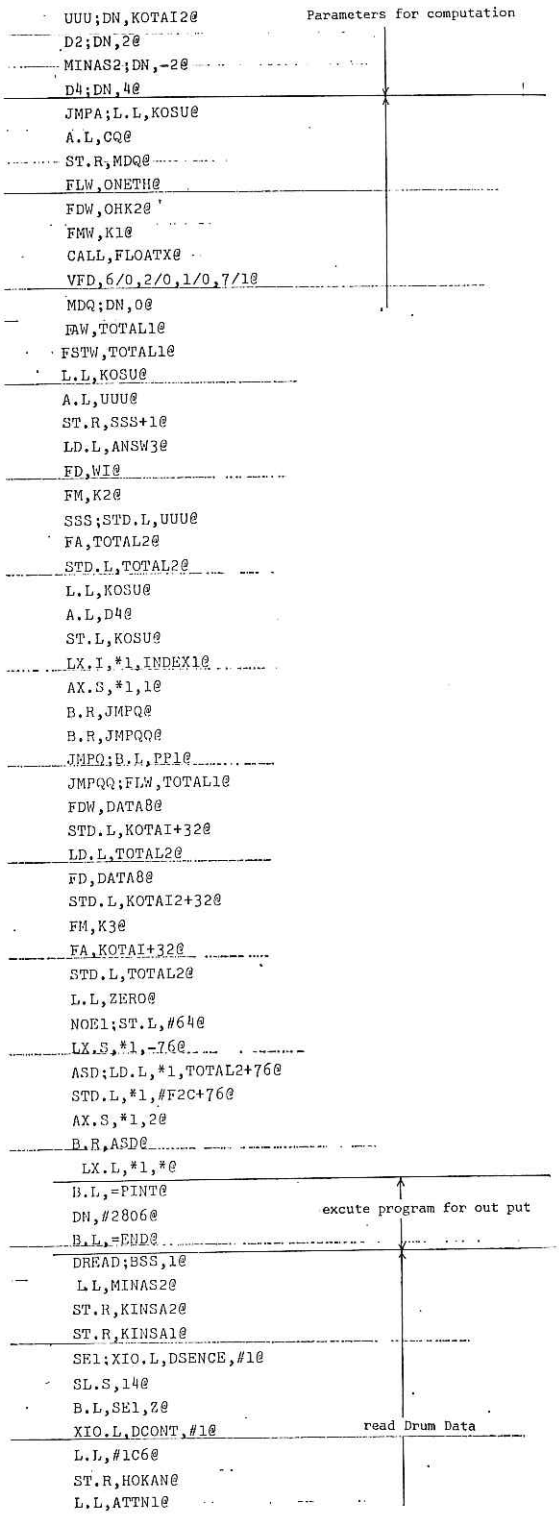


```
      UUU;DN,KOTAI2@
      D2;DN,2@
      MINAS2;DN,-2@
      D4;DN,4@
      JMPA;L.L,KOSU@
      A.L,CQ@
      ST.R,MDQ@
      FLW,ONETH@
      FDW,OHK2@
      FMW,K1@
      CALL,FLOATX@
      VFD,6/0,2/0,1/0,7/1@
      MDQ;DN,0@
      FAW,TOTAL1@
      FSTW,TOTAL1@
      L.L,KOSU@
      A.L,UUU@
      ST.R,SSS+1@
      LD.L,ANSW3@
      FD,WI@
      FM,K2@
      SSS;STD.L,UUU@
      FA,TOTAL2@
      STD.L,TOTAL2@
      L.L,KOSU@
      A.L,D4@
      ST.L,KOSU@
      LX.I,*1,INDEX1@
      AX.S,*1,1@
      B.R,JMPQ@
      B.R,JMPQQ@
      JMPQ;B.L,PP1@
      JMPQQ;FLW,TOTAL1@
      FDW,DATA8@
      STD.L,KOTAI+32@
      LD.L,TOTAL2@
      FD,DATA8@
      STD.L,KOTAI2+32@
      FM,K3@
      FA,KOTAI+32@
      STD.L,TOTAL2@
      L.L,ZERO@
      NOE1;ST.L,#64@
      LX.S,*1,-76@
      ASD;LD.L,*1,TOTAL2+76@
      STD.L,*1,#F2C+76@
      AX.S,*1,2@
      B.R,ASD@
       LX.L,*1,*@
      B.L,=PINT@
      DN,#2806@
      B.L,=END@
      DREAD;BSS,1@
       L.L,MINAS2@
      ST.R,KINSA2@
      ST.R,KINSA1@
      SE1;XIO.L,DSENCE,#1@
      SL.S,14@
      B.L,SE1,Z@
      XIO.L,DCONT,#1@
      L.L,#1C6@
      ST.R,HOKAN@
      L.L,ATTN1@
```

Table 14. (Continued)

```
        ST.L,#1C6@
        KIN1;L.L,KINSA1@
        B.L,KIN1,P@
        KIN2;L.R,KINSA2@
        B.L,KIN2,P@
        B.I,DREAD@
        QUAD@
        DSENCE;DN,#A100,CA@
        DCONT;DN,#C100,CADD@
        READ;DN,#2000,DATA2,100@        Drum read parameters
        QUAD@
        CADD;DN,#1000@
        DRA;DN,0@
        CA;BSS,2@
        ATTN2;DN,BLAN2@
        HOKAN;BSS,1@
        RONE;DN,#100@
        ATTN1;DN,BLAN1@                 Drum interruption processing parameter area
        KINSA1;BSS,1@
        KINSA2;BSS,1@
        BLAN1;XIO.L,DSENCE,#1@
        XIO.L,READ,#1@
        L.R,ATTN2@
        ST.R,KINSA1@
        ST.L,#1C6@                      Drum interruption processing area
        B.I,#187@                       (Interruption processing and Read Error check)
        BLAN2;XIO.L,DSENCE,#1@
        L.R,HOKAN@
        ST.R,KINSA2@
        ST.L,#1C6@
        B.I,#187@
        FCVT;BSS,1@
        CALL,FXFL@
        BP;DN,#31@                      decimal to binary conversion
        B.I,FCVT@
        QUAD@
        ANSW1;BSS,4@
        ANSW2;BSS,4@
        ANSW3;BSS,4@
        ONETH;BSS,4@
        OHK2;BSS,4@
        TOTAL1;BSS,4@
        TOTAL2;BSS,4@
        KOTAI;BSS,36@
        KOTAI2;BSS,36@
        OUTAR;BSS,12@
        WS1;BSS,4@                      Parameters for computation
        WS2;BSS,4@                      Drum read Data                  area
        FZERO;EFLD,0@
        DONE;EFLD,1@
        WI;EFLD,2956877@
        TISG;BSS,2@
        TPSG;BSS,2@
        DATA1;DA,900@
        DATA2;DA,128@
        INDEX1;BSS,1@
        INDEX3;DN,444@
        ZERO;DN,0@
        ONE;DN,1@
        KOSU;BSS,1@
        CV1;DN,31@
        CV2;DN,43@
        DATAPU;DN,#2B@
```

Table 14. (Continued)

```
QUAD@
K1;EFLD,410572+5@
K2;EFLD,168569367+13@
K3;EFLD,0.0018@
OMEGA;FLD,1,3,6,10,15,21,28,36,45,55,66,78,91,105
,120,136,153,171,190,210,231,253,276,300,325,351,
378,406,435,465,496,528,561,595,630,666,703,741,7
80,820,861,903,946,990,1035,1081,1128,1176,1225,1
275,1326,1378,1431,1485,1540,1596,1653,1711,1770,
1830,1891,1953,2016,2080,2145,2211,2278,2346,2415
,2485,2556,2628,2701,2775,2850,2926,3003,3081,316
0,3240,3321,3403,3486,3570,3655,3741,3828,3916,40
05,4095,4186,4278,4371,4465,4560,4656,4753,4851,4
950,5050,5150,5250,5350,5450,5550,5650,5750,5850,
5950,6050,6150,6250,6350,6450,6550,6650,6750,6850
,6950,7050,7150,7250,7350,7450,7550,7650,7750,785
0,7950,8050,8150,8250,8350,8450,8550,8650,8750,88
50,8950,9050,9150,9250,9350,9450,9550,9650,9750,9
850,9950,10050,10149,10247,10344,10440,10535,1062
9,10722,10814,10905,10995,11084,11172,11259,11345
,11430,11514,11597,11679,11760,11840,11919,11997,
12074,12150,12225,12299,12372,12444,12515,12585,1
2654,12722,12789,12855,12920,12984,13047,13109,13
170,13230,13289,13347,13404,13460,13515,13569,136
22,13674,13725,13775,13823,13869,13913,13955,1399
5,14033,14069,14103,14135,14165,14193,14219,14243
,14265,14285,14303,14319,14333,14345,14355,14363,
14369,14373@
END@
¥PRBLSPRG100005¥STOP
```

weight function storage area

low level program 2(Type out program)

```
EXTN,CTPFW@
CALL,OPNT@
DN,CTPFW@
B.R,*@
BB.L,CRPRT@
L.L,#D80@
CALL,IBDC@
DN,OUTAR+1@
BB.L,PRINT1@
BB.L,CRPRT@
LX.S,*1,-36@
P1;LD.L,*1,#F30+36@
BB.L,DCS@
BB.L,PRINT1@
AX.S,*1,4@
B.R,P1@
BB.L,CRPRT@
LX.S,*1,-36@
P2;LD.L,*1,#F30+72@
BB.L,DCS@
BB.L,PRINT2@
AX.S,*1,4@
B.R,P2@
LD.L,#F2C@
BB.L,DCS@
BB.L,PRINT1@
BB.L,CRPRT@
CALL,CLST@
B.L,=END@
PRINT1;BSS,1@
LX.S,*2,-4@
```

Table 14. (Continued)

```
    L.L,SP@
    PR;BB.L,PRINT@
    AX.S,*2,1@
    B.R,PR@
    LX.S,*2,-6@
    PR2;L.L,*2,OUTAR+7@
    BB.L,PRINT@
    AX.S,*2,1@
    B.R,PR2@
    B.I,PRINT1@
    PRINT2;BSS,1@
    LX.S,*2,-3@
    L.L,SP@
    P21;BB.L,PRINT@
    AX.S,*2,1@
    B.R,P21@
    LX.S,*2,-4@
    P22;L.L,*2,OUTAR+5@
    BB.L,PRINT@
    AX.S,*2,1@
    B.R,P22@
    LX.S,*2,-3@
    P23;L.L,*2,OUTAR+11@
    BB.L,PRINT@
    AX.S,*2,1@
    B.R,P23@
    B.I,PRINT2@
    CRPRT;BSS,1@
    L.L,CR@
    BB.L,PRINT@
    B.I,CRPRT@
    PRINT;BSS,1@
    CALL,PUTT@
    B.R,*@
    B.I,PRINT@
    DCS;BSS,1@
    CALL,FBDCS@
    DN,OUTAR@
    DN,0@
    B.I,DCS@
    CR;DN,#0A@
    SP;DN,#20@
    OUTAR;BSS,12@
    END@
    ¥PSTO*  CANCEL
    ¥PSTOP
```

154									
978616	978619	978619	978616	978612	978609	978609	978611	978614	
3028-01	2665-01	2644-01	3113-01	3891-01	4392-01	4265-01	3678-01	3459-01	978620
155									
978602	978602	978604	978606	978608	978610	978610	978611	978607	
2719-01	2501-01	2287-01	2247-01	2420-01	2637-01	2702-01	2658-01	2521-01	978611
156									
978606	978605	978605	978605	978605	978605	978607	978609	978606	
3076-01	3159-01	3103-01	3025-01	3041-01	3039-01	2927-01	2763-01	3016-01	978611
157									
978605	978604	978603	978602	978600	978599	978598	978598	978601	
3392-01	3294-01	3082-01	2843-01	2772-01	2847-01	2950-01	2904-01	3011-01	978606
158									
978602	978604	978606	978607	978608	978608	978608	978608	978606	
3082-01	2820-01	2728-01	2799-01	2869-01	2813-01	2635-01	2430-01	2772-01	978611
159									
978608	978606	978606	978605	978603	978603	978603	978603	978605	
3264-01	3085-01	2900-01	2826-01	2911-01	3095-01	3135-01	2929-01	3018-01	978610
160									
978603	978603	978602	978600	978599	978599	978600	978602	978601	
2408-01	2272-01	2588-01	3115-01	3546-01	3692-01	3627-01	3519-01	3096-01	978607
162									
978598	978598	978601	978601	978601	978602	978602	978602	978601	
3850-01	3409-01	2629-01	1912-01	1552-01	1605-01	1870-01	2131-01	2370-01	978605

VIII.2.4. Batch Processing Program for Computing the Corrected Depth, Bouguer Correction and the Eotovos Correction

by

T. Igarashi

1. The program was made for the purpose of the second stage of the gravity analysis. The input data shown in Table 16 are manually punched on the paper tapes, and the items in the Table 17 are the output of the computer.

Table 16. Input

1) Time; year, month and day
2) Time difference between J.S.T. and ship time
3) Specification of the area according to the Matthews table for the correction of the echo sounder depth
4) Time; hour and minute
5) Ship position at arbitraly time measured by 10 min unit
6) Echo sounder depth
7) Total magnetic force

Table 17. Output

1) The ship position at every 10 min interpolated from the given data
2) The corrected depth
3) Bouguer correction
4) Eotvos correction

The examples of input data format and the output of the computer are shown in Table 18 and 19, respectively.

2. Computation formula

1) Eotvos correction

T; Time difference measured by the unit of 10 minutes

L; Longitude difference in 10 minutes

T; Latitude difference in 10 minutes

2) Correction of echo sounder depth

$D = D' + \Delta D$

$\Delta D = k + ld + md + nd$

$d = D/10000$

D'; Echo sounder depth

D; Corrected depth

Numerical constants k, l, m, n are determined by A. Tokuhiro, Hydrographic Office, by means of the least square method to best fit to the table of Mathews.

3) Bouguer correction

$g_B = D \times 69/1000$ mgals

3. The flow chart of the program (program name SAMOA) is shown in Figure 88. Batch processing program written in the FASP is shown in Table 20.

4. Remarks

1) Ship position should be given at the time of the multiple of integer of 10 min.

2) Time interval between the consecutive ship position should be less than 110 minutes, and the ship position should be given at least every 2 hours.

The program was at first tried to operate with the real time processing together with the on line gravity data processing by time sharing. This was given up, because of the serious miss punching inevitable to the manual tape punching. This sometimes resulted in free running of the program beyond its limit. It is very difficult to make a program capable of processing all kinds of expected error contained in the manually punched tapes, and making such complete program will be tried in the next chance.

Table 18. Example of input of computer.

	690119P	+3R	28A			
	2000H	69278S	169515W	4130D	6524K	6527F
	1CH			4120D	6528K	6526F
	2CH			4000D	6526K	6529F
	3CH			4000D	6532K	6533F
	4CH			4000D	6533K	6527F
	5CH	69235S	170142W	3700D	6516K	6504F
	2100H	69218S	170216W	3200D	6497K	6500F
	1CH	69195S	170290W	4100D	6508K	6516F
	2CH			4230D	6520K	6525F
	3CH			4240D	6531K	6539F
	4CH			4220D	6546K	6555F
	5CH			4210D	6560K	6564F
	2200H	69139S	170530W	4130D	6559K	6553F
	1CH			4150D	6546K	6538F
	2CH			4200D	6532K	6538F
	3CH			4210D	6531K	6534F
	4CH	69078S	171190W	4210D	6538K	6544F
	5CH			4210D	6550K	6556F
	2300H	69075S	171282W	4170D	6559K	6553F
	1CH	69074S	171328W	4070D	6544K	6535F
	2CH			4210D	6530K	6529F
	3CH			4210D	6529K	6532F
	4CH			4210D	6536K	6542F
	5CH			4200D	6548K	6553F
	69012CP	+3R	28A			
	0000H	69003S	172016W	4200D	6551K	6546F
	1CH			4210D	6542K	6537F
	2CH			4200D	6534K	6532F
	3CH			4200D	6530K	6530F
	4CH			4210D	6531K	6533F
	5CH			4210D	6538K	6544F
	0100H	68539S	172320W	4200D	6550K	6555F

Table 19. Example of output of computor.

1500H	44191S	179206W	750	746	51	5794	5793	60
10H	44201	179180	830	826	57	5795	5797	
20H	44211	179154	870	865	59	5798	5799	
30H	44221	179128	900	895	61	5795	5795	
40H	44231	179102	940	935	64	5796	5796	
50H	44241	179076	960	955	65	5797	5798	
690108P								
1600H	44256S	179048W	980	966	66	5798	5798	60
10H	44267	179022	1039	1027	70	5799	5800	
20H	44278	178596	1000	986	68	5800	5801	
30H	44289	178570	1050	1037	71	5801	5802	
40H	44300	178544	1079	1066	73	5802	5802	
50H	44311	178518	1109	1096	75	5802	5802	
1700H	44322S	178490W	1150	1135	78	5803	5803	61
10H	44333	178464	1169	1155	79	5802	5802	
20H	44344	178438	1199	1184	81	5801	5801	
30H	44355	178412	1250	1233	85	5801	5800	
40H	44366	178386	1250	1233	85	5800	5800	
50H	44377	178360	1260	1243	85	5800	5799	
1800H	44388S	178329W	1260	1243	85	5798	5798	61
10H	44399	178303	1269	1253	86	5798	5797	
20H	44410	178277	1289	1273	87	5797	5797	
30H	44421	178251	1299	1282	88	5796	5796	
40H	44432	178225	1299	1282	88	5796	5795	
50H	44443	178199	1299	1282	88	5795	5795	
1900H	44455S	178168W	1359	1341	92	5795	5794	61
10H	44466	178141	1380	1361	93	5793	5792	
20H	44477	178114	1359	1341	92	5792	5791	
30H	44488	178087	1440	1420	98	5790	5789	
40H	44499	178060	1469	1450	100	5788	5787	
50H	44510	178033	1520	1499	103	5786	5785	
2000H	44522S	178006W	1599	1578	108	5785	5785	59
10H	44533	177580	1680	1657	114	5785	5787	
20H	44544	177554	1769	1746	120	5791	5794	
30H	44555	177528	1789	1766	121	5795	5794	
40H	44566	177502	1799	1776	122	5790	5785	
50H	44577	177476	1850	1825	125	5783	5783	
2100H	44588S	177448W	1869	1845	127	5785	5786	61
10H	44599	177421	1899	1875	129	5787	5790	
20H	45010	177394	1949	1924	132	5792	5796	
30H	45021	177367	2000	1974	136	5801	5805	
40H	45032	177340	2050	2023	139	5808	5808	
50H	45043	177313	2130	2103	145	5806	5806	
2200H	45055S	177285W	2119	2093	144	5806	5807	57
10H	45066	177260	2160	2133	147	5806	5807	
20H	45077	177235	2199	2172	149	5806	5808	
30H	45088	177210	2210	2182	150	5811	5810	

Table 20. Batch processing program for gravity calculation.

```
    EXTN,CTROKI,CTPFW@
    CALL,OPNT@
    DN,CTPFW@
    B.R,E1@
    CALL,OPNR@
    DN,CTROKI@
    B.R,E1@
    B.R,B1@
    E1;BABS.S,=END@                          Data read
    B1;LX.S,*1,-22@
    B3;LX.S,*3,0@
    STX.L,*3,INDEX3@
    B2;CALL,GETR@
    B.R,E1@
    LX.I,*3,INDEX3@
    SKP.S,P@
    B.R,B2@
    B.L,STRAT@
    SP;DN,#20@
    CR;DN,#A@
    P;DN,#50@
    R;DN,#52@
    A;DN,#41@
    H;DN,#48@
    N;DN,#4E@
    S;DN,#53@
    E;DN,#45@
    W;DN,#57@
    D;DN,#44@
    K;DN,#4B@          Parameters for discreminate control mark of Data
    DN,#46@
    OWARI;DN,#3B@
    BRNCH;B.L,B2@
    B.L,B2@
    B.L,PP@
    B.L,B3@
    B.L,AA@
    B.L,HH@
    B.L,NN@
    B.L,SS@
    B.L,EE@
    B.L,WW@
    B.L,DD@
    B.L,KK@
    B.L,FF@
    CALL,CLSR@
    L.R,K@
    ST.L,ENDD@
    B.L,T0@
    STRAT;ST.L,*3,RE@
    STX.L,*3,INDEX3@
    LX.S,*2,-14@
    LX.S,*3,0@
    BRN;EOR.L,*2,SP+14@     discreminate control mark of Data
    B.L,*3,BRNCH,PW@
    EOR.L,*2,SP+14@
    AX.S,*3,2@
    AX.S,*2,1@
    B.R,BRN@
    LX.I,*2,INDEX2@
    LX.I,*3,INDEX3@
    AX.S,*3,1@
    STX.L,*3,INDEX3@                         Index control
```

Table 20. (Continued)

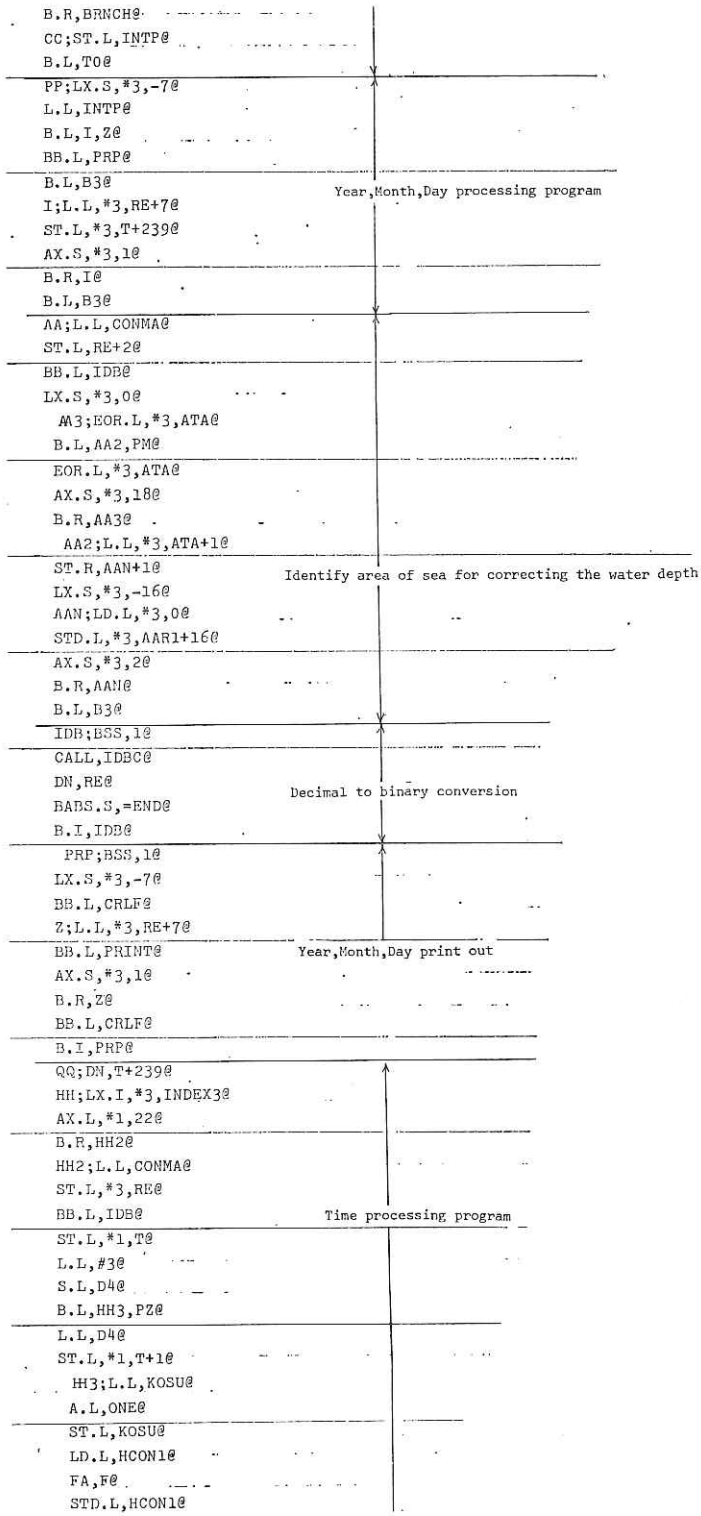

Table 20. (Continued)

```
    STD.L,*1,T+3@
    L.L,ZCONT@
    B.L,TAPR,Z@
    B.L,ST@1
    TAPR;L.L,*1,T-21@
    B.L,GK,P@
    S.L,*1,T+1@
    B.L,CC,PM@
    GK;AX.L,*1,-22@
    B.R,T0@
    T0;STX.L,*1,INDEX1@
    LX.L,*1,0@
    JMP6;L.L,*1,T+1@
    B.L,T2,PM@
    BB.L,CRLF@
    T2;L.L,*1,T@
    BB.L,IBD@
    LX.S,*3,-5@
    T3;L.L,*3,RE+6@
    BB.L,PRINT@
    AX.S,*3,1@
    B.R,T3@
    L.L,H@
    BB.L,PRINT@
    BB.L,SPECE@
    AX.L,*1,4@
    LD.L,*1,T@
    BB.L,ARSM@
    L.L,*1,T+2@
    B.L,BRN9,Z@
    L.L,SP@
    BRN9;BB.L,PRINT@
    BB.L,SPECE@
    ID.L,*1,T@
    BB.L,ARSM@
    L.L,*1,T-1@
    B.L,BRN99,Z@
    L.L,SP@
    BRN99;BB.L,PRINT@
    BB.L,SPECE@
    AX.L,*1,2@
    LX.S,*3,-6@
    JMP5;STX.L,*3,INDEX3@
    LD.L,*1,T@
    B.L,JMP7,Z@
    BB.L,ZCONT@
    B.R,JMP8@
    JMP7;BB.L,CVTFL@
    JMP8;LX.I,*3,INDEX3@
    AX.L,*1,2@
    AX.S,*3,1@
    B.R,JMP5@
    BB.L,CRLF@
    L.L,#1@
    S.L,INDEX1@
    B.L,JMP6,Z@
    L.L,ENDD@
    B.L,L,Z@
    L.L,T+237@
    B.L,Q,PM@
    L.L,QQ@
    ST.L,Z+1@
    BB.L,PRP@
```

Out put processing program

Table 20. (Continued)

```
    Q;LX.S,*3,-26@
    JJ1;LD.L,*1,T@
    STD.L,*3,RE+26@
    AX.L,*1,2@
    AX.S,*3,2@
    B.R,JJ1@
    SLD.S,32@
    LX.L,*1,-240@
    JJ3;STD.L,*1,T+240@
    AX.L,*1,2@
    B.R,JJ3@
    ST.L,PCONT@
    L.L,INTP@
    B.L,GG,2@
    ST.L,KOSU@
    LD.L,RE@
    STD.L,T@
    LD.L,RE+2@
    STD.L,T+2@
    B.L,B3@
    GG;LX.S,*1,-26@
    JJ4;LD.L,*1,RE+26@
    STD.L,*1,T+26@
    AX.S,*1,2@
    B.R,JJ4@
    LX.L,*1,22@
    L.L,ONE@
    ST.L,KOSU@
    B.L,B3@
    L;CALL,CLST@
    BABS.S,=END@
    NN;L.L,RE+2@
    ST.L,RE+10@
    L.L,RE+5@
    ST.L,*1,T+6@
    L.L,CONMA@
    ST.L,RE+5@
    ST.L,RE+2@
    BB.L,IDB@
    M.L,D600@
    STD.L,*1,T+4@
    L.L,RE+10@
    ST.L,RE+2@
    CALL,IDBC@
    DN,RE+2@
    B.R,N2@
    B.R,N3@
    N2;BABS.S,=END@
    N3;SRAD.S,16@
    AD.L,*1,T+4@
    STD.L,*1,T+4@
    B.L,B3@
    EE;L.L,RE+3@
    ST.L,RE+10@
    L.L,RE+6@
    ST.L,*1,T+7@
    L.L,CONMA@
    ST.L,RE+3@
    ST.L,RE+6@
    BB.L,IDB@
    M.L,D600@
    STD.L,*1,T+8@
    L.L,RE+10@
```

Latitude processing program

Table 20. (Continued)

```
    ST.L,RE+3@
    CALL,IDBC@          Londitude processing program
    DN,RE+3@
    B.R,N2@
    SRAD.S,16@
    AD.L,*1,T+8@
    STD.L,*1,T+8@
    L.L,INTP@
    B.L,INTPO,Z@
    L.R,EE@
    ST.L,INTP@
    B.L,B3@
    SS;EQU,NN@
    WW;EQU,EE@
    INTPO;L.L,T+6@
    EOR.L,*1,T+6@
    B.L,INT2,Z@
    LD.L,*1,T+4@
    SD.L,T+4@
    INT5;D.L,KOSU@
    SRAD.S,16@
    LX.I,*3,KOSU@
    LX.S,*2,0@
    AX.S,*3,-1@         Interpolate Latitude
    B.R,*@
    STD.L,RE+10@
    AD.L,T+4@
    INT4;AX.S,*3,-1@
    B.R,INT3@
    AX.L,*2,22@
    STD.L,*2,T+4@
    AD.L,RE+10@
    B.R,INT4@
    INT2;LD.L,*1,T+4@
    AD.L,T+4@
    B.R,INT5@
    INT3;L.L,T+7@
    EOR.L,*1,T+7@
    B.L,INT33,Z@
    LD.L,*1,T+8@
    SD.L,T+8@
    INT36;STD.L,RE+8@
    CALL,FXFL@
    DN,31@
    STD.L,PAID@
    L.L,T+7@
    EOR.L,W@            Interpolate Longitude
    B.L,WWW,Z@
    LD.L,M1F@
    FM,PAID@
    STD.L,PAID@
    WWW;LX.I,*3,KOSU@
    AX.S,*3,-1@
    B.R,*@
    LX.S,*2,0@
    LD.L,RE+8@
    D.L,KOSU@
    SRAD.S,16@
    STD.L,RE+8@
    AD.L,T+8@
    INT35;AX.S,*3,-1@
    B.R,INT34@
    AX.S,*2,22@
```

Table 20. (Continued)

```
      STD.L,*2,T+8@
      AD.L,RE+8@
      B.R,INT35@
INT33;L.L,DMNT@
      M.L,D10@
      SD.L,*1,T+8@
      STD.L,RE+10@
      L.L,DMNT@
      M.L,D10@
      SD.L,T+8@
      AD.L,RE+10@
      B.R,INT36@
INT34;LD.L,*1,T+2@          calculate Eotvos effect
      FS,T+2@
      STD.L,RE+8@
      LD.L,T+4@
      CALL,FXFL@
      DN,31@
      FM,PAI@
      CALL,COS@
      STD.L,RE+10@
      FM,RE+10@
      FM,PAID@
      FM,D45@
      FD,RE+8@
      FD,F@
      STD.L,T+20@
      L.R,DD@
      ST.L,PCONT@
      B.L,B3@
DD;BB.L,FDB@
      STD.L,*1,T+10@
      FD,D10000@
      STD.L,RE@
      LD.L,*1,T+10@
                            calculate depth correction and Bouguer correction
      FS,D1000@
      B.L,DD1,MZ@
      LX.S,*3,0@
      BB.L,DEEP@
      B.L,B3@
DD1;LX,L,*3,8@
      BB.L,DEEP@
      B.L,B3@
DEEP;BSS,1@
      ID.L,*3,AAR1+2@
      FM,RE@
      STD.L,RE+2@
      LD.L,RE@
      FM,RE@
      STD.L,RE+10@
      FM,RE@
      FM,AAR1+6,3@
      STD.L,RE+4@
      LD.L,RE+10@
      FM,AAR1+4,3@
      FA,RE+2@
      FA,RE+4@
      FA,AAR1,3@
      FA,T+10,1@
      STD.L,*1,T+12@
      FD,D1000@
      FM,D69@
      STD.L,*1,T+14@
```

Table 20. (Continued)

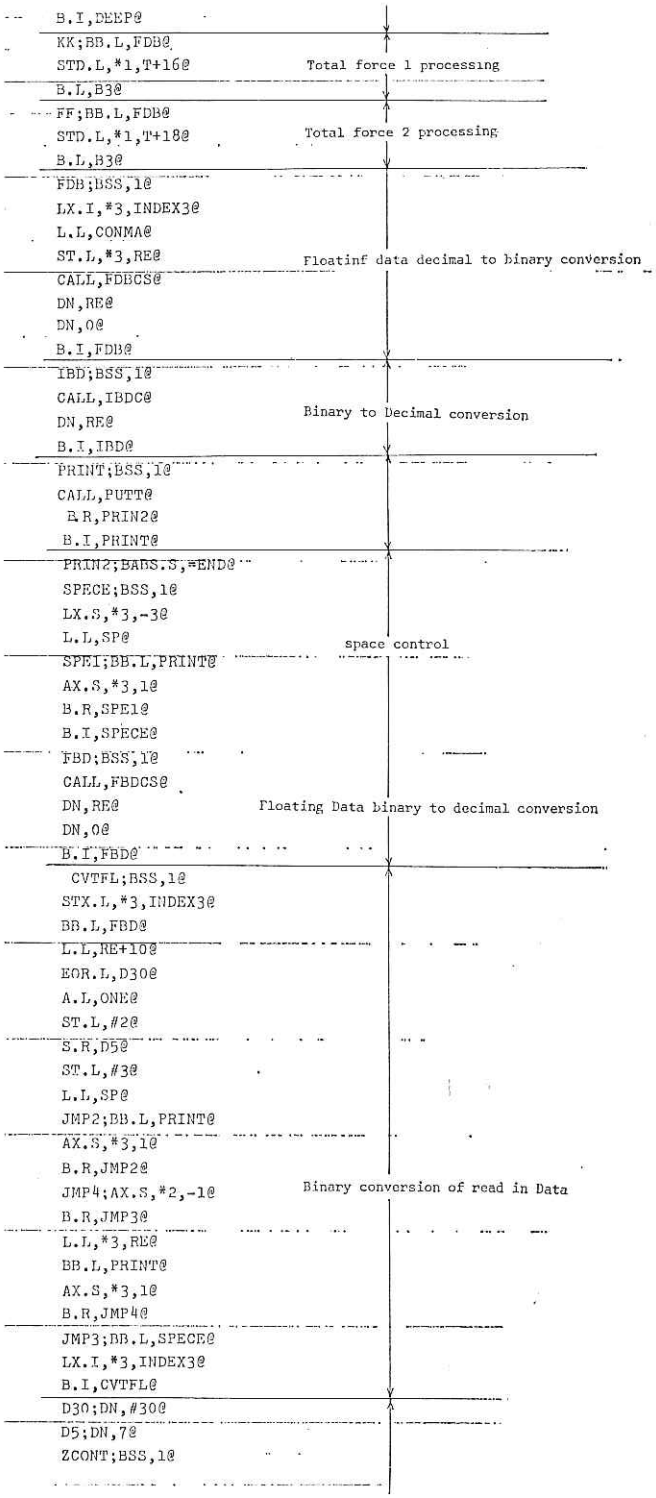

Table 20. (Continued)

```
LX.S,*3,-10@
L.L,SP@
JMP10;BB.L,PRINT@
AX.S,*3,1@
B.R,JMP10@
B.I,ZCONT@
```

Zero Data control

```
CRLF;BSS,1@
L.L,CR@
BB.L,PRINT@
STX.R,*1,CRC1@
LX.I,*1,CRC2@
AX.S,*1,1@
B.R,JCR@
LX.S,*1,-10@
JCR2;BB.L,PRINT@
AX.S,*1,1@
B.R,JCR2@
LX.S,*1,-56@
B.R,JCR@
JCR;STX.L,*1,CRC2@
LX.I,*1,CRC1@
B.I,CRLF@
```

Type writer L.F. control

```
CRC2;DN,-56@
CRC1;DN,0@
ARSM;BSS,1@
D.L,D600@
STD.L,WS@
BB.L,IBD@
LX.S,*3,-3@
T4;L.L,*3,RE+6@
BB.L,PRINT@
AX.S,*3,1@
B.R,T4@
L.L,WS+1@
BB.L,IBD@
LX.S,*3,-3@
T5;L.L,*3,RE+6@
EOR.L,D30@
SR.S,4@
B.L,V,2@
L.L,*3,RE+6@
TT;BB.L,PRINT@
AX.S,*3,1@
B.R,T5@
B.I,ARSM@
V;L.L,D30@
B.R,TT@
EVEN@
```

out put control

```
AAR1;BSS,8@
AAR2;BSS,8@
RE;BSS,26@
T;BSS,240@
HCON1;FLD,0@
F;FLD,10@
WS;BSS,2@
D1000;FLD,1000@
D10000;FLD,10000@
PAID;BSS,2@
PAI;FLD,0.00002908881@
D45;FLD,450@
D69;FLD,69@
M1F;FLD,-1@
KOSU;DN,-1@
```

parameter area

Table 20. (Continued)

```
ONE;DN,1@
RAREA;BSS,1@
ENDD;BSS,1@
INTP;BSS,1@
INDEX1;BSS,1@
INDEX2;BSS,1@
INDEX3;BSS,1@
D4;DN,4@
D600;DN,600@
DMNT;DN,10800@
D10;DN,10@
PCONT;BSS,1@
INTARP;BSS,I@
CONMA;DN,#2C@
EVEN@
ATA;DN,42,ATA+18@
FLD;2.367,-57.33,-275.3,777,20.2,-293.7,567.5,28.
                                                    Data for depth correction storage area
17@
DN,46,ATA+36@
FLD,0.8999,146.9,-1947,5099,23.8,-269.7,539,39.04
@
DN,22,ATA+54@
FLD,1.199,-3656,-1321,4492,14,-301.7,580.6,21.18@
DN,23,ATA+72@
FLD,1.033,-177.2,335.1,-412.8,15.03,-326.6,612.4,
8.353@
DN,24,ATA+90@
FLD,-1,-136.2,-611.9,-3059,8.967,-314.2,596.2,15.
15@
DN,25,ATA+108@
FLD,0.6,-278.5,648.3,-558.5,2.995,-295.2,584.8,-9
2.14@
DN,26,ATA+126@
FLD,-0.2999,-293,572.5,-242.8,0.6898,-306.2,583.4
,-61.37@
DN,27,ATA+144@
FLD,-1.4,-288.2,339.5,607,-4.347,-256,330,244@
DN,28,ATA+162@
FLD,-0.6667,-316.3,480.8,437.1,-4.481,-257.7,303.
3,251.3@
END@
¥PSTOP
```

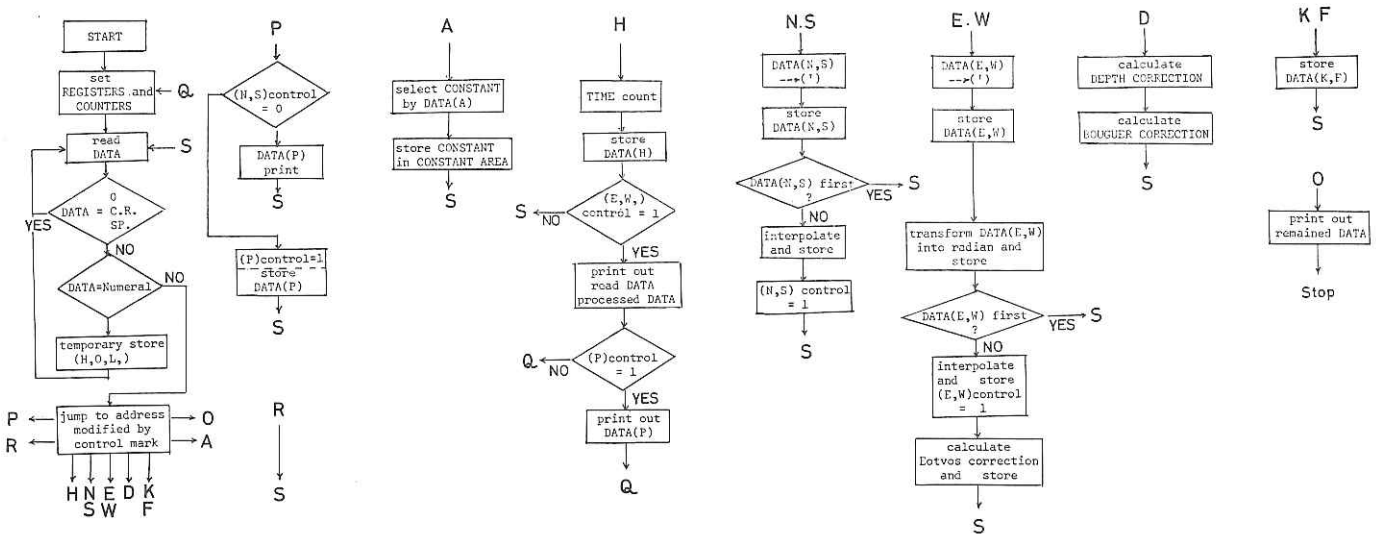

Fig. 88. Flow chart of the program (SAMOA).

P, R,.....A, O, represent following processing routine, respectively.

- P: Year, Month, Day processing routine.
- R: Time difference between J.S.T. and Ship time processing routine.
- H: Time processing routine.
- N or S: Latitude processing routine.
- E or W: Longitude processing routine.
- D: Depth processing routine.
- K or F: Total magnetic force processing routine.
- A: Specification of area in Matthews table processing routine.
- O: End of data processing routine.

VIII.2.5. Terrestrial Heat Flow

by

K. Nagasaka

Object. The measurement of terrestrial heat flow was proposed during this cruise to obtain the data especially in the South Pacific near the Antarctica, where the knowledge on terrestiral heat flow is rather limited.

Stations. A summary of the stations occupied for the heat flow study is given in Table 21, containing the location, water depth, the depth of peneration of the probe and length of the core.

Table 21. List of the terrestrial heat flow stations

Terrestrial heat flow measurements were tried at the following stations. A complete set of the device was missed at station 33–3 (37°58.5′S, 169°57.7′W).

Station No.	Date ('68/69)	Position		Depth in m	Penetration in cm	Core length in cm
		Lat.	Long.			
2–3	Nov. 23	30°01.6′N	170°04.0′W	5510	Full	43
11–3	27	21°02.7′	170°04.0′	4865	Full	30 (11–2)*
15–2	30	11°58.0′	169°56.2′	5815	Full	39
18–2	Dec. 4	3°03.0′	169°58.6′	5505	Full	40
21–2	7	6°09.8′S	170°06.8′	5390	0	0
29–3	20	25°54.0′	170°18.5′	5545	Full	50
31–2	23	31°57.5′	169°57.0′	5670	Full	41
32–2	24	35°00.0′	169°59.1′	5195	0	1
32–3	24	36°17.7′	170°01.1′	5215	0	0
38–2	Jan. 10	47°59.5′	170°03.3′	5260	Full	—
39–3	11	56°06.0′	169°57.7′	5120	Full	53 (39–2)*
43–2	15	58°17.7′	169°55.2′	5100	Full	—
45–3	16	61°56.0′	169°52.5′	3310	0	23 (45–2)*
46–2	17	63°57.1′	170°04.8′	2850	Full	—
49–2	19	69°32.0′	170°00.0′	4205	Full	70 (49–3)*
51–2	21	66°28.0′	170°08.0′E	3235	Full	—
53–2	24	60°00.7′	155°04.8′	2915	0	—
54–2	25	57°03.0′	155°01.5′	3630	0	—
55–2	27	53°58.8′	155°10.0′	4215	0	—
56–2	28	51°12.3′	155°26.0′	4295	125	—
57–2	29	48°00.3′	155°06.8′	4825	135	—
59–2	30	44°00.0′	155°05.0′	4655	Full	—
60–3	Feb. 1	38°25.7′	155°05.8′	4650	Full	46 (60–2)*

* Sample of pilot corer with piston corer.

Measurement. The measurement of the geothermal gradient in the ocean floor was carried out with Tokyo University type sea bottom thermograd-meter (Figure 89). The probe used in this cruise had two pairs of thermistor sensor inside and was 2 m long and 21 mm in diameter.

During the Leg I and II, it was lowered into sea floor with a small gravity-type corer (80 cm long and 44 mm in diameter) as shown in Figure 89. However, during the Leg III, only the probe was lowered into the bottom, because of the missing of the devices. The bottom contact of the devices was recognized by observing the wire tension.

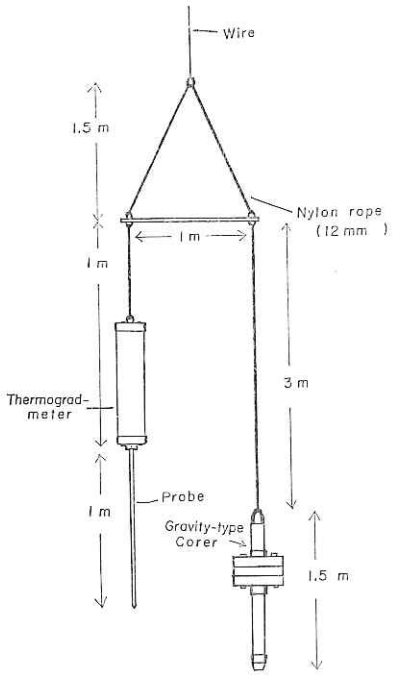

Fig. 89. Schematic diagram showing the combination of a gravity-type corer and a thermograd-meter.

The recovered core samples were used for the measurement of the thermal conductivity after they reached the thermal equilibrium with ambient temperature of the laboratory aboard. The von Herzen and Maxwell's needle probe technique was employed for the determination of the thermal conductivity.

Rough description of the results. Among 23 stations occupied during this cruise, 16 trials were successful. It is very difficult to mention rough aspects of the distribution of the heat flow values, because the number of measurements were not enough compared with the area covered.

It may be said that the values are slightly high in the area of the Tasman Sea and that they are almost normal in the other area.

Detail study of the results will be reported elsewhere in near future.

VIII.2.6. Possibility of Magnetization Measurement of the Pelagic Sediments on Board

by

K. Kitazawa

Measurements of magnetization of sediments collected from ocean bottom by piston corer are important in the study of the ancient geomagnetic field. Magnetization, both intensity and direction, has so far been measured in the laboratory on land after the sampling ship returns. If magnetization can be measured on board, sampling of the sediments will become more effective than it has been. Moreover, it is possible to increase efficiency of the study by obtaining the measured results of magnetization during a cruise. For the purpose of fulfilling these two requirements, a stable and sensitive magnetometer was designed and constructed.

There are two types of magnetometer. One is an astatic magnetometer which has a pair of small permanent magnets suspended by an elastic string made by phosphor bronze. Intensity of magnetization is obtained by measuring the torsion of the string and direction of magnetization is calculated from those obtained intensities. The other is a spinner magnetometer by which both intensity and direction of magnetization of sample can be measured. Magnetized sample is set in a sample holder attached at an end of shaft rotating above a search coil. Both voltage and phase induced in the coil are measured. The voltage is proportional to the intensity of magnetization and the phase indicates the direction of magnetization. The former magnetometer is not suitable for use on a cruising ship because of its mechanical weakness. The latter is theoretically workable on a ship but practically it is necessary to compensate noises peculiar to the moving steel vessel.

The present model of magnetometer follows the latter principle. The design is somewhat similar to Foster's model built at Lamont Geological Observatory but two troidal flux gate sensors in a pair as shown in Plate 6 are used to avoid any undesirable influence of local distorsion of the ambient magnetic field which varies as the ship pitches, rolls or changes its direction. A phase sensitive detector with low pass filters is adopted to detect the signals from noises which can not be eliminated yet. The block diagram of this apparatus is shown in Figure 90. Standard frequency of 1 kHz generated by piezo-electric oscillator is supplied to primary coil in each of the sensors. The secondary coils of two sensors are connected antiparallelly with each other to cancel out the ambient noises. Output intensity is thus proportional to the intensity difference of the magnetic field surrounding each troidal coil. The output of secondary coils becomes 2 kHz signal modulated with 8 Hz signal when a magnetized sample is revolved with a constant speed of 480 RPM in the gap of one of a pair of troidal coils. This signal is fed to the phase detector to select 8 Hz signal alone and then the 8 Hz signal is amplified and recorded.

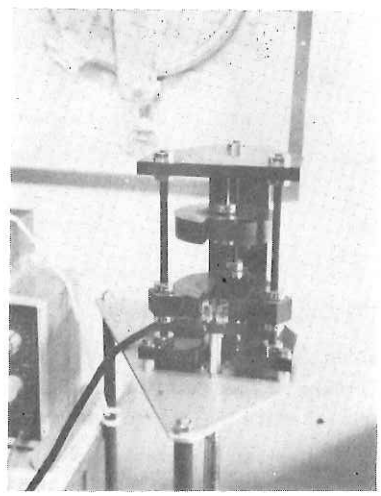

Plate 6.

One of the rock samples, of which intensity and direction of magnetization has been measured with an astatic magnetometer in the laboratory on land, was used as a standard sample to test the sensitivity of this magnetometer. This basaltic rock was collected from the bottom of the North Pacific Ocean in the last cruise of the Hakuhō Maru

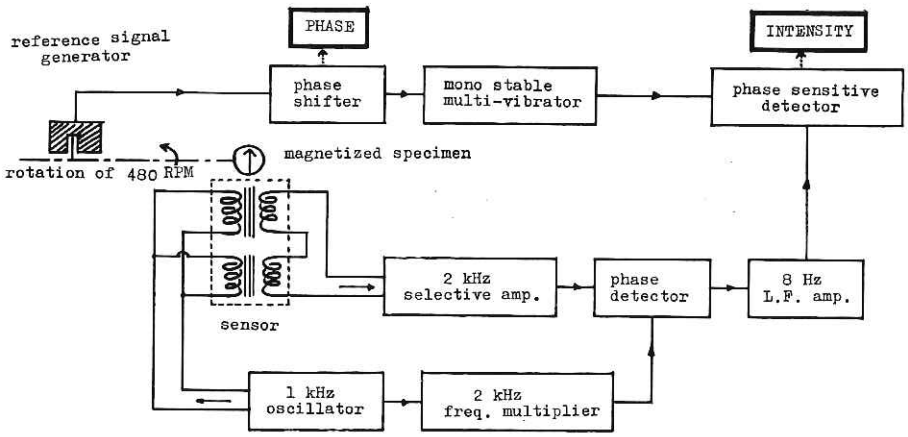

Fig. 90. Block diagram of spinner magnetometer.

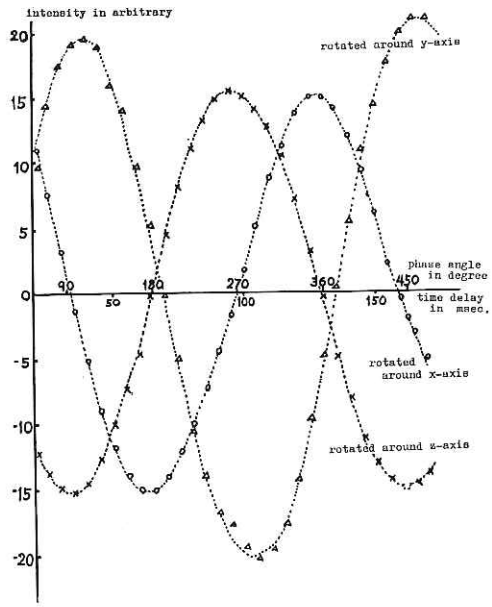

Fig. 91. Magnetization measurement of standard rock sample.

(KH–68–3). A cubic specimen, 2 cm in each edge, was cut from the rock. Both intensities and directions in each plane of this standard specimen are listed in Table 22. The change of the phase-detected output intensity according to the phase change of the reference signal is measured when the shaft of the magnetometer, with a specimen and a reference signal generator, is revolved with a constant speed by a synchronous motor. An example of the changes of the output intensity is shown in Figure 91. Choosing an axis (X, Y or Z) of cubic specimen as a rotation axis, one of the three curves in the figure is obtained. The amplitude of these three curves is proportional to the intensity of magnetization in each plane and the phase angle of the peak in each curve shows the direction of magnetization in each plane. If the conversion factor is given so as to equalise the measured intensity of magnetization in the xy-plane with the absolute value

Table 22. Standard Rock Sample

	Intensity		Direction	
	Astatic Magnetometer	Spinner Magnetometer	Astatic Magnetometer	Spinner Magnetometer
xy-plane	5.46×10^{-4}emu/g		from x-axis 163°	
yz-plane	5.83	5.43	y-axis 74°	79°
zx-plane	7.66	7.33	z-axis 317°	319°
Total	7.82	7.70		

Table 23. Sediment Specimen

	Intensity	Direction
xy-plane	5.34×10^{-5} emu/g	from x-axis 177°
yz-plane	3.86	y-axis 254°
zx-plane	4.32	z-axis 286°
Total	5.57	

determined by an astatic measurement, intensities of magnetization in *yz*- and *zx*-planes become the values listed in Table 23. The directions of magnetization in each plane are also listed in Table 23 under the assumption that the angle from *x*-axis in the *xy*-plane measured by spinner magnetometer is equal to that determined by an astatic magnetometer. Every measured value in Table 22 is satisfactorily consistent, if measurement errors are taken into account.

Figure 92 shows the result of measurement with a sediment sample collected at station 22–2 (10°57′S, 169°59′W) in the present cruise. Output intensity of specimen was measured on the two different ways of setting. The sediment specimen is reset in the 180° rotated position with the same rotation axis after one measurement is completed in order to eliminate the magnetic noises from the mechanical parts of the apparatus which are rotated with the specimen. If the rotating parts of the apparatus especially the sample holder and the shaft are ferromagnetic the output intensity is the vector sum of the magnetization of the specimen and the magnetization of the mechanical parts. When the specimen is reset in the sample holder on the opposite position with the same rotation axis, different two curves of (a) and (b) in Figure 92 are obtained. Both intensity and direction of magnetization of this sediment specimen are acquired from Figure 92 by

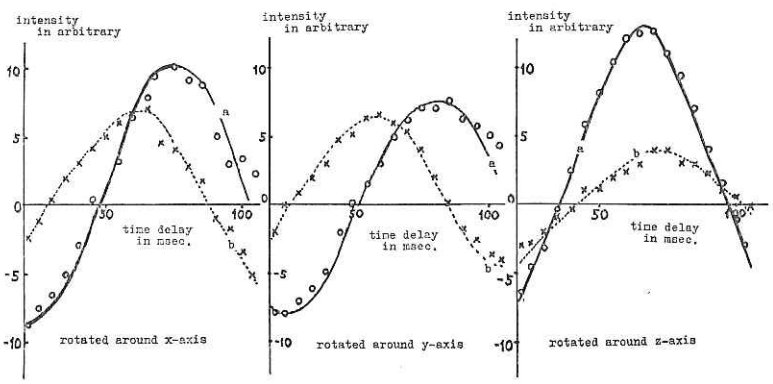

Fig. 92. Magnetization measurement of a sediment sample (Curve a, solid line). Dotted lines b show results after resetting on the opposite position with the same rotation axis.

averaging the two curves after shifting the curve (b) by 180° (65 msec) and these values are listed in Table 22. In this case the *xy*-plane of the specimen is chosen in the level, therefore the inclination of magnetization is −16°. Magnetic noise of this apparatus is equivalent to a magnetic body of 4.43×10^{-5} emu/g in its intensity and the direction of magnetization is 202°.

VIII.2.7. Observation of Atmospheric Electricity

by

M. Kanada

In the fine or fair weather region on the earth surface, the electric conduction current of the order of 10^{-12} A/m^2 continually flows vertically into the earth from the upper atmosphere. The main generator of the current is considered to be the world-wide thunderstorm activity, because the air-earth current density or the atmospheric electric field under a fair weather condition shows a diurnal variation that is independent of local time and in phase with the thunderstorm activity variation accumulated all over the world. Then we could picture the global electric current circuit, which starts from thunderclouds mainly distributed in tropical continents, passes through the upper conductive atmosphere and terminates at the fair weather ground and sea surface.

As emphasized in the "Atmospheric Electricity Ten-Year Program" (Resolution of Joint Committee on Atmospheric Electricity of IAMAP and IAGA, IUGG, 1965), a basic requirement of the fair weather measurement is to differentiate between the effects of global electric circuit and of disturbances locally caused by meteorological and industrial conditions around the observation point.

As to the meteorological effects, we could keep it out by selecting the records for so called calm days. Disturbances due to human activity, however, would be unavoidable so far as we would stay on the land where industries pollute circumstances day and night. Atmosphere on the sea surface could be much clean compared with that on the land, when one would leave any sea coast several tens of kilometers. One of the main objects of the present observation is to investigate the global effect of the atmospheric elements without the influence of land pollution. As it would be understood from the construction of global circuit, two factors, the geographic distribution of thunderstorms as the generators of it and the latitude dependence of electrical conductivity in the upper atmosphere mostly related to the ionization by cosmic ray, would have influence on the values of current or electric field at various localitites. In this respect, the present long cruise including a longitudinal routes along 170°W from 30°N to 69°30′S was very suitable for investigating the geophysical characteristics of atmospheric electricity. Moreover, the later half of the cruise fortunately coincides with a partial period of the Atlantic expedition by German and American research vessels, on which the same kind of atmospheric electric measurement as ours will be carried out, and the cooperative program is set forward between the observations in the Pacific and Atlantic Ocean. It would much enhance our understanding of the global circuit under the present condition that we do not have any effective worldwide networks to observe the daily storm occurrences, which would have considerable fluctuations from a day to another.

The sea surface, on the other hand, affects the electrical nature of the atmosphere very close to it. The preliminary observation done a year before on R.V. Tansei Maru suggested a possibility of the existence of space charge close to the sea surface, which would be thought to depend on the generation of electric charge due to splashing sea water and the existence of aerosols, mostly concerned with sea salt nuclei. During the whole period of the cruise exceeding three months, good results were obtained to study

on the contribution of the sea to the atmospheric electricity.

Measurements.

1. Atmosheric electric field.

A field meter of mechanical collector type was used for the measurement of electric field on Hakuho Maru. The main role of the field sensible unit is played by a set of rotor and stator, both of which have similar butterfly-like shapes. The rotor is periodically exposed to and shielded from the external electric field corresponding to the mutual displacement between the rotor and the grounded stator. Synchronized with the rotatory motion of the rotor, it is instantaneously connected in turn to the ground directly or through a parallel circuit of capacitance and high resistance. Thus the electric charge induced on the rotor is accumulated on the capacitance. The simple estimation will give that the final value of the capacitor potential is

$$\varepsilon SE/C\left\{1-\exp\left(-\frac{\tau}{CR}\right)\right\},$$

where E is the field, ε the dielectric constant in air, S the surface area of the rotor, C and R the total capacitance and resistance o fthe rotor system, and τ the period of rotatory motion. The capacitor potential is the order of 10 mv, which is amplified and recorded, for the used meter and for calm days.

A problem on the field measurement is in setting of the apparatus, because the field is usually disturbed by the surrounding objects and the apparatus itself modifies the natural field. The experimental procedure to obtain the absolute value of natural field on a plane surface, which is called as the reduction to plane, is done by the comparison with other devices, for example, the measurement of the potential of a long wire horizontally stretched 1 to 2 meters above the flat ground, when the wire is regarded as of the same potential as the surrounding atmosphere by equipped with a radioactive or smoke collector.

2. Air-earth current.

The air-earth current was measured by the use of a receiving plate. The current received with a plate includes the displacement current $\varepsilon(dE)/dt$ in addition to the conduction current i, which is the quantity to be measured. Some devices are necessary to take the term of displacement current off the record. Since i and E are combined with the conductivity λ, the current on the receiving plate would be given as

$$i+\frac{\varepsilon}{\lambda}\frac{di}{dt},$$

where ε/λ is called the time constant of the atmosphere and of the order of several minutes. If we would connect the receiving plate to the ground through such a parallel circuit of C and R that the product CR is equal to ε/λ, the voltage drop across the resistance R would be iR, which we might amplify and record. Although the conductivity λ is not always constant, the error expected from the variation of λ is usually small. The receiving plate used on the Hakuhō Maru is a square of 0.65 m, and the values of R and CR are 10^{12} ohm and 500 sec, respectively. The ouptut voltage from the plate is of the order of 0.1 v for a fair weather condition.

3. Atmospheric electrical conductivity

The Gerdien type aspiration cylindrical condenser was used for the measurement of electrical conductivity on the Hakuhō Maru. The condenser is consisted of two parts, outer and inner electrodes. Suppose an ion that enters the condenser just from the surface of the outer electrode at the entrance and trapped at the end of inner electrode under the

influence of electric field between outer and inner electrodes. The mobility of the ion is defined as the critical mobility of the system. The critical mobility is given by

$$K_c = \left(\frac{\varepsilon}{C}\right) \cdot \frac{\Phi}{V},$$

where Φ is the rate of airflow, V the voltage between two electrodes, C the capacity of the condenser and ε is the dielectric constant of air. The current i flowing into the inner electrode is given by

$$i = e\Phi\left[\int_{K_c}^{\infty} f(k)dk + \frac{1}{K_c}\int_0^{K_c} Kf(k)dk\right],$$

where e is the elementary charge and $f(K)$ is the distribution function, that is, the number of ions dn with mobility between K and $K + dK$ is given by $f(K)dK$. When the mobility of ions is less than the critical mobility of the system, the system acts as conductivity meter. The conductivity λ is given by

$$\lambda = \left(\frac{\varepsilon}{C}\right)\frac{i}{V}$$

Thus, the conductivity can be measured with the applied voltage of DC 6.3 volt and with the rate of airflow of 300 liter per minute. The current is the order of 10^{-13} ampere for the used meter and for calm days.

4. Atmospheric small ion mobility spectrum

The mobility spectrum of atmospheric small ions was measured by the use of an ion mobility spectrometer. The spectrometer is an aspiration cylindrical condenser which is composed of inner and outer electrodes. The inner electrode placed along the central axis of the cylinder is devided into two portions, first and second electrodes. Some of the ions that enter the condenser are trapped by the first and the second electrodes and the current i_2 consisting of ions collected by the second electrode is given by

$$i_2 = e\Phi\left[\int_{K_d}^{K_c} f(K)dK + \frac{1}{K_d}\int_0^{K_d} Kf(K)dK - \frac{1}{K_c}\int_0^{K_c} Kf(K)dK\right],$$

where Φ is the rate of airflow, e the elementary charge, K_c and K_d the critical mobilities of the first and the second electrodes and $f(K)$ the distribution function. The concentration of ions with mobility between K_c and K_d is deduced from

$$\frac{d(i_2/V)}{dK_c} = \frac{C_1}{\varepsilon} e \int_{K_d}^{K_c} f(K)dK,$$

where V is the applied voltage between outer and inner electrode. In the measurement on the Hakuho Maru, i_2 is the order of 10^{-13} ampere for a fair weather condition, and in this time the first electrode is grounded. The applied voltage was changed stepwise from 4.5 volt up to 186 volt and Φ was taken 600 liter per minute or 800 liter per minute.

VIII.3. Biological Works

To investigate the present condition of the stocks of both commercially important and protected species of whales, estimation of the quantitative and qualitative population densities of the whales in their breeding and feeding regions is very important. However, the sighting records on the larger whales and the smaller toothed whales in the mid Pacific Ocean has not yet been accumulated enough for this object.

On this account, we carried out sighting observations on those cetaceans throughout the course of the expedition. During the practical observations, the occurrence of sea-birds and marine mammals of other than cetacea were also checked by the name of the each species and numbers of individuals; since they were a significant sign of the presence of whales, especially in the southern whaling ground at the higher latitude. During the sighting observations, various phenomena of the sea such as the slick and discolored water were also recorded.

At the hydrographic stations plankton sampling with three kinds of net, and the simultaneous recording of the DSL were carried out to obtain the knowledge on the abundance of food organisms of baleen whales and sea-birds in relation to their distributions.

VIII.3.1. Sighting Records of Whales and Sea-birds

by

A. Kawamura and K. Kureha

1. Whales

The sighting observations were started on November 15, 1968 at 33°05.6′ N, 143°33.2′E and ended on February 28, 1969 at 30°21.7′ N, 137°49.5′ E. The observations were carried out continuously at the upper deck of the ship from sunrise to sunset whenever the ship was cruising. When the ship stopped at the hydrographic stations, the observations were paused.

The total distance that the observation has been carried out was as far as 9070.3 nautical miles, and the general features of the observations were shown in Figures 93a–c.

As the upper deck was at 11.8 m above the water level, the theoretical radius of visibility from the upper deck is calculated as about 7.1 nautical miles. It can be said in general that the sighting observations were made within the visibility range of 7 miles or a little more.

As shown in Legs. I and II (Figure 93a) at least one observer was in charge of watching at the upper deck throughout the daytime. As the ship cruised from New Zealand down to the southern sea (Leg. III), the duration of daytime grew longer, and we watched in four shifts a day. Two types of binocular telescope were used. One of them was a 12 cm, 20 × 3° (Nikon); it was quite sufficient for the sight of great distant object.

The following items were recorded in the observation: species name, their sighted positions and orientations, the number of individuals, accompany with a calf or not, sighting angle between the bow direction and the whales, sea-birds followed or not, and other remarkable conditions or phenomena. The sighting angle and the distance of the whales from the ship were recorded as exactly as possible because these factors are quite important for the stock assessment of larger whales (Figure 94). In addition to the aboves, the conditions of the sea, *i.e.*, water and air temperatures, weather, visibility, force and direction of wind, wave and swell, abundance of white edges of breaking waves in four grades were recorded.

The name of whales observed were listed in Table 24. In the records, some individuals among the sei whales in the tropical or subtropical seas, are considered to be Bryde's whale: *Balaenoptera edeni* ANDERSON which has been caught as the sei whale. However, as it was difficult to distinguish the Bryde's whale from the sei whale from that distance, they were recorded as the sei whale in Tables 24, 25, and Table 28. The numbers of larger whales and smaller toothed whales sighted throughout the cruise were as much as 83 and 553 respectively (Table 25), and the records of the sighted whale are shown in Tables 26–39 in detail.

2. Pinipeds

During the expedition, seven individuals of leopard seal: *Hydrurgal leptonyx* BLAINVILLE and an individual of southern fur seals *Arctocephalus* sp. were observed. The leopard seals were sighted three times on the ice pack near by the north-east shore of Sturge Islands (67°09.9′ S, 165°05.0′ E) on January 22, 1969. *Arctocephalus* sp. was sighted at 48°00.9′ S, 170°05.6′ W on January 10, 1969.

3. Sea-Birds

Although the principal objectives of this investigation were focussed on whales and other marine mammals, sea-birds occurred within the sighting range were also recorded with the number of individuals and species of each flock for having interest in the relationship between whales and birds.

For identifications of the sea-birds at sea, we referred to the following documents.

B. King: Preliminary Smithonian Identification Manual; Seabirds of the tropical Pacific Ocean. U. S. Nat. Mus. Smithsonian Inst., Washington (1967)

R. A. Falla, R. B. Sibson and E. G. Turbott: A field guide to the birds of New Zealand and outlying islands. Collins, London (1966)

B. Roberts (Edited): Edward Wilson's birds of the Antarctic. Blandford Press, London (1967)

K. Ozawa: Distribution of sea birds in austral summer season in the southern ocean. Ant. Rec., No. 29 (1967)

CSK Working Group: Manual for optical observations. (1966)

The name of the observed sea-birds, and the positions of appearance and vanishing were recorded in Tables 37 and 38. Some among the petrels, more examination on their species is required, though they were included in Table 37. Most of the species shown in Table 37 was found in the area between longitude 170°W and 155°E except several species such as Antarctic petrels, Snow petrel and Silvery-grey fulmar whose occurrence were restricted within the Antarctic regions between longitude 170°W and 155°E.

VIII.3.2. Plankton Sampling and Observation of the DSL

by

A. Kawamura and K. Kureha

1. Sampling with Norpac net

The quantitative and qualitative distributions of zooplankton along the longitudinal section of 170°W gives an idea on the distributional relationship between zooplankton and sea-birds. Large biomass were usually found in the equatorial Pacific regions where Cromwell Current is prevailing.

Another aim of the plankton sampling was to know the quantitative distributions of copepods, particularly that of *Calanus tonsus* BRADY which is thought to be important as a food of the sei whale (*Balaenoptera borealis*) and the little piked whale (*Balaenoptera*

bonaerensis) in the southern whaling ground. For this purpose, we made 118 vertical hauls at 63 stations. The net having 0.33 mm mesh-openings was towed from 150 m deep to the surface at a speed of 1 m/sec. The flow-meter was attached to the mouth ring of the net. The sampling was duplicated in most cases.

The wet weight and displacement volume of samples were determined by using aspiration filtering apparatus. Unusual large organisms such as fishes, squids, *Phronima* sp., jellyfish, salpa etc, were removed before the measurements, and these numbers were counted separately.

The wet weight and displacement volume per haul were then converted to those per 1000 m^3 of water. The sampling data and results are shown in Table 39.

2. Sampling with Petersen type vertical closing net*

In order to know the organisms which are presumed to be partly responsible for the DSL formation in the southern seas, the net was towed vertically at several different depths of water at 17 stations, at which the DSL was observed on the fish recorder. In all: 41 samples were obtained. The net used was a Petersen type closing net, 70 cm in mouth diameter and 210 cm long: its filtering portion was made of Pylen 24, 1.0 mm in mesh-openings. The net was towed at a speed of 1.8 m/sec, and closed by using a release mechanism at each desired depth.

The Norpac net sampling was also operated in the most cases besides the Petersen net sampling for the purpose of comparison.

The records of sampling are shown in Table 40.

3. Sampling with larva net

To get lanternfishes and other larval forms, surface towing with a larva net was done 44 times and 38 groups of samples were obtained. The net, 2m in mouth diameter and 5.5 m long, was designed by the Tohoku Regional Fisheries Research Laboratory for collecting saury larva. The filtering portion was made of bolting cloth, 7.0 mm in mesh-openings. It was attached to the 160 cm mouth ring of a ORI net at the operation. At the hydrographic stations in Legs. I–III, the net was drifted just beneath the surface for 1–2 hours at the mercy of the movement of the ship. The mouth ring of the net was kept vertically with two bouys attached to the sides of the ring. Smaller bouys were also attached to the filtering part of net to keep it open horizontally during the sampling.

In Leg. IV, on the way from Noumea, New Caledonia, to Tokyo, horizontal surface towings with larva net were operated at 6 stations. The net was towed for 30 minutes from side of the ship by the aid of boom at a speed of 2 knots. Each sampling was made at night. The records of sampling are shown in Table 41.

The records of samples collected with Norpac net and Petersen type vertical closing net have been reserved for later examination at The Whales Research Institute, and those collected with larva net have been deposited in the Ocean Research Institute, University of Tokyo.

During the cruising from November 22, 1968 at 30°03.8′ N, 171°26.3′ W to February 27, 1969 at 24°09.2′ N, 138°07.1′ E, the observations of the DSL by a fish finder were made. Sanken's New Fish-finder Model TL–32 was used and the total duration of the present observation attained 386.5 hours. The fish-finder was operated with 28 KC in wave frequency in most cases and the DSL was recorded on the "Tomy-Echo" recording paper. Usually the observations were made three times a day; namely, for 3 hours at times of sunrise and sunset, and 2 hours in mid-day. At the hydrographic stations a duration of observation varied considerably according to the conditions of plankton

* A. Kawamura: Bull. Plankt. Soc. Japan, **15**, No. 1. (1968).

net towing and of the another works at the opposite deck side.

The objectives of DSL observation were to get the organisms in the DSL and, to find the depth at which the DSL occurs especially at dusk and dawn in the Antractic regions in relation to the daily feeding habit of the baleen whales. The plankton sampling with Petersen type vertical closing net (shown in Table 39) was done for this purpose.

In the Indian sector of the Antarctic Ocean, patterns of the DSL are known (Kumagori *et al.*, 1964)*, and four of them, *i.e.*, belt-, line-, spot- and block-like DSL were recorded in this expedition. One of the characteristics of the DSL observed in the Antarctic Ocean was that: the stable and dense layer was found at the shallow water above 60 m, and 2 or 3 significant DSL were usually observed below the former layer. The former consisted of Diatoms-Copepods populations, and the latters comprised mainly Copepods-Chaetognaths or Euphausiids-Chaetognaths populations. The latter scatteres showed a remarkable diurnal migration: they ascended near to the surface at dusk, and descended to 400 or 500 meter level at dawn. The speed of the vertical movement of the scatterers was less than 4 m/min in ascent and more than 6 m/min in descent.

Table 24. The scientific and common name of whales observed

	Scientific name	Common name
Family	Balaenopteridae	
	Balaenoptera musculus (LINNAEUS)	blue whale
	B. physalus (LINNAEUS)	fin whale
	B. borealis LESSON	sei whale
Family	Physeteridae	
	Physeter catodon LINNAEUS	sperm whale
Family	Delphinidae	
	Stenella vaeruleo-alba (MEYEN)	blue white dolphin
Family	Globicephalidae	
	Globicephala melaena (TRAILL)	pilot whale
	Pseudorca crassidens OWEN	false killer whale
	Orcinus orca LINNAEUS	killer whale
Family	Grampidae	
	Grampus gruseus (CUVIER)	Risso's dolphin

Table 25. The numbers and the frequencies of whales sighted

Species	Number of whales sighted	Frequency
Larger whales		
blue whale	2	2
fin whale	5	5
sei whale	18	110
sperm whale	42	15
unidentified	16	9
Smaller whales		
blue white dolphin	348	9
pilot whale	134	9
false killer whale	29	4
killer whale	1	1
Risso's dolphin	30	1
unidentified	21	7

* *J. Tokyo Univ. Fish.*, 7, No. 2. (1964)

Table 26. Record of larger whales
P.: Port, S.B.: Starboard

Blue Whale: *Balaenoptera musculus* (LINNAEUS)

Date	Ship's time	Position	Number of individual	Sighted angle from ship's head	Sighted distance (mile)	Direction of swimming	Weather	Visibility (mile)	Wind direction	Wind force	Air temperature (°C)	Sea temperature (°C)
Dec. 6	0730	2°02.5S 170°01.5W	1	S.B. 60	3	W→E	bc	8	E	4	27.6	28.3
Feb. 23	1235	4°04.8N 139°43.0E	1	P. 70	5	SSE→NNW	bc	8	NE	3	28.2	28.9

Table 27. Record of larger whales
P.: Port S.B.: Starboard

Fin Whale: *Balaenoptera physalus* (LINNAEUS)

Date	Ship's time	Position	Number of individual	Sighted angle from ship's head	Sighted distance (mile)	Direction of swimming	Weather	Visibility (mile)	Wind direction	Wind force	Air temperature (°C)	Sea temperature (°C)
Dec. 29	0855	45°06.0S 173°58.6W	1	S.B. 20	3	—	o	8	W	3	13.2	14.1
Jan. 17	0440	63°54.7S 169°59.5W	1	P. 10	0.5	W→E	bc	7	NE	2	1.3	2.5
	1350	64°43.0S 170°05.8W	1	S.B. 70	3	N→S	c	7	SE	4	1.6	2.3
Jan. 22	2253	65°54.2S 162°24.3E	1	P. 48	2.5	NW→SE	bc	8	SW	5	−0.1	0.4
Nov. 1	0850	38°32.1S 155°04.9E	1	S.B. 20	3	W→E	bc	8	ENE	2	19.2	20.9

Table 28. Record of larger whales
P.: Port, S.B.: Starboard

Sei Whale: *Balaenoptera borealis* LESSON

Date	Ship's time	Position	Number of individual	Sighted angle from ship's head	Sighted distance (mile)	Direction of swimming	Weather	Visibility (mile)	Wind direction	Wind force	Air temperature (°C)	Sea temperature (°C)
Dec. 6	0738	2°02.5S 170°01.5W	1	P. 90	1	W→E	b	8	E	4	27.6	28.3
Dec. 23	1634	33°26.8S 169°56.3W	1	P. 60	3	N→S	c	8	SSE	3	19.0	19.5
Dec. 29	0655	45°12.0S 173°30.8W	2	S.B. 130	2	N→S	o	8	W	3	13.1	13.7
	0710	45°07.0S 173°39.0W	4	S.B. 80	2	ESE→WNW	o	8	W	3	12.9	13.6
Jan. 1	1115	42°32.6S 173°48.0E	1	P. 45	0.5	NE→SW	b	8	NE	4	15.0	15.0
Jan. 17	1330	64°39.3S 170°05.8W	2	S.B. 130	2	SW→NE	c	7	N	3	2.0	2.9
Jan. 23	0710	64°41.0S 159°04.0E	3	S.B. 10	1.5	NE→SW	bc	8	S	4	−1.5	−0.5
	0720	64°40.0S 159°04.0E	1	P. 45	0.3	SE→NW	bc	8	SW	4	−1.6	−0.5
	1440	63°29.9S 156°32.3E	1	P. 10	3	—	bc	8	NNE	3	1.7	1.0
Nov. 3	0745	33°08.8S 153°51.9E	2	S.B. 50	2	N→S	bc	8	ESE	5	23.0	26.0

Table 29. Record of larger whales
P.: Port, S.B.: Starboard

Sperm Whale: *Physeter catodon* LINNAEUS

Date	Ship's time	Position	Number of individual	Sighted angle from ship's head	Sighted distance (mile)	Direction of swimming	Weather	Visibility (mile)	Wind direction	Wind force	Air temperature (°C)	Sea temperature (°C)
Nov. 18	1105	30°07.5N 161°41.0E	3	0	3	S→N	bc	7	SE	5	23.3	23.6
Nov. 25	1625	24°00.3N 169°58.5W	1	180	0.01	—	c	8	SW	2	25.8	25.6
Nov. 27	1520	19°20.0N 170°05.0W	1	S.B. 30	3	W→E	bc	9	ENE	3	27.1	27.8
Dec. 15	1630	17°17.0S 170°04.0W	1	S.B. 10	5	ESE→WNW	bc	8	ESE	3	28.0	28.2
Dec. 23	1817	33°44.5S 169°57.9W	9	S.B. 20	3	N→S	c	8	SSE	4	18.9	19.3
Jan. 19	0530	69°32.0S 170°00.0W	1	S.B. 80	1.5	ENE→WSW	s	7	S	4	−1.0	0.0
Jan. 20	1825	67°16.0S 179°56.0W	1	S.B. 80	3	SSW→NNE	bc	8	NE	1	1.0	1.0
Jan. 20	1835	67°13.0S 179°56.0W	1	P. 10	1	S→N	bc	8	NE	1	1.0	0.7
Jan. 22	1000	67°14.5S 165°29.0W	3	—	—	—	s	3	SSE	5	−2.0	−1.7
Jan. 23	1820	63°01.8S 155°05.7E	1	S.B. 35	2	NNE→SSW	b	8	NE	5	1.4	1.4
Feb. 2	2040	33°10.3S 156°39.3E	1	S.B. 40	1.5	E→W	c	8	SE	5	20.8	23.2
Feb. 11	1130	27°12.3S 159°06.5E	4	S.B. 20	3.5	NNW→SSE	c	8	SE	2	23.8	24.6
	1415	26°42.1S 159°30.7E	5	P. 10	1	SW→NE	o	7	SE	3	23.0	24.8
Feb. 23	0745	3°00.4N 140°06.3E	1	S.B. 50	1	WNW→ESE	be	8	N	5	28.2	28.7
Feb. 27	0900	24°23.0N 138°04.5E	9	P. 5	2.5	NNE→SSW	bc	8	S	4	23.3	24.8

Table 30. Record of larger whales
P.: Port, S.B.: Starboard

Unidentified

Date	Ship's time	Position	Number of individual	Sighted angle from ship's head	Sighted distance (mile)	Direction of swimming	Weather	Visibility (mile)	Wind direction	Wind force	Air temperature (°C)	Sea temperature (°C)
Dec. 28	1845	45°55.0S 170°33.0W	1	P. 20	1.5	—	c	8	W	2	12.8	13.7
Dec. 29	1630	44°40.0S 175°47.0W	2	S.B. 12	1	—	bc	8	SW	4	20.1	20.0
Jan. 17	1210	64°21.8S 170°05.8W	2	S.B. 50	2.5	NNE→SSW	s	7	N	3	2.1	2.7
	1530	65°07.0S 170°05.8W	2	P. 45	3	E→W	c	8	SE	3	0.2	2.2
Jan. 22	2040	66°14.0S 163°15.0E	1	S.B. 15	4	—	bc	7	SW	7	-0.1	0.4
	2130	66°07.6S 162°58.5E	1	—	—	—	bc	7	SW	7	0.0	0.2
Jan. 30	0835	44°54.3S 155°07.1E	2	P. 42	3.5	—	bc	8	W	3	12.3	12.8
	0905	44°49.0S 155°06.4E	1	P. 10	1	—	bc	8	W	3	12.2	13.0
Feb. 19	0700	6°59.5S 155°00.7E	4	P. 45	2	WNW→ESE	bc	8	NW	5	28.7	28.9

Table 31. Record of smaller toothed whales
P.: Port, S.B.: Starboard

Blue White Dolphin: *Stenella caeruleo-alba* (MEYEN), and others.

Date	Ship's time	Position	Number of individual	Sighted angle from ship's head	Sighted distance (mile)	Direction of swimming	Weather	Visibility (mile)	Wind direction	Wind force	Air temperature (°C)	Sea temperature (°C)
Dec. 23	1300	32°39.0S 169°57.0W	50	0	2	W→E	bc	8	SW	4	20.1	20.0
	1340	32°43.0S 169°56.0W	30	S.B. 40	1	N→S	bc	8	SW	4	19.8	19.9
Dec. 24	0750	35°17.7S 169°59.7W	50	S.B. 45	3	S→N	bc	7	SSW	1	18.2	18.9
Jan. 25	1010	57°34.3S 155°07.4E	8	S.B. 5	2	S→N	o	6	NNE	4	5.8	5.2
Feb. 2	0750	36°09.3S 155°42.0E	30	P. 90	1	NE→SW	o	8	ESE	3	20.1	20.9
	0820	36°02.5S 155°44.7E	50	P. 40	4	SSW→NNE	o	8	ESE	3	20.1	22.5
	1010	35°37.5S 155°54.6E	100	S.B. 20	3	SSW→NNE	c	8	ESE	3	20.2	22.2
	1510	34°31.6S 156°19.6E	25	P. 60	2	S→N	bc	8	ESE	5	20.6	21.8
Feb. 4	0530	33°57.2S 151°42.0E	5	S.B. 50	0.01	NE→SW	b	8	NNE	2	20.9	22.3

Table 32. Record of smaller toothed whales
P.: Port, S.B.: Starboard

Pilot Whale: *Globicephala melaena* (TRAILL)

Date	Ship's time	Position	Number of individual	Sighted angle from ship's head	Sighted distance (mile)	Direction of swimming	Weather	Visibility (mile)	Wind direction	Wind force	Air temperature (°C)	Sea temperature (°C)
Jan. 8	1250	44°05.0S 179°55.0W	5	S.B.—	0.3	SE→NW	b	8	N	6	16.2	19.8
Jan. 11	1110	50°07.2S 169°58.9W	50	0	0.01	N→S	c	8	WSW	4	13.2	12.5
	1830	50°33.0S 169°56.0W	20	P. 40	3.5	NE→SW	bc	8	WSW	3	12.9	12.4
Jan. 25	0820	57°56.5S 155°07.5E	8	P. 55	1.0	S→N	o	5	N	4	5.6	5.3
	0840	57°51.7S 155°07.5E	7	P. 70	2.0	S→N	o	5	N	4	5.8	5.3
	0854	57°48.4S 155°07.5E	15	0	3.0	N→S	o	6	N	4	5.9	5.3
	0905	57°47.0S 155°07.5E	20	S.B.120	3.0	N→S	o	6	N	4	5.9	5.3
	1040	57°24.1S 155°06.6E	7	P. 80	1.0	NW→SE	r	6	NNE	4	6.0	5.2
Feb. 3	1915	33°10.0S 152°47.0E	2	S.B. 45	1.0	W→E	bc	9	ESE	4	22.8	25.7

Table 33. Record of smaller toothed whales
P.: Port, S.B.: Starboard

False Killer Whale: *Pseudorca crassidens* OWEN

Date	Ship's time	Position	Number of individual	Sighted angle from ship's head	Sighted distance (mile)	Direction of swimming	Weather	Visibility (mile)	Wind direction	Wind force	Air temperature (°C)	Sea temperature (°C)
Dec. 4	1530	1°58.0N 170°00.0W	2	S.B. 45	5	W→E	bc	9	Calm	3	28.0	30.0
Dec. 5	1135	0°03.6N 170°11.9W	15	S.B.150	0.2	NW→SE	b	9	E	3	28.3	28.4
Dec. 31	1420	43°05.0S 178°36.0E	2	S.B. 20	1	WNW→ESE	bc	8	S	4	14.0	15.0
Feb. 12	0800	24°13.3S 163°05.1E	10	S.B. 45	1	NE→SW	c	7	SE	1	25.1	25.0

Table 34. Record of smaller toothed whales
P.: Port, S.B.: Starboard

Killer Whale: *Orcinus orca* LINNAEUS

Date	Ship's time	Position	Number of individual	Sighted angle from ship's head	Sighted distance (mile)	Direction of swimming	Weather	Visibility (mile)	Wind direction	Wind force	Air temperature (°C)	Sea temperature (°C)
Jan. 16	1205	61°59.5S 169°58.8W	1	P. 30	0.025	W→Z	c	7	SW	6	2.2	4.0

Table 35. Record of smaller toothed whales
P.: Port, S.B.: Starboard

Risso's Dolphin: *Grampus griseus* (CUVIER)

Date	Ship's time	Position	Number of individual	Sighted angle from ship's head	Sighted distance (mile)	Direction of swimming	Weather	Visibility (mile)	Wind direction	Wind force	Air temperature (°C)	Sea temperature (°C)
Dec. 20	1025	25°51.6S 170°18.0W	30	S.B. 60	3	W→E	bc	8	SW	1	23.2	23.6

Table 36. Record of smaller toothed whales
P.: Port, S.B.: Starboard

Unidentified

Date	Ship's time	Position	Number of individual	Sighted angle from ship's head	Sighted distance (mile)	Direction of swimming	Weather	Visibility (mile)	Wind direction	Wind force	Air temperature (°C)	Sea temperature (°C)
Dec. 7	1130	5°51.0S 170°01.0W	2	S.B. 20	1	NNE→SSW	bc	8	NE	1	23.2	23.6
Dec. 28	1935	45°53.0S 170°37.0W	1	S.B.110	0.3	—	c	8	WNW	4	12.4	13.6
Jan. 8	1035	43°48.8S 179°30.2E	1	P.	0.02	NE→SW	bc	8	N	6	15.6	15.5
Jan. 22	1630	66°58.0S 164°48.7E	5	—	1	NE→SW	c	7	SW	7	−0.8	−1.1
Feb. 20	1155	6°23.0S 150°22.0E	10	S.B. 25	0.1	W→E	bc	8	S	2	29.1	29.1
Feb. 25	0955	13°34.8N 137°45.2E	1	S.B. 70	1	SW→NE	b	8	ENE	6	26.6	26.6
	0958	13°34.8N 137°45.2E	1	P. 25	0.5	W→E	b	8	ENE	6	26.6	26.6

Table 37. The scientific and common names of sea-birds observed

	Scientific name	Common name
Family	Diomedeidae	Albatrosses
	Diomedea cauta	Shy mollymawk
	D. chrysostoma	Grey-headed albatross
	D. eremita	Chatham Island mollymawk
	D. epomophora	Royal albatross
	D. exulans	Wandering albatross
	D. immutabilis	Laysan albatross
	D. melanophris	Black-browed albatross
	D. nigripes	Black-footed albatross
	Phoebetria palpebrata	Light-mantled sooty albatross
Family	Phalaerocoracidae	Shags or Cormorant
	Phalacrocrax melanoleucos brevirostris	Little shag
	P. sulcirostris	Little black shag
Family	Hydrobatidae	Storm petrels
	Oceanodroma castro	Harcourt's storm petrel
	O. furcata	Fork-tailed petrel
	O. leucorhoa	Leach's storm petrel
	O. tristrami	Sooty storm petrel
	Oceanites oceanicus	Wilson's storm petrel
	Fregetta grallaria	White-bellied storm petrel
	F. tropica	Black-bellied storm petrel
	Mesofregetta albigularis	White-throated storm petrel
	Pelagodroma marina	White-faced strom petrel
	Garrodia mereis	Grey-backed storm petrel
Family	Procellariidae	Petrels, Shearwaters and Fulmars
	Pterodroma alba	Phoenix petrel
	P. arminjoniana heraldica	Herald petrel
	P. cooki cooki	Cook's petrel
	P. externa externa	Juan Fernandez petrel
	P. externa cervicalis	White-necked petrel
	P. hypoleuca	Bonin petrel
	P. lessoni	White-headed petrel
	P. leucoptera	White-winged petrel
	P. inexpectata	Peale's petrel
	P. neglecta	Kermadec petrel
	P. hypoleuca nigripennis	Black-winged petrel
	P. phaeopygia	Dark-rumped petrel
	P. solandri	Solander's petrel
	Bulweria bulweri	Bulwer's petrel
	Puffinus bulleri	New Zealand shearwater
	P. carneipes	Pale-footed shearwater
	P. griseus	Stooty shearwater
	P. nativitatus	Christmas shearwater
	P. pacificus	Wedge-tailed shearwater (N. islands lt. ph.) (S. islands dk. ph.)

Table 37. (Continued)

	Scientific name	Common name
	P. gavia	Fluttering shearwater
	P. tenuirostris	Slender-billed shearwater
	Calonectris leucomelas	Streaked shearwater
	Daption capensis	Cape pigeon
	Fulmarus glacialoides	Silver-grey fulmar
	Halobaena caerulea	Blue petrel
	Macronectes giganteus	Giant petrel
	Pachyptila spp.	Prions
	Pagodroma nivea	Snow petrel
Family	Fregatideae	Frigatebirds
	Fregata ariel	Lesser frigatebird
	F. minor	Great frigatebird
Family	Sulidae	Gannets and Boobies
	Sula dactylatra	Blue-faced booby
	S. leucogaster	Brown booby
	S. sula	Red-footed booby
Family	Phaethontidae	Tropicbirds
	Phaethon lepturus	White-tailed tropicbird
	P. rubricauda	Red-tailed tropicbird
Family	Laridae	Gulls, Terns and Noddies
	Larus dominicanus	Southern black-backed gull
	L. novaehollandiae	Silver gull
	Sterna dougalli	Roseate tern
	S. fuscata	Sooty tern
	S. lunata	Grey-backed tern
	S. sumatrana	Black-naped tern
	Anous stolidus	Brown noddy
	Gygis alba	White tern
	Thalasseus bergi	Crested tern
Family	Stercorariidae	Skuas
	Catharacta skua	Great skua
	Stercorarius pomarinus	Pomarine jaegar
Family	Spheniscidae	Penguins
	Pygoscelis papua	Gentoo penguin (?)
	P. antarctica	Chinstrap penguin

Table 38. The first and the last positions where the successful occurrence of sea-birds was observed along the 170°W and 155°E longitude

Species	First sight			Last sight		
	Date	Position	Sea temp. (°C)	Date	Position	Sea temp. (°C)
Laysan albatross	Nov. 15, 1968	32°57.5 N 143°47.8 E	22.3	Nov. 25, 1968	24°00.3 N 169°58.5 W	25.6
Black-footed albatross	Nov. 18, 1968	30°07.2 N 161°26.0 E	23.6	Nov. 29, 1968	13°22.3 N 170°02.1 W	27.5
Wandering albatross	Dec. 23, 1968	32°07.8 S 169°56.4 W	19.8	Jan. 17, 1969	65°28.4 S 170°07.0 W	1.7
	Jan. 20, 1969	69°28.7 S 169°55.0 W	0.0	Jan. 21, 1969	66°31.7 S 173°22.5 E	0.3
	(Near Scott Island)					
	Jan. 26, 1969	54°31.5 S 155°50.0 E	7.2	Feb. 2, 1969	33°07.7 S 156°38.0 E	22.9
	(Near Macquarie Island)					
Chatham Island mollymawk	Dec. 29, 1968	44°43.4 S 175°39.3 W	14.3	Dec. 29, 1968	44°23.5 S 176°44.2 W	14.3
	(Near Pyramid Rock, Chatham Island)					
Black-browed albatross	Dec. 28, 1968	46°00.4 S 169°54.0 W	13.6	Dec. 31, 1968	43°25.6 S 179°48.9 E	14.7
	Jan. 13, 1969	54°20.0 S 169°38.0 W	8.7	Jan. 31, 1969	44°02.3 S 155°05.0 E	14.3
	(There were no occurrence on Jan. 19 and 22. The ship's noon positions of these two days were 69°29.7 S; 169°58.0 W and 67°29.0 S; 165°26.5 W, respectively)					
Grey-headed albatross	Dec. 31, 1968	43°25.6 S 179°48.9 E	14.7	Jan. 15, 1969	59°43.8 S 170°03.0 W	6.3
	Jan. 25, 1969	58°27.7 S 155°07.5 E	4.2	Jan. 31, 1969	41°44.3 S 155°08.2 E	15.7
Shy mollymawk	Jan. 31, 1969	42°06.0 S 155°08.5 E	15.4	Jan. 31, 1969	41°00.7 S 155°00.3 E	17.2
Light-mantled sooty albatross	Jan. 15, 1969	58°18.0 S 169°54.5 W	7.2	Jan. 28, 1969	48°46.2 S 155°22.4 E	11.1
Giant petrel	Dec. 28, 1968	46°00.4 S 169°54.0 W	13.6	Jan. 11, 1969	50°48.4 S 169°56.2 W	12.0
	Jan. 23, 1969	63°03.3 S 155°13.0 E	1.4	Jan. 26, 1969	54°05.5 S 155°25.7 E	6.7
White-winged petrel	Dec. 18, 1968	23°10.8 S 174°49.2 W	24.1	Jan. 12, 1969	53°14.1 S 169°58.1 W	10.5
Wedge-tailed shearwater (dk. ph.)	Dec. 3, 1968	05°40.1 S 169°51.1 W	29.0	Dec. 28, 1968	45°44.0 S 170°22.4 W	13.7
Wedge-tailed shearwater (lt. ph.)	Nov. 16, 1968	30°00.5 N 150°07.6 E	24.1	Nov. 25, 1968	24°03.9 N 169°59.5 W	25.7
Sooty shearwater	Jan. 11, 1969	50°09.6 S 169°56.3 W	13.2	Jan. 30, 1969	44°02.3 S 155°01.0 E	14.3
	The southern limit of occurrece was 67°48.4 S; 169°58.2 W with sea temperature 0.7°C.					
Cape pigeon	Dec. 29, 1968	44°46.2 S 175°26.8 W	14.1	Jan. 1, 1969	43°53.9 S 173°21.0 E	16.3
	Jan. 16, 1969	61°20.5 S 169°42.0 W	4.1	Jan. 26, 1969	54°00.5 S 155°17.0 E	6.7
Antarctic petrel	Jan. 17, 1969	65°28.4 S 170°07.0 W	1.7	Jan. 23, 1969	64°01.7 S 157°47.4 E	0.8

Table 38. (Continued)

Species	First sight			Last sight		
	Date	Position	Sea temp. (°C)	Data	Position	Sea temp. (°C)
	The southern limit of occurrence was Jan. 19, 69°29.7 S; 169°58.0 W with sea temperature −0.1°C.					
Snow petrel	Jan. 19, 1969	69°17.0 S 170°05.5 W	0.2	Jan. 23, 1969	64°39.6 S 159°19.3 E	−0.8
Silver grey fulmar	Jan. 20, 1969	67°29.5 S 179°28.0 W	1.4	Jan. 23, 1969	63°36.0 S 156°41.0 E	1.3
	(Near Scott Island)					
Great frigatebird	Nov. 27, 1968	19°14.6 N 170°02.5 W	27.8	Dec. 10, 1968	13°40.0 S 171°44.2 W	27.8
Boobies (Brown, blue-faced and red-footed)	Nov. 28, 1968	17°05.2 N 170°03.4 W	27.8	Dec. 15, 1968	17°00.4 S 170°02.0 W	27.9
Red-tailed tropicbird	Dec. 6, 1968	02°46.0 S 170°00.5 W	28.8	Dec. 22, 1968	30°50.1 S 169°58.4 W	20.6
White-tailed tropicbird	Nov. 29, 1968	14°08.4 S 170°06.0 W	27.6	Dec. 20, 1968	25°58.3 S 170°10.2 W	23.6
	Feb. 11, 1969	28°01.3 S 157°55.9 E	24.4	Feb. 12, 1969	24°21.5 S 162°52.4 E	24.7
Sooty tern	Dec. 3, 1968	05°19.4 S 169°51.6 W	28.9	Jan. 8, 1969	44°01.3 S 179°53.4 W	15.0

Table 39. Data on plankton sampling with Norpac net and the biomass in the upper 150 m.

Station	Date	Position	Ship's time	Estimated depth net reached (m)	Volume of water filtered (m^3)	Wet wight of sample: per haul (g)	Wet wight of sample: per 1000 m^3 (g)	Displacement volume of sample: per haul (ml)	Displacement volume of sample: per 1000m^3 (ml)	Dominant organisms in the sample
1	Nov. 19	30°01.2 N 166°46.6 E	1415 1423	118.2	31.65	0.8	25.28	0.6	18.96	Copepods Chaetognaths Euphausiids
2	Nov. 22	30°00.5 N 170°02.2 W	1857 1904	132.0	24.24	0.7	28.88	0.5	20.63	Copepods
			1907 1913	102.3	26.41	0.9	34.07	0.8	30.29	Euphausiids
3	Nov. 23	28°59.2 N 170°06.3 W	1957 2002	138.2	20.17	0.3	14.87	0.4	19.83	Copepods
			2006 2012	142.5	19.61	0.7	35.69	0.6	30.59	Euphausiids
4	Nov. 24	28°00.7 N 170°01.2 W	0141 0147	138.0	20.70	0.8	38.65	1.0	48.31	Copepods Euphausiids
			0151 0156	141.8	21.29	0.7	32.88	0.8	37.58	Chaetognaths
5	Nov. 24	26°50.5 N 170°00.7 W	1716 1722	138.2	22.32	1.0	44.80	1.0	44.80	Copepods Euphausiids
			1726 1732	107.9	25.45	0.5	19.65	0.7	27.50	Chaetognaths
6	Nov. 24	26°01.0 N 170°04.0 W	2233 2240	128.6	23.90	0.8	33.47	0.7	29.29	Copepods
			2243 2249	128.6	24.42	0.7	28.67	0.5	20.48	Chaetognaths
7	Nov. 25	25°00.7 N 170°00.8 W	0635 0642	142.5	21.22	0.3	14.14	0.3	14.14	Copepods
			0645 0652	144.2	19.93	0.5	25.09	1.0	50.18	
8	Nov. 25	24°00.3 N 169°58.5 W	1730 1736	165.8	23.99	0.3	12.50	0.5	20.84	Copepods
			1741 1747	147.3	19.99	0.5	25.12	0.4	20.05	Chaetognaths

Table 39. (Continued)

Station	Date	Position	Ship's time	Estimated depth net reached (m)	Volume of water filtered (m^3)	Wet weight of sample: per haul (g)	Wet weight of sample: per 1000m^3 (g)	Displacement volume of sample: per haul (ml)	Displacement volume of sample: per 1000m^3 (ml)	Dominant organisms in the sample
9	Nov. 25–26	23°00.3 N 169°59.9 W	2346 2350	148.1	21.97	0.3	13.66	0.3	13.66	Copepods
			2359 0005	140.1	20.76	0.8	38.54	0.6	28.90	Chaetoghaths
10	Nov. 26	21°59.3 N 170°02.4 W	0632 0638	146.1	20.63	0.6	29.08	0.7	33.93	Salpa Chaetognaths
			0642 0648	148.1	20.90	0.7	33.50	0.6	28.71	Copepods
11	Nov. 26	20°59.9 N 170°00.9 W	1925 1932	154.0	24.54	0.6	24.40	0.6	24.40	Copepods
			1947 1953	143.4	21.17	1.0	47.24	1.0	47.24	Chaetognaths
12	Nov. 27	19°59.8 N 170°02.0 W	1118 1124	135.9	23.30	0.8	34.34	0.5	21.46	Copepods
			1128 1134	131.3	24.49	0.7	28.58	0.8	32.66	Chaetognaths
13	Nov. 27	17°59.7 N 170°01.9 W	2329 2330	150.0	22.71	0.2	8.81	0.3	13.21	Copepods
			2341 2348	146.1	21.33	0.5	23.44	0.6	28.13	
14	Nov. 28	14°58.2 N 170°00.0 W	2027 2033	140.1	22.27	0.5	22.45	0.5	22.45	Salpa Copepods
			2046 2053	133.7	26.46	0.1>	3.8>	0.1>	3.8>	Chaetognaths
15	Jan. 29	11°59.5 N 169°59.5 W	2034 2039	88.2	26.17	0.1	3.82	0.1	3.82	Copepods
			2042 2047	120.7	26.29	0.3	11.41	0.2	7.61	

16	Dec. 1	09°01.7 N 170°00.2 W	2009 2014	129.9	20.81	0.6	28.83	0.8	38.44	Copepods
			2016 2022	122.9	21.52	0.7	32.53	0.8	37.18	Chaetognaths
17	Dec. 3	06°05.0 N 169°55.5 W	0131 0137	122.2	23.74	0.3	12.64	0.3	12.64	Copepods
			0148 0154	141.9	24.39	0.4	16.40	0.5	20.50	Euphausiids
18	Dec. 3	03°02.0 N 169°56.0 W	2006 2012	122.9	23.78	1.2	50.46	1.1	46.26	Copepods
			2015 2020	122.9	22.89	2.1	91.75	1.9	83.01	Euphausiids
C	Dec. 4	00°59.3 N 170°03.5 W	2147 2153	140.1	23.43	2.6	110.97	2.7	115.24	Copepods Euphausiids
			2156 2201	140.1	22.89	3.0	131.07	2.9	126.70	Chaetognaths
E	Dec. 5	00°02.2 N 170°09.7 W	0633 0639	122.9	34.24	2.5	73.03	2.8	81.79	Copepods
			0645 0650	133.5	28.45	3.2	112.5	3.0	105.40	Chaetognaths
G	Dec. 5	01°01.1 S 170°00.7 W	2213 2219	139.2	22.70	2.7	110.94	2.8	123.34	Copepods Cheatognaths
			2224 2228	140.1	23.08	3.2	138.66	3.0	120.99	Euphausiids Hydromedusae
1	Dec. 6	02°01.3 S 170°01.5 W	0625 0631	138.0	24.53	3.0	122.31	2.9	118.23	Copepods
			0633 0639	122.9	23.40	3.4	145.31	3.1	132.49	Chaetognaths
20 (K)	Dec. 6	03°00.9 S 170°00.3 W	1954 2000	137.1	21.48	1.8	83.09	1.9	88.45	Euphausiids Copepods
			2003 2009	137.1	21.74	2.1	96.6	2.0	92.0	Chaetognaths
21	Dec. 7	06°09.8 S 170°07.0 W	2004 2010	139.2	20.81	2.3	110.52	2.1	100.91	Copepods Chaetognaths
			2040 2046	144.9	20.95	2.1	100.23	1.9	90.69	Hydromedusae Euphausiids

Table 39. (Continued)

Station	Date	Position	Ship's time	Estimated depth net reached (m)	Volume of water filtered (m^3)	Wet weight of sample: per haul (g)	Wet weight of sample: per 1000m^3 (g)	Displacement volume of sample: per hual (ml)	Displacement volume of sample: per 1000m^3 (ml)	Dominant organisms in the sample
22	Dec. 8	09°03.0 S 169°52.8 W	2039 2045	137.1	23.23	0.6	25.83	0.5	21.53	Copepods
			2050 2055	140.1	21.80	0.6	27.52	0.6	27.52	Chaetognatus
23	Dec. 9	11°59.5 S 170°01.1 W	1957 2006	146.3	20.96	0.5	23.86	0.4	19.08	Copepods
			2009 2015	140.1	20.96	0.5	23.86	0.4	19.08	Chaetognaths
24	Dec. 15	17°00.0 S 170°00.0 W	0842 0848	141.0	21.50	0.3	13.95	0.4	18.60	Copepods Chaetognaths
			0853 0900	141.9	20.82	0.5	24.02	0.6	28.82	Hydromedusae
25	Dec. 16	20°00.0 S 170°03.8 W	0637 0642	141.0	19.98	0.5	25.03	0.5	25.03	Copepods
			0646 0652	139.2	20.53	0.5	24.36	0.6	29.23	Chaetognaths
26	Dec. 17	23°10.8 S 169°57.2 W	0906 0913	129.9	31.58	0.2	6.33	0.2	6.33	Copepods
			0915 0922	119.7	23.84	0.3	12.59	0.2	8.39	Chaetognaths
27	Dec. 18	23°09.8 S 174°39.0 W	1708 1714	140.1	21.77	0.8	36.74	0.8	36.74	Copepods Chaetognaths
			1716 1723	140.1	22.31	0.7	31.37	0.7	31.37	Scyphomodusae
28	Dec. 19	23°16.1 S 176°30.4 W	0523 0530	150.0	19.37	0.9	46.47	0.9	46.47	Copepods
			0533 0539	149.7	16.86	0.9	53.38	0.9	53.38	

29	Dec. 20	26°02.0 S 170°00.3 W	2133 2139 2141 2147	149.1 149.4	18.98 19.15	1.4 1.5	73.77 78.33	1.4 1.5	73.77 78.33	Copepods
30	Dec. 22	28°59.8 S 170°01.6 W	0620 0627 0630 0635	138.0 137.0	20.23 21.00	0.1> 0.1>	4.94> 4.76>	0.1> 0.1>	4.94> 4.76>	Salpa
31	Dec. 23	31°57.5 S 169°57.0 W	0448 0454 0457 0503	138.0 142.7	23.56 22.21	0.4 0.4	16.98 18.01	0.5 0.4	21.22 18.01	Copepods Scyphomodusae
32	Dec. 24	35°00.0 S 169°59.1 W	0308 0314 0336 0342	148.4 146.7	19.48 19.02	1.3 1.2	66.73 63.10	1.4 1.1	71.86 57.84	Copepods
33	Dec. 25	37°59.7 S 169°54.1 W	2100 2106 2109 2115	149.4 149.1	18.77 19.18	0.4 0.4	21.31 20.86	0.5 0.5	26.64 26.07	Euphausiids Copepods
34	Dec. 26	39°59.6 S 170°04.8 W	1423 1428 1432 1438	122.9 139.2	21.11 19.73	0.1> 0.1>	4.7> 5.7>	—— ——	—— ——	Salpa
35	Dec. 27	42°02.5 S 170°04.0 W	0641 0647 0650 0656	122.9 127.1	25.92 24.79	0.1> 0.1>	3.9> 4.0>	—— ——	—— ——	Salpa
36	Dec. 27	44°00.0 S 170°00.3 W	2019 2025 2027 2033	121.4 119.7	26.50 26.60	0.4 0.7	15.10 26.31	0.5 0.7	18.87 26.31	Euphausiids Copepods
37	Dec. 28	46°00.0 S 169°58.5 W	0902 0908 0912 0919	122.9 132.5	18.93 19.73	1.3 1.4	68.68 70.95	1.5 1.6	79.25 81.10	Copepods Chaetognaths

Table 39. (Continued)

Station	Date	Position	Ship's time	Estimated depth net reached (m)	Volume of water filtered (m^3)	Wet weight of sample: per haul (g)	Wet weight of sample: per 1000m^3 (g)	Displacement volume of sample: per haul (ml)	Displacement volume of sample: per 1000m^3 (ml)	Dominant organisms in the sample
38	Jan. 10	47°57.5 S 170°00.0 W	0158 0205	105.9	28.55	2.5	87.58	2.6	91.08	Copepods Euphausiids
			0208 0214	111.5	27.15	2.7	99.44	2.7	99.44	
39	Jan. 11	49°52.1 S 170°00.6 W	0703 0709	118.1	24.53	3.2	130.46	3.2	130.46	Copepods Chaetognaths
			0711 0716	113.1	22.89	4.5	196.61	4.5	196.61	
40	Jan. 12	51°56.9 S 169°55.7 W	0228 0334	142.7	28.25	5.0	177.00	5.0	177.00	Copepods Euphausiids
			0337 0343	143.3	26.07	2.9	111.24	3.1	118.92	Chaetognaths
41	Jan. 13	54°02.0 S 169°54.2 W	0620 0627	148.5	18.07	7.7	426.12	7.8	431.65	Copepods Chaetognaths
			0634 0640	86.0	28.97	5.2	179.50	5.2	179.50	
42	Jan. 14	55°54.4 S 169°57.0 W	1227 1233	116.6	28.54	1.6	56.06	1.8	63.07	Copepods
			1235 1240	109.7	28.66	2.0	69.78	2.0	69.78	
43	Jan. 15	57°55.3 S 170°00.0 W	0012 0020	132.0	22.61	5.0	221.15	4.8	212.30	Copepods Euphausiids
			0025 0031	131.3	22.39	5.5	245.63	5.5	245.63	Chaetognaths Salpa
44	Jan. 15	59°58.5 S 169°51.9 W	2325 2331	98.4	26.80	11.2	417.87	10.8	402.95	Copepods Euphausiids
			2337 2342	100.2	24.39	4.4	180.40	4.3	176.30	

45	Jan. 16	61°58.0 S 169°56.2 W	1502 1507 1510 1516	100.2 107.7	22.38 21.65	7.7 9.5	344.04 438.81	8.1 10.2	361.91 471.14	Diatoms Copepods
46	Jan. 17	63°57.1 S 170°04.8 W	0825 0831 0834 0840	141.8 149.4	18.05 16.05	11.8 2.3	653.72 143.31	12.0 2.6	664.80 162.01	Diatoms
47	Jan. 17	66°00.0 S 170°00.0 W	2001 2008 2012 2018	147.8 148.4	15.64 13.90	4.0 4.1	255.76 294.95	4.0 4.3	255.76 309.34	Diatoms Salpa
48	Jan. 18	68°00.3 S 170°05.5 W	1503 1509 1514 1520	146.7 147.8	14.19 13.67	3.2 5.6	255.50 409.64	2.8 4.8	197.32 351.12	Diatoms Salpa
49	Jan. 19	69°30.0 S 169°59.5 W	1021 1030 1041 1049	157.9 145.5	18.30 17.75	2.7 2.8	147.53 157.75	2.7 2.7	147.53 152.12	Copepods
50	Jan. 20	66°45.0 S 180°00.0	2103 2110	145.1	18.66	8.3	444.80	9.0	482.31	Diatoms Salpa
51	Jan. 21	66°30.5 S 170°07.9 E	1844 1850	149.7	18.47	0.5	27.07	0.8	43.31	Salpa, Euphausiids Amphipods
52	Jan. 23	63°01.8 S 154°56.8 E	1938 1945	135.5	20.19	18.7	919.00	19.0	934.00	Diatoms
53	Jan. 24	60°00.5 S 155°03.5 E	1711 1718	144.8	19.57	10.4	531.44	11.0	562.10	Diatoms
54	Jan. 25	57°03.0 S 155°01.5 E	1410 1416	122.6	11.37	19.7	1732.62	20.0	1759.00	Diatoms
55	Jan. 27	53°56.0 S 155°07.1 E	0020 0027 0029 0035	121.4 118.9	24.83 23.08	8.0 6.0	322.16 259.98	8.0 6.0	322.16 259.98	Copepods Chaetognaths

Table 39. (Continued)

Station	Data	Position	Ship's time	Estimated depth net reached (m)	Volume of water filtered (m^3)	Wet weight of sample: per haul (g)	Wet weight of sample: per 1000m^3 (g)	Displacement volume of sample: per haul (ml)	Displacement volume of sample: per 1000m^3 (ml)	Dominant organisms in the sample
56	Jan. 28	51°02.0 S 154°59.8 E	0012 0018	121.4	23.38	3.7	158.25	3.7	158.25	Copepods Euphausiids
			0020 0026	124.2	25.34	3.5	138.11	3.5	138.11	Chaetognaths
57	Jan. 29	48°00.5 S 155°05.2 E	0822 0828	96.4	28.84	0.5	17.34	0.5	17.34	Chaetognaths
			0831 0838	111.5	31.21	0.5	16.02	0.5	16.02	
59	Jan. 30	44°02.3 S 155°02.9 E	1603 1609	146.1	18.49	0.3	16.24	0.3	16.24	Euphausiids
60	Jan. 31	41°02.0 S 155°01.6 E	1607 1611	147.1	19.58	0.1	5.11	0.4	20.40	Copepods Euphausiids
61	Feb. 1	38°02.9 S 154°54.8 E	2122 2126	144.1	19.30	0.3	15.56	0.3	15.56	Euphausiids
			2151 2157	147.1	19.07	0.7	36.70	0.7	36.70	

Table 40. Data on plankton sampling with Norpac net and Petersen type vertical closing net in relation to the appearance of the Deep Scattering Layer

N: Norpac net, P: Petersen type vertical closing net

Station	Date	Position	Ship's time	Net used	Haul (m)	Estimated depth net reached (m)	Volume of water filtered (m^3)	Wet weight of sample: per haul (g)	Wet weight of sample: per $1000m^3$ (g)	Displacement volume of sample: per haul (ml)	Displacement volume of sample: per $1000m^3$ (ml)
41	Jan. 13	54°02.0 S 169°54.2 W	0707 0710	N	60– 0	46.0	10.32	4.3	416.67	4.0	387.60
			0711 0715	N	100– 0	69.4	18.33	5.1	278.26	5.1	278.26
42	Jan. 14	55°54.4 S 169°57.0 W	1258 1301	N	70– 0	55.1	11.69	0.5	42.77	0.6	51.32
			1302 1305	N	45– 0	35.4	——	0.2	——	0.2	——
45	Jan. 16	61°58.0 S 169°56.2 W	1832 1835	N	50– 0	47.0	5.86	9.9	1689.44	10.6	1808.89
46	Jan. 17	63°57.1 S 170°04.8 W	0902 0904	N	40– 0	39.4	5.24	4.5	858.78	4.8	916.03
			0910 0920	P	300– 0	300.0	——	11.8	——	12.6	——
			0922 0930	P	350– 0	350.0	——	4.8	——	4.8	——
47	Jan. 17	66°00.0 S 170°00.0 W	2041 2043	N	50– 0	49.8	4.55	3.7	813.19	3.7	813.19
48	Jan. 18	68°00.3 S 170°05.5 W	1559 1610	P	400–150	389.6 146.1	——	4.2	——	4.0	——
			1621 1629	P	150– 70	144.8 67.6	——	3.5	——	3.2	——
			1634 1635	P	70– 0	68.5	——	1.5	——	1.5	——

Table 40. (Continued)

Station	Date	Position	Ship's time	Net used	Haul (m)	Estimated depth net reached (m)	Volume of water filtered (m^3)	Wet weight of sample: per haul (g)	Wet weight of sample: per $1000m^3$ (g)	Displacement volume of sample: per haul (ml)	Displacement volume of sample: per $1000m^3$ (ml)
49	Jan. 19	69°30.0 S 169°59.5 W	1124 1127	N	40– 0	38.6	4.13	0.4	96.85	0.3	72.64
			1235 1246	P	200– 0	194.8	——	7.5	———	7.0	———
			1338 1346	P	200– 0	197.0	——	4.8	———	4.5	———
50	Jan. 20	66°45.0 S 180°00.0	2255 2300	P	150– 0	146.1	51.52	2.6	50.47	2.7	52.41
			2305 2308	P	50– 0	48.1	19.25	1.5	77.93	1.5	77.93
			2138 2143	N	90– 0	88.4	7.70	8.1	1051.95	9.0	1168.83
51	Jan. 21	66°30.5 S 170°07.9 E	1932 1935	N	60– 0	58.9	7.41	0.5	67.48	0.5	67.48
52	Jan. 23	63°01.8 S 154°56.8 E	2009 2011	N	60– 0	56.0	3.71	11.1	2619.00	12.5	2960.00
			2058 2104	P	160– 0	129.4	55.62	13.7	246.33	14.0	251.72
53	Jan. 24	60°00.5 S 155°03.5 E	1740 1742	N	60– 0	58.9	6.20	5.5	887.10	5.8	935.5
			1813 1822	P	300– 0	285.3	94.03	6.1	64.84	6.8	72.28
			1827 1832	P	100– 0	99.4	32.49	5.5	169.29	5.9	181.60
54	Jan. 25	57°03.0 S 155°01.5 E	1419 1421	N	60– 0	53.9	4.41	12.4	2811.82	12.8	2902.53
			1544 1554	P	350– 0	215.6	134.11	29.5	220.07	31.5	234.99
			1559 1604	P	150– 0	114.9	59.85	10.3	172.11	10.6	177.13

55	Jan. 27	53°57.7 S 155°08.8 E	0142 0158	N	350–	0	247.1	57.94	6.0	103.56	6.0	103.56
55	Jan. 27	53°58.8 S 155°10.0 E	0341 0356	P	400–	0	251.6	163.44	7.3	44.68	7.0	42.84
			0401 0409	P	240–	0	154.3	96.32	3.5	36.33	3.5	36.33
57	Jan. 29	48°00.5 E 155°05.2 E	0900 0906	P	200–	0	125.9	83.08	1.0	12.04	1.0	12.04
59	Jan. 30	44°02.3 E 155°02.9 E	1530 1541	N	300–	0	276.0	41.60	0.8	26.57	0.8	26.57
			1613 1618	P	170–	0	161.5	56.55	0.5	8.84	0.7	12.37
			1623 1632	P	300–	0	277.9	96.20	1.9	19.79	1.8	18.75
60	Jan. 31	41°02.0 S 155°01.6 E	1613 1630	N	500–	0	466.5	63.40	1.5	23.65	1.5	23.65
			1718 1724	P	170–	0	165.5	53.40	0.6	11.24	0.7	13.11
			1728 1746	P	500–	0	479.5	153.10	3.0	19.58	2.3	18.27
61	Feb. 1	38°01.4 S 154°57.6 E	1818 1825	P	180–	0	173.8	55.00	0.2	3.62	0.2	3.62
		38°02.5 S 154°54.4 E	1828 1843	P	500–	0	463.0	173.90	1.0	5.75	1.0	5.75
		38°02.9 S 154°54.8 E	2033 2041	P	300–	0	276.1	84.30	0.3	3.56	0.3	3.56
			2129 2132	N	80–	0	79.5	10.42	0.1	9.59	0.1	9.59

Table 41. Records of surface tow with larva net.

St.	Date	Hour	Position	Haul	Dominant organisms collected
24	Dec. 15	0950–1230	13°00.4 S, 169°59.5 W	Drifting	*Physalia* sp.
25	Dec. 16	0500–0900	20°00.0 S, 170°03.8 W	"	Hydromedusae, *Antennarius* sp.
26	Dec. 17	0400–0615	23°10.4 S, 169°59.4 W	"	*Diphyes* sp.
31	Dec. 22	2235–2335	31°59.6 S, 170°01.0 W	"	———
	Dec. 23	2340–0140	31°56.5 S, 169°56.0 W	"	*Diphyes* sp.
32	Dec. 24	0250–0430	34°58.3 S, 169°59.3 W	"	*Diphyes* sp.
33	Dec. 25	2025–2225	37°59.7 S, 169°54.1 W	"	———
34	Dec. 26	1422–1622	39°58.0 S, 170°01.7 W	"	*Velella, Physalia* sp.
36	Dec. 27	2020–2050	44°00.0 S, 170°00.0 W	"	*Cavolinia* sp.
40	Jan. 12	0840–1040	51°57.1 S, 169°55.6 W	"	Amphipoda
42	Jan. 14	1230–1330	55°54.4 S, 169°57.0 W	"	———
43	Jan. 15	0115–0215	57°55.3 S, 170°00.0 W	"	Chaetognatha
	Jan. 15	1223–0323	" "	"	Chaetognatha
45	Jan. 16	1225–1425	61°59.8 S, 169°59.0 W	"	Amphipoda
47	Jan. 17	2100–2300	66°00.0 S, 170°00.0 W	"	*Salpa* sp. Amphipoda
48	Jan. 18	1435–1635	68°02.0 S, 170°09.0 W	"	*Salpa* sp. Copepoda
	Jan. 18	1650–2050	" "	"	———
49	Jan. 19	1105–1150	69°32.0 S, 170°00.0 W	"	Squid, Fish larva
50	Jan. 20	2135–2235	66°45.0 S, 180°00.0	"	*Salpa* sp. Amphipoda
	Jan. 20	2305–2335	" "	"	*Salpa* sp. Amphipoda
51	Jan. 21	2300–2320	66°30.5 S, 170°09.9 E	"	*Saopa* sp. Amphipoda, Euphausiacea
53	Jan. 24	1840–1940	60°00.5 S, 155°04.8 E	"	*Sapla* sp. Amphipoda
	Jan. 24	1950–2050	" "	"	*Salpa* sp. Amphipoda
	Jan. 24	2207–2237	" "	Horizontal	*Salpa* sp. Amphipoda, Squid
54	Jan. 25	1535–1630	57°03.0 S, 155°01.5 E	Drifting	———
	Jan. 25	1817–1847	" "	Horizontal	———
55	Jan. 27	0135–0235	53°57.7 S, 155°08.8 E	Drifting	*Salpa* sp., Amphipoda, Chaetognatha
	Jan. 27	0449–0519	54°00.0 S, 155°11.7 E	Horizontal	*Salpa* sp., Amphipoda, Squid
56	Jan. 28	0244–0322	51°02.0 S, 154°59.8 E	Drifting	*Salpa* sp., Chaetognatha
	Jan. 28	0702–0732	51°06.4 S, 155°04.9 E	Horizontal	*Salpa* sp., Chaetognatha
H-1	Jan. 28	2219–2249	48°38.8 S, 156°18.0 E	"	Amphipoda, Chaetognatha, Squid
58	Jan. 29	2119–2149	46°56.2 S, 155°05.0 E	"	*Salpa* sp., Amphipoda, Chaetognatha
59	Jan. 30	1540–1740	44°01.0 S, 155°05.0 E	Drifting	Hydromedusae
H-2	Jan. 30	2208–2238	43°47.4 S, 155°06.6 E	Horizontal	*Salpa* sp., Amphipoda, Chaetognatha
60	Jan. 31	1605–1805	41°02.0 S, 155°01.6 E	Drifting	Phyllosoma
H-3	Jan. 31	2207–2237	40°27.5 S, 155°03.6 E	Horizontal	*Salpa* sp., Lantern fish, Saury
61	Feb. 1	2256–2326	38°01.7 S, 154°55.8 E	"	Hydromedusae, *Physalia* sp., Saury
H-4	Feb. 2	2107–2137	33°07.7 S, 156°36.9 E	"	*Physalia* sp., Lantern fish, Leptocephalus
H-5	Feb. 22	2108–2138	00°48.8 N, 141°07.2 E	"	*Salpa* sp., Alima larva of decapoda
H-6	Feb. 23	2057–2127	05°58.5 N, 139°13.0 E	"	*Salpa* sp., Lantern fish, Leptocephalus
H-7	Feb. 24	2057–2127	10°44.2 N, 137°54.0 E	"	*Salpa* sp., Leptocephalus
H-8	Feb. 25	2100–2130	16°05.3 N, 137°45.0 E	"	*Salpa* sp., Alima larva of decapoda
H-9	Feb. 26	2100–2130	21°40.0 N, 137°55.3 E	"	Ctenophore
H-10	Feb.27	2100–2130	27°11.5 N, 137°50.1 E	"	*Salpa* sp., Leptocephalus, Lantern fish

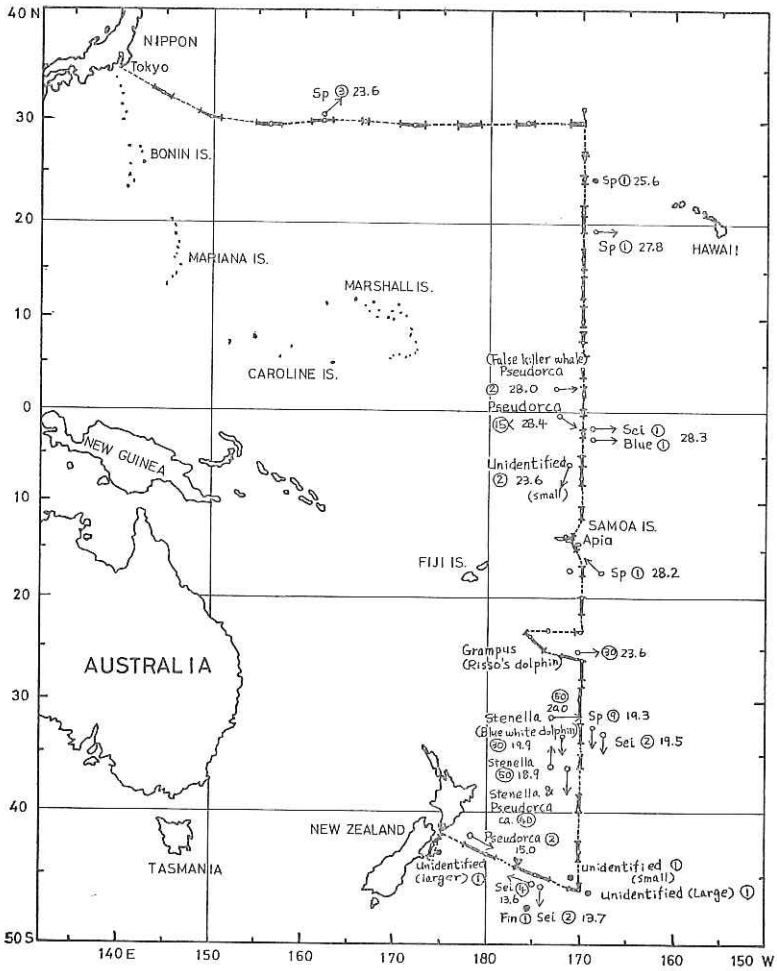

Fig. 93a. Whales sighted. Solid line: observed section, open circles: noon position, arrow: direction of whale movement when sighted, number encircled; number of whales sighted, numeral: surface sea temperature (°C).

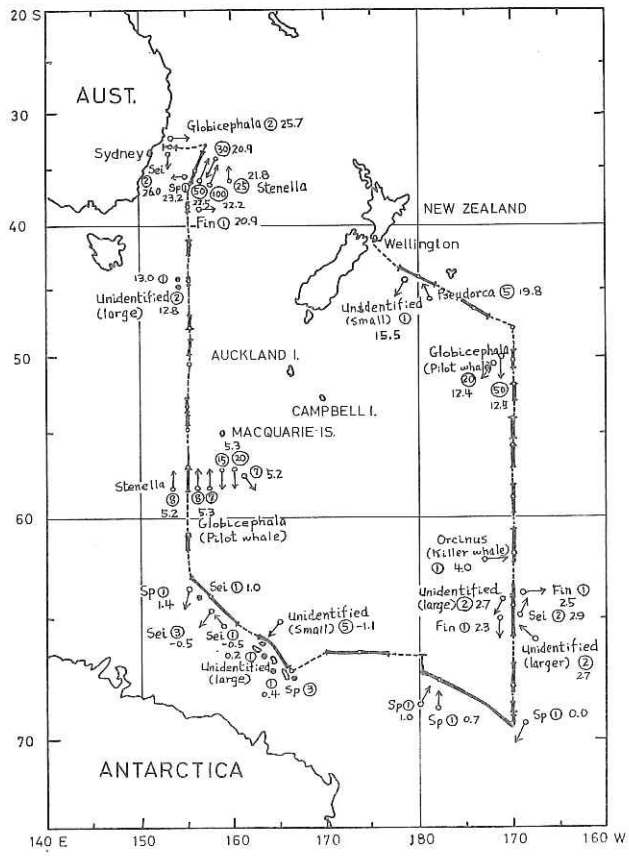

Fig. 93b. Whales sighted. Legend as in Figure. 93a.

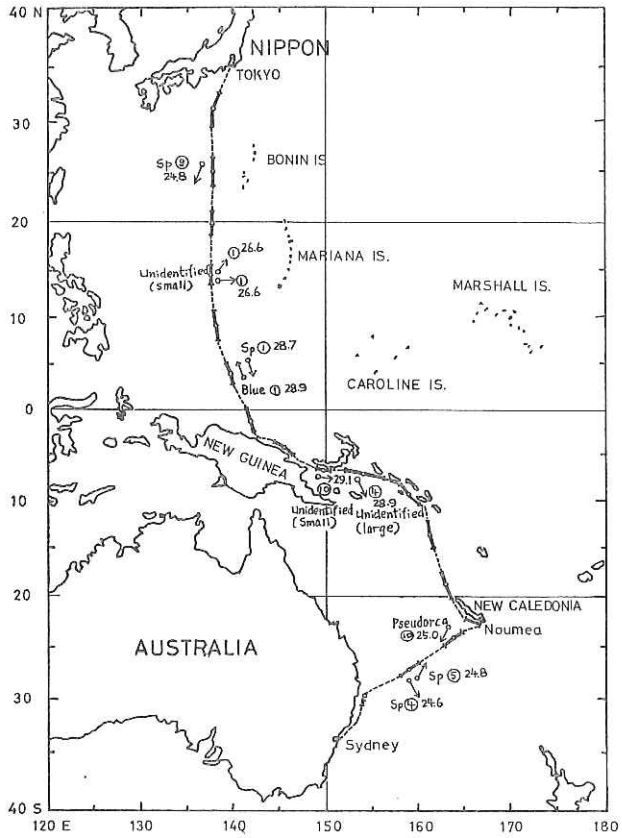

Fig. 93c. Whales sighted. Legend as in Figure. 93a.

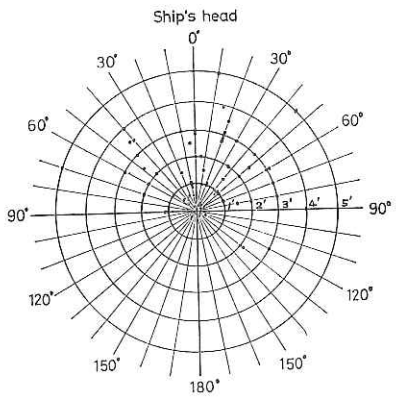

Fig. 94. Direction and distance frequencies of sighted whales.

VIII.3.3. Jet Net

by

T. Nakai, K. Hasumoto, and H. Otobe

Object. Clarke Jet Net [J. Mar. Res., 22, 284–287 (1964)] was operated at the cruising speed of the Hakuhō Maru. The object of the test is to find the best conditions for stable towing, especially towing- and depressor-position.

Method. Jet Net was towed over the side by wire rope and boom, and was launched and recovered with hoist. The wire rope is about 33 meter long and 16 mm in diameter, and the boom is about 4 meter long.

Result. Jet Net was tested at cruising speed of 10 to 14 knots. It was found that Jet Net is towed in a stable condition at towing position No. 3, and depressor position No. 1 in Figure 95 at 5 meters below sea surface. Plankton collected was in excellent condition. Also, the shape and size of wings were found to play very important role for stabilizing Jet Net in water, and that a small deformation of wings makes the Jet Net unstable.

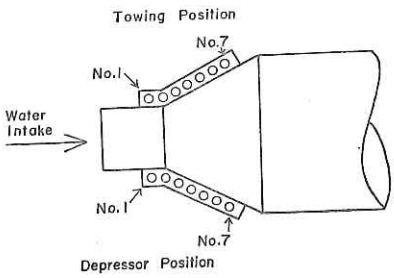

Fig. 95. Jet Net showing the optimum position of towing and depressor.